

**NON-LINEAR FINITE ELEMENT ANALYSIS  
OF STEEL FRAMES IN FIRE CONDITIONS**

by

**HASSAN A. SAAB**

*B.Sc.(Hons.), M.Sc., D.I.C.*

A thesis submitted to the Department of Civil  
and Structural Engineering in partial fulfilment  
of the requirements for the Degree of  
Doctor of Philosophy

University of Sheffield

June, 1990

*To*

*My Parents, Brothers and Sisters*

*My Wife*

*with love*

# Contents

<b>List of Figures</b>	<b>ix</b>
<b>List of Tables</b>	<b>xvi</b>
<b>Acknowledgement</b>	<b>xvii</b>
<b>Declaration</b>	<b>xviii</b>
<b>Summary</b>	<b>xix</b>
<b>Notations</b>	<b>xxi</b>
<b>1 Introduction</b>	<b>1</b>
1.1 Fire development and growth . . . . .	2
1.2 Standard fire exposure . . . . .	3
1.3 Fire safety measures . . . . .	4
1.4 Fire engineering approaches . . . . .	5
1.5 Objectives and scope of the research . . . . .	6
<b>2 Literature Review</b>	<b>8</b>
2.1 Introduction . . . . .	8

2.1.1	Temperature growth in a compartment . . . . .	10
2.1.1.1	Determination of the fire load . . . . .	11
2.1.1.2	The ventilation factor . . . . .	12
2.1.1.3	Thermal properties of the bounding materials . . . . .	12
2.1.2	Prediction of temperatures of structural steel elements . . . . .	13
2.1.2.1	Effect of the location of the steelwork . . . . .	13
2.1.2.2	Effect of steel size and shape . . . . .	14
2.1.3	Assessment of the structural response . . . . .	15
2.2	Review of previous experimental work . . . . .	16
2.2.1	Creep buckling tests . . . . .	21
2.3	Review of previous theoretical work . . . . .	23
2.3.1	Analytical investigations . . . . .	23
2.3.2	Numerical analyses . . . . .	26
2.3.3	Method of analysis of BS5950 Pt.8 (1990) . . . . .	34
2.4	Observations . . . . .	36
<b>3</b>	<b>Mechanical Properties of Structural Steel at Elevated Temperatures</b>	<b>38</b>
3.1	Introduction . . . . .	38
3.1.1	Tests under steady state heating conditions . . . . .	39
3.1.2	Tests under transient heating conditions . . . . .	40
3.2	The available data on stress-strain-temperature relationships . . . . .	40
3.3	Temperature dependent mechanical properties of steel . . . . .	42
3.3.1	The elastic modulus . . . . .	42

3.3.1.1	Brockenbrough (1970) . . . . .	43
3.3.1.2	C.T.I.C.M (1982) . . . . .	43
3.3.1.3	E.C.C.S (1983) . . . . .	44
3.3.1.4	The adopted model . . . . .	44
3.3.2	The yield strength . . . . .	45
3.3.2.1	Brockenbrough (1970) . . . . .	45
3.3.2.2	C.T.I.C.M (1982) . . . . .	45
3.3.2.3	E.C.C.S (1983) . . . . .	45
3.3.2.4	The adopted model . . . . .	46
3.3.2.5	Fire resistant steel . . . . .	46
3.3.3	Coefficient of thermal expansion . . . . .	47
3.4	Stress-strain-temperature relationship. . . . .	47
3.5	Summary . . . . .	50
<b>4</b>	<b>Nonlinear Inelastic Analysis of Fire-Exposed Frames</b>	<b>51</b>
4.1	Introduction . . . . .	51
4.2	Description of the program INSTAF . . . . .	54
4.3	Structural analysis at elevated temperatures . . . . .	55
4.3.1	Temperature distribution within each member . . . . .	55
4.3.2	Definition of the problem and main assumptions . . . . .	57
4.3.3	Finite element formulations . . . . .	61
4.3.3.1	Evaluation of the tangent stiffness $(k_T)_{ij}$ and the incremental unbalanced force $\Delta Q_i$ . . . . .	64
4.3.3.2	Evaluation of the section properties . . . . .	65

4.3.3.3	Evaluation of the incremental stress resultant vector	67
4.3.4	Solution procedure	70
4.3.4.1	Load-deformation characteristics under increasing load and a given temperature level	70
4.3.4.2	Load-deformation characteristics under increasing temperature and subject to given load level	71
4.4	Computer program	72
4.5	Summary	74
<b>5</b>	<b>Comparison with Experimental and Analytical Data</b>	<b>75</b>
5.1	Room temperature comparison	76
5.2	Comparison with elevated temperature tests	78
5.2.1	Comparison with Aasen (1985)	78
5.2.2	Comparison with Rubert and Schaumann (1986)	79
5.3	Comparison with analytical results	80
5.4	Review of verification studies	82
5.5	Conclusions	84
<b>6</b>	<b>Behavioural Studies</b>	<b>85</b>
6.1	Inelastic buckling of steel columns at elevated temperatures	86
6.2	Frame response at elevated temperatures	88
6.2.1	Effect of slenderness ratio	89
6.2.2	Effect of stress-strain relationships and material properties expressions	91
6.2.2.1	Comparison between bilinear and continuous stress-strain relationships using BS 5950 material models	92

6.2.2.2	Comparison between bilinear and continuous $\sigma - \epsilon$ relationships using CTICM material models . . .	93
6.2.2.3	Comparison between bilinear and continuous $\sigma - \epsilon$ relationships using ECCS material models . . . .	93
6.2.2.4	Comparison between bilinear and continuous stress-strain representations using the three material models (BS 5950, CTICM, ECCS) . . . . .	94
6.2.3	Effects of various forms of protection . . . . .	94
6.2.4	Effect of magnitude of residual strains . . . . .	96
6.2.5	Effect of thermal gradient along and across the section . .	98
6.2.5.1	Effect of thermal gradient across the section . . .	98
6.2.5.2	Effect of thermal gradient along the members . .	100
6.3	On the strength - temperature relationships of steel frames . . . .	101
6.3.1	The elevated temperature sway frame response . . . . .	101
6.3.2	An approximate strength - temperature curve for uniformly heated steel frames . . . . .	103
6.3.3	Verification of the obtained curve . . . . .	103
6.4	Variation of internal moment with temperature . . . . .	104
6.5	Concluding remarks . . . . .	108
<b>7</b>	<b>Strength and Stability of Sway Frames in Fire</b>	<b>111</b>
7.1	Introduction . . . . .	111
7.2	Behaviour of fixed base frames . . . . .	113
7.3	Behaviour of pin ended frames . . . . .	116
7.4	Concluding remarks . . . . .	118

<b>8 Conclusions and Recommendations</b>	<b>120</b>
8.1 Scope of the work . . . . .	120
8.2 Concluding remarks . . . . .	122
8.3 Recommendations for future work . . . . .	125
<b>References</b>	<b>127</b>
<b>Appendix A</b>	<b>141</b>



## LIST OF FIGURES

- Fig. 1.1** - Three periods of fire development [58].
- Fig. 1.2** - ISO standard temperature-time relationship.
- Fig. 3.1** - Variation of the adopted modulus of elasticity with temperature compared with CTICM and ECCS models.
- Fig. 3.2** - Variation of the adopted effective yield strength model with temperature compared with CTICM and ECCS models.
- Fig. 3.3** - Comparison between the adopted effective yield strength model and Fire Resistance Steel [78].
- Fig. 3.4** - Variation of coefficient of thermal expansion  $\alpha$  with temperature [58].
- Fig. 3.5** - Comparison between present stress-strain-temperature relationships and BSC data [17].
- Fig. 4.1** - Load-deformation relationships as predicted by various types of analysis.
- Fig. 4.2** - Logical sequence of INSTAF.
- Fig. 4.3** - Various protection configurations and temperature distributions [64].
- Fig. 4.4** - Assumed temperature distribution across the section of an element.
- Fig. 4.5** - Finite element deformations.
- Fig. 4.6** - Local nodal displacements.
- Fig. 4.7** - Global nodal displacements.
- Fig. 4.8** - Transformed section of a plate segment.

**Fig. 4.9** - Residual strain distribution.

**Fig. 4.10** - Newton-Raphson iterative procedure at constant temperature.

**Fig. 4.11** - Newton-Raphson iterative procedure at increasing temperature.

**Fig. 4.12** - Logical sequence of the program.

**Fig. 5.1** - Frame geometry and loadings for room temperature comparison.

**Fig. 5.2** - Comparison between predicted lateral deflections and test results [7].

**Fig. 5.3** - Comparison between predicted and measured critical temperatures [1].

**Fig. 5.4** - Mid-height deflection of column No.8.

**Fig. 5.5** - Frame types for comparison with Ref.[77].

**Fig. 5.6** - Comparison between predicted and measured critical temperatures [77].

**Fig. 5.7** - Comparison between calculated and measured deflections of frame EHR3 [77].

**Fig. 5.8** - Comparison between calculated and measured deflections of frame EGR1 [77].

**Fig. 5.9** - Comparison between calculated and measured deflections of frame ZSR1 [77].

**Fig. 5.10** - Beam and frame configurations for comparison with analytical results [33].

**Fig. 5.11** - Comparison with Furumura [33] for simply supported beam.

**Fig. 5.12** - Comparison with Furumura [33] for hinged ends beam.

**Fig. 5.13** - Comparison with Furumura [33] for fixed-ended beam.

**Fig. 5.14** - Comparison with Furumura [33] for frame results.

**Fig. 6.1** - Residual stress distribution.

**Fig. 6.2** - Variation of failure stress with column slenderness ratio at increasing temperature.

**Fig. 6.3** - Comparison between calculated column buckling curves and ECCS [29] at increasing temperature.

**Fig. 6.4** - Variation of failure stress with temperature at increasing slenderness ratio.

**Fig. 6.5** - Frame geometry and loading for parametric studies.

**Fig. 6.6** - Variation of failure load with temperature at increasing slenderness using BS5950 expressions and continuous  $\sigma - \epsilon$ .

**Fig. 6.7** - Variation of failure load with temperature at increasing slenderness.

**Fig. 6.8** - Variation of failure load with temperature at increasing slenderness using BS5950 expressions and bilinear  $\sigma - \epsilon$ .

**Fig. 6.9** - Variation of failure load with temperature at increasing slenderness using CTICM expressions and continuous  $\sigma - \epsilon$ .

**Fig. 6.10** - Variation of failure load with temperature at increasing slenderness using CTICM expressions and bilinear  $\sigma - \epsilon$ .

**Fig. 6.11** - Variation of failure load with temperature at increasing slenderness using ECCS expressions and continuous  $\sigma - \epsilon$ .

**Fig. 6.12** - Variation of failure load with temperature at increasing slenderness using ECCS expressions and bilinear  $\sigma - \epsilon$ .

**Fig. 6.13** - Comparison of frame response using different strength expressions ( $\bar{\lambda} = 0.27$ ).

**Fig. 6.14** - Comparison of frame response using different strength expressions ( $\bar{\lambda} = 0.30$ ).

**Fig. 6.15** - Comparison of frame response using different strength expressions ( $\bar{\lambda} = 0.54$ ).

**Fig. 6.16** - Comparison of frame response using different strength expressions ( $\bar{\lambda} = 0.89$ ).

**Fig. 6.17** - Frame geometry and loading.

**Fig. 6.18a** - Ambient temperature failure mode.

**Fig. 6.18b** - Failure mode of uniformly heated frame.

**Fig. 6.19** - Failure mode for various forms of protection.

**Fig. 6.20** - Temperature-sway deflection relationships for various forms of protection.

**Fig. 6.21** - Variation of failure load with temperature at increasing residual stress level ( $\bar{\lambda} = 0.89$ ).

**Fig. 6.22a** - Variation of failure load/failure load of uniformly heated section with increasing temperature ( $\bar{\lambda} = 0.27$ ).

**Fig. 6.22b** - Variation of failure load/failure load of uniformly heated section with increasing temperature ( $\bar{\lambda} = 0.33$ ).

**Fig. 6.22c** - Variation of failure load/failure load of uniformly heated section with increasing temperature ( $\bar{\lambda} = 0.89$ ).

**Fig. 6.23** - Typical temperature distribution along a column length [92].

**Fig. 6.24** - Variation of failure load with temperature using different longitudinal temperature distributions.

**Fig. 6.25a** - Frame geometry and loading.

**Fig. 6.25b** - Variation of failure load with temperature at increasing slenderness for sway frame.

**Fig. 6.26** - Applied load level Vs. critical temperature at increasing slenderness.

**Fig. 6.27** - Schematic representation of method of analysis.

**Fig. 6.28** - Proposed strength-temperature curve for uniformly heated frames.

**Fig. 6.29** - Frame geometry and loadings for curve verification.

**Fig. 6.30** - Frame geometry and loadings for curve verification.

**Fig. 6.31** - Verification of the proposed strength-temperature curve for uniformly heated frames.

**Fig. 6.32** - Frames geometry and loadings.

**Fig. 6.33** - Variation of bending moment distribution with temperature.

**Fig. 6.34** - Variation of bending moment distribution with temperature at mid-span of the beam.

**Fig. 6.35** - Variation of bending moment distribution with temperature.

- Fig. 6.36** - Variation of bending moment distribution with temperature.
- Fig. 6.37** - Variation of bending moment distribution with temperature.
- Fig. 7.1** - Frame geometry and loadings of fixed base frame.
- Fig. 7.2** - Lateral deflection-temperature relationships for heating conditions shown in Table 7.1.
- Fig. 7.3** - Ambient temperature failure mode.
- Fig. 7.4** - Deformed shape of uniformly heated frame ( $F_1$ ).
- Fig. 7.5** - Deformed shape of frame ( $F_2$ ) at  $550^\circ C$ .
- Fig. 7.6** - Deformed shape of frame ( $F_4$ ) at  $550^\circ C$ .
- Fig. 7.7** - Bending moment distribution of frame ( $F_2$ ) at  $550^\circ C$ .
- Fig. 7.8** - Bending moment distribution of frame ( $F_4$ ) at  $550^\circ C$ .
- Fig. 7.9** - Bending moment distribution of frame ( $F_6$ ) at  $550^\circ C$ .
- Fig. 7.10** - Frame geometry and loadings.
- Fig. 7.11** - Lateral deflection-temperature relationships for the heating conditions shown in Table 7.2.
- Fig. 7.12** - Bending moment distribution of frame ( $P_4$ ) at  $400^\circ C$ .
- Fig. 7.13** - Bending moment distribution of frame ( $P_5$ ) at  $400^\circ C$ .
- Fig. 7.14** - Bending moment distribution of frame ( $P_3$ ) at  $560^\circ C$ .
- Fig. 7.15** - Bending moment distribution of frame ( $P_5$ ) at  $560^\circ C$ .
- Fig. A.1** - Member deformations due to thermal bowing.

**Fig. A.2** - Thermal bowing of pin-ended members.

**Fig. A.3** - Thermal bowing of a cantilever.

## LIST OF TABLES

**Table 5.1** - Input data and results for ambient temperature comparison.

**Table 5.2** - Input data and results for comparison with column tests [1].

**Table 5.3** - Input data and results for comparison with frame tests [77].

**Table 6.1** - Input data for calculation of  $\bar{\lambda}$ .

**Table 6.2** - Various forms of protection and corresponding critical temperatures.

**Table 6.3** - Input data and results for curve verification.

**Table 6.4** - Input data and results for curve verification.

**Table 7.1** - Various forms of heating conditions and corresponding critical temperatures.

**Table 7.2** - Various forms of heating conditions and corresponding critical temperatures.



## Acknowledgement

The author is indebted to Professor D A Nethercot and Dr. I W Burgess for their excellent supervision, guidance and many valuable discussions. He also wishes to thank Professor T H Hanna, Head of Department, and all the departmental staff for their help.

The author is grateful to the Hariri Foundation for their financial support during the period of this work.

Finally, the support of my parents, brothers and sisters is greatly appreciated. The endless support and patience of my wonderful wife is affectionately acknowledged.

## Declaration

Except where specific reference has been made to the work of others, this thesis is the result of my own work. No part of it has been submitted to any University for a degree, diploma or other qualification.

H A SAAB

## Summary

The present work is concerned with the development of a finite element approach and its subsequent use for behavioural studies on steel frames in fire conditions. The nonlinear structural analysis is based on a tangent stiffness formulation using large deformation theory. Deterioration in material strength and stiffness at increasing temperature is represented by a set of nonlinear stress-strain-temperature relationships using a Ramberg-Osgood equation in which creep effects are implicitly included. The clearly nonlinear form of steel material properties at elevated temperatures is better represented as a set of continuous stress-strain relationship than in a bilinear form although provision is made for any form of relationship to be included. Structures subject to increasing loads or temperatures are analysed using an incremental Newton-Raphson iterative procedure. The analysis permits collapse load or critical temperature to be calculated at a specified temperature or load level respectively, and provides a complete load-deformation and temperature-deformation history for two-dimensional multistorey steel frames. A nonlinear method of frame analysis, based on large-deformation theory, has been used which includes the effect of geometric non-linearity, temperature-dependent nonlinear material behaviour and variation in temperature distribution both along and across the section. The effects of thermal strains, residual stresses and thermal bowing are also included and different values of the elastic stiffnesses of the support conditions can be considered. A beam element with two nodes and three degrees of freedom at each node is used in the analysis. Gradual penetration of yielding through the cross-section is accounted for using the transformed area approach. The validity of this method is tested by comparing with experimental and analytical data covering as wide a range of problem parameters as possible. The comparisons show good agreement

with this data.

The method has been used to study a number of aspects of frame behaviour in fire. The influence of slenderness ratio, stress-strain representation and material models, various forms of protection, magnitude of residual stress and thermal gradient along and across the section of a frame are investigated. An approximate curve based on statistical analysis of the derived results is suggested as a simple means of predicting the critical temperature or collapse load of a uniformly heated steel frame. Further examples are presented which illustrate the special form of moment redistribution that occurs at elevated temperatures for frames that contain partially heated elements.

Finally, general conclusions and recommendations for future work are presented.

## NOTATIONS

$b_r$	Thickness of a plate region
$b_{rt}$	Transformed thickness of a plate region
$e$	Eccentricity
$k$	End elastic stiffness
$l_r$	Plate region length
$n, m, m^*$	Stress resultants
$\{q\}$	Element displacement vector
$r$	Plate region
$t$	Time
$t_k$	Plate segment thickness
$u_o, v_o$	Displacement functions for a beam element
$A$	Area
$A^t$	Transformed area
$E_{20}$	Young's modulus
$E_\theta$	Effective modulus of elasticity at temperature $\theta$
$E_t$	Tangent modulus at ambient temperature
$E_t(\theta)$	Tangent modulus at temperature $\theta$
$F$	Applied load
$F_u$	Failure load

$F_{u,20}$	Failure load at ambient temperature
$F_{u,\theta}$	Failure load at ambient temperature
$[K_T]$	Element tangential stiffness matrix
$L/r$	Column slenderness ratio
$\{Q\}$	External load vector
$W_0$	Initial-out-of-straightness
$\{\Delta R\}$	Assembled unbalanced load vector
$\alpha$	Coefficient of thermal expansion
$\theta$	Temperature variable
$\theta_{cr}$	Critical temperature
$\bar{\lambda}$	Frame slenderness ratio
$\epsilon$	Effective strain
$\epsilon_e$	Elastic strain
$\epsilon_r$	Residual strain
$\epsilon_{th}$	Thermal strain
$\epsilon_z$	Axial strain
$\epsilon_{zt}$	Total Axial strain
$\sigma$	Effective stress
$\sigma_{cr}$	Critical stress
$\sigma_{y,20}$	Ambient temperature yield stress

$\sigma_{y,\theta}$

Effective yield stress at temperature  $\theta$

# Chapter 1

## Introduction

The occurrence of a fire in a steel structure would, if the structure were not at least partly shielded from the heating effect, lead to a significant deterioration in material strength and stiffness and consequently cause large losses both in lives and property. This is because the physical properties of steel are temperature-dependent. However, recent appraisals of the cost of steel construction carried out in the UK in 1982 [74] showed that fire protection of a steel structure accounts for around 30% of the total cost of the structure.

For much of this century, steel has been the favoured material for building frames. While most development in improving its cost-effectiveness has been achieved in reducing the steel weight and erection cost, a comparable improvement has yet to be achieved by reducing fire protection cost. This requires better understanding of the behaviour of steel structures at elevated temperatures. Hence the need for a reliable fire engineering system to quantify both real fire conditions and the structural response of structures under such conditions.



## 1.1 Fire development and growth

In general, fire starts because a combustible material is ignited by a heat source. Depending upon the circumstances in the enclosure, the accumulation of heat may ignite other existing combustible materials and the fire will spread rapidly. When all combustible materials are ignited, the fire becomes fully developed before it starts to decay when these materials are burnt to ash.

The temperature history during fire is illustrated in Fig.1.1 [58]. Phase  $A-B$  represents the growth period when the temperature in the room is relatively low though close to that of the burning materials. In this period, the chance of escape is relatively high and, if the fire is put down, the damage inflicted on the structure is relatively low. The rising temperature in the room ignites other combustible materials before flashover occurs at  $B$  when all combustible materials are burning actively. At this stage the burning period starts and the temperature starts to rise sharply. During this period the fire is fully developed and the temperature in the enclosure continues to increase, though at a decreasing rate, until conduction of the heat between the heat sources and the surroundings becomes small. At  $C$ , the burning period ends and the temperature starts to fall sharply, signalling the decay period. The temperature is still high enough at the beginning of this period that fire can spread to the surroundings through propagation or radiation if partitions collapse.

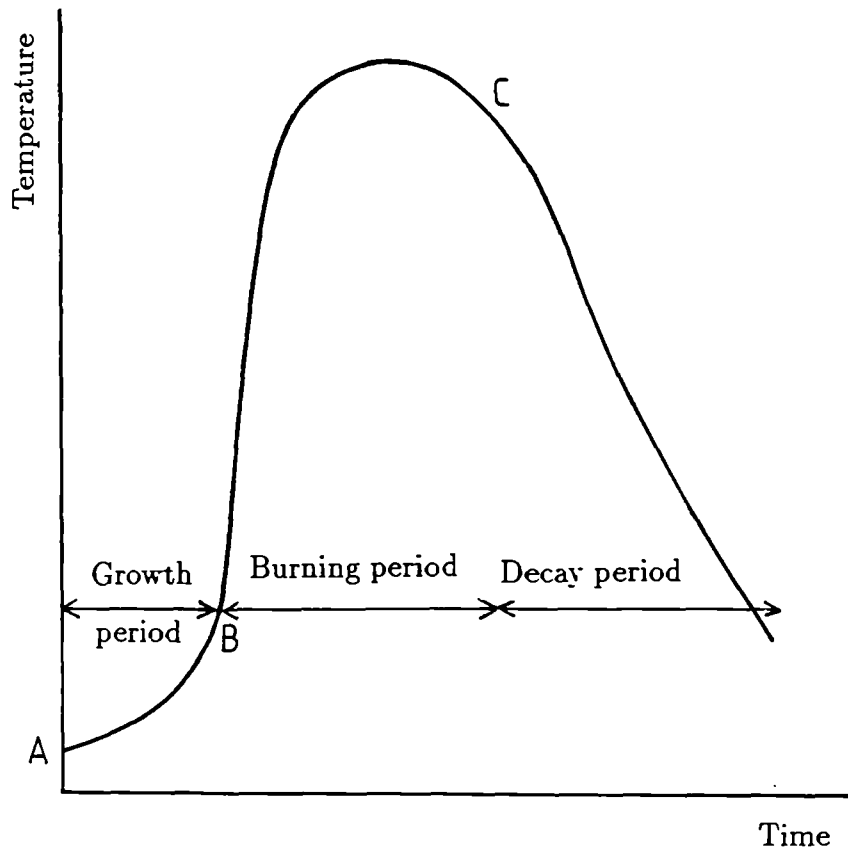


Fig. 1.1 - Three periods of fire development [58].

## 1.2 Standard fire exposure

The time-temperature relationships adopted by different countries have similar shapes due apparently to these curves being based on the same data taken from actual fires. The standard ISO gas temperature-time relationship assumes that the growth of a fire follows a single curve (Fig.1.2) which has the following relationship :

$$\theta - \theta_0 = 345 \log_{10}(8t + 1) \quad (1.1)$$

where :

$t$  = time in minutes,

$\theta$  = furnace temperature in  $^{\circ}C$  at time  $t$ ,

$\theta_0$  = initial furnace temperature in  $^{\circ}C$  at time  $t_0$ .

The ISO standard time-temperature relationship [42] was drawn following the fire load concept proposed by Ingberg (1928). The fire load is defined as the weight of wood with heat content equivalent to that of combustible material per unit floor area of a building or a fire compartment. The fire load concept is based on the following two assumptions :

1. The fire resistance depends only on the fire severity. The fire severity can be represented by the area under the temperature-time curve beyond a certain temperature level,  $572^{\circ}C$  according to Ingberg.
2. Fire severity depends only on the fire load density.

It is clear that the assumption that real fires follow the ISO standard curve is somewhat oversimplified since both of the above assumptions are untenable [87]. Structural materials respond differently to a short intensive fire and a long but

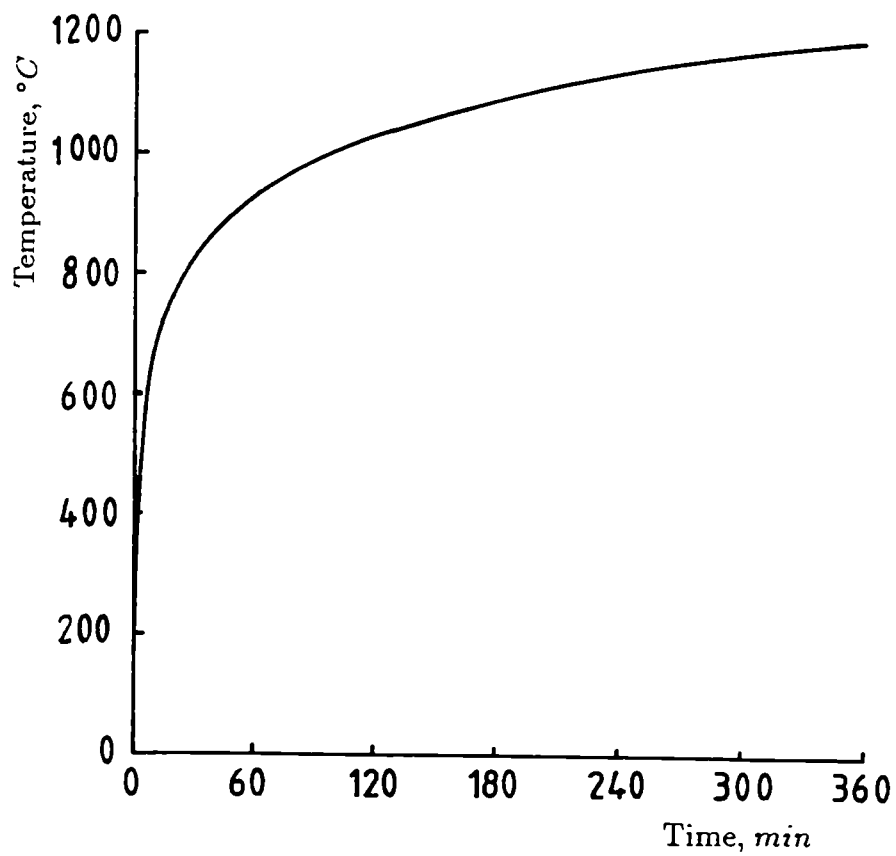


Fig. 1.2 - ISO standard temperature-time relationship.

less intensive one, though both fires may have the same severity according to the first assumption. In addition, fire severity does not only depend on the fire load but also on a number of other factors such as ventilation, rate of burning, mass of noncombustible materials and thermal properties of walls, floors and ceiling of the compartment [87].

The main distinction between a real fire (Fig.1.1) and the standard time-temperature relationship (Fig.1.2) is the absence of a full growth period in the standard curve. This is of major importance during a fire since most damage is inflicted on the structure during this phase. None the less, it is widely accepted that the standard curve forms a useful basis for fire resistance comparison between different structural elements, or as a means of appraising the relative performance of structures and materials for regulation purposes.

### 1.3 Fire safety measures

Fire protection cannot ensure complete fire safety. In addition, measures ought to be taken to ensure that the chance of a fire occurring is minimal or to mitigate the consequences of a fire should it occur. Such measures include some permanent features such as structural fire protection, escape routes, fire brigade access routes and control of combustible materials. Other measures which will be activated in the event of a fire include early detection and alarm systems, sprinklers and smoke control, all of which can be operated automatically. Above all, a structure should have enough inherent fire resistance to prevent collapse while evacuation takes place and rescue services can arrive.

## 1.4 Fire engineering approaches

Approaching the problem of the behaviour of a structure under fire conditions is primarily an analytical one and can be treated in one or both of the following categories :

1. The evolution of heat due to a fire and prediction of the temperature history within the structure.
2. The structural performance of a steel structure under a specified temperature distribution.

The first approach has been studied in detail over the last two decades. Temperature rise was assumed to follow that obtained from burning wooden cribs and the effects of factors such as fire load density, size and shape of windows, size and shape of compartments and thermal properties of the surrounding materials were considered. Theoretical models have been developed in order to predict time-temperature relationships and temperature distribution within the structural elements. These models resemble the natural fire curve and were based on the balance between the heat produced by the fire and that lost to the surroundings [56]. This is investigated in more detail in section 2.1.

In the second approach, prediction of the deformation history as well as the collapse load and critical temperature would normally be attempted. Several analytical studies have been carried out in which temperature distribution is given as an input, and stresses and deformations are the only output. This is reviewed in more detail in section 2.3. This research project deals with the fire problem from the second point of view.

Recently, BS5950 Pt.8 (1990) has adopted a more analytical approach to assess the fire resistance of steel elements based upon quantitative methods. Using these methods, the limiting temperatures of beams, columns and tension members can be determined. These methods will be reviewed in section 2.3.3.

## 1.5 Objectives and scope of the research

This research project aims to develop a practical tool for the structural analysis of steel frames under fire conditions using the finite element method. The analysis is based on the tangent stiffness formulation. A beam element with two nodes and three degrees of freedom at each node is used in the analysis. Deterioration in material strength and stiffness at increasing temperatures is represented by a set of nonlinear stress-strain-temperature relationships using a Ramberg-Osgood equation in which creep effects are implicitly included. Structures subject to increasing loads or temperatures are analysed using an incremental Newton-Raphson iterative procedure. The analysis permits the deformation history and either the collapse load or critical temperature to be calculated at specified temperature or load levels respectively. It includes the effects of geometric non-linearity, temperature-dependent nonlinear material behaviour and variations in temperature distribution both along and across the section. The effects of thermal strains, residual stresses and thermal bowing are also included, and different material models and constitutive relationships can be used.

In Chapter 2 a detailed review of previous experimental and analytical investigations of the behaviour of steel members in fire is presented. Chapter 3 outlines the effect of testing procedures on the material data for the properties of steel at elevated temperatures. It also summarizes some of the reported data

and compares the adopted material model with those of CTICM and ECCS.

In Chapter 4 a formulation for the nonlinear analysis of steel frames under fire conditions using the finite element method is presented. The validity of this approach is checked in Chapter 5 against experimental and analytical data covering as wide a range of problem parameters as possible. An extensive parametric study is carried out in Chapter 6 in order to investigate the effects of some parameters which are known to affect the behaviour of *fire-exposed steel frames*. These include : slenderness ratio, stress-strain representation and material models, various forms of protection, the magnitude of residual strains and thermal gradient along and across the section. An approximate curve based on statistical analysis of the derived results is suggested as a simple means of predicting the critical temperature or collapse load of a uniformly heated steel frame from a knowledge of the behaviour of the same frame at room temperature. Further examples are presented which illustrate the special form of moment redistribution that occurs at elevated temperatures for frames which contain particular heated elements.

In Chapter 7 the stability and strength of sway frames in fire is investigated. The stabilising influence of the cooler part of the frame and the effects of localised heating on the overall behaviour of sway frames is studied. The effects of deterioration of the stiffness of the beam forming the roof of a fire compartment on the column strength is also investigated together with the effects of additional forces produced in the structure due to restraint of the heated elements from expansion by adjacent cooler members.

Finally, in Chapter 8 general conclusions are drawn and suggestions for future work are presented.



# Chapter 2

## Literature Review

### 2.1 Introduction

Current building regulations dealing with structural fire design specify minimum periods of fire resistance for load bearing elements, which depend upon the size and function of the buildings, for which these elements do not violate certain performance criteria when heated in a furnace. In the UK, guidance on the required periods for fire resistance of structural elements (including walls, floors and columns) is given by a document entitled 'Fire Grading Report' [63] in a tabular format, and may vary from 30 minutes to 4 hours. In most countries, classification of these structural elements in terms of the length of time they can resist collapse is based on a standard time - temperature function for the fire to which the structure is exposed. The standard test is therefore a means by which the performance of one element can be compared with that of another under standardised heating conditions; it does not necessarily measure the performance of an element under actual loading and heating conditions.

Whilst the principle of these regulations has remained unaltered since their publication in 1946, considerable progress has been made towards better understanding of real fires in buildings and interpretation of standard fire test results. Advances have also been made in understanding the structural response of the heated elements and the development of new design methods to improve the load bearing capacity, integrity and insulation of the construction materials under fire conditions (Kirby (1986)).

The good fund of knowledge of all aspects of the problem now makes it possible to assess and thus to design for the fire resistance of structures using an alternative fire engineering approach in order to overcome the inflexibility of the existing legislations. At present, there is a clear tendency in many countries towards the development of regulations containing more functionally based requirements and performance criteria [85]. The European Convention for Constructional Steelwork (ECCS) Technical Committee 3 has published its European Recommendations which have already been implemented in the national regulations and design guidance of Switzerland, Germany and Sweden [57]. In the UK, BS5950 : The Structural Use of Steelwork in Buildings; Part8 : Code of Practice for Fire Resistance Design will be published in 1990. Parallel activities have been carried out in France by The Conseil International du Batiment (CIB) which led to a Design Guide based on research carried out in Sweden (Lawson (1987)).

The subject of fire engineering has been developed in many countries with a view to providing more flexibility to designers based upon quantitative methods [84]. This primarily analytical approach can be sub-divided into three main areas as follows [47].

### 2.1.1 Temperature growth in a compartment

As previously outlined, a real fire has significantly different characteristics from the curve offered by the standard time-temperature relationship. It has been recognised that factors such as fire load, the size and shape of the compartment and the thermal properties of the surrounding surfaces influence the atmospheric time-temperature relationship [47]. Research work has been carried out in order to relate these factors to the time-temperature relationship by means of a mathematical model based on the concept of balance between the heat produced and that removed in a compartment fire. Usually, part of the heat produced by combustion of the compartment content (i.e fire load) is absorbed by the surrounding structure as well as by the gases in the enclosure. Heat losses result from radiation from the windows, outflow of hot gases, outflow of unburned gases which burn outside the compartment, and outflow of suspended, unburned particles [60]. The temperature rise can therefore be calculated knowing the heat produced and that lost at all times. Some of the factors that determine heat production and losses such as material properties, compartment and opening dimensions, emissivity of flames and exposed materials, can be determined with reasonable accuracy. Others, such as the heat loss due to gases that burn outside the compartment, emission of unburned particles through windows and temperature differences in the compartment can only approximately be considered. Several other parameters which may affect the temperature rise, such as wind velocity, the amount, surface area and arrangement of the combustible contents, and outside temperature at the time of the fire cannot be predicted at all. However, based on this concept, studies have been carried out in Sweden to produce a comprehensive set of gas temperature-time relationships for a number of typical and representative fire compartments [85]. These curves have been presented as a function of the

fire load, ventilation conditions and thermal properties of the surrounding surfaces. A probabilistic approach has been used by other researchers to derive fire temperature-time curves that are unlikely to be exceeded in the event of fire [60].

#### 2.1.1.1 Determination of the fire load

The fire load may be defined as the amount of combustible material per unit of the internal bounding surfaces of the fire compartment. The combustible material can be part of the structure (static) or its contents (mobile). The fire load is normally expressed as the fire load density  $q$ , which can be defined as the equivalent amount in wood in  $kg/m^2$  of floor area which has the same heating content or calorific value of combustible material per unit area of bounding surfaces as :

$$q = \frac{\sum mH}{A_t} \quad (MJ/m^2) \quad (2.1)$$

where :

$m$  = mass of item (kg),

$H$  = calorific content (MJ/kg),

$A_t$  = total area of bounding surfaces (i.e walls, floor and ceiling) ( $m^2$ ).

The heat contents of various materials is well established and therefore  $q$  can be determined with good accuracy.

However, in the event of fire, a safe fire engineering calculation is based on 100% burn-out although such a complete burn-out does not necessarily occur due to the intervention of the fire fighting services.

### 2.1.1.2 The ventilation factor

The ventilation factor  $F$  is related to the dimensions of the window opening and is generally expressed as :

$$F = \frac{A\sqrt{h}}{A_t} \quad (2.2)$$

where :

$A$  = area of openings in the compartment ( $m^2$ ),

$h$  = height of opening ( $m$ ),

$A_t$  = area of bounding surfaces ( $m^2$ ).

For the same available fire load, a large ventilation factor results in a fire with relatively high temperatures but short duration; a small ventilation factor produces a fire with relatively low temperatures and longer duration. Thus, the ventilation factor influences the intensity and duration of a fire whilst the fire load affects only its duration in that the higher the fire load, the longer the time that elapses before the fire starts to decay [60].

The size and shape of a compartment also influences the burning rate and consequently the atmosphere temperature during the fire. This is implicitly taken into account when calculating the fire load and ventilation factor through the area of bounding surfaces  $A_t$ . In general, for the same floor coverage, a tall room will have a greater volume of air and a larger wall area over which heat can be lost.

### 2.1.1.3 Thermal properties of the bounding materials

The type of construction material influences the atmosphere heating rate. For example, the better the insulating quality of the walls, the higher the temperature in the room becomes. It should, however, be noted that the influence of the

bounding materials is relatively small compared with that of the fire load and the ventilation factor. The temperature - time curves obtained using the above technique resemble the behaviour of a natural fire where the three periods of growth, full development and decay are simulated.

It is also worth noting that the accumulated data on the behaviour of structural steel elements subjected to the standard fire tests can be related to compartment fires using methods such as equivalent fire severity [47].

## **2.1.2 Prediction of temperatures of structural steel elements**

Temperature rise in structural elements that are exposed to fire can be determined both experimentally and numerically. At present, both protected and unprotected steel members can be considered. Several factors are known to affect the heating rate and maximum temperature of the elements. The most important are: the location of the steelwork relative to the fire source and, the steel sectional size and shape [47].

### **2.1.2.1 Effect of the location of the steelwork**

The amount of heat transferred by radiation and convection to a structural member is affected by its location relative to the heat source. This will result in differential heating rates and differential temperatures within the heated element. A typical situation is that of a steel beam supporting a concrete slab, where the flame reaches and travels along the underside of the soffit while the slab acts as a heat sink, thus reducing the heating rate of the beam. Also, internal columns

which are totally exposed to fire will heat at a higher rate than edge columns encased in walls.

#### 2.1.2.2 Effect of steel size and shape

It is logical to expect that a steel member which has a smaller flange thickness will heat at a faster rate and thus reach a higher temperature than another which has a larger flange thickness for the same exposure duration. Also, the thickness of the insulating materials keeps down the heating rate since the protection time offered by the insulation material increases with its thickness. Hence, the time for which a steel member is exposed to fire is of special importance in determining the temperature distribution. This is due to the fact that, although steel is a relatively good conductor of heat, it still requires some time before the temperature reaches the atmospheric level. For example, the thermal gradient between the hotter and cold flanges of a section becomes less if it is exposed to the same heating condition but for a longer duration.

To express the effect of steel size and shape on heating rate, reference is often made to the concept of  $H_p/A$ , where  $H_p$  is the perimeter in metres of the section directly exposed to the fire, and  $A$  is the cross-sectional area in square metres of the entire steel member.

A considerable amount of analytical work has been carried out in order to determine the thermal response of the structural steel [47][10][85] and thus a considerable amount of data are available. However, more sophisticated thermal analysis based on the finite element method is also available [89][12].

### 2.1.3 Assessment of the structural response

This area aims at predicting the full deformation behaviour and stress distribution for a structure under fire conditions. This can be achieved using tests carried out on loaded structures or analyses based upon structural models.

Experimentally, a large number of fire tests have been carried out on structural elements. Only a few tests have investigated the potentially beneficial interaction of these elements in a framed structure. Most of the full scale tests on individual elements have followed the standard fire testing procedure with few tests ever being carried out on real structures exposed to natural fires [47]. Some of the previous experimental work will be reviewed in section 2.2.

Computer-based analyses of steel structures have been widely used in design and are gradually being extended to fire design. Such analyses, using the finite element technique for example, are based upon theoretical assumptions validated through experimental tests. A number of such programs already exist and will be reviewed in section 2.3. On the other hand, several attempts have been made to provide more simplified but practical approaches for the fire problem. These will also be reviewed in section 2.3.

A versatile fire engineering system which incorporates all aspects of the problem has not been possible up to now. None the less, computer programs which deal with the three aspects of fire engineering already exist [81]. It can be seen that it is possible to deal with the structural aspect of the problem separately providing temperature distributions are given as input. This has been considered by several authors and it is the subject of this research project.



## 2.2 Review of previous experimental work

Experimental investigation into the behaviour of structural elements in fire dates back to 1885 when Bauschinger appears to have been the first to conduct experimental studies on columns. Tests were carried out on columns placed and loaded horizontally, heated then sprinkled with water. Temperatures were determined by means of various metals having different melting points. *The results showed* that cast iron is a more fire resistant material than both wrought iron and mild steel.

During the last hundred years a large number of tests have been carried out on beams and columns. The various experimental programs carried out in Germany, England and the United States during 1920 - 1957 are reviewed by Boue (1959) [1].

During the last two decades a considerable amount of experimental work has been carried out in many countries on structural elements, mostly subjected to the standard fire heating. Knublauch *et al.* (1974) carried out a series of tests on 23 columns having different types of cross-sections and insulated with box-shaped vermiculite insulating plates. Heating was applied to 80% of the column lengths. Loading was axially applied and kept constant while heating progressed. Thermal expansion was not restrained. He concluded that 95% of the tested columns attained critical temperatures of  $500^{\circ}\text{C}$  or more when subjected to a design load according to DIN 4114. A considerable increase in these temperatures was obtained by Kerstma *et al.* (1979) who carried out calculations of those columns with an assumed elastic restraint at the column base instead of hinges.

At the University of Ghent, Vandamme and Janss (1981) and Janss and

Minne (1981/1982) tested a total of 25 insulated and 2 uninsulated columns. The applied load was kept constant and there was no restriction on axial restraint as temperature increased. Rotational restraint was imposed on the column ends with the aid of a special device. Their analytical model, based on the ECCS buckling curve *c* and a modification factor proposed by Pettersson and Witteveen (1979/1980), accurately predicted the measured critical temperatures. This approach has been adopted by the ECCS-T3 (1983).

At the University of Aalborg [37] a total of 24 hinged-end columns with different lengths were tested in a horizontal position in a special furnace in order to ensure in-plane buckling. From these columns 18 were tested at prescribed temperature levels with a constant rate of loading whilst the remaining columns were subjected to a constant axial load as heating progressed. In no case was there any axial restraint.

In France, at the University of Rennes, Aribert and Randriantsara (1980) and (1983) tested a total of 33 unprotected pinned steel columns. The tested columns had the same cross-sections and lengths, and were vertically placed in a furnace with the entire length, including the end bearings, being heated. The testing program consisted of loading at a prescribed temperature level with and without end moment at the top, or heating at constant axial load with and without axial restraint. The main aim of the tests was to demonstrate that creep effects become significant at temperatures above  $450^{\circ}C$ .

A comprehensive set of column tests was carried out at the Technical University of Brunswick [38]. A total of 75 columns was tested with the following varying parameters : column slenderness, load level, eccentricity of loading, axis of buckling, hinged or clamped end conditions, thermal gradient along the columns

due to partial protection, types of steel sections, rate of heating and full axial restraint. Tests on simple frames have also been carried out.

Aassen (1985) has carried out 20 tests on steel columns under the following varying parameters : slenderness ratio, load level, rotational and axial restraint, load eccentricity and rate of heating and temperature gradient. The load was applied in increments at ambient temperature to a prescribed level and kept constant while electric heating progressed.

An equally large number of beam tests have also been carried out. Witteveen *et al.* (1976) have carried out tests on small scale model beams with rectangular cross-section. The beams, having a span of 400 *mm*, were loaded with a constant two-point load and subjected to uniform heating. Linear heating rates of  $50^{\circ}\text{C}/\text{min}$ ,  $10^{\circ}\text{C}/\text{min}$  and  $5^{\circ}\text{C}/\text{min}$  were chosen in order to study the effect of rate of heating. Results have shown that for practical heating rates (i.e. between 5 and  $50^{\circ}\text{C}/\text{min}$  and temperatures not exceeding  $600^{\circ}\text{C}$ ) the influence of the heating rate is quite modest.

Kruppa (1979) has reported the results of 10 tests carried out in France on simply supported steel beams. Four European section sizes ranging in depth from 140 to 280*mm* were used. Seven of these beams were box- protected while the remaining three were either unprotected or contour protected. The beams were subjected to loads ranging from 30% to 65% of their ambient temperature ultimate load. Rubert and Schaumann (1986) have carried out tests on 17 simply supported medium scale beams made of standard rolled sections. These tests were carried out in order to derive temperature-stress-strain relationships. The beams, subject to a constant single load at mid-span, were heated uniformly along their entire length. A uniform temperature distribution was possible to <sup>be</sup> achieved with

the aid of an electronic temperature control system. The beams, having a span of  $1140\text{mm}$ , were subjected to load ratios of between 0.05 and 0.85 of their ambient temperature ultimate load capacity. Fully analytical stress-strain-temperature relationships were then derived.

Quite recently, a major testing program was carried out by British Steel Swinden Laboratories as a part of a joint program with BRE Fire Research Station. Robinson (1989) reported tests undertaken at the Warrington Research Centre on unprotected and partially exposed beams subjected to the standard fire heating in a gas fired furnace. A total of 23 tests was carried out on unprotected simply supported steel beams covering a wide range of section sizes and load ratios with the beams having a span of  $4500\text{mm}$ , out of which at least  $4000\text{mm}$  was completely submerged in flames. Results of the tests have shown that the limiting temperatures given by BS5950 Pt.8 are conservative since they relate to a beam depth of  $225\text{mm}$ . It was also concluded that since this depth is generally lower than that of a practical beam, deeper beams will exhibit higher limiting temperatures. On the other hand, the effect of temperature gradients on beam behaviour has also been investigated. Eight simply supported shelf angle steel beams were partially exposed to fire and tested under a wide range of load ratios and floor depths so that the maximum temperature difference between the lower and upper flanges was typically between  $600$  and  $800^{\circ}\text{C}$ . The beam span was  $4500\text{mm}$ . Results have shown that significant increase in limiting temperatures and endurance time occur in cases where large thermal gradient across the section exists.

Few experimental results have been reported regarding the potentially beneficial interaction between beams and columns in fire. Most of the frames tested have been model frames due to lack of suitable furnaces for full-scale frame tests.

Witteveen *et al.* (1977) tested 4 braced and 11 unbraced small-scale simple model steel frames. The frames, having rectangular column and beam cross-sections, have a column height of  $100mm$  and beam span of  $400mm$ . The frames were loaded with concentrated loads corresponding to the range 0.2 - 0.6 of the ambient temperature ultimate load. Results of the tests showed that unbraced frames exhibited lower critical temperatures than those of braced frames due to the additional sway effect.

In Japan, an experimental testing program has been carried out on medium scale steel frames in order to study the effects of thermal stress distribution at elevated temperatures. Koike *et al.* (1982) tested 22 two-storey two-bay frames with only one or two girders heated. Typical beam spans were  $2000mm$  and typical column heights  $1500mm$ . The members were heated at a constant rate in an electric furnace up to temperature levels not high enough to cause any significant loss of strength. Ooyanagi *et al.* (1983) applied a similar heating arrangement to test 16 three-dimensional two-storey two-bay medium scale model frames. Results of both analyses have shown that large thermal stresses appeared in the frames not only in the fire-exposed members but also in other structural members. These stresses are due to the fact that thermal expansions of heated members are partially restrained by other structural members. It has also been shown that the principle of superposition with regard to axial thermal strain is approximately valid.

A series of 20 medium-scale frame tests have been reported by Rubert and Schaumann (1985b). Typical spans  $l$  were  $1200mm$  with typical column heights  $h$  of  $1170mm$ . Frame slenderness ratio, defined as the square root of the simple plastic collapse load divided by the elastic critical load, varied between 0.33 and 1.00. The applied load was varied between 38% and 79% of the ambient temper-

ature ultimate load. All frames were uniformly heated at a constant rate using electrical elements, except that the beams in two frames were kept at ambient temperature and 3 frames had one beam and one column insulated. Results of the tests have shown that collapse temperatures can be determined as a function of load factor and system slenderness ratio.

Results from a natural fire test on a full-size steel frame have recently been reported by Cooke and Latham (1987). The frame, fully loaded, had a beam span of  $4500\text{mm}$  and column height of approximately  $3500\text{mm}$ . A fire compartment was built for this purpose in the FRS facility at Cardington with heating obtained from burning wooden cribs. The frame had pinned feet with the webs of the columns infilled with block-work; precast concrete slabs were placed on the top flange of the beam. The columns were loaded with an externally applied load of  $552\text{ kN}$  and the beam was loaded at four positions along the span each with a load of  $39.6\text{ kN}$ . Results have shown better performance than that of individual elements due to the beneficial effects of beam-to-column interaction and to the effect of blocking-in the webs of the columns.

### 2.2.1 Creep buckling tests

Creep, defined as a time-dependent increase in strain without corresponding increase in stress, has been shown to have a considerable effect on steel behaviour beyond a certain temperature level, approximately  $450^{\circ}\text{C}$ . Several methods have been suggested to account for this effect. The effect of creep on the buckling strength of steel columns has been investigated by many researchers. Eggwertz (1976) carried out a creep-buckling analyses for a steel column with a slenderness ratio of 45 subjected to a certain temperature - time history. The analysis was

based on Norton's creep law modified to conform with Dorn-Harmathy theory [35]. Thus only secondary creep was considered. The analysis shows that creep has a detrimental effect on column strength at high temperatures. Aribert and Randriantsara (1980) have conducted creep buckling tests on 33 HEA100 pin-ended uninsulated columns. The test specimen was about 2000 *mm* long with a slenderness ratio of 80, with bending occurring about its minor axis. Loading was applied at prescribed temperature levels with and without axial restraint. It was shown that creep effects on the column strength become more noticeable at temperatures in excess of 545°C. This effect varies with the column slenderness ratio and the amount of load applied. For example, with very low load level and temperatures in excess of 600°C, the reduction in the column bearing capacity due to the creep effects is about 9% for a column with a slenderness ratio of 80. They also derived an interaction formula on the basis of a similar creep model proposed by Eggwertz (1976). The equilibrium condition is established only at the mid-height of a column assuming the deformed shape as a half-sine curve. Furthermore, Fujimoto *et al.* (1982) investigated the effect of creep on buckling strength by testing fixed-ended H-section columns having a slenderness ratio of 25.1. The column specimens were subjected to various constant loads with varying eccentricities at temperature levels ranging from 475 to 550°C. It was shown that the eccentricity of loading, as well as the actual load and temperature levels, affect the creep-buckling behaviour of columns. The results were numerically verified but there was about 50% underestimation of the bearing capacity theoretically. None the less, both theory and experiment exhibit similar modes of creep-buckling behaviour. The theoretical model was later amended by using a modified tangent modulus-temperature relationship and a creep model that resulted in more consistency between theory and the experiments carried out by Fujimoto *et al.* (1983) on another set of H-columns with slenderness ratio of 46.9.

However, the adoption of a time-independent approach has been justified by Witteveen and Twilt (1972) and by Witteveen *et al.* (1976). From experimental investigations carried out on model structural steel elements, it was established that the collapse temperature is time-independent and consequently is not influenced by the heating history. Results for a column with a slenderness ratio of 45 calculated at  $600^{\circ}\text{C}$  coincided with the buckling analysis result of Eggwertz (1976).

## 2.3 Review of previous theoretical work

### 2.3.1 Analytical investigations

Attempts towards the development of an adequate yet simplified and practical fire engineering system have been made by many researchers. Culver (1972) investigated the effect of non-uniform heating along the length of a column on its performance. A finite difference scheme was employed along with a tangent modulus approach for determining the buckling loads of an axially loaded column at room temperature. The effect of temperature on the column strength was considered through its effect on the material elastic modulus and yield strength. It was found that the pin-ended column, in which the maximum temperature occurred at the mid-height, exhibited the largest decrease in buckling strength. It was also shown that for other boundary conditions, the case in which the maximum temperature is closest to the strongest boundary usually results in the largest decrease in strength. Culver *et al.* (1973) have studied the buckling behaviour of pin-ended steel columns subjected to a uniform heating. Various buckling curves have been derived for different cross-sections and residual stress patterns.



It was concluded that residual stresses have the same effect on column buckling at elevated temperatures as at room temperature. Furthermore, Ossenbruggen *et al.* (1973) have studied the effect of thermal gradient across the section using a moment-load-curvature-temperature approach. This included both thermal and residual stresses. Thermal bowing was approximated by a certain amount of initial imperfection. It was concluded that thermal gradient is detrimental to the performance of axially loaded columns.

A similar attempt to provide column design curves at elevated temperatures has been carried out in Sweden by Magnusson *et al.* (1976). Curves were derived from the following buckling equations :

$$\frac{\sigma_{cr,\theta}}{\sigma_{y,\theta}} = \beta - \sqrt{\beta^2 - \frac{1}{\bar{\lambda}^2}} \quad (2.3)$$

in which :

$$\beta = \frac{1 + \lambda^2 \times 4.8 \times 10^{-5} + \bar{\lambda}^2}{2\bar{\lambda}^2} \quad (2.4)$$

and

$$\bar{\lambda} = \frac{\lambda}{\pi} \sqrt{\frac{\sigma_{y,20}}{E_{20}}} \quad (2.5)$$

where

$$\lambda = \frac{L}{r} \quad (2.6)$$

Vandamme and Janss (1981) proposed similar curves based on the ambient temperature design curve but allowing for the influence of elevated temperatures on the yield stress and modulus of elasticity. The European design curve at room temperature may be expressed by eq.2.3 provided that

$$\beta = \frac{1 + \alpha(\bar{\lambda} - 0.2) + \bar{\lambda}^2}{2\bar{\lambda}^2} \quad (2.7)$$

where  $\alpha$  is the imperfection parameter ranging from 0.206 to 0.489 for buckling curves *a* to *c*.

The Swedish buckling curves are related to the conventional proportionality slenderness ratio  $\lambda_0$ , while the ECCS curves are related to the relative slenderness ratio  $\bar{\lambda}$ .

The ECCS buckling curves at elevated temperatures [29] are derived from eqs.2.3 and 2.7 based on the room temperature curve  $c$  but allowing the effect of temperature on the yield strength to be considered using the ECCS material characteristics (eqs.3.3 and 3.7). Comparison between expressions 2.4 and 2.7 shows that, at room temperature, agreement between the two formulae is good assuming curve  $c$  and  $\sigma_{y,20} = 235 \text{ N/mm}^2$  but large discrepancies exist with increasing yield stress. A remarkable deviation between these two design approaches exists at elevated temperatures, due to the fact that the modulus of elasticity is replaced by the secant modulus and the 0.2% proof stress by the 0.5% proof stress in the Swedish buckling equations. Furthermore, Proe *et al.* (1986a) have investigated the validity of the ECCS and CTICM expressions for the reduction of yield strength and modulus of elasticity on the prediction of column strength. It was concluded that estimations of buckling stress based on the ECCS material characteristics are considerably more conservative than those predicted on the basis of the CTICM expressions.

The poor repeatability and reproducibility of the test results have made discrepancies between experimental and calculated results inevitable. This is thought to be mainly due to the difference between the nominal and actual values of the mechanical properties at elevated temperatures, to imperfections, to non-uniform temperature distribution along and across heated members and, to end restraint. To overcome these discrepancies, Pettersson and Witteveen (1979/1980) have developed a simple approach given by :

$$P_u = f \times P_{cr,\theta} \quad (2.8)$$

where  $P_{cr,\theta}$  is the theoretical buckling load at elevated temperature for a uniform temperature distribution and  $P_u$  is the failure test result. The magnification factor  $f$  has been defined in Ref.[69] for columns and simple and continuous beams, whilst the ECCS (1983) recommendations have adopted the value of  $f = 1.18$ . On the other hand, Vandamme and Janss (1981) and Janss and Minne (1981/1982) have shown that the consistency between analytically and experimentally determined fire resistance can be improved by using the actual yield stress instead of nominal values in the analytical calculations. However, Setti (1983) has carried out numerical simulation of the column tests conducted by the Universities of Aalborg and Rennes and has concluded that a more favourable buckling curve than curve  $c$  of ECCS can be obtained, provided that representative estimates of the structural and geometrical imperfections are considered.

### 2.3.2 Numerical analyses

Analysis of frame structures under fire conditions generally considers the structure as being subjected to a constant load but at increasing temperatures. For a certain fixed temperature pattern, analytical procedures can be applied as in the usual ambient temperature environment. If a new temperature pattern is to be introduced within the structure, a similar analysis can be carried out with the current solution being modified to accommodate the effects of the newly-introduced temperatures. Thus the analysis becomes a repeated procedure, usually nonlinear, but essentially similar to those commonly used at ambient temperature. The effect of time-dependent creep may be considered explicitly as indicated before, or implicitly in the stress-strain curve, as will be discussed in Chapter 3.

The stiffness matrix method is now well established for structural analy-

sis of problems where deformation solutions are required. Joint displacements, and hence internal forces, are obtained by solution of the system of equilibrium equations. Although this method has been developed for the analysis of linear systems where the principle of superposition is valid, special techniques can be used for problems where geometric and material nonlinearities are considered. Such techniques consist of iterative methods to overcome the nonlinearities. This means that the external loads are applied in small increments assuming that the structure behaves linearly at each load increment. Thus the nonlinear analysis is replaced by the superposition of the analyses of a series of linear structures, each of which is subjected to an increment of the applied load. This solution technique is particularly suitable for problems where a complete load-deformation history is required.

The incremental analysis approach assumes that deformations due to a new load increment progress in the direction of the tangent to the actual load-deformation curve. A tangent stiffness matrix is therefore produced according to the current geometry of the structural member. In many cases, this causes an underestimation of the actual displacements, and may lead to a large cumulative error depending upon the degree of nonlinearity of the problem. To reduce this effect, a local iteration technique such as the Newton-Raphson procedure may be employed as well as reducing the load increment step. On the other hand, the secant stiffness approach assumes that the current geometry and member forces are known. The new values of the current geometry and member forces obtained after an iteration cycle are then used in the following cycle. This sequence is repeated until convergence is obtained. This is achieved when the difference of the member forces and deformed shape between two consecutive cycles of calculation is smaller than a prescribed tolerance limit.

A comparison between these two methods of analysis reveals that the tangent stiffness approach is more suitable for tracing the collapse load and producing the full load-deformation history of a structure. On the other hand, the tangent stiffness approach controls its error at local incremental level, and requires the use of small increments in order to obtain sufficiently accurate results. The secant stiffness approach is not sensitive to the loading history of the structure.

The concept of stiffness matrix analysis deals essentially with structures which can be discretised into a finite number of structural elements interconnected at a number of joints. However, the enormity of the potential number of elements in a continuous solid gives an indication of the difficulty of numerical approaches. None the less, the finite element method is now well established and has been shown to be an effective tool to deal with complicated problems. However it requires computers with considerable execution speed and data storage capacity.

The recent development of powerful digital computers makes the finite element method very suitable to handle complicated structural problems in which large deformations and large rotations occur. Recently, this method has been adopted by many researchers to *predict the behaviour of structures in fire*. Cheng and Mak (1975) and Cheng (1983) have developed a general theory and algorithm to investigate the thermo-creep deformation and buckling behaviour of steel structures at elevated temperatures. Furumura and Shinohara (1978) have applied an elasto-plastic-creep analysis including the influence of geometrical imperfections. Muzeau and Lemaire (1980) used a nonlinear elastic-plastic creep model to study the behaviour of steel structures. Creep was implicitly included in the stress-strain relationship. Jain and Rao (1983) developed a numerical technique to study the deformation history of steel frames in fire. The analysis includes a visco-plastic model, geometric nonlinear effects, the effect of creep and large de-

formations. Contro *et al.* (1987) used a nonlinear numerical analysis to predict the response of steel beams in fire. Aribert and Abdel-Aziz (1987) have developed a numerical method for the analysis of steel columns in fire. The analysis allows for partial restraint and bending moment at the ends of the column to be considered in order to simulate the effect of the rest of the structure. Kouhia *et al.* (1988) have used a nonlinear analysis to model multistorey buildings in fire. The analysis includes material nonlinearity and large deformations. Their finite element program is applicable to three-dimensional beams and frames.

As mentioned earlier, modelling the response of steel structures in fire can be subdivided into two phases. In the first phase, the temperature distribution along and across the structural members is determined, then the structural response of these members within the calculated thermal environment is assessed. It has been shown that several methods of analysis and computer programs already exist in the literature which deal with either thermal or structural response and, in some cases, with both phases of the analyses. Typical examples of such programs which will be reviewed in the following section are : FIRES-T3, TASEF-2, FASBUS and CEFICOSS. All these programs are based on the finite element method.

### Thermal programs

The problem of thermal analysis involves solution of the nonlinear heat flow equation. This nonlinearity is due to the temperature-dependence of the thermal properties of the structural materials as well as the heat transfer mechanism. Hence, numerical rather than analytical methods are usually employed to predict the thermal responses of structural elements subjected to a heating environment.

The program FIRES-T3 (FIre REsponse of Structures - Thermal) devel-

oped by Bresler *et al.* (1977) is based on the finite element method coupled with time-step integration to solve the nonlinear heat flow problem. An implicit backward-difference time integration is used to solve the nonlinear heat flow problem. Different types of structural materials can be considered, as well as composite structures. The program can also solve two-dimensional and three-dimensional heat flow problems.

The program TASEF-2 (Temperature Analysis of Structures Exposed to Fire - Two Dimensional Version) has been developed by Wickstrom (1979) for the thermal analysis of a variety of structures under fire conditions. The program uses the finite element method coupled with an explicit forward-difference time integration scheme to solve the nonlinear heat flow problem. The program takes into account the heat exchange caused by radiation and convection due to voids inside the structure.

#### Structural programs

FASBUS (Fire Analysis of Steel BUilding Systems) is a nonlinear finite element computer program developed by Bresler and Iding (1981) to enable the analysis under fire conditions to be made of floor systems in steel framed construction. It models both the support beams and the floor slab behaviour. The steel beams are modelled using a beam finite element with three degrees of freedom at each node while the concrete slab is modelled using a plate finite element with three nodes and five degrees of freedom per node. The program uses nonlinear stress-strain-temperature characteristics for steel and concrete and a bilinear stress-strain curve for the reinforcing steel. The material constitutive law of concrete is approximated by a piecewise linear curve expressed in terms of yield strength, initial elastic modulus, crushing strain and maximum tensile strain.

These parameters, as well as the coefficient of thermal expansion of concrete, are temperature dependent. The elements used in the structural idealisation are layered in order to take into account gradual yielding and cracking. Five temperature regions are assumed across the beam and slab cross-section. An extensive model is included in the program to deal with the creep effects. However, in the program the beam is assumed to be laterally restrained, and thus no loading may be applied transverse to the beam. In addition, forces applied to a slab element at a node are assumed to be distributed over the element; thus no local effects may be predicted. Furthermore, the program assumes that the column support system remains unaffected by fire, and thus provides constant end conditions which ignore any instability effects. Reported results of the analysis of a beam supporting a concrete slab using the thermal response as predicted by FIRES-T3 showed good agreement with test results.

CEFICOSS (Computer Engineering of Fire resistance for COmposite and Steel Structures) is another finite element computer program developed by ARBED-Research, Luxembourg and the University of Liege, Belgium. The program is capable of modelling steel and composite frames in fire [80][81]. The integral thermal analysis within this program is determined using a finite difference method based on the heat balance between adjacent elements. The solution procedure is carried out in two phases. Firstly, at ambient temperature the load is applied in small increments. After each load increment the internal forces and deformations are calculated based on the tangent stiffness approach. The equilibrium of the structure is then restored using an iterative Newton-Raphson procedure. When the service load has been reached it is kept constant during the next thermal simulation. At this stage a short time-step of about one minute is introduced and the thermal part of the program is employed in order to determine the temperature distribution within the structure. Next, the structural part of the program cal-



culates the new deformed shape of the structure which corresponds to the newly introduced heating environment. This procedure performs alternating thermal and structural calculations up to the moment where equilibrium can no longer be sustained. This is equivalent to the ultimate fire endurance time of the structure. This alternating solution has the advantage of considering the influence of the structural analysis on the thermal analysis. For example, the spalling of concrete or a fire-protective coating at any stage of the analysis will affect the thermal analysis and consequently the overall response of the structure. The program uses beam elements with two nodes and three degrees of freedom at each node. The cross-section of the element is subdivided into sub-slices forming a rectangular mesh. A bilinear set of stress-strain-temperature relationships has been used for steel, whilst for concrete the stress-strain-temperature characteristics have nonlinear ascending branches and linear descending branches. Creep effects have been considered to be implicitly included in the stress-strain curves. Several fire tests on full-scale beams, columns and frame have been carried out in order to calibrate and verify the program [81].

At the University of Sheffield, a major theoretical programme has been carried out to investigate the structural response of steel members in fire. Olawale and Plank (1988) applied an elasto-plastic finite strip method to analyse the behaviour of steel columns at increasing temperatures. The method includes the effect of plastification of component plates using the deformation theory of plasticity. It incorporates local, overall and interactive buckling modes. Burgess *et al.* (1988) have developed a secant stiffness approach for the analysis of flexural members. A modified Ramberg-Osgood equation was used to represent the moment-curvature-temperature relationship. Unlike incremental analysis, the method checks an assumed equilibrium state of the structure. This state is then used to describe the stiffness of the structural elements in terms of the secant-stiffness

coefficients which relate moment to curvature. Thus the correct equilibrium state will satisfy both compatibility of deformations and the moment-curvature relationship. An iterative procedure was used for convergence. The analysis includes non-uniform temperature distribution across the section of the beam. The work has resulted in a computer program which is now being further developed to be run for framed structures including the  $P - \Delta$  effect.

An existing finite element program INSTAF [95] has been available for some time at the University of Sheffield. The program, developed at the University of Alberta, is a versatile tool for the in-plane analysis of braced and unbraced multistorey I-section steel frames bending about both major and minor axes. The analysis is based on a stiffness formulation which accounts for geometric as well as material nonlinearities. The effect of axial load on the stiffness and strength of the individual members is considered. Gradual development of plastic zones is considered using a transformed area approach, in which the cross-section is divided into a number of plates and the strain of each plate is evaluated. Each plate thickness is then factored by the ratio of the current tangent modulus to the original modulus of elasticity. The formulation permits consideration of extended plastic regions rather than discrete hinges in beams and beam-columns. The analysis considers the effect of residual stress as well as any prescribed values for the elastic stiffnesses of the boundary conditions. In the finite element formulation the element is treated as a beam element with two nodes and three degrees of freedom at each node (i.e two translations and one rotation). An iterative Newton-Raphson technique is employed to solve the equilibrium equations in order to obtain the load-deformation characteristics of the structure. The solution procedure involves applying the load in small increments. After each load increment, the internal forces and deformations are calculated based on the tangent stiffness approach. Convergence is obtained using Newton-Raphson it-

eration until the vectors of unbalanced forces and displacement increments are simultaneously small.

Modification to INSTAF was carried out by Lai (1988) to allow the program to be run for welded aluminium frames, including the consideration of a greater range of cross-sections. Part of the work involved the use of two continuous stress-strain curves, one for the heat-affected zone where the welding has taken place, and one for the remainder of the member. This modified version was further developed by Sharples (1987) to allow the program to be run for steel columns at elevated temperatures. The work involved the inclusion of a set of stress-strain-temperature curves. The load-deformation characteristics of a column can therefore be determined at a prescribed temperature level using the corresponding stress-strain curve. The original program, together with its modifications, has been checked against a wide range of data. In all cases, excellent agreement has been obtained, which has established the capability of the original theory to deal with sophisticated problems in which large deformations occur.

### **2.3.3 Method of analysis of BS5950 Pt.8 (1990)**

Recently, BS5950 Pt.8 has adopted a more analytical approach to assess the fire endurance of steel members using the limiting temperature method and the moment capacity method. Using these methods, the limiting temperatures of beams, columns and tension members can be determined.

The code defines two temperatures : the design temperature and the limiting temperature. The first is defined as the temperature that the critical element will reach at the end of the specified period of fire resistance in the standard test.

The limiting temperature is defined as the temperature of the critical element of a member at failure under fire conditions.

The limiting temperature is given in the code in table 5 for various members as a function of the load ratio at the fire limit state. The load ratio for beams, columns in simple and continuous construction and tension members are given in the code in terms of the applied moment at the fire limit state and the moment capacity of the cross-section at ambient temperature. The design temperature is given in tabulated form and is obtained using the dimensions of the cross-section and the required period of fire resistance.

The limiting temperature method is used to determine the behaviour in fire of columns, tension members and beams with low shear load. The code specifies that, if the limiting temperature for the applicable load ratio is not less than the design temperature at the required period of fire resistance, the member may be considered to have adequate fire resistance without protection. Protection is needed if this limiting temperature is less than the design temperature.

The moment capacity method is applicable only to beams which have webs which satisfy the requirements for a plastic or compact section as defined in Part 1 of BS5950. It is applicable for beams whose temperature profile can be defined. For such beams, the moment capacity of the cross-section  $M_{cf}$  is calculated using the elevated temperature profile for the required period of fire resistance and the appropriate values of the strength reduction factor. When the applied moment  $M_f$  does not exceed  $M_{cf}$ , the member may be considered to have adequate fire resistance without protection.

Comparison between Tables 5, 6 and 7 of the code reveals that for the majority of practical cases the limiting temperatures are less than design tem-

peratures even for elements subjected to a very low load ratio. The code thus requires fire protection for most structural elements. No method is given for the assessment of the behaviour of frames in fire. In addition, the influence of other structural members of the frame on the behaviour of the heated beams and columns has not been considered by the code. This influence is of major importance when structural elements of a frame are individually considered as will be discussed in Chapters 6 and 7.

## 2.4 Observations

Based on the above review, the following principal observations may be drawn.

1. A large amount of work has been carried out to assess the behaviour of structural members in fire. Although tests have largely been carried out under standard fire conditions, the good fund of available data has been a useful means of assessing the relative performance of structures and materials for regulation purposes.
2. There has been a clear tendency in the last decade towards the development of numerical analyses as an alternative to fire tests. This has been adopted by various national codes and it is also recognised by BS 5950 Pt.8.
3. It is noted that the performance of structural elements in a framed structure has been assessed without consideration of the effects of the rest of the structure. Clearly these elements form an integral part of the frame and should therefore be assessed with respect to the temperature level and distribution of the rest of the frame.

4. It has been assumed that failure occurs once the temperature of a critical element reaches a certain level. Temperature variation around the structure and within elements has a considerable influence on critical temperatures, and appropriate fire protection may therefore delay failure until considerably higher temperatures are reached.

## Chapter 3

# Mechanical Properties of Structural Steel at Elevated Temperatures

### 3.1 Introduction

The strength and deformation properties of steel are temperature dependent and must therefore be known in order to predict the structural response of steel structures under fire conditions. Considerable progress has been made in the measurement of the mechanical response of steel at elevated temperatures, leading to mathematical models of such properties. The properties of interest comprise : tensile strength, compressive strength, modulus of elasticity, stress - strain relationship and creep. Such properties are well known at room temperature when it is assumed that steel has the same properties in tension and compression. These properties are generally determined from testing. Tension tests are generally per-

formed for steel in which the relationship between elongation of the test specimen and the applied stress is obtained.

During the last two decades, several such tests have been carried out at elevated temperatures ; these show some scatter in results due to the testing procedures and types of specimen used. Other factors such as rate of loading and rate of heating of the specimen have shown some influence on the steel behaviour.

There has been recognition of a number of testing procedures from which various characteristics of steel at elevated temperatures can be obtained. These can be grouped as steady state tests and transient tests [62].

### **3.1.1 Tests under steady state heating conditions**

In this type of test, the unloaded specimen is heated at a certain rate before any load is applied. The specimen is then strained at a uniform rate while the applied stress is recorded as a function of elongation. The strain measured before the load is applied corresponds to the thermal strain. A family of load-elongation relationships can be obtained by repeating the test at different temperature levels. These relationships can yield the following strength and deformation characteristics :

- Stress-strain relationship, stress rate controlled. Data can be obtained on modulus of elasticity, strength and ultimate strain.
- Stress-strain relationship, strain rate controlled. The obtained data include dissipation of mechanical energy.
- Creep , at constant temperature and constant load. Strain is measured during a certain period of time (2 - 4 hours).



### **3.1.2 Tests under transient heating conditions**

In this form of test, the specimen is loaded and the load is maintained constant while temperature is increased at a given rate. The change in specimen length is recorded by means of high temperature extensometers. Also, the load can develop during heating by restraint against thermal expansion. This type of test can be carried out with either load or strain control. Failure temperature and restraint forces are normally recorded.

The two types of testing procedures provide information on different features of behaviour. Tests carried out under transient conditions are considered to represent truly the behaviour of structures in fire, and thus provide data of direct relevance [62].

The aim of this chapter is to report material test results carried out by different authors using different testing techniques. Some mathematical models on the variation of mechanical properties with temperature are presented and a suitable formulation for these properties is derived for use in the subsequent analytical work.

## **3.2 The available data on stress-strain-temperature relationships**

Considerable progress has been made during the last decade in the development of test data relating to the stress - strain relationship at elevated temperature. This data differs considerably due to the variation in testing procedures and room temperature material properties as well as the method adopted to deal

with creep effects, defined as a continuous time-dependent deformation under constant loading and constant temperature level.

Many researchers have studied the effect of creep on steel members at elevated temperatures. It is concluded that creep effects become significant once temperatures are in excess of a certain level, generally about 400°C [5] [31].

Harmathy (1967) developed a comprehensive creep model based on Dorn's creep theory. This was further modified by Anderberg (1988) where the creep effect was explicitly taken into account. However, the adoption of a time-independent analysis was justified by Witteveen and Twilt (1972) and Witteveen *et al.* (1976). From tests carried out on steel beams and columns they concluded that the critical temperatures of these members were not affected by the rate of heating in a significant way, provided that the heating rate falls within 5 to 50°C/min (to be expected in building fires) and that the critical temperature does not exceed 600°C. They also found that the result for a column tested at 600°C coincides with a creep buckling analysis by Eggwertz (1976). They also carried out warm creep tests [94] in order to obtain the temperature-strain relationships at constant loading so as to eliminate the effect of rate of loading. These relationships were then transformed into stress-strain curves in which creep is implicitly included. Similar tests were carried out by Rubert and Schaumann (1985a) on simply supported steel beams loaded at mid-span. The beams were under constant loading and increasing temperature. Mathematical formulae were then drawn from the test results.

In the UK, investigation into the mechanical properties of steel at high temperatures dates back to 1964 when tensile properties were reported by Woolman and Mottram and Skinner [25]. Holmes *et al.* (1982) examined the tensile

strength properties of hot rolled grade 43 steel up to 700°C under steady state conditions. Data including tensile strength, elastic modulus and ultimate strength were derived from the tests. More recently, Kirby and Preston (1988) reported an extensive testing programme on small-scale tensile tests carried out by BSC under both isothermal and transient heating conditions. Data on the hot rolled, structural steels were provided and a series of stress-strain -temperature relationships have been derived for a temperature range of 20 - 900°C.

### **3.3 Temperature dependent mechanical properties of steel**

Considerable progress has been made in analytically describing the mechanical properties of steel at high temperatures. Usually, the stress-strain relationship is described by two parameters, namely elastic modulus and yield strength. The elastic modulus is defined as the slope of the stress-strain curve at infinitely small stress, which is similar to Young's modulus except that at elevated temperature it becomes stress-dependent. The yield strength is defined as the stress corresponding to a pre-defined strain after which the stress level is assumed to remain constant. These two parameters are usually expressed as the ratios of their elevated temperature values to the room temperature values.

#### **3.3.1 The elastic modulus**

The value of the modulus of elasticity of steel decreases as temperature increases. The rate of decrease depends on the type of steel used. It was reported [87] that

the modulus of elasticity decreases linearly up to a certain temperature level (e.g. 370°C for carbon steel, 480°C for alloyed ferritic steel and 704°C for stainless steel) before the decrease becomes more rapid.

Reported data on the elevated temperature elastic modulus shows a wide variation in the mathematical models suggested in relation to temperature. As discussed in section 3.1, this variation may be at least partly due to the testing method and equipment used.

Several such methods have been reported which show the modulus of elasticity  $E_\theta$  at a temperature  $\theta$  as a ratio to its room temperature value  $E_{20}$ . The following are examples of the commonly used expressions.

### 3.3.1.1 Brockenbrough (1970)

Brockenbrough (1970) suggested an expression for the elastic modulus derived by fitting curves to the data obtained from conventional short-term elevated temperature tests :

$$\begin{aligned} E_\theta &= E_{20} \left[ 1.0 - \left( \frac{\theta - 100}{5000} \right) \right] & 100 < \theta \leq 700^\circ F \\ &= E_{20} \left[ (500,000 + 1.333\theta - 1.111\theta^2) \times 10^{-6} \right] & 700 < \theta \leq 1200^\circ F \end{aligned} \quad (3.1)$$

### 3.3.1.2 C.T.I.C.M (1982)

$$E_\theta = E_{20} \left[ 1.0 + \frac{\theta}{2000 \ln \left( \frac{\theta}{1100} \right)} \right] \quad 0 < \theta \leq 600^\circ C$$

$$= E_{20} \left[ \frac{690 - 0.69\theta}{\theta - 53.5} \right] \quad 550 < \theta \leq 800^\circ C \quad (3.2)$$

### 3.3.1.3 E.C.C.S (1983)

$$\begin{aligned} E_\theta = E_{20} [ & 1.0 - 17.2 \times 10^{-2} \theta^4 + 11.8 \times 10^{-9} \theta^3 - 34.5 \times 10^{-7} \theta^2 \\ & + 15.9 \times 10^{-5} \theta ] \quad 0 < \theta \leq 600^\circ C \\ & \text{not defined} \quad \theta > 600^\circ C \end{aligned} \quad (3.3)$$

### 3.3.1.4 The adopted model

In the present work, expressions for the modulus of elasticity were modelled to approximately satisfy the BS 5950 Pt.8 stress-strain-temperature data relationships. These expressions are given by Sharples (1987):

$$\begin{aligned} E_\theta &= E_{20} \left[ 1.0 - 2.8 \left( \frac{\theta - 20}{1485} \right)^2 \right] \quad 80 < \theta \leq 550^\circ C \\ &= E_{20} \left[ 1.0 - 3.0 \left( \frac{\theta - 20}{1463} \right)^2 \right] \quad 550 < \theta \leq 800^\circ C \end{aligned} \quad (3.4)$$

Comparison between the adopted model and those proposed by ECCS and CTICM is shown in Fig. 3.1. A good agreement between the different models is shown up to 400°C. Beyond this temperature level all three curves drop sharply with the ECCS curve being the most conservative.

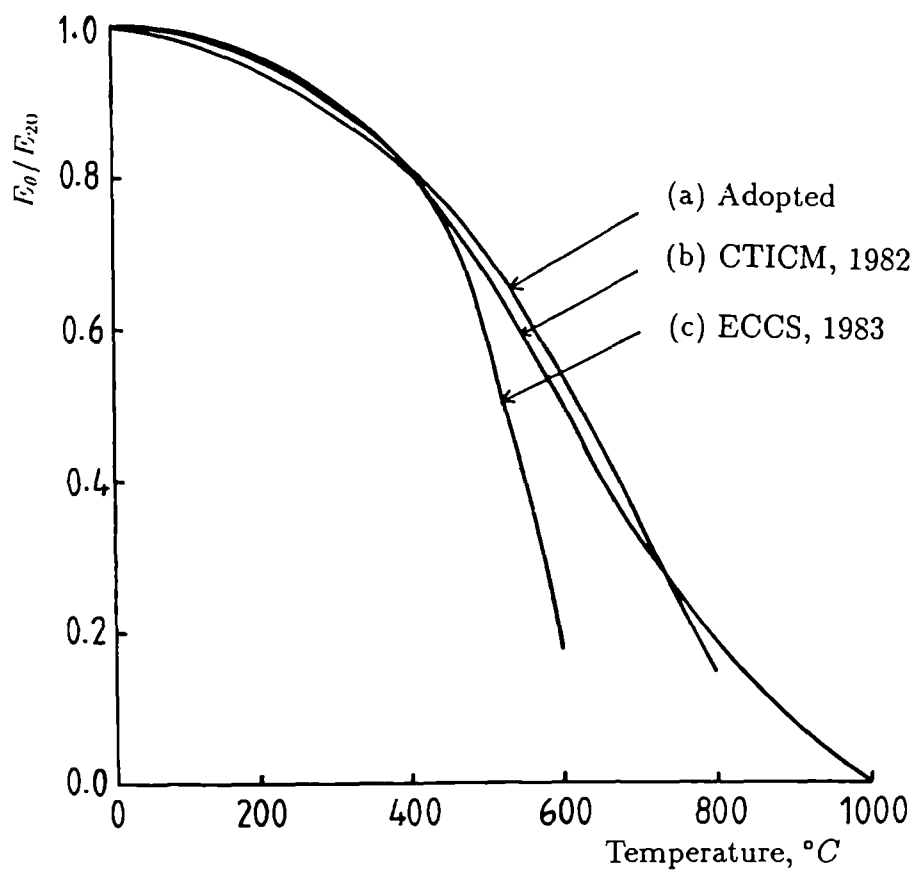


Fig. 3.1 - Variation of the adopted modulus of elasticity with temperature compared with CTICM and ECCS models.

### 3.3.2 The yield strength

As will be discussed later (section 3.4), the stress-strain relationship of steel becomes markedly nonlinear as temperature increases, thus deviating considerably from the assumed elastic-perfectly plastic relationship commonly used at room temperature. These curves become more rounded at higher temperatures and thus possess no definite yield point; defined as the stress at which the strain exhibits a large increase without a corresponding increase in stress. The effective yield strength is therefore the proof stress often corresponding to 0.2%<sup>inelastic</sup> strain.

#### 3.3.2.1 Brockenbrough (1970)

$$\begin{aligned}\sigma_{y\theta} &= \sigma_{y20} \left[ 1.0 - \frac{\theta - 100}{5833} \right] & 100 < \theta \leq 800^\circ F \\ &= \sigma_{y20} \left[ (-720,000 + 4200\theta - 2.75\theta^2) \times 10^{-6} \right] & 800 < \theta \leq 1200^\circ F\end{aligned}\quad (3.5)$$

#### 3.3.2.2 C.T.I.C.M (1982)

$$\begin{aligned}\sigma_{y\theta} &= \sigma_{y20} \left[ 1.0 + \frac{\theta}{200 \ln \left( \frac{\theta}{1750} \right)} \right] & 20 < \theta \leq 600^\circ C \\ &= \sigma_{y20} \left[ \frac{340 - 0.34\theta}{\theta - 240} \right] & 600 < \theta \leq 1000^\circ C\end{aligned}\quad (3.6)$$

#### 3.3.2.3 E.C.C.S (1983)

$$\begin{aligned}\sigma_{y\theta} &= \sigma_{y20} \left[ 1.0 + \frac{\theta}{767 \ln \left( \frac{\theta}{1750} \right)} \right] & 0 < \theta \leq 600^\circ C \\ &= \sigma_{y20} \left[ \frac{108 \left( 1 - \frac{\theta}{1000} \right)}{\theta - 440} \right] & 600 < \theta \leq 1000^\circ C\end{aligned}\quad (3.7)$$

### 3.3.2.4 The adopted model

The adopted yield strength expressions were appropriately modelled in order to satisfy the BS 5950 Pt.8 data.

$$\begin{aligned}\sigma_{y\theta} &= \sigma_y \left[ 0.987 - 0.034 \frac{\theta}{350} \right] & 80 < \theta \leq 400^\circ C \\ \sigma_{y\theta} &= \sigma_y \left[ 1.553 - 0.155 \frac{\theta}{100} \right] & 400 < \theta \leq 550^\circ C \\ \sigma_{y\theta} &= \sigma_y \left[ 2.340 - 0.220 \frac{\theta}{70} \right] & 550 < \theta \leq 600^\circ C \\ \sigma_{y\theta} &= \sigma_y \left[ 1.374 - 0.078 \frac{\theta}{50} \right] & 600 < \theta \leq 690^\circ C \\ \sigma_{y\theta} &= \sigma_y \left[ 1.120 - 0.128 \frac{\theta}{100} \right] & 690 < \theta \leq 800^\circ C\end{aligned} \quad (3.8)$$

The reported models of the variation of yield strength with temperature are plotted in Fig.3.2 for comparison.

### 3.3.2.5 Fire resistant steel

Recently, Nippon Steel of Japan has developed a fire resistant steel for columns and beams which are now used in office buildings [78]. At 600°C this steel retains over 2/3 of its ambient temperature strength and thus requires only 1/2 to 1/3 of the fire protection needed for conventional structural steel. This is achieved by adding 1% of such alloying components as nickel, chrome and molybdenum to the conventional steel and precisely controlling the temperature of the rolling process. Plates, H-shapes and hollow sections, welding materials and high tensile bolts have been developed which meet all the requirements for building material including good weldability and low cost.



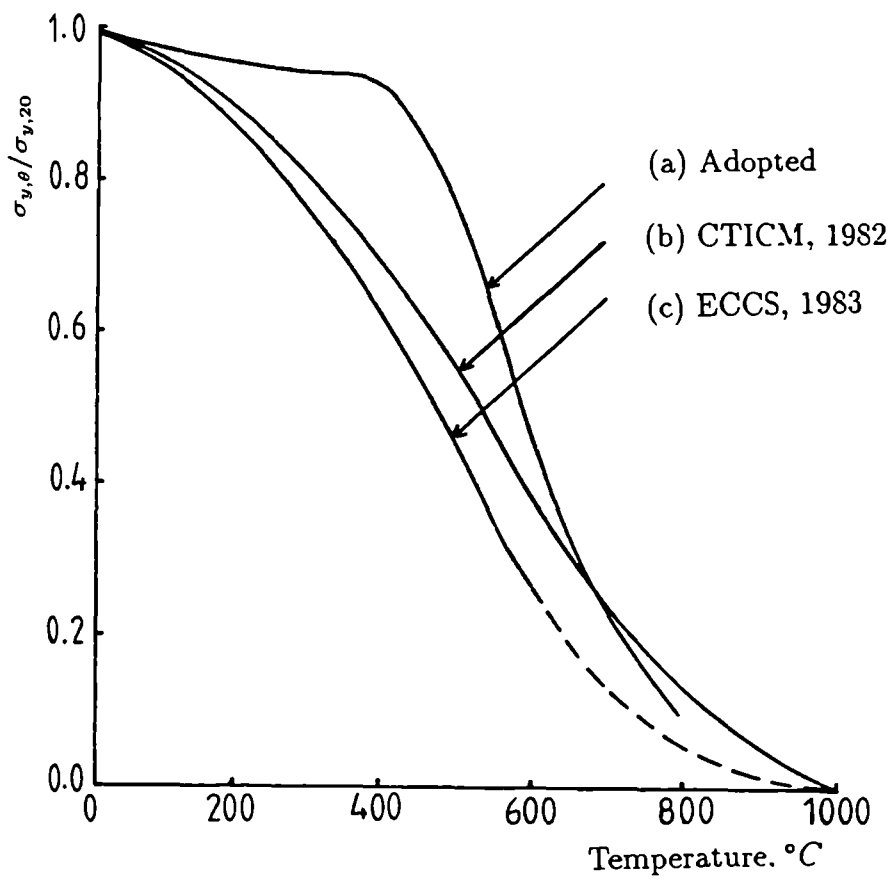


Fig. 3.2 - Variation of the adopted effective yield strength model with temperature compared with CTICM and ECCS models.

A comparison between the adopted model for yield strength and the material strength test results for this steel is given in Fig.3.3. The beneficial use of this material in structural elements will be checked in section 6.3.3.

### 3.3.3 Coefficient of thermal expansion

Investigation into the effect of temperature on the coefficient of thermal expansion  $\alpha$ , that is the rate at which steel expands as a function of temperature, shows good agreement between all reported data. Results of this investigation have shown that the value of  $\alpha$  increases slowly with temperature up to  $700^{\circ}\text{C}$  approximately where a sudden drop in its value occurs due to a sudden shrinkage of the steel caused by transformation of the material into austenite [58]. The type of steel, strength characteristics and temperature level seem to have no significant influence on this relationship (Anderberg (1988)). It can be seen from Fig.3.4 that the effect of temperature on  $\alpha$  can be neglected in theoretical analysis. An average value of  $1.4 \times 10^{-5}$  is usually recommended for  $\alpha$  which will be used throughout the present work.

## 3.4 Stress-strain-temperature relationship.

The simplest form of the stress-strain relationship is two-straight lines, where the elastic modulus and yield strength are the only information needed to describe the behaviour of steel members. This relationship between the stress  $\sigma$  and the strain  $\epsilon$  is normally expressed as :

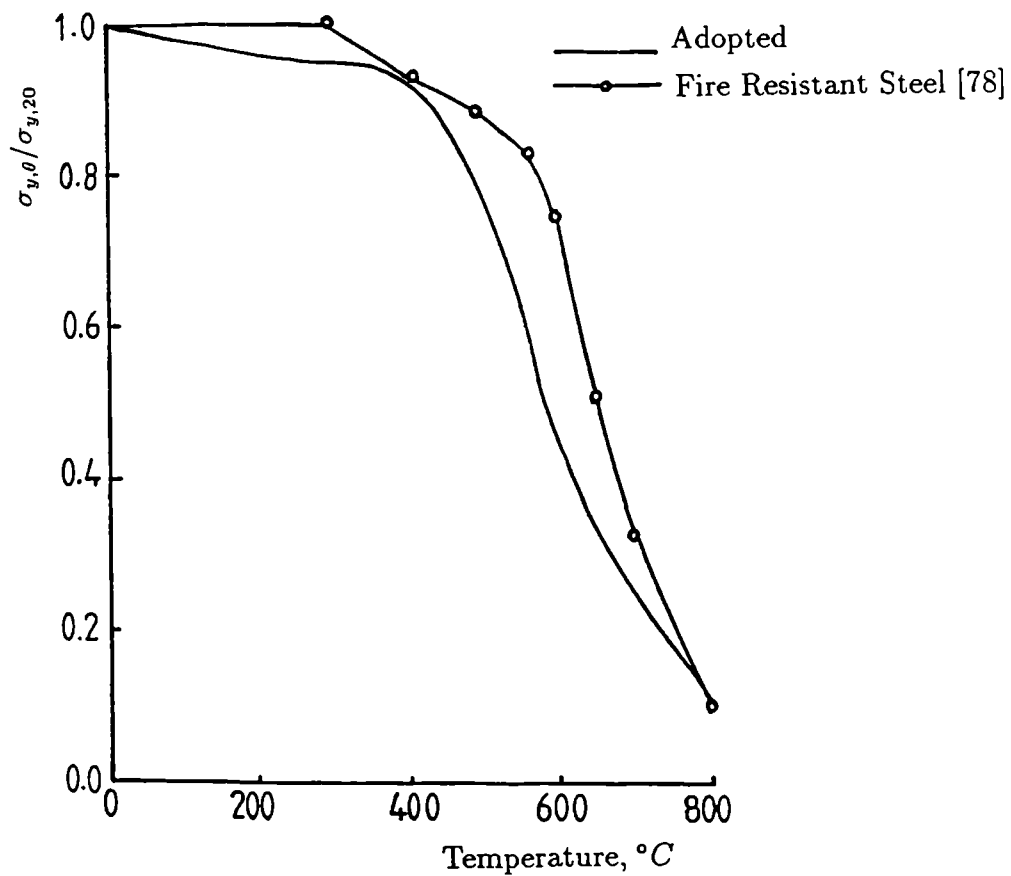


Fig. 3.3 - Comparison between the adopted effective yield strength model and Fire Resistance Steel [78].

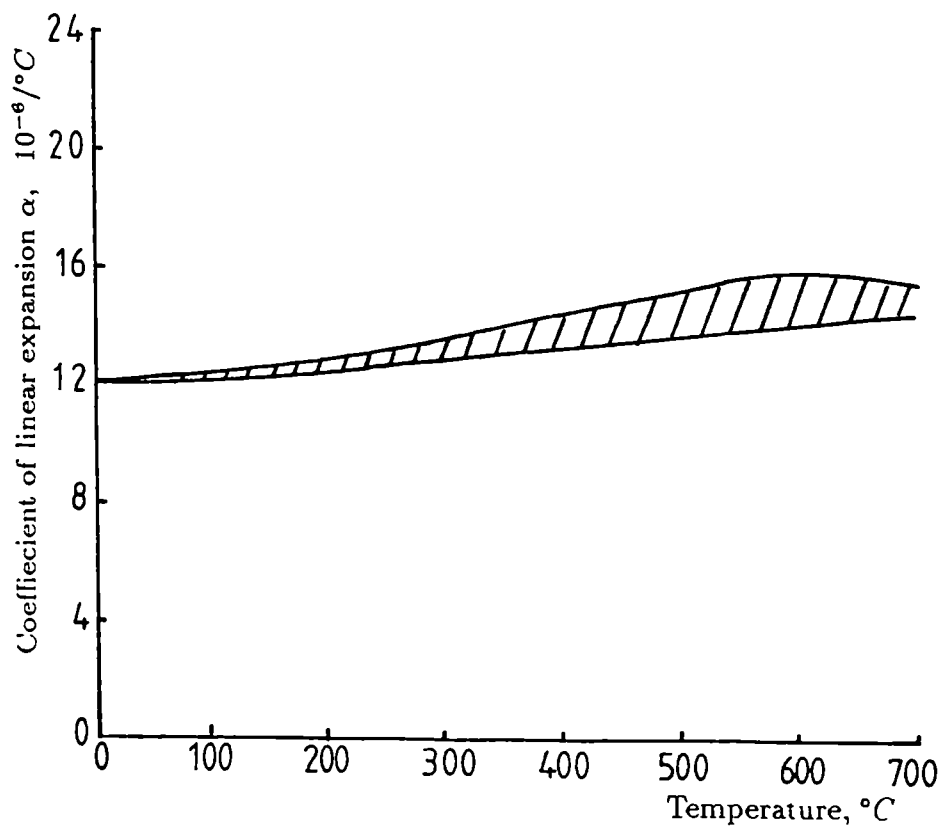


Fig. 3.4 - Variation of coefficient of thermal expansion  $\alpha$  with temperature [58].

$$\sigma = \begin{cases} E_1 \epsilon & \epsilon \leq \epsilon_1 \\ E_1 \epsilon_1 + E_2 (\epsilon - \epsilon_1) & \epsilon > \epsilon_1 \end{cases} \quad (3.9)$$

In this relationship only the main features of steel behaviour are represented. The initial slope  $E_1$  represents the elastic behaviour up to the limit of proportionality defined by  $\epsilon_1$ . The second slope  $E_2$  represents the plastic behaviour. When pure plastic response is assumed,  $E_2$  tends to zero and the expression becomes the elastic-perfectly plastic relationship commonly used in structural design.

Although the elastic-plastic stress-strain relationship is still popular because of its simplicity or when ultimate load is the only item needed, tests have shown that there is a gradual transition from the elastic straight line for loaded members to the horizontal plastic line which starts at progressively lower load levels when temperature increases. Thus a uniform stretching or an affine transformation of coordinates from an assumed bilinear room temperature relationship by replacing the elastic modulus and yield strength with their corresponding elevated temperature values fails to fit test data. Hence there is a need for parameters other than the elastic modulus and yield strength in the stress-strain relationship formulation in order to take into account variation in transition phase between the elastic and plastic phases.

The continuous form of stress-strain relationship given by the Ramberg-Osgood formulae [73] seems to be the most suitable form to fit the test data for these relationships at elevated temperatures. Its shape is continuously increasing as if it possesses strain hardening from the beginning. This formula is given by :

$$\epsilon = \frac{\sigma}{E_{20}} + 0.002 \left( \frac{\sigma}{\sigma_{0.2}} \right)^\eta \quad (3.10)$$

Where

$\epsilon$  = strain

$\sigma$  = stress at a given strain

$\sigma_{0.2}$  = 0.2% proof stress

The first term of the right hand side of eq.3.10 represents the elastic component of the strain and the second term represents the plastic component.  $\eta$  is the knee factor which describes the shape of the curve. A high value of  $\eta$  represents a sharp knee and if  $\eta \rightarrow \infty$  eq.3.10 becomes the elastic-perfectly plastic relationship.

In the present work, the Galambos modified version of the formula is used for temperatures below 80°C together with a modified form of the formula for higher temperatures. These formulae are given in Ref.[83] as:

$$\begin{aligned}\epsilon &= \frac{\sigma}{E_{20}} + \frac{3}{7} \left( \frac{\sigma_{y20}}{E_{20}} \right) \left( \frac{\sigma}{\sigma_{y20}} \right)^{50} & 0 < \theta \leq 80^\circ C \\ &= \frac{\sigma}{E_\theta} + 0.01 \left( \frac{\sigma}{\sigma_{y\theta}} \right)^{\eta_\theta} & 80 < \theta \leq 800^\circ C\end{aligned}\quad (3.11)$$

Where :

$E_{20}$  is the Young's modulus of elasticity at ambient temperature

$\sigma_{y20}$  is the yield strength at ambient temperature

$\epsilon$  is the effective strain

$\sigma$  is the effective stress

$E_\theta$  is the effective modulus of elasticity at temperature  $\theta$

$\sigma_{y\theta}$  is the effective yield strength at temperature  $\theta$

$\eta_\theta$  is the material constant at elevated temperatures.

$E_\theta$  and  $\sigma_{y\theta}$  were modelled to approximately satisfy the BS 5950 Pt.8  $\sigma - \epsilon$

-  $\theta$  data and were given by eqs.3.4 and 3.8 respectively.

$\eta_\theta$  expressions at elevated temperatures are :

$$\begin{aligned}
 \eta_\theta &= \frac{4600}{\theta} + \alpha & 80 < \theta \leq 200^\circ C \\
 \eta_\theta &= \frac{2650}{\theta} + \alpha & 200 < \theta \leq 400^\circ C \\
 \eta_\theta &= \frac{2400}{\theta} + \alpha & 400 < \theta \leq 550^\circ C \\
 \eta_\theta &= \frac{3900}{\theta} + \alpha & 550 < \theta \leq 600^\circ C \\
 \eta_\theta &= \frac{3600}{\theta} + \alpha & 600 < \theta \leq 690^\circ C \\
 \eta_\theta &= \frac{4600}{\theta} + \alpha & 690 < \theta \leq 800^\circ C
 \end{aligned} \tag{3.12}$$

where :

$$\alpha = \frac{\theta}{500 \ln \left( \frac{\theta}{1750} \right)} \tag{3.13}$$

Fig.3.5 compares these relationships with original data obtained by BSC tests [17].

### 3.5 Summary

This chapter has outlined the effect of testing procedures on the material data for the properties of steel at elevated temperatures as provided by various authors. It has also summarized some of the reported data and has compared the adopted models with those of CTICM and ECCS. Attention has been drawn to a fire resistant steel which is already in use in office buildings.

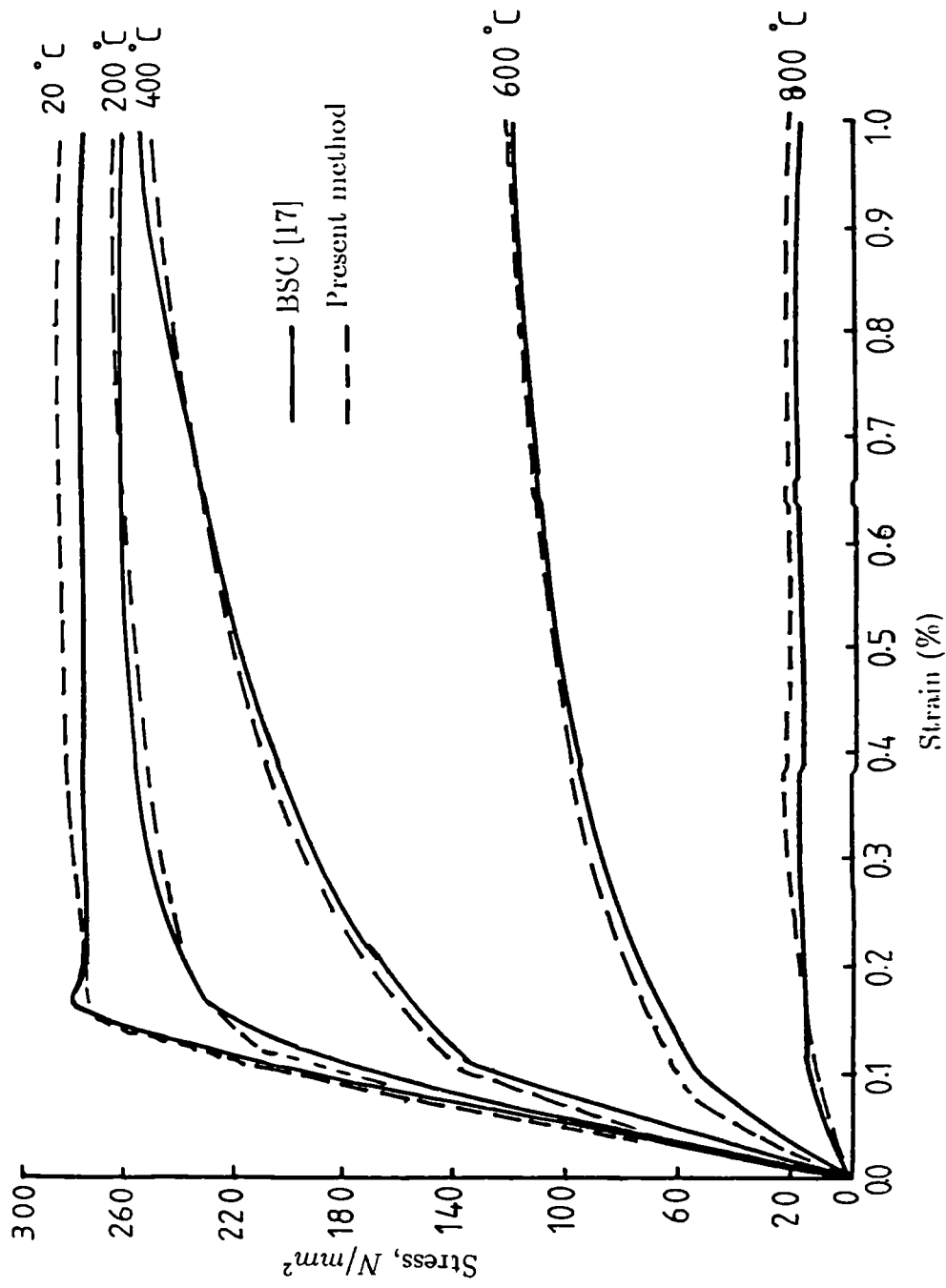


Fig. 3.5 - Comparison between present stress-strain-temperature relationships and BSC data [17].

## Chapter 4

# Nonlinear Inelastic Analysis of Fire-Exposed Frames

### 4.1 Introduction

The various possible types of frame analysis may be illustrated with reference to Fig.4.1 in which the relationship between the applied load  $P$  and the lateral deflection  $\Delta$  at the top of a simple portal frame as predicted by various approaches is shown.

The simplest form of analysis which may be performed to predict the structural response is linear elastic analysis where  $P$  is proportional to  $\Delta$  over an unrestricted range resulting in the straight line  $OA$ , normally referred to as first-order linear elastic analysis. Such methods of analysis include normal moment distribution, most energy methods and conventional slope-deflection analysis [49]. If, however, the effect of deformations on the equilibrium equations (i.e  $P - \delta$  due



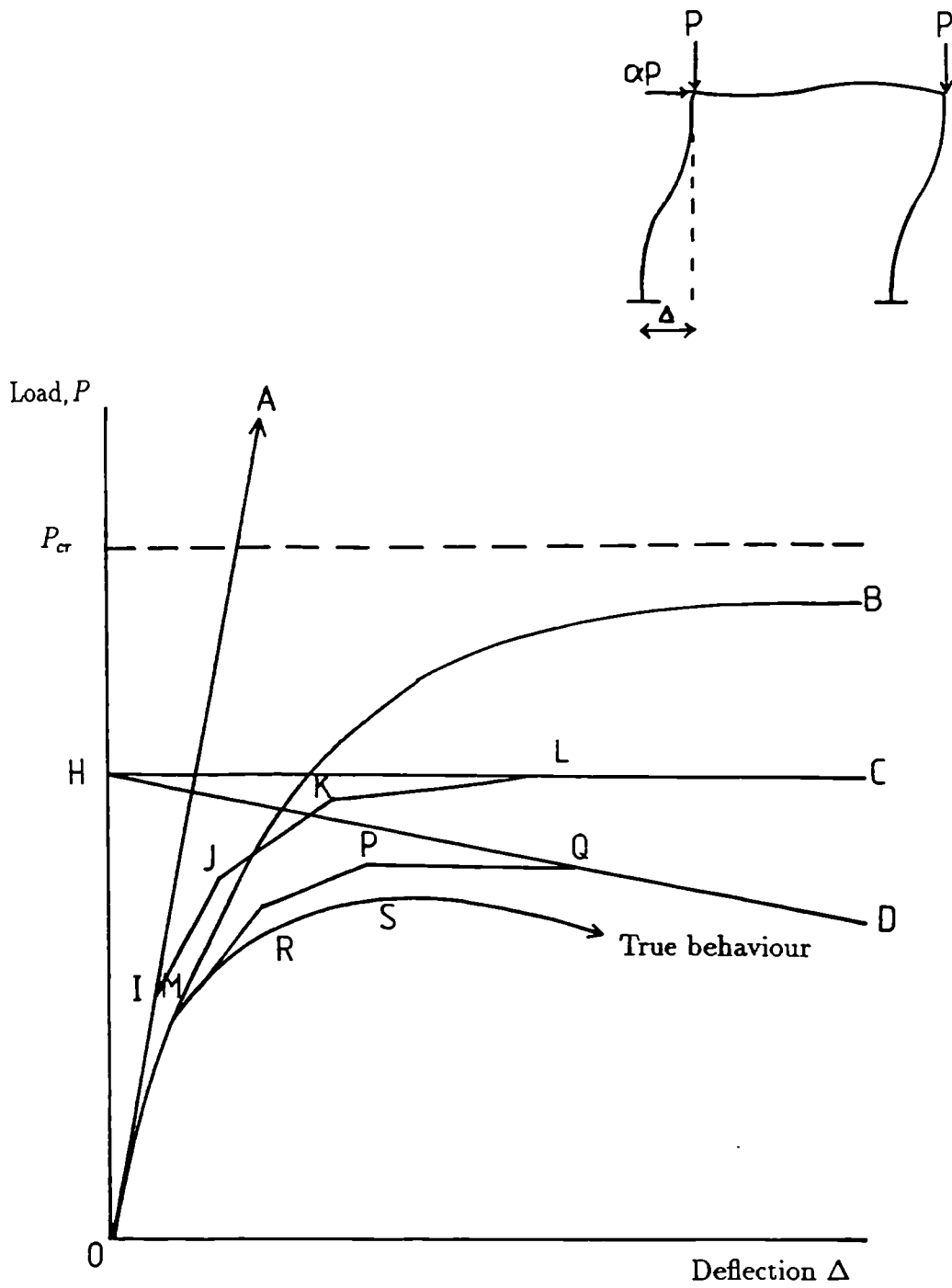


Fig. 4.1 - Load-deformation relationships as predicted by various types of analysis.

to the load  $P$  acting through  $\delta$  and loss of bending stiffness due to compressive load) is recognised, then the analysis, known as second-order elastic analysis, will result in the curve  $OB$  which results in larger deflections than those predicted by linear elastic theory. The curve  $OB$  is tangential to the linear elastic characteristic at the origin and asymptotic to the line  $P = P_{cr}$  at large deflections. Hence, the elastic critical load  $P_{cr}$  is an upper bound to the failure load of the frame. Such methods include use of the familiar slope deflection equations but including the nonlinear stability coefficients  $s$  and  $c$  ( Kirby and Nethercot (1979)).

If, instead of perfectly elastic behaviour, rigid-plastic behaviour is assumed (in which the modulus of elasticity  $E$  is assumed to be infinite), then no deformation occurs until the formation of the final hinge which converts the structure into a mechanism. Such a method of analysis results in the load - deflection curve  $OHC$ , denoted simple rigid-plastic behaviour. The straight portion  $HC$  of this curve ceases to be a horizontal line if the effects of deformations on the equilibrium equations are considered. The inclusion of these effects implies that the rigid-plastic load-deflection relationship takes the form of the rigid-plastic mechanism curve  $OHD$  which is frequently described as the drooping plastic characteristic ( Horne and Merchant (1965)).

More sophisticated analyses, often suitable for computer-orientated approaches, begin with linear elastic analysis coupled with the concept of plastic hinges. The resulting curve  $OIJKL$ , usually referred to as first-order elastic-plastic analysis, takes the form of a series of straight lines changing slopes abruptly as successive hinges form. These slopes represent the linear stiffnesses of the frame with frictionless pins inserted at locations where plastic hinges have formed at the corresponding load levels. When the effects of change in frame geometry on the equilibrium equations are considered, the load - deflection curve becomes

$OMNPQ$  denoted as second-order elastic-plastic analysis (Horne(1965)).

Both the rigid-plastic and the elastic treatments represent idealisations of the true behaviour. The elastic curve  $OB$  represents the true behaviour of the frame only up to point  $M$  when the corresponding load level causes the bending moment at some location to reach the fully plastic moment of resistance at that section. Here, considering the structure modified by the insertion of a frictionless pin at the location of the plastic hinge, new linear and nonlinear elastic stiffnesses (defined by the slope  $MN$  on the nonlinear elastic-plastic curve) can be determined as it is considered that the section is unable to resist any additional moment for an increment of load. The modified structure has also a new reduced elastic critical load which can represent an upper value of the failure load if no further hinges are formed as load increases. If the section shape factor were unity (i.e moment at this section equals the fully plastic moment  $M_p$ ) then the load - deflection curve would follow  $OMN$ . However, for members with practical cross-section, the shape factor is normally greater than unity and the true behaviour is therefore rounded off below the curve  $OMN$ . The curve  $OMN$  thus forms an upper bound to the true behaviour  $ORS$ .

Once again the load level is increased and a further hinge will form. The process is repeated until the load parameter becomes approximately equal to the elastic critical load of the structure in the current deteriorated situation. Nevertheless, the true behaviour has still not been obtained due to the large number of mathematical idealisations still present. These include neglect of residual stresses, initial lack of straightness, material variability, finite member and joint sizes, real joint stiffness which may vary with increasing load and so on. Yet it must be pointed out that these complications do not prevent the prediction of a form of behaviour which is normally sufficiently accurate, especially when the uncertain-

ties in the input parameters such as loading and material properties are taken into account.

This chapter aims at modelling the structural response of a steel frame under fire conditions. A computer program has been developed based on the original room temperature ultimate strength analysis program INSTAF [95]. This program attempts to handle closely the true behaviour given by curve *ORS* in Fig.4.1 by allowing for both the gradual development of plastic zones and the effects of instability.

## 4.2 Description of the program INSTAF

The original program INSTAF is a versatile program developed at the University of Alberta for the in-plane analysis of braced and unbraced multistorey I-section steel frames. The analysis is based on a stiffness formulation which accounts for geometric as well as material nonlinearities. The effect of axial load on the stiffness and strength of the individual members is considered and partial plastification is taken into account as well as the effects of residual stresses. The formulation permits consideration of extended plastic regions rather than discrete hinges in beams and beam-columns. In the finite element formulation, the element is treated as a beam element and an iterative Newton-Raphson technique is then employed to solve the equilibrium equations in order to obtain the load - deformation characteristics of the structure. This formulation is well documented by El-Zanaty et al (1980). The logical sequence of INSTAF is illustrated by Fig.4.2.

Modification to INSTAF was carried out at Sheffield University by Lai

- (1) START
- (2) Read problem control parameters
- (3) Read nodal geometry, member properties, connectivities and boundary conditions
- (4) Assemble load vector
- (5) Set approximate displacements
- (6) *GO TO* (9)
- (7) Read information from previous step
- (8) Assemble load vector
- (9) Form and assemble tangent stiffness matrix
- (10) Evaluate vector of unbalanced forces
- (11) Calculate increment in displacements to equilibrate the unbalanced forces
- (12) Update displacements
- (13) Check convergence
- (14) Return to (9) if no convergence
  - Stop if divergence
  - Output displacements and stresses if converged
- (15) Check load level
  - Maximum load level exceeded?
  - If NO return to (7)
  - If YES stop
- (16) END.

**Fig. 4.2** - Logical sequence of INSTAF.

(1988) to allow the program to be run for welded aluminium frames, including the consideration of a greater range of cross-sections. Part of the work involved the use of two continuous stress-strain curves, one for the heat affected zone where the welding has taken place, and one for the remainder of the member. It is this modified version that has been further modified by Sharples (1987) to allow the program to be run for steel columns at elevated temperatures. The work involved development of a set of stress-strain-temperature curves approximately satisfying the BS5950 Pt.8 material data. The program was then employed to predict the collapse load at a certain temperature level using the corresponding stress-strain relationship. In all cases, the results obtained were in very good agreement with experimental data, thus establishing the capability of the original theory to deal with sophisticated problems in which large deformations occur.

The present work uses the previously developed material constitutive relationships to model the structural behaviour of steel frames under fire conditions. The program has been further modified to give a more complete and profound treatment of the response of steel frames at elevated temperatures. This has resulted in a complete remodelling of the program parallel to the original formulations which will be described in the following section.

## **4.3 Structural analysis at elevated temperatures**

### **4.3.1 Temperature distribution within each member**

When a frame is exposed to fire, the temperature distribution may vary along and across each member. This may be due to the heating procedure or to the

partial protection offered when the steel is in contact with another material.

The temperature distribution in a structural member depends on the position of this member in the structure relative to the heating source. Thus the case for external columns, when columns are built into walls or when webs of I-sections are encased in brickwork will all be different. For a beam supporting a concrete floor, the temperature of the bottom flange is often much greater than that of the top flange. Schematic temperature distributions across some structural members are shown in Fig.4.3.

Variation of temperature across the section of a member is generally a beneficial effect since the strength and stiffness of those parts of these members at lower temperature levels are retained. However, an induced bowing towards the heating source if the element is not restrained is expected due to this variation in temperature, as well as an induced bending moment if the member is rotationally restrained at its ends. The magnitude of this bowing, due to the internal strains caused by the temperature gradient over the cross-section, depends on the temperature distribution and level within the section. This thermal problem becomes more complicated when the phenomenon of reversed bowing, often observed in column tests [24] due to deterioration in material properties of the hot parts and shift of the effective neutral axis towards the cold parts as temperature increases, is to be considered. This is because early bowing of the member towards the heat source is overshadowed by the deterioration of the stiffness of the hot parts of the section. This, in turn, causes the resultant of the internal forces to be shifted towards the colder parts which results in an apparent eccentricity of the loading, and consequently partly compensates for this early thermal bowing. Which of these effects governs depends on the temperature level and distribution across the section. In the present work, this thermal effect is considered to be equivalent

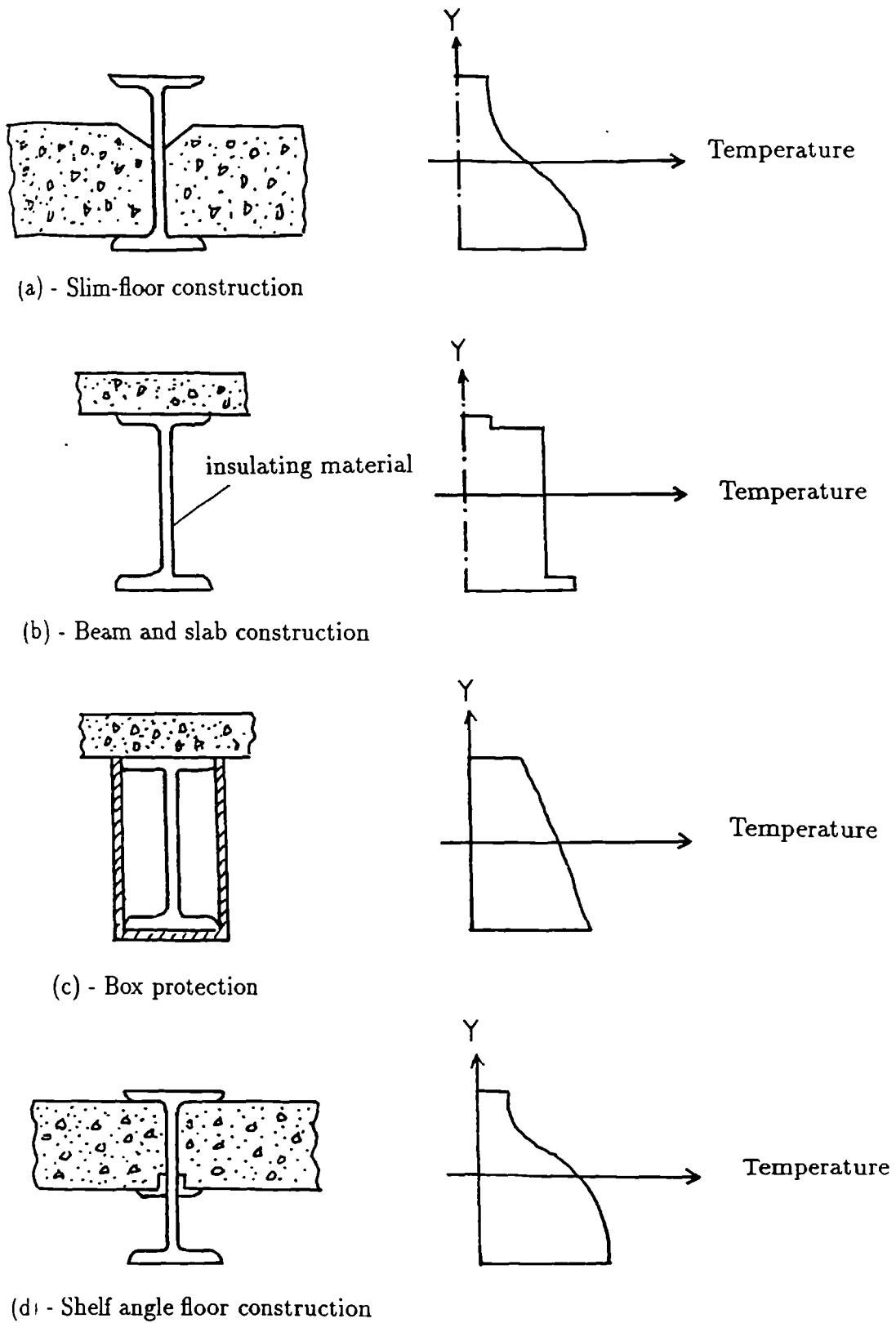


Fig. 4.3 - Various protection configurations and temperature distributions [64].



to an initial lack of straightness at the beginning of each temperature increment. Appendix A presents a simple method used in the analysis to calculate the maximum deflection due to this thermal effect based on the assumption of a circular deformed shape and a linear temperature distribution over the section.

Temperature profiles across the section must be known as a function of the depth. However, due to the wide range of profiles which may exist, a justifiable approximation can be made by assuming the profile in a stepped form over a finite number of regions across the section depth. In this work, along each finite element four different temperature levels can be considered across the section as shown by Fig.4.4. This assumption is justified by actual fire data when top flange, bottom flange and the web of a section may be exposed to different heating levels.

### **4.3.2 Definition of the problem and main assumptions**

1. When steel frames are exposed to a fire they may be expected to undergo axial thermal expansion at increasing temperatures. Only axial forces may be expected to be induced in elements that are uniformly heated if such expansion is completely restrained.
2. The presence of a thermal gradient over the cross-section produces differential expansion between the hot and cold parts. For the cross-section to remain plane this expansion must be coupled with rotation. Bowing of the member towards the heat source will produce additional bending moments, interacting with the externally applied loading system if the member is rotationally restrained.
3. Plane sections are assumed to remain plane under flexural deformations. No out-of-plane or torsional actions are considered.

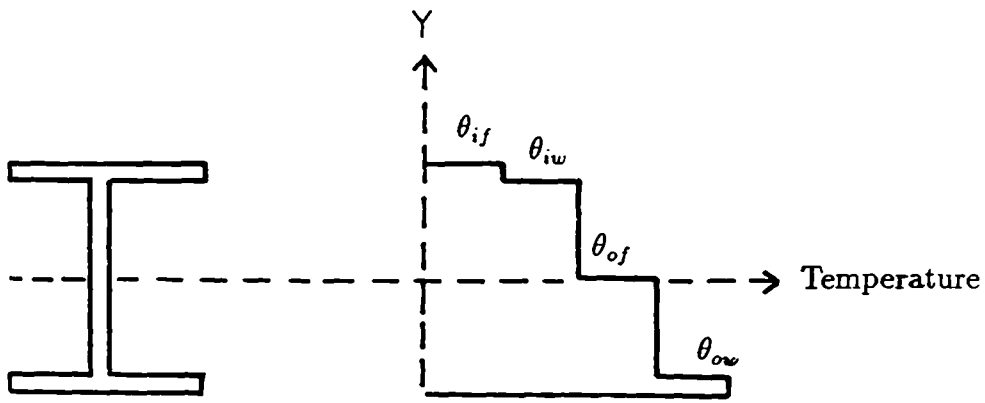


Fig. 4.4 - Assumed temperature distribution across the section of an element.

4. Shear deformations are very small in framed structures and can be neglected.

5. The in-plane element deformation components are as shown by Fig.4.5. The slope at any point along the reference axis assumed in INSTAF is given by:

$$v'_o = \frac{\Delta v_o}{\Delta z} = \sin \theta \quad (4.1)$$

6. The gradient of the displacement  $\Delta z$  is negligible compared with its slope  $v'$ . Expression 4.1 remains valid for problems in which <sup>nonlinear</sup> displacements and rotations occur.

Referring to Fig.4.5, the displacement functions  $u$  and  $v$  of an arbitrary point A can be expressed in terms of the displacements of the reference axis  $u_o$  and  $v_o$  of the beam as follows:

$$\begin{aligned} u &= u_o - y \sin \theta \\ v &= v_o - y(1 - \cos \theta) \end{aligned} \quad (4.2)$$

Using eq.4.1, eqs.4.2 can be written as :

$$\begin{aligned} u &= u_o - yv'_o \\ v &= v_o - y(1 - \cos \theta) \end{aligned} \quad (4.3)$$

The total axial strain at A may be obtained from the large displacement equations as [79] :

$$\epsilon_z = u' + \frac{1}{2} [(u')^2 + (v')^2] \quad (4.4)$$

Differentiating  $v$  of eq.4.2 with respect to  $z$  yields :

$$v' = v'_o - y \sin \theta \frac{d\theta}{dz} \quad (4.5)$$

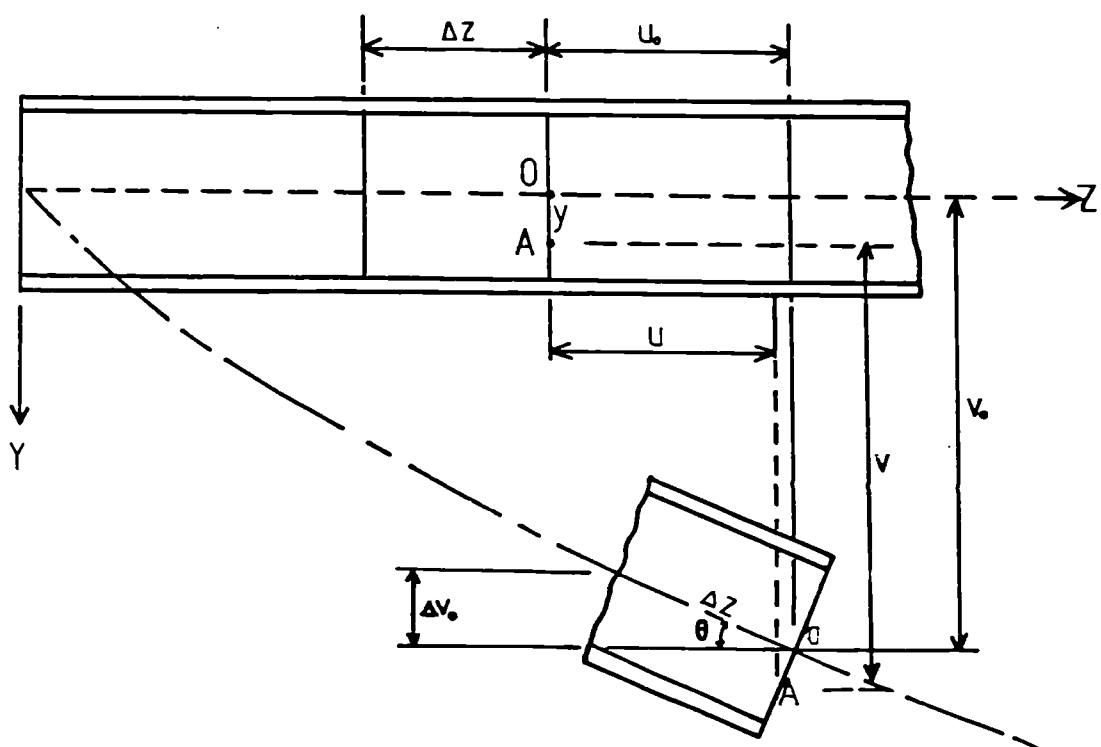


Fig. 4.5 - Finite element deformations.

Differentiating eq.4.1 for  $v'_o$  we obtain :

$$v''_o = \cos \theta \frac{d\theta}{dz} \quad (4.6)$$

from which

$$\frac{d\theta}{dz} = \frac{v''_o}{\cos \theta} \quad (4.7)$$

Referring to Fig.4.5,  $\cos \theta$  can be expressed as :

$$\cos \theta = \sqrt{1 - (v'_o)^2} \quad (4.8)$$

Substituting eq.4.7 into eq.4.5 and using eqs.4.1 and 4.8, eqs.4.2 can be written as :

$$\begin{aligned} u' &= u'_o - yv''_o \\ v' &= v'_o - \frac{yv'_ov''_o}{\sqrt{1 - (v'_o)^2}} \end{aligned} \quad (4.9)$$

Finally substituting eq.4.9 into eq.4.4 yields the strain - displacement relationship for nonlinear formulation:

$$\begin{aligned} \epsilon_z &= u'_o + \frac{1}{2} \left\{ (u'_o)^2 + (v'_o)^2 \right\} - yv''_o \left\{ 1 + u'_o + \frac{(v'_o)^2}{\sqrt{1 - (v'_o)^2}} \right\} \\ &+ \frac{1}{2} y^2 (v''_o)^2 \left\{ 1 + \frac{(v'_o)^2}{1 - (v'_o)^2} \right\} \end{aligned} \quad (4.10)$$

Eq.4.10 is the strain-displacement relationship at any arbitrary point A accounting for geometric nonlinearity since both nonlinear terms of eq.4.4 are retained. The total strain  $\epsilon_{zt}$  can be expressed in terms of the elastic strain  $\epsilon_e$ , residual strain  $\epsilon_r$  and the thermal strain  $\epsilon_{th}$  as follows :

$$\epsilon_{zt} = \epsilon_z + \epsilon_r = \epsilon_e + \epsilon_{th} \quad (4.11)$$

where the thermal strain due to thermal expansion of steel caused by a temperature increment  $\Delta\theta$  is given by :

$$\epsilon_{th} = \int_{\theta_{t_0}}^{\theta_{t_0} + \Delta\theta} \alpha_\theta d\theta \quad (4.12)$$

The principle of virtual work results in the following energy equation :

$$\delta W = \int_V \sigma_z \delta \epsilon_z dV - \langle Q \rangle \{\delta q\} = 0 \quad (4.13)$$

in which  $\langle Q \rangle^T$  is the vector of externally applied load and  $\{\delta q\}$  is the nodal displacement vector.

The elastic strain  $\epsilon_e$  is related to the stress  $\sigma_z$  by the stress - strain relationship :

$$\begin{aligned} \sigma_z &= C \epsilon_e \\ &= C (\epsilon_z + \epsilon_r - \epsilon_{th}) \end{aligned} \quad (4.14)$$

Let stress resultants be defined as :

$$\begin{aligned} n &= \int_A \sigma_z dA \\ m &= \int_A \sigma_z y dA \\ m^* &= \int_A \sigma_z y^2 dA \end{aligned} \quad (4.15)$$

Differentiating eq.4.10,  $\delta \epsilon_z$  can be written in matrix form as :

$$\begin{aligned} \delta \epsilon_z &= \{B\}^T \{\delta U\} \\ &= \{B\}^T \{V\} \end{aligned} \quad (4.16)$$

where  $\{U\}$  is the displacement vector and  $\{V\}$  are the velocities :

$$\begin{aligned} \{U\} &= \langle u'_o \quad v'_o \quad v''_o \rangle^T \\ \{V\} &= \langle \delta u'_o \quad \delta v'_o \quad \delta v''_o \rangle^T \end{aligned} \quad (4.17)$$

Using eqs.4.15 and 4.17, eq.4.13 can be written as :

$$\int_l \{A\}^T \{\delta U\} dz - \langle Q \rangle \{\delta q\} = 0 \quad (4.18)$$

in which

$$\{A\}^T = \int_A \sigma_z \{B\}^T dA \quad (4.19)$$

### 4.3.3 Finite element formulations

To discretize eq.4.18 by the finite element method, the displacements  $u_0$  and  $v_0$  can be approximated as functions of  $N$  discrete nodal displacements  $q_i$ . Eq.4.18 can therefore be written as a set of  $N$  nonlinear equations [96]

$$\psi_i = 0 \quad (4.20)$$

in which

$$\psi_i = \int_l \{A\}^T \frac{\delta}{\delta q_i} \{U\} dz - Q_i \quad (4.21)$$

$i = 1, \dots, N$

Since eqs.4.21 are not satisfied, Newton-Raphson iteration can be used to calculate  $\Delta q_i$ , the correction increments to displacements  $q_i$ . According to eq.4.13:

$$\Delta \psi_i = 0 \quad (4.22)$$

where :

$$\Delta \psi_i = \psi_i + \frac{\partial \psi_i}{\partial q_j} \Delta q_j \quad (4.23)$$

$j = 1, \dots, N$

Substituting eq.4.21 into eq.4.22 yields:

$$\left[ \int_l \frac{\partial}{\partial q_j} \{A\}^T \frac{\partial}{\partial q_i} \{U\} dz \right] \Delta q_j = Q_i - \int_l \{A\}^T \frac{\partial}{\partial q_i} \{U\} dz \quad (4.24)$$

Eq.4.24 is the basic Newton-Raphson equilibrium equation for an element and may be used to deal with material and geometric nonlinearities of steel at high

temperatures. This equation relates the incremental tangent stiffness matrix  $[k_T]$  and the unbalanced load vector  $\{\Delta Q\}$  as follows :

$$[k_T] \{\Delta q\} = \{\Delta Q\} \quad (4.25)$$

In order to evaluate the tangent stiffness matrix for an inelastic element, it is necessary to evaluate the increments in stress resultants. These variations in stress resultants at any stage of loading and temperature may arise from variation of the displacement and temperature levels. Differentiating eq.4.14 and using eq.4.16 yields :

$$\delta \sigma_z = C \left( \{B\}^T \{V\} - \delta \epsilon_{th} \right) \quad (4.26)$$

For any time step  $t + \Delta t$ ,  $\delta \epsilon_{th}$  can be computed from :

$$\delta \epsilon_{th} = \left[ \epsilon_{th}^{t+\Delta t} - \epsilon_{th}^t \right] \quad (4.27)$$

where  $\epsilon_{th}^{t+\Delta t}$  and  $\epsilon_{th}^t$  are determined from eq.4.12.

The stiffness matrix  $[k_T]$  in eq.4.25 has been calculated with respect to the nodal displacement vector  $\{q\}$  referred to a local coordinate system as shown by Fig.4.6.  $\{q\}$  can therefore be written as :

$$\{q\} = \left\{ \{q^I\}, \{q^J\} \right\} \quad (4.28)$$

in which :

$$\{q^I\} = \left\{ u^I, v^I, \theta^I, \left( \frac{\partial u}{\partial z} \right)^I \right\} \quad (4.29)$$

However, it is convenient to express these displacements in a global coordinate system  $\{r_E\}_G$  as shown in Fig.4.7.  $\{r_E\}_G$  can therefore be expressed as:

$$\{r_E\}_G = \left\{ \{r_E^I\}, \{r_E^J\} \right\}_G \quad (4.30)$$



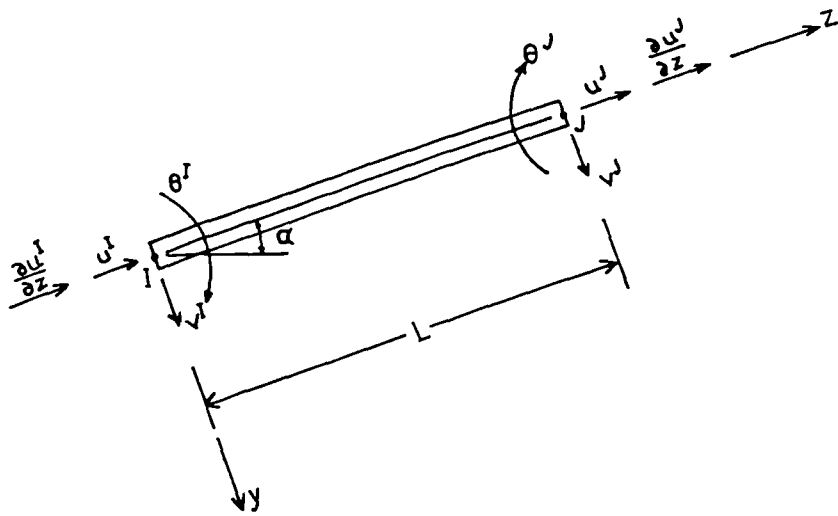


Fig. 4.6 - Local nodal displacements.

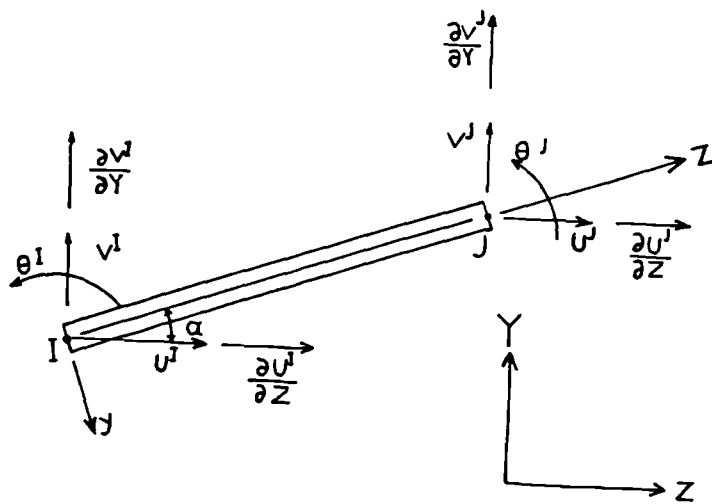


Fig. 4.7 - Global nodal displacements.

in which :

$$\{r_E^I\} = \left\{ U^I, V^I, \theta^I, \left(\frac{\partial U}{\partial z}\right)^I, \left(\frac{\partial V}{\partial Y}\right)^I \right\} \quad (4.31)$$

thus, the element displacements with respect to the local coordinate system  $\{q\}$  can be computed from those in the global coordinate system  $\{r_E\}_G$  using the transformation matrix  $[T]$  as :

$$\{q\} = [T] \{r_E\}_G \quad (4.32)$$

If  $\{R_E\}_G$  is the vector of nodal forces corresponding to global nodal displacements  $\{r_E\}_G$  then by assuming that these forces must perform the same amount of work in both the local and global coordinate systems :

$$\{q\}^T \{Q\} = \{r_E\}_G^T \{R_E\}_G \quad (4.33)$$

Substituting eq.4.32 into eq.4.33 yields :

$$\{r_E\}_G^T [T]^T \{Q\} = \{r_E\}_G^T \{R_E\}_G \quad (4.34)$$

or

$$\{r_E\}_G^T \{[T]^T \{Q\} - \{R_E\}_G\} = 0 \quad (4.35)$$

from which

$$\{R_E\}_G = [T]^T \{Q\} \quad (4.36)$$

Eq.4.25 can therefore be written as :

$$[K_T] \{\Delta r_E\}_G = \{\Delta R_E\}_G \quad (4.37)$$

Assembling the element equations by the direct stiffness method forms the equilibrium equations :

$$[K_T] \{\Delta r\} = \{\Delta R\} \quad (4.38)$$

in which :

$[K_T]$  is the assembled incremental tangent stiffness matrix,

$\{\Delta r\}$  is the assembled vector of incremental nodal displacements in the global coordinate system,

$\{\Delta R\}$  is the assembled vector of unbalanced nodal forces which accounts for thermal effects.

Eq.4.38 is the basic incremental solution using the iterative Newton- Raphson procedure.

#### 4.3.3.1 Evaluation of the tangent stiffness $(k_T)_{ij}$ and the incremental unbalanced force $\Delta Q_i$ .

The incremental equilibrium equation for an element was given by eq.4.24 in which the influence coefficient  $(k_T)_{ij}$  of the tangent stiffness is given by :

$$(k_T)_{ij} = \int_l \left( \frac{\partial a_1}{\partial q_j} \frac{\partial u'_o}{\partial q_i} + \frac{\partial a_2}{\partial q_j} \frac{\partial v'_o}{\partial q_i} + \frac{\partial a_3}{\partial q_j} \frac{\partial v''_o}{\partial q_i} \right) dz \quad (4.39)$$

To evaluate the stiffness coefficient  $(k_T)_{ij}$  and the incremental unbalanced forces  $\Delta Q_i$ , the stress resultants  $n$ ,  $m$ , and  $m^*$  of eqs.4.15 and their derivatives  $\frac{\partial n}{\partial q_j}$ ,  $\frac{\partial m}{\partial q_j}$ , and  $\frac{\partial m^*}{\partial q_j}$  must be evaluated.

To accomplish this, assuming that the stress-strain-temperature relationship is defined and the strain distribution is known, the stress resultants may then be calculated numerically in the  $x - y$  reference plane from their definition [95]. Thus, each plate of the cross-section is divided into 5 regions as shown by Fig.4.8. Eqs.4.15 become :

$$n = \sum_{k=1}^n \sum_{r=1}^5 \frac{1}{2} l_r t_k (\sigma_{ir} + \sigma_{jr})$$

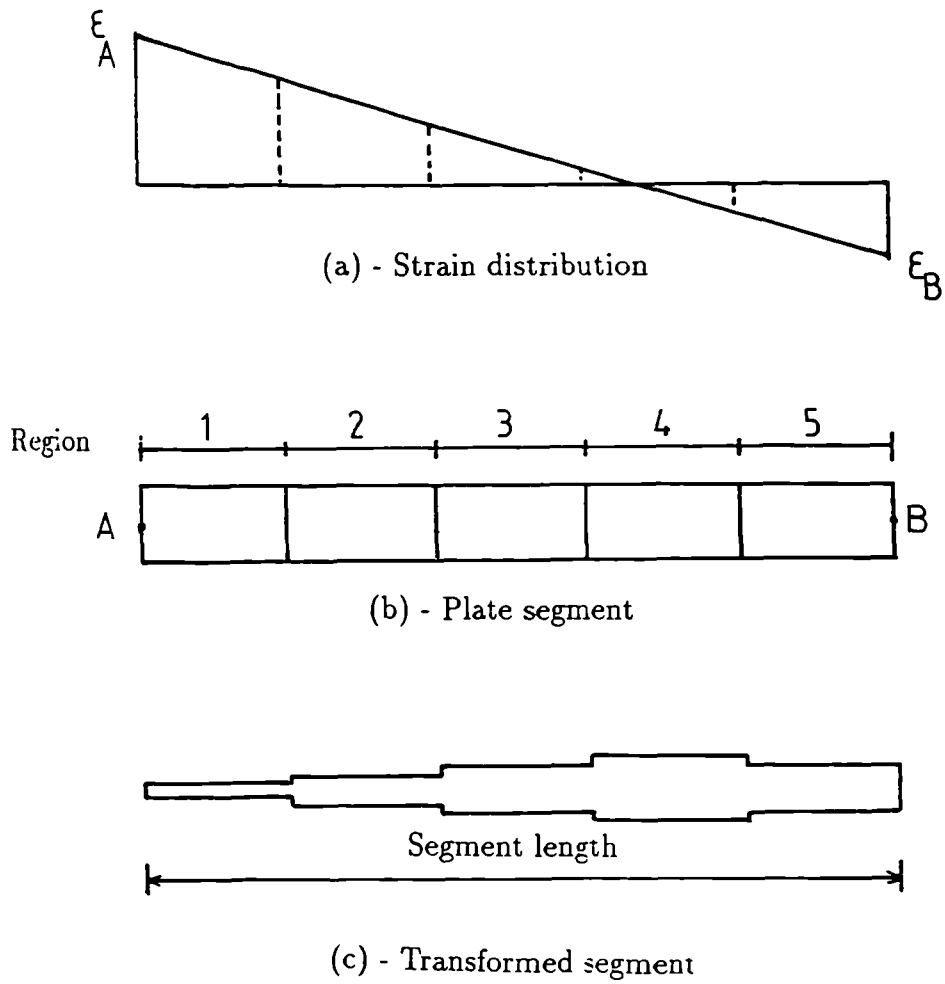


Fig. 4.8 - Transformed section of a plate segment.

$$\begin{aligned}
m &= \sum_{k=1}^n \sum_{r=1}^5 \frac{l_r t_k}{6} [\sigma_{ir}(y_{jr} + 2y_{ir}) + \sigma_{jr}(y_{ir} + 2y_{jr})] \\
m^* &= \sum_{k=1}^n \sum_{r=1}^5 \frac{l_r t_k}{12} [\sigma_{ir}(4y_{ir}^4 + 2y_{jr}^2 - l_r^2) \\
&\quad + \sigma_{jr}(4y_{jr}^4 + 2y_{ir}^2 - l_r^2)] \tag{4.40}
\end{aligned}$$

in which :

$r$  is the plate region,

$n$  is the number of plate segments,

$t_k$  is the plate segment thickness,

$l_r$  is the plate region length,

$i$  and  $j$  refer to the two ends of each region.

This discretisation of the internal forces is particularly suitable for the analysis in which thermal gradient across the section is considered since it allows the calculation of these forces over 4 plate segments with 5 different regions in each plate. Each plate therefore exhibits different resistance to the applied loading depending upon the stress-strain curve at the corresponding temperature level. It is also suitable for the analysis about the weak axis.

The evaluation of the section properties is based on the transformed area approach which allows for nonlinearity in the material to be considered. This method is briefly reviewed in the following section but full details are provided in Ref.[95].

#### 4.3.3.2 Evaluation of the section properties

If each element area is such that the product of the current tangent modulus at any temperature,  $E_t(\theta)$ , times the original element area  $A$ , is equal to the original

effective modulus,  $E_\theta$ , times the element of transformed area  $A^t$ , then :

$$E_t(\theta) A = E_\theta A^t \quad (4.41)$$

from which :

$$b_r^t = \frac{E_t(\theta) b_r}{E_\theta} \quad (4.42)$$

in which  $b_r^t$  is the transformed thickness of a particular region  $r$  and  $b_r$  is the original thickness of the region. The tangent modulus  $E_t(\theta)$  is obtained from the stress-strain-temperature relationship as :

$$E_t(\theta) = \frac{1}{\frac{d\epsilon}{d\alpha}} \quad (4.43)$$

where :

$$\frac{d\epsilon}{d\sigma} = \frac{1}{E_\theta} + 0.01 \eta_\theta \left( \frac{\sigma}{\sigma_{y\theta}} \right)^{\eta_\theta - 1} \frac{1}{\sigma_{y\theta}} \quad (4.44)$$

Thus the section is transformed and the cross-section properties are evaluated as given below :

$$\begin{aligned} A^t &= \int_{A_t} dA^t \\ &= \sum_{k=1}^n A_k \\ I_1^t &= \int_{A_t} y dA^t \\ &= \sum_{k=1}^n A_k Y_k \\ I_2^t &= \int_{A_t} y^2 dA^t \\ &= \sum_{k=1}^n (I_{xx})_k + \sum_{k=1}^n A_k Y_k^2 \\ I_3^t &= \int_{A_t} y^3 dA^t \\ &= 3 \sum_{k=1}^n (I_{xx})_k Y_k + \sum_{k=1}^n A_k Y_k^3 \\ I_4^t &= \int_{A_t} y^4 dA^t \\ &= \sum_{k=1}^n (I_{4xx})_k Y_k^2 + \sum_{k=1}^n A_k Y_k^4 \end{aligned} \quad (4.45)$$

in which  $(I_{xx})_k$  is the moment of inertia of segment  $k$  about the centroidal axis  $x - x$  and  $(I_{4xx})_k$  is defined as :

$$(I_{4xx})_k = \int_A y^4 dA \quad (4.46)$$

#### 4.3.3.3 Evaluation of the incremental stress resultant vector

The incremental stress resultant vector necessary to calculate the vector of internal forces is calculated by differentiating eqs.4.15 :

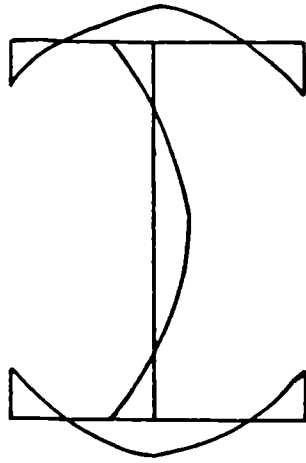
$$\begin{aligned} \delta n &= \int_A E_t(\theta) \delta \epsilon dA \\ \delta m &= \int_A E_t(\theta) \delta \epsilon y dA \\ \delta m^* &= \int_A E_t(\theta) \delta \epsilon y^2 dA \end{aligned} \quad (4.47)$$

using the transformed area approach, eqs.4.45 can be written as :

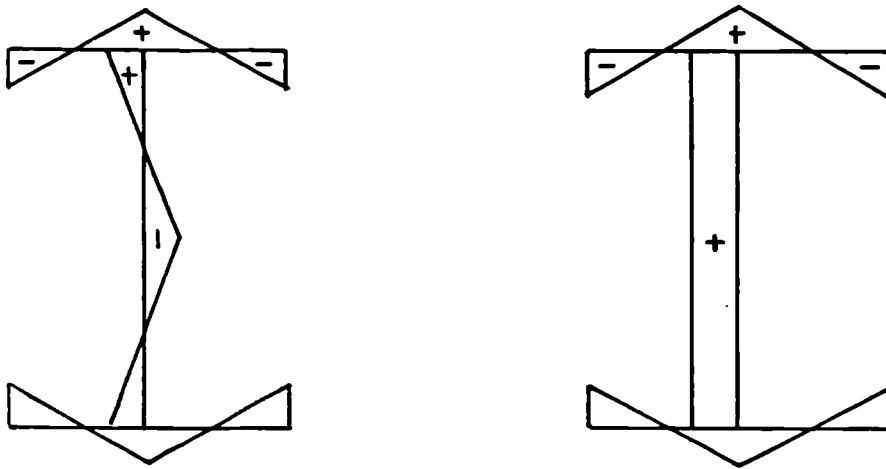
$$\begin{aligned} \frac{\partial n}{\partial q_j} &= \int_{A^t} E_\theta \frac{\partial \epsilon}{\partial q_j} dA^t \\ \frac{\partial m}{\partial q_j} &= \int_{A^t} E_\theta \frac{\partial \epsilon}{\partial q_j} y dA^t \\ \frac{\partial m^*}{\partial q_j} &= \int_{A^t} E_\theta \frac{\partial \epsilon}{\partial q_j} y^2 dA^t \end{aligned} \quad (4.48)$$

from which the values of  $\frac{\partial a_1}{\partial q_j}$ ,  $\frac{\partial a_2}{\partial q_j}$  and  $\frac{\partial a_3}{\partial q_j}$  necessary to evaluate the influence coefficient  $(k_T)_{ij}$  of eq.4.39 is computed.

For any set of nodal displacements, the strain at any point on the element  $\epsilon_z$  due to axial and bending displacements can be evaluated from eq.4.10. Adding the residual strain  $\epsilon_r$  at this stage results in the total strain  $\epsilon_{zt}$  given by eq.4.11. If the residual strains vary across the section, this variation can be approximated by linear segments as shown by Fig.4.9. This is to maintain a linear strain distribution across a plate segment since the total strain distribution will also



(a) - Actual residual strain



(b) - Assumed residual strain

Fig. 4.9 - Residual strain distribution.



be linear in the segment after superposition. The system of residual strains is self-equilibrating, hence :

$$\begin{aligned}\int_A \sigma_r dA &= 0 \\ \int_A \sigma_r y dA &= 0\end{aligned}\tag{4.49}$$

Therefore, for any temperature profile, and given that the strain distribution across the section is known, the stresses are computed from the corresponding stress-strain curve at the relevant temperature level. Since  $\sigma$  is not an explicit function of  $\epsilon$  in the original formula of eq.3.11, the curve is modified into a piecewise form by dividing it into 90 linear pieces. The technique used to find the corresponding stress becomes a comparison rather than the standard computing 'trial and error' technique which is more time consuming. It has been shown that the computer processing time is usually speeded up by 10 to 30 times, with the difference in the calculated stress less than 0.1% between the original and the piecewise forms of the Ramberg-Osgood formula [55]. This, however, does not affect the calculation of the current tangent modulus since it is determined analytically from eq.4.44.

The stress resultants and their derivatives are therefore calculated. The stiffness matrix and the vector of unbalanced forces are also computed and assembled, and the load-deformation characteristics of the structure can therefore be traced using the Newton-Raphson iterative procedure. In order to trace the load-deflection characteristics beyond the peak of the curve, a special treatment must be adopted in order to obtain the descending branch [95]. The descending branch of the load-deflection curve in the inelastic region is characterized by a negative definite stiffness matrix. The determinant of the tangent stiffness matrix undergoes a 'gradient test', that is a check on sign change to determine whether

the stiffness matrix is still positive definite. If this sign changes, then the load is decremented in order to maintain equilibrium.

Before applying the boundary conditions, the tangential stiffness matrix of a structure is singular and therefore cannot be decomposed. In a real steel structure, a variety of boundary conditions may exist :

1. fixed conditions where the corresponding degree of freedom equals to zero.
2. flexible elastic boundary conditions in which the corresponding boundary condition is represented by its elastic spring stiffness.
3. free boundary conditions.

This program represents more realistically the frame boundary conditions by incorporating their elastic stiffnesses (i.e three springs corresponding to the nodal degrees of freedom for each node). Hence, for a fixed boundary condition, a large number is assigned to the corresponding spring stiffness ( $10^{21}$  for example). For a flexible boundary condition, any value can be given to the spring stiffness to allow for a prescribed resistance while zero is assigned for unrestrained condition.

The use of the transformed area approach allows the yielding in the material to penetrate gradually. Dividing the cross-section area into a number of segments allows thermal gradient to be considered when analysing members about both axes of bending. It also allows for the effect of this thermal gradient on the shift of the resultant of internal forces of resistance to be automatically considered when using the appropriate stress-strain curve at the relevant temperature of the segment. The induced moment resulting from this apparent eccentricity of loading is therefore automatically included in the analysis. This is similar to

the apparent eccentricity, prescribed by BS5950 Pt.5, of load produced by loss of effectiveness of thin plating with compressive forces. The iterative procedure adopted in order to determine the load-deformation characteristics of the structure is explained in the following section.

#### 4.3.4 Solution procedure

The solution procedure may best be illustrated with reference to Figs.4.10 and 4.11 for a system with one degree of freedom in which the Newton-Raphson iterative solution technique has been adopted in order to determine the collapse load at a certain temperature level or the critical temperature under sustained loading. This technique has proven to be one of the most useful solution techniques available for nonlinear analysis.

##### 4.3.4.1 Load-deformation characteristics under increasing load and a given temperature level

Referring to Fig.4.10, the load-deformation characteristics under increasing load and constant temperature are found as follows :

1. Set the temperature at  $T_0$  and the load level at  $R_0$ .
2. At the temperature level  $T_0$ , for any approximate set of displacements  $\{r\}_n$ , the stiffness matrix  $[K_T]$  and the vector of unbalanced forces  $\{\Delta R\}_n$  are evaluated as described in section 4.3.3.1.
3. The incremental displacements  $\{\Delta r\}$  necessary to equilibrate the unbalanced forces are evaluated using eq.4.38. The displacements are therefore

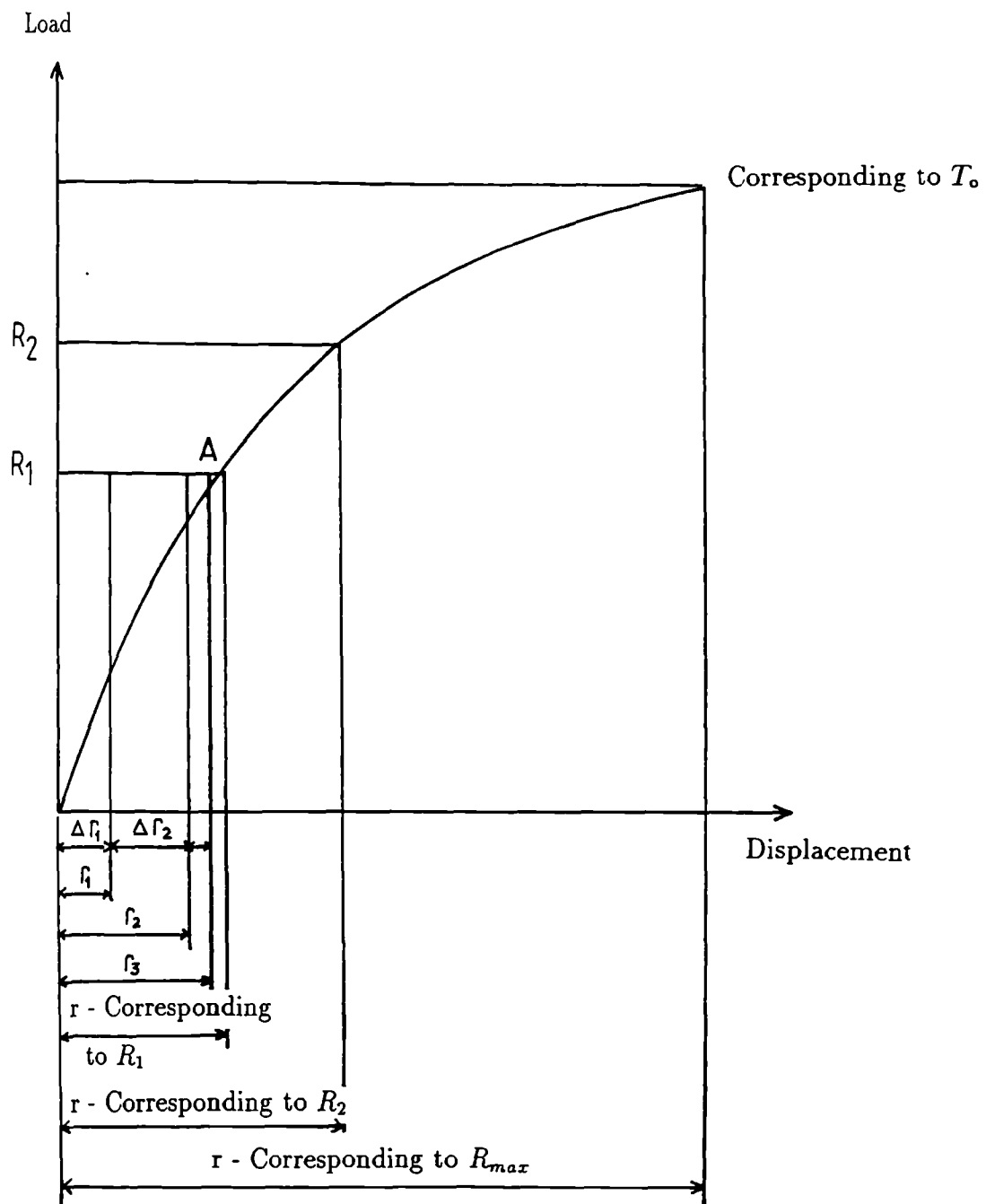


Fig. 4.10 - Newton-Raphson iterative procedure at constant temperature.

updated.

4. Steps 2 and 3 are repeated until the vector of unbalanced forces  $\{\Delta R\}$  and the displacement increments  $\{\Delta r\}$  are sufficiently small. At this stage a point  $A$  on the load-deflection curve is thus obtained.
5. A new load level is applied and steps 2 to 4 are repeated until the load level reaches the maximum required level (Fig.4.10).

This iterative procedure enables the collapse load at a given temperature level to be obtained, together with the load-deformation history of the structure.

#### 4.3.4.2 Load-deformation characteristics under increasing temperature and subject to given load level

Fig.4.11 illustrates the technique used in order to predict the critical temperature of a structure as well as the load-deformation characteristics under increasing temperature. The solution procedure is as follows :

1. Set the temperature at  $T_0$  and the load level at  $R_0$ .
2. At the temperature level  $T_0$ , for any approximate set of displacements  $\{r\}_n$ , the stiffness matrix  $[K_T]$  and the vector of unbalanced forces  $\{\Delta R\}_n$  are evaluated as described in section 4.3.3.1.
3. The incremental displacements  $\{\Delta r\}$  necessary to equilibrate the unbalanced forces are evaluated using eq.4.38. The displacements are therefore updated.

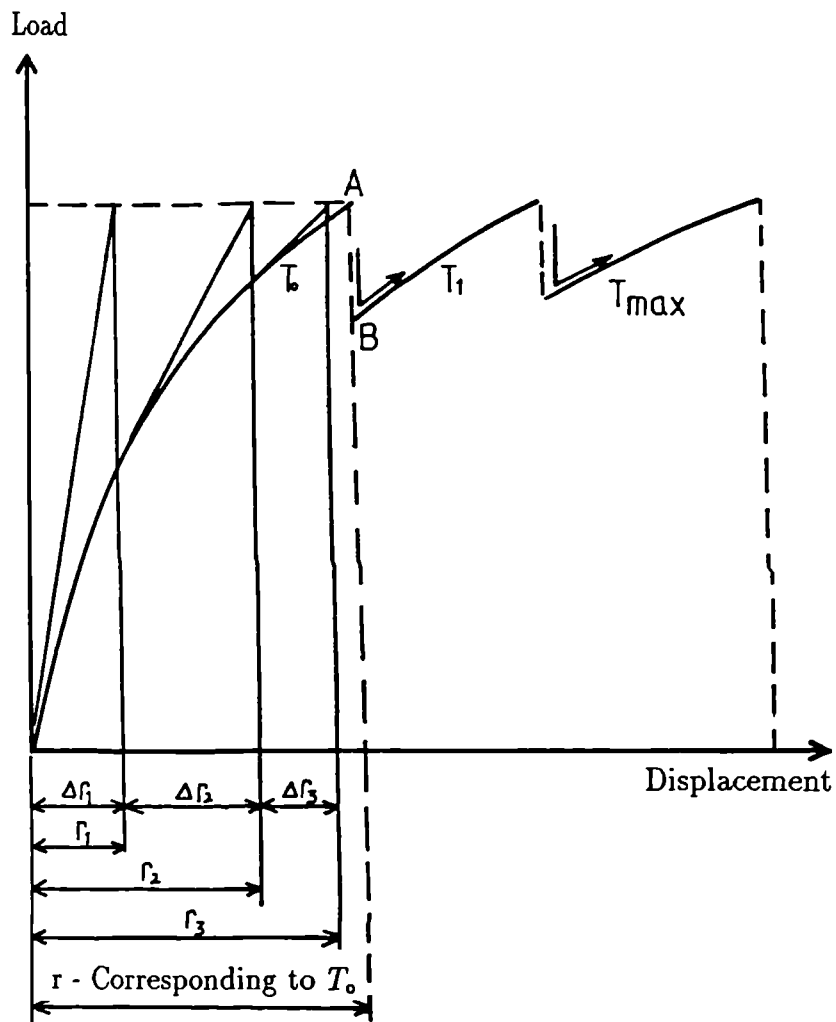


Fig. 4.11 - Newton-Raphson iterative procedure at increasing temperature.

4. Steps 2 and 3 are repeated until the vector of unbalanced forces  $\{\Delta R\}$  and the displacement increments  $\{\Delta r\}$  are arbitrarily small. At this stage a point  $A$  on the load-deflection curve is thus obtained.
5. A new temperature level is applied while the load level is kept constant. New material properties and stress-strain relationship are thus introduced, and a new load-deformation curve corresponding to the current temperature level is also introduced. At this stage, the previously calculated set of displacements, which corresponds to a lower load level, is stored in order to save computing time and used as initial deformations for subsequent analysis. Using the analysis described in section 4.3.3.1, the internal stress resultants are therefore evaluated and thus a point  $B$  on the newly introduced curve is obtained. Incompatibility in displacements necessitates that steps 2 to 4 are repeated in order to restore equilibrium and consequently to find the appropriate set of displacements which corresponds to the applied load level.

This solution procedure is repeated at each temperature level until the temperature reaches the maximum required level. This results in the prediction of the critical temperature and the full deformation history of the structure (Fig.4.11).

## 4.4 Computer program

A finite element computer program has been developed using the above formulation to predict the deformational behaviour, collapse load and critical temperature of steel frames. However, since the basic iterative solution procedure becomes independent of temperature once the corresponding material properties

and stress-strain relationship are introduced, this program makes use of the basic stiffness subroutine of INSTAF.

The procedure described in this chapter has been implemented in INSTAF. The temperature profile is required as an input either in a continuous form or as a set of discrete points. The section is then discretised into four different plates allowing for 4 different heating zones to be considered. The internal forces and moments are then evaluated for each plate from eq.4.40 using the appropriate material characteristics. This has the advantage of producing the additional moment due to the shift of the effective stress resultant which overshadows the effect of thermal bowing as calculated from Appendix A at the beginning of each temperature increment and is considered as an initial lack of straightness. Both the continuous and bilinear representations of the stress-strain curve have been added to the program as well as the ECCS, CTICM and BS5950 material properties. The division of the cross-section into a large number of segments allows yielding in the material to penetrate gradually over the section using the transformed area approach. Failure could be detected by imposing a limit on the strain or deformation rate although a full deformation history can be obtained if no limits are imposed. The program also allows different cross-sections, material types and temperature profiles to be considered along the member as well as the effects of residual strains and initial lack of straightness.

The program is written in FORTRAN 77 language and implemented on IBM 3083 machine. A general flowchart of the logical steps of the program is given in Fig.4.12.



- (1) START
- (2) Input : nodal geometry, member properties, boundary conditions, Loads,  
Temperature profile, Nonlinear control analysis
- (3) Assemble load vector
- (4) Set approximate displacements
- (5) *GO TO* (8)
- (6) Read information from previous step
- (7) Assemble load vector if temperature is constant  
Introduce new temperature profile if temperature is increasing
- (8) Evaluate tangent stiffness matrix
- (9) Evaluate vector of unbalanced forces
- (10) Calculate increment in displacements to equilibrate the unbalanced forces
- (11) Update displacements
- (12) Check convergence
- (13) Return to (8) if no convergence  
Stop if divergence  
Output displacements and stresses if converged
- (14) Check if temperature is increasing
- (15) *GO TO* (6) if temperature is constant  
If temperature is increasing : introduce new material characteristics
- (16) *GO TO* (6)
- (17) END.

**Fig. 4.12** - Logical sequence of the program.

## 4.5 Summary

A formulation for the nonlinear analysis of two dimensional steel frames under fire conditions using the finite element method has been presented. Deterioration in material strength with increasing temperatures is represented by a set of nonlinear stress-strain-temperature relationships using a Ramberg-Osgood equation in which creep effects are implicitly included. Structures subject to increasing loads or temperatures are analysed using an incremental Newton-Raphson iterative procedure. The analysis permits the deformation history and either collapse load or critical temperature to be calculated at specified temperature or load levels respectively. It includes the effects of geometric nonlinearity, temperature dependent nonlinear material behaviour and variations in temperature distributions both along and across the section. The effects of thermal strains, residual stresses and thermal bowing are also considered and different material models and constitutive relationships can be used. The validity of the present approach is verified in the next chapter.

## Chapter 5

# Comparison with Experimental and Analytical Data

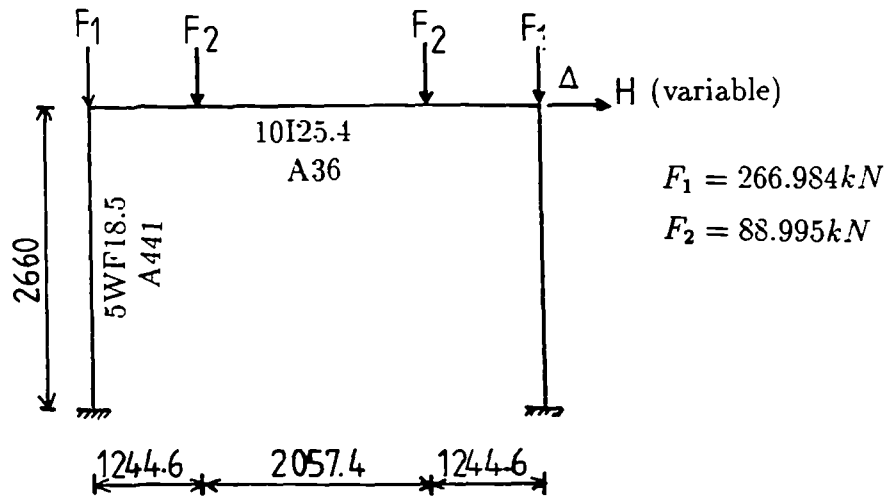
In order to establish the validity of the present approach as developed in Chapter 4, the program has been thoroughly checked against a selection of test results that represent a wide range of problem parameters. These include : an initial comparison with a room temperature frame test, column tests and frame tests, as well as comparison with theoretical results in which temperature gradient effects are present. The room temperature comparison was undertaken in order to check the basic ability of the program to deal with load - deformation response. The elevated temperature studies include a range of frame slenderness, end conditions, load levels and temperature profiles.

The analyses are based on the reported heating histories; and the stress-strain-temperature relationships described in section 2.4 are used unless otherwise stated. Collapse load or critical temperature are those given by the experimental results. In those cases where these critical states are not provided, failure is

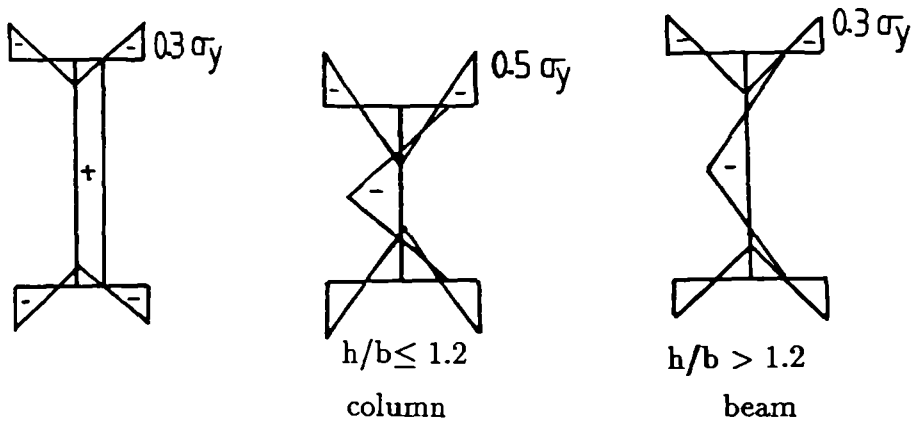
assumed when deformations anywhere on the frame increase in an uncontrollable fashion, corresponding to the last converged solution obtained from the program.

## 5.1 Room temperature comparison

Arnold et al (1968) have provided results for a test on the frame shown in Fig.5.1(a). This was designed so that the geometry and relative stiffnesses would be representative of the lower stories of a multistorey frame. Loading was intended to produce failure by a combined beam and column mechanism, involving significant instability effects. The test procedure involved the application of a constant vertical load followed by increase of lateral load to failure. The yield stress, modulus of elasticity and residual strains were measured at six locations around the cross-sections of the beam and column. Using these values, five analyses were carried out, with each using one set of yield stress, elastic modulus and residual strain values as shown in Table 5.1. It can be seen from Table 5.1 that all calculations lead to results for the ultimate load that are in basic agreement with the test results. The difference between the calculated and test results has resulted mainly from the values of the yield stress and modulus of elasticity used in the analyses. The influence of each of the material characteristics on the collapse load is clear from calculations nos.3,4,5. The highest collapse load was obtained on the basis of calculation no.3 in which the highest values of the yield stress and modulus of elasticity were used, whereas lower collapse loads were obtained from calculations nos.4 and 5 when low values of either one or both of the material characteristics were used. This is due to the fact that this frame fails in a combined material yielding and elastic overall instability mode, and therefore both the stiffness and yield strength of the material are effective in preventing collapse



(a) - Test frame and loads.



(b) all members

(c) ECCS values

Fig. 5.1 - Frame geometry and loadings for room temperature comparison.

		1	2	3	4	5
$\sigma_y$ ( $N/mm^2$ )	Beam	266.002 <sup>(b)</sup>		286.235 <sup>(a)</sup>	255.197 <sup>(c)</sup>	
	Column	387.393 <sup>(b)</sup>		390.380 <sup>(a)</sup>	384.865 <sup>(c)</sup>	
$E$ ( $kN/mm^2$ )	Beam	203.317 <sup>(b)</sup>		204.201 <sup>(a)</sup>		202.537 <sup>(c)</sup>
	Column	215.457 <sup>(b)</sup>		257.889 <sup>(a)</sup>		203.305 <sup>(c)</sup>
$\sigma_{res}$	Beam	(d)	(e)		(f)	
	Column					
$H_{ult}$ ( $kN$ )	Calculated	70.9	71.14	77.7	70.9	67.65
		-4%	-3.68%	+5.2%	-4%	-8.4%
Tested $H_{ult}$ ( $kN$ )		73.86				

(a) highest values.

(b) measured mean values.

(c) lowest values.

(d) measured values.

(e) Fig.5.1(b).

(f) ECCS values, Fig.5.1(c).

Table 5.1 - Input data and results for ambient temperature comparison.

of this frame. Furthermore, the contribution of the yield stress and modulus of elasticity were different as can be seen from calculations nos.4 and 5. A decrease of about 9% in the ultimate load resulted mainly from the lower values of the yield stress used in calculation no.4, whereas a further decrease of only 4% was obtained when lower values of the elastic modulus were used in case no.5. This is due to the fact that heavy concentrated vertical loads were kept constant whilst only the horizontal load was increased. Hence the influence of the yield stress is more predominant in delaying the collapse of this frame. On the other hand, using the measured mean values of the material properties in cases nos.1 and 2 has resulted in the value of the collapse load which approximately represents the average value of the calculated collapse loads. Moreover, it can be seen from calculations nos.1 and 2 that residual stress magnitude and distribution have no significant influence on the calculated collapse loads of this frame.

The predicted responses are shown by solid lines in Fig.5.2 in which the predicted deflections compare very favourably with test results. The test deflections are somewhat higher than those predicted by calculations nos. 3 and 4, and lower than deflections predicted on the basis of calculations nos. 1, 2 and 5. Whilst the values of the yield stress and modulus of elasticity have significantly affected the collapse load of this frame, these values have resulted in different effects on the sway deflections of the frame. The relatively lower lateral deflection exhibited on the basis of calculations nos.3 and 4 has resulted mainly from the high values of modulus of elasticity used in the analyses, although calculation no.4 results in a lower collapse load. A relatively higher sway was exhibited by calculations nos.1,2,5 regardless of the values of yield stress used in the analyses. In all of these calculations lower values of the modulus of elasticity were used. The fact that using high values for the elastic modulus in calculation no. 4 results in lower lateral deflection is justified by the fact that only horizontal load is

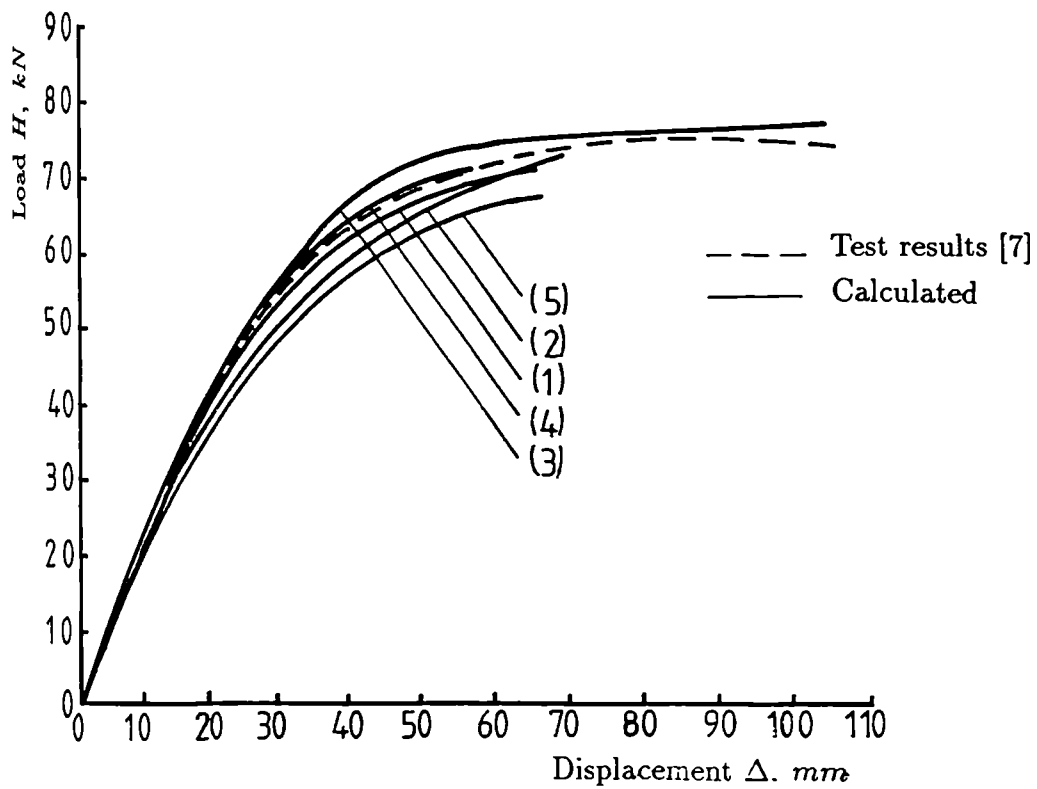


Fig. 5.2 - Comparison between predicted lateral deflections and test results [7].



increased whereas heavy concentrated vertical loads have been taken as constant. This suggests that using high stiffness material, especially for the columns, leads to a smaller sway of this frame.

The above comparison confirms the ability of the program to deal with ambient temperature behaviour.

## 5.2 Comparison with elevated temperature tests

### 5.2.1 Comparison with Aasen (1985)

Aasen (1985) has reported tests on 15 pin-ended and 5 end restrained steel columns milled from IPE 160 sections. All specimens were made from high strength steel with a measured average value of ambient temperature yield strength of  $448 \text{ N/mm}^2$ . Three columns, nos. 7, 11, 15, were provided with rotational restraint through beams at both ends of the column. In those cases, the beams were kept cold throughout the testing programme which provided these columns with a constant degree of restraint  $k$  given in Table 5.2. In the analytical simulation, a constant degree of end restraint is given as an input and this is kept constant during the analysis. Although initial geometric imperfections were reported, no details of residual stresses were provided. The columns had slenderness ratios of between 92 and 169 and were subject to loading of between 30% and 100% of the room temperature pin-ended buckling load. The highest load level  $1.0P_e$  was chosen for tests nos. 7, 11 and 15 in order to demonstrate the beneficial effect of end restraint for those columns. Heating was provided by low voltage electrical elements attached to the outside of each flange. Temperature distributions were

measured during the tests and were found to vary both along and across the sections of the structural elements. These temperatures were reported, and are used in this comparison.

Table 5.2 summarises the main test parameters used in the calculations together with the measured and calculated failure temperatures. The complete set of tests embraced a wide range of column slenderness, rotational restraint conditions, end eccentricities and temperature gradients both along and across the columns. In all cases very good agreement was obtained between the predicted failure temperatures and those reported from the tests as indicated both from the individual values of Table 5.2 and the overall comparison of Fig.5.3. The relatively large difference between the calculated and tested critical temperatures of column no. 12 can be explained by comparison with column no. 14 in which the initial lack of straightness is the only difference in input data. This alone cannot be responsible for the lower critical temperature of column no. 12 which suggests that other unknown effects have resulted in a weaker column during the test. On the other hand, agreement between the predicted and measured lateral deflections at mid-height of the columns are equally good as can be seen from Fig.5.4 which represents a typical load-deflection curve.

## 5.2.2 Comparison with Rubert and Schaumann (1986)

Rubert and Schaumann (1986) have tested the series of frames shown in Fig.5.5. Typical spans  $l$  were 1200 mm with typical column heights  $h$  of 1170 mm. The ambient temperature yield strength and modulus of elasticity were approximately 400 N/mm<sup>2</sup> and 210 kN/mm<sup>2</sup> respectively. Frame slenderness ratios  $\bar{\lambda}_{sys}$ , defined as the square root of the simple plastic collapse load divided by the elastic critical

No.	$\lambda$	$P$ (kN)	$P/P_{cr,20}$	$W_{o\ max}$ (mm)	ecc. $e$ (mm)	end res. $k$ (kNm/rd)	crit. temp. ( $^{\circ}C$ )	
							test	calc.
2	169	91.20	0.7	4.21	-	-	471	480
5	169	68.10	0.5	7.91	-	-	527	537
6	169	90.90	0.7	3.40	-	-	460	480
7	169	143.0	1.0	3.20	-	1711	632	600
8	120	168.9	0.7	3.97	-	-	452	460
9	120	129.9	0.5	4.26	-	-	525	540
10	120	168.8	0.7	0.59	-	-	481	470
11	120	246.9	1.0	1.10	-	1711	619	600
12	92	246.7	0.7	2.90	-	-	351	456
13	92	181.9	0.5	2.21	-	-	466	500
14	92	246.6	0.7	0.86	-	-	473	460
15	92	363.9	1.0	1.80	-	1711	584	585
16	92	98.00	0.3	1.36	-	-	679	678
19	92	98.00	0.3	1.91	13.8	-	575	520
20	92	97.90	0.3	0.80	19.7	-	564	530

Table 5.2 - Input data and results for comparison with column tests [1].

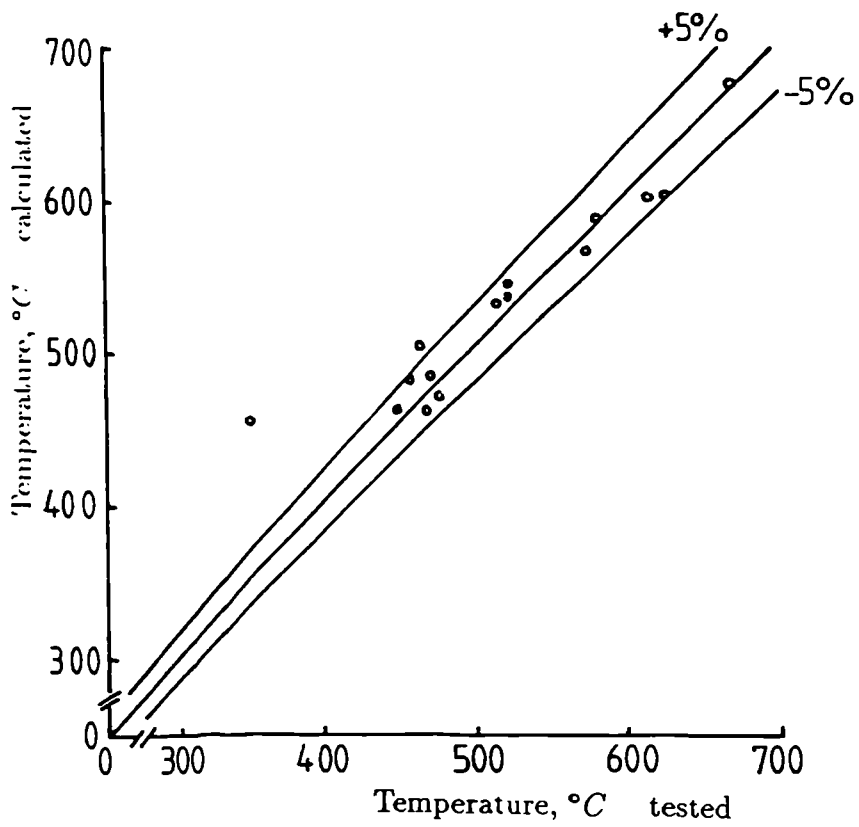


Fig. 5.3 - Comparison between predicted and measured critical temperatures [1].

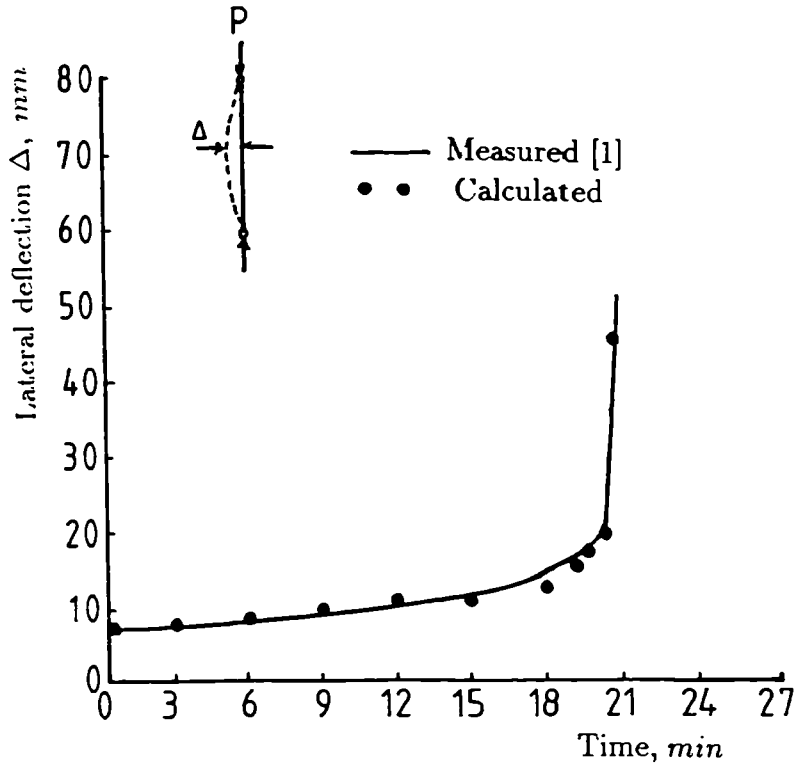


Fig. 5.4 - Mid-height deflection of column No.8.

load, varied between 0.33 and 1.00. The applied vertical load was varied between 38% and 79% of the ambient temperature ultimate load with the lateral load being held at 1.9% of the vertical load for frame type *EGR* and 1.28% for frame type *ZSR*. Table 5.3 summarises the main test parameters used in the calculations. All frames were uniformly heated at a constant rate using electrical elements. The *EHR* type frames were subjected to uniform temperature rises, whilst the beams in two frames of the *EGR* type were kept at ambient temperature and the *ZSR* frames had one beam and one column insulated. Table 5.3 gives the predicted critical temperatures, defined as the maximum temperature anywhere on the frame, at which deformations increased in an uncontrollable fashion and corresponding to the last converged solution from the program. These compare very favourably with those reported from the tests of Ref.[77], as indicated by the graphical comparison of Fig.5.6. More detailed comparisons of the temperature-deformation history for those three tests for which such data are available are given in Figs. 5.7, 5.8, 5.9. In all cases the analysis correctly follows the trend of the test behaviour, with the quantitative agreement being particularly good for frames *EGR1* and *ZSR1*. In the case of *EHR3* agreement is not quite as good, especially for the beam deflections; while the fact that the analysis of Ref.[77] was also less close to the experimental results in this case suggests the possibility of less representative input data being used.

### 5.3 Comparison with analytical results

Furumura and Shinohara (1978) reported results of the analysis of a beam and a single-bay portal frame using an elastic-plastic computer program based on large deformation theory. The nonlinear inelastic analysis which is based on a stiffness

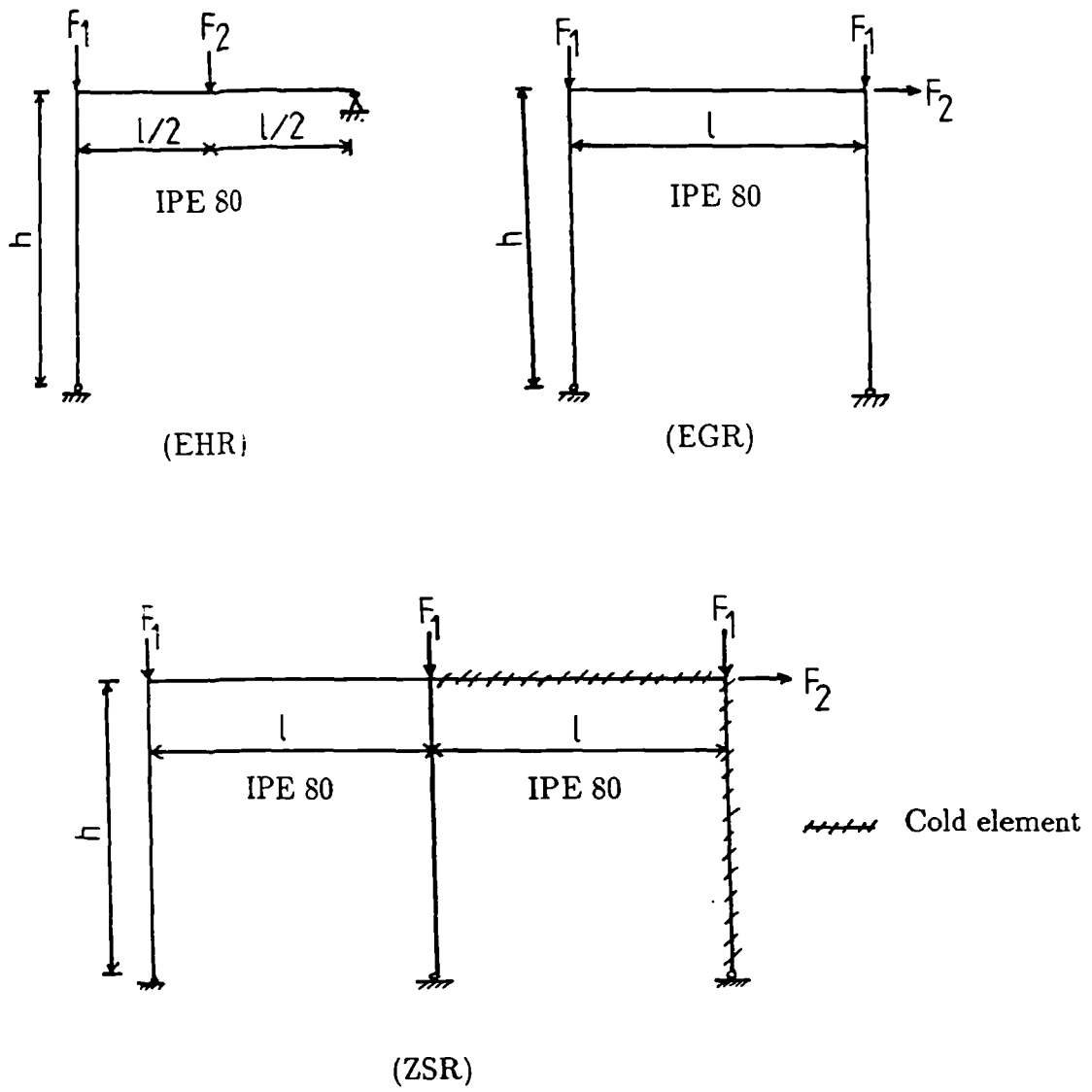


Fig. 5.5 - Frame types for comparison with Ref.[77].

Type	$l$ (mm)	$h$ (mm)	$\sigma_y$ (N/mm <sup>2</sup> )	$F_1$ (kN)	$F_2$ (kN)	$F/F_u$	$\bar{\lambda}_{sys}$	Critical temp.		*
								test (°C)	calculated (°C)	
<i>EHR1</i>	1190	1170	395	56	14	0.38	0.33	600	608	(a)
<i>EHR2</i>	1240	1170	395	84	21	0.59	0.33	530	550	
<i>EHR3</i>	1240	1170	382	112	28	0.82	0.33	475	476	
<i>EHR4</i>	1250	1500	389	20	5	0.59	0.65	562	540	(b)
<i>EHR5</i>	1250	1500	389	24	6	0.71	0.65	460	460	
<i>EHR6</i>	1250	1500	389	27	6.7	0.79	0.65	523	514	
<i>EGR1</i>	1220	1170	382	65	2.5	0.55	0.93	515	506	(c)
<i>EGR2</i>	1220	1170	385	40	1.6	0.34	0.93	612	574	
<i>EGR3</i>	1220	1170	385	77	3.0	0.66	0.93	388	400	
<i>EGR4</i>	1220	1170	412	77	3.0	0.63	0.96	424	408	
<i>EGR5</i>	1220	1170	412	88	3.4	0.72	0.96	335	341	
<i>EGR6</i>	1220	1170	412	88	3.4	0.72	0.96	350	341	
<i>EGR7</i>	1220	1170	320	68.5	2.6	0.65	0.84	454	420	(d)
<i>EGR8</i>	1220	1170	385	77	3.0	0.7	0.89	464	425	
<i>ZSR1</i>	1200	1180	355	74	2.85	0.6	0.94	547	525	(e)
<i>ZSR2</i>	1200	1180	380	84.5	3.25	0.66	0.97	479	476	
<i>ZSR3</i>	1200	1180	432	68.5	2.64	0.5	1.00	574	582	

\*

- (a) Fully heated : Major axis bending.  
(b) Fully heated : Minor axis bending.  
(c) Fully heated : Major axis bending.  
(d) Cold beam : Major axis bending.  
(e) Partial heating, Fig.5.5 : Major axis bending.

Table 5.3 - Input data and results for comparison with frame tests [77].

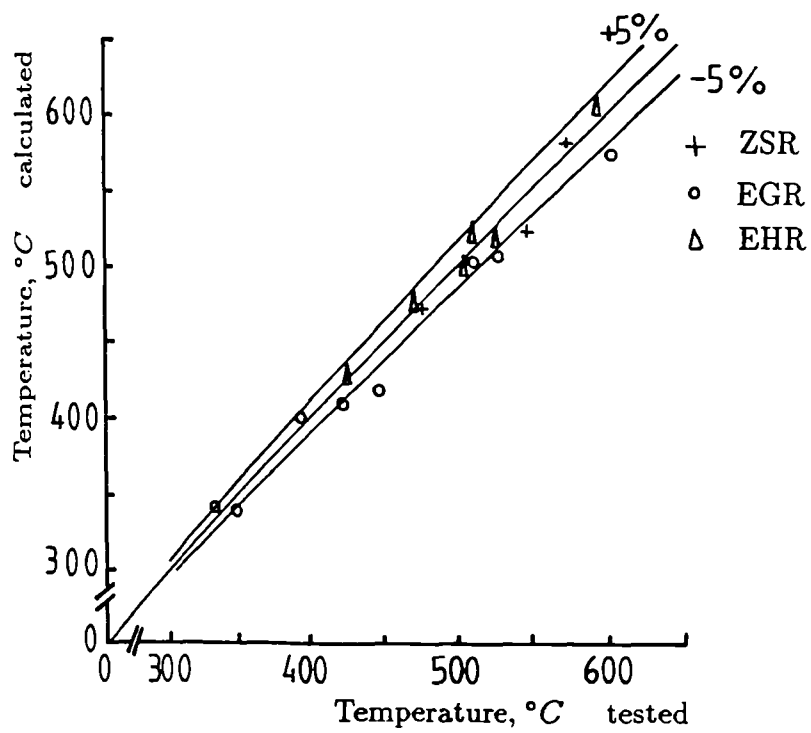


Fig. 5.6 - Comparison between predicted and measured critical temperatures [77].



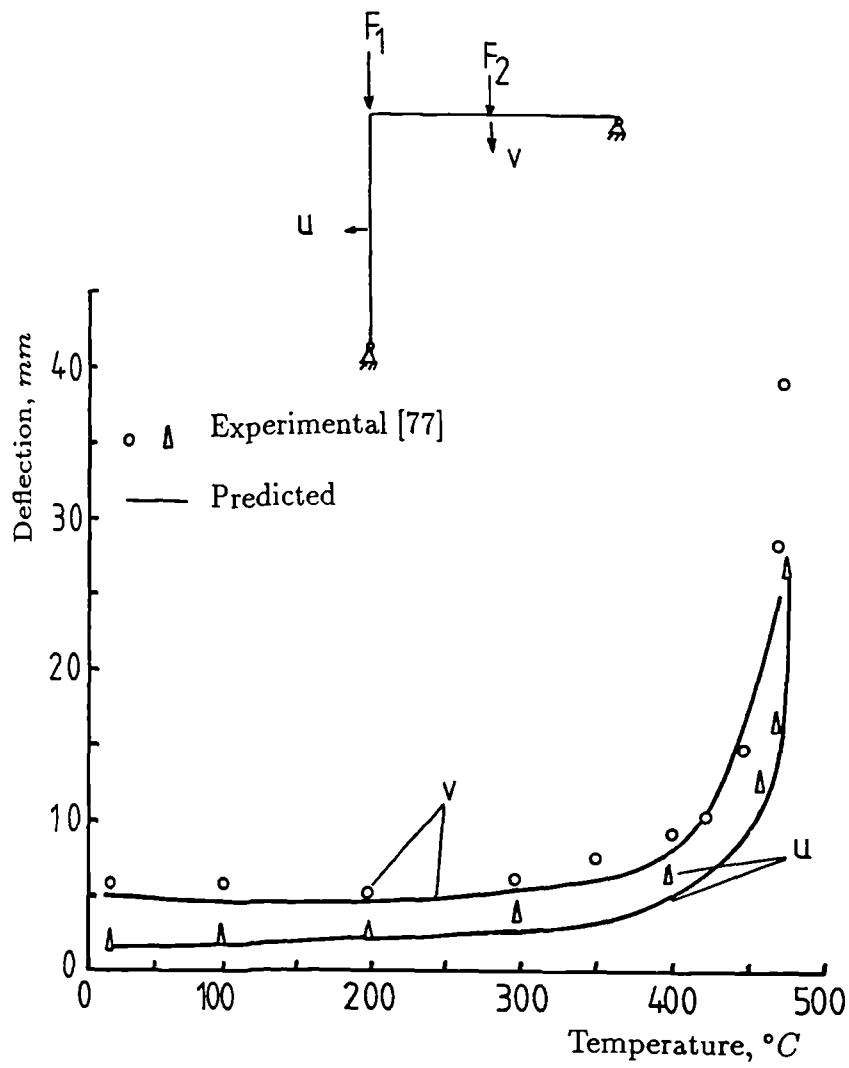


Fig. 5.7 - Comparison between calculated and measured deflections of frame EHR3 [77].

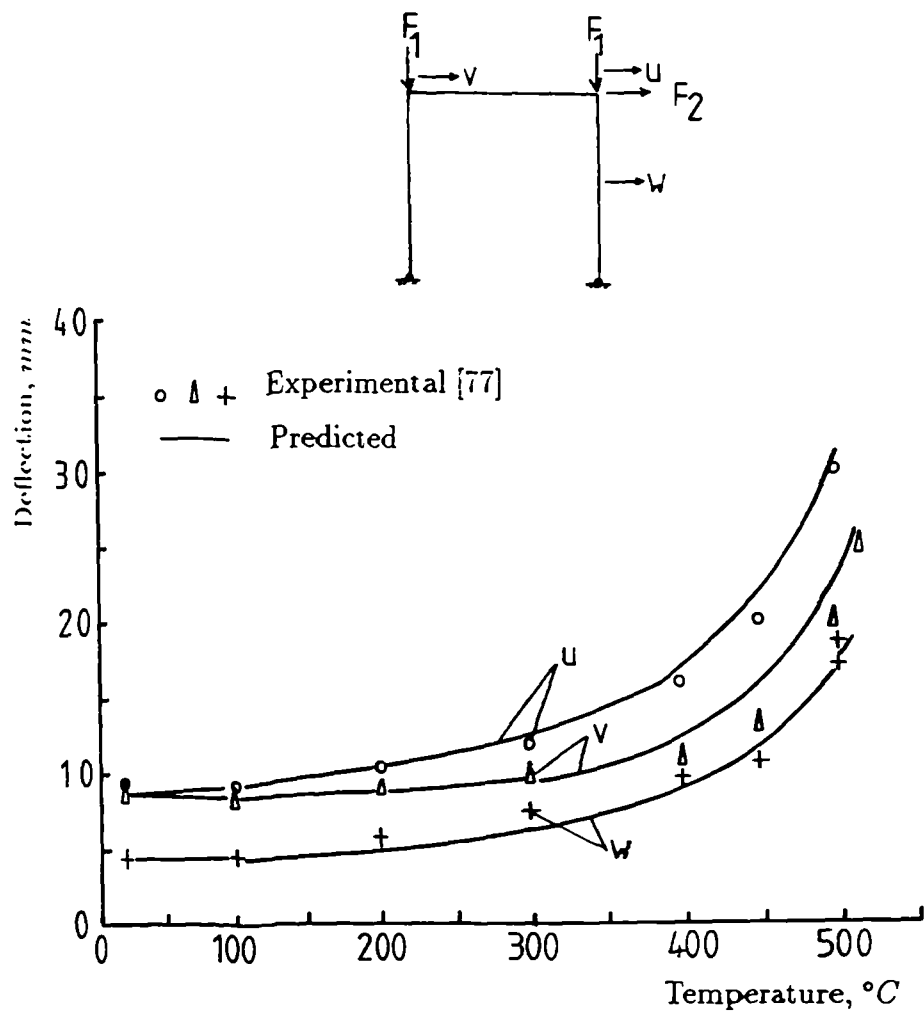


Fig. 5.8 - Comparison between calculated and measured deflections of frame EGR1 [77].

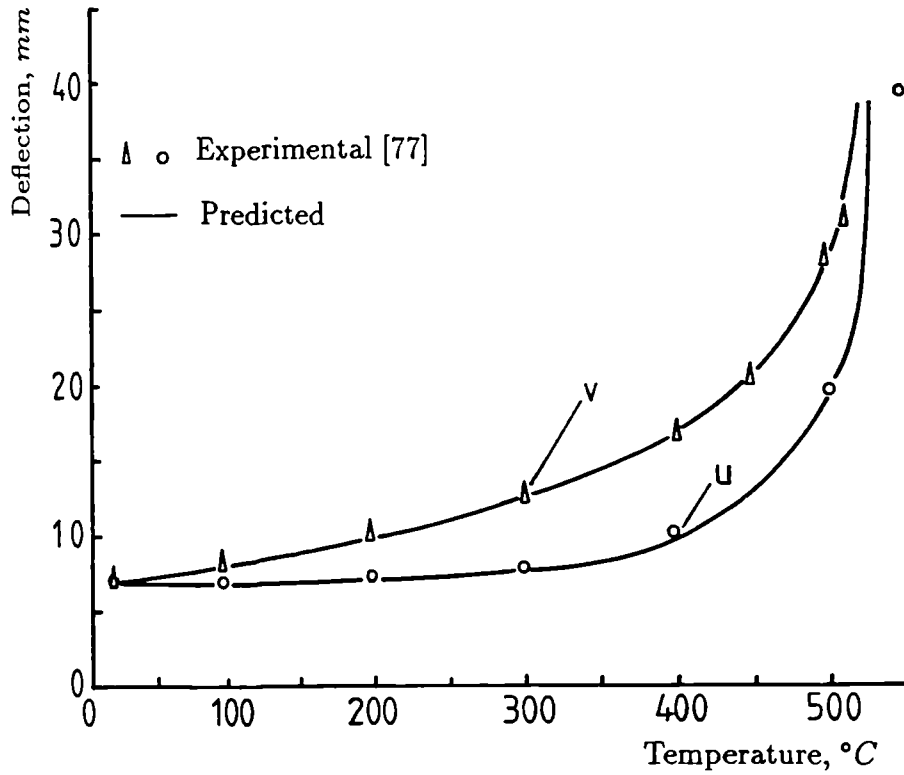
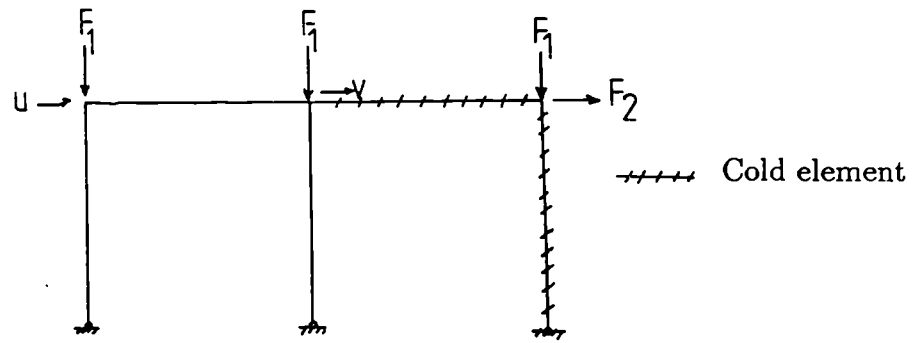


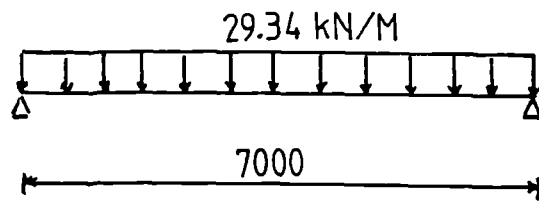
Fig. 5.9 - Comparison between calculated and measured deflections of frame ZSR1 [77].

formulation, includes geometric nonlinearity and an extensive model to deal with the effects of creep. A set of bilinear stress-strain-temperature relationships was used in which the values of the elastic modulus at elevated temperature were combined with a constant yield strain. The coefficient of thermal expansion was considered as a function of temperature. The ambient temperature yield strength and modulus of elasticity were taken from the stress-strain curves as  $345 \text{ N/mm}^2$  and  $216 \text{ kN/mm}^2$  respectively. Temperature gradients across the beam and column sections were calculated using a thermal analysis computer program with an assumed gas temperature rise taken from fire tests. The structural analysis was carried out with a relatively small time step of 30 seconds up to the time limit of 120 minutes.

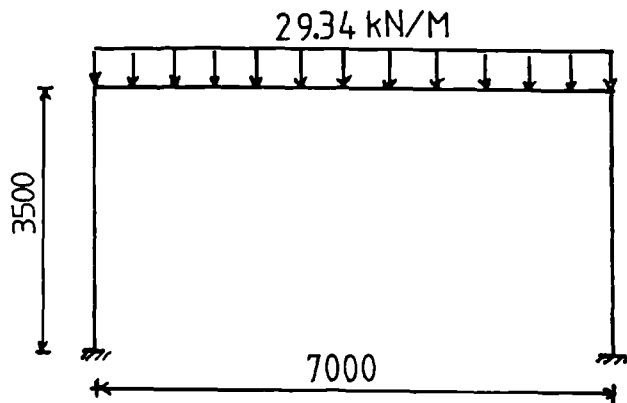
Calculations were carried out for the beam and frame shown in Fig.5.10(a) and Fig.5.10(b) respectively. The beam, having a span of  $7\text{m}$ , was loaded by a uniformly distributed load of  $29.34 \text{ kN/m}$ . Three calculations were undertaken for this beam representing different end restraints : a simply supported, hinged ends (i.e lateral movement of the beam is restrained) and both ends fixed. The frame, which has similar beam span and cross-section, has a column height of  $3.5 \text{ m}$  and was loaded by the same distributed load on its beam only. In all cases, calculations were carried out using the same stress-strain-temperature curves, material properties and temperature profiles.

Results of the analysis carried out with a time step of 15 minutes compare very favourably with the reported data in which creep effects have been excluded, as shown by Figs.5.11 - 5.14 which represent the simply supported, hinged ends and both ends fixed beams, and the frame respectively. The horizontal expansion  $d_H$  of the simply supported beam shown in Fig.5.11 increases sharply beyond 30 minutes following the increase in the section temperatures. This has kept the

Beam section : 400x200x8x13    Column section : 350x350x12x19



(a)



(b)

Fig. 5.10 - Beam and frame configurations for comparison with analytical results [33].

central deflection  $d_v$  of the beam at a relatively low level. Furthermore, Fig.5.12 shows that the axial force  $P$  developed by the hinge-ended beam as a result of restraining its ends against expansion increases to a peak of approximately 1300  $kN$  while the deflection is still relatively small. This axial force starts to decrease as a result of an abrupt increase in the central deflection of the beam. In the case where the central deflection remains at a lower level due to the built-in conditions of the ends of the beam (Fig.5.13), the axial force continues to increase, though at a decreasing rate after 30 minutes approximately, until a higher temperature level is reached which reduces the axial rigidity of the section. This causes the axial forces to decrease and the central deflection to increase up to failure. The central deflection of the frame shown in Fig.5.14 is plotted only for data points at which this deflection was provided. The upward deflection of the beam, which has a comparatively smaller flexural rigidity than that of the column, follows the bowing of the columns towards the compartment fire up to 45 minutes approximately before it starts to deflect in the direction of the applied load.

In all cases, the analysis correctly follows the behaviour predicted by Ref.[33] with the quantitative agreement being particularly good up to 75 minutes approximately. The fact that the analysis of Ref.[33] was noticeably higher beyond this time level when the effects of creep have been included suggests the need for more representative material data at high temperatures.

## 5.4 Review of verification studies

A total of 41 test and analytical results covering a wide range of problem parameters have been simulated in this chapter. Five calculations have been carried

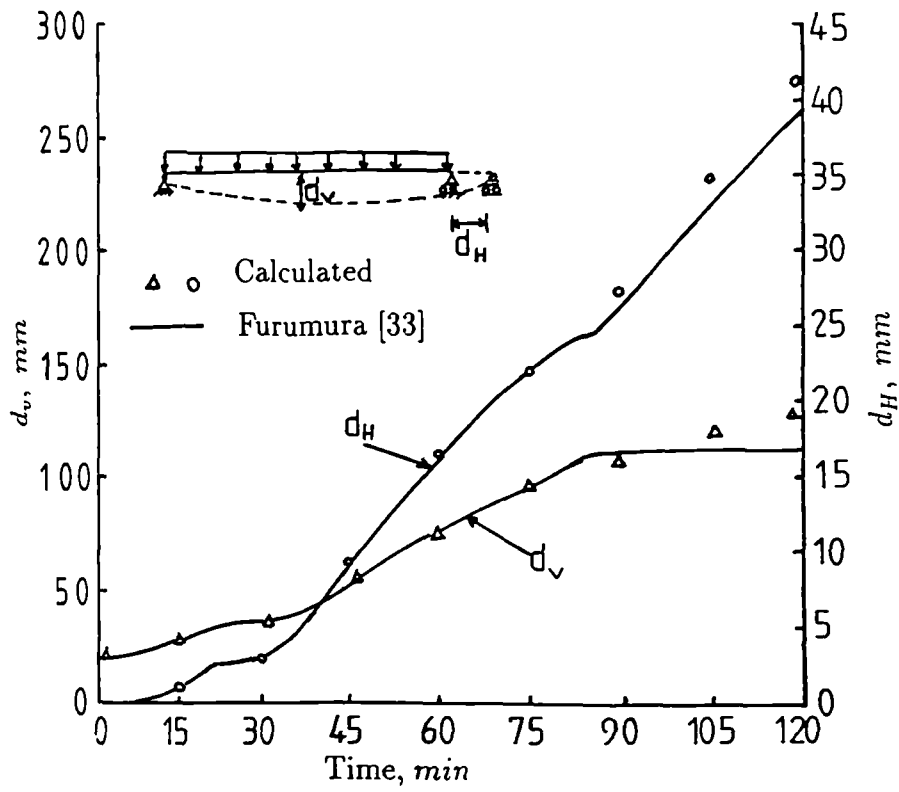


Fig. 5.11 - Comparison with Furumura [33] for simply supported beam.

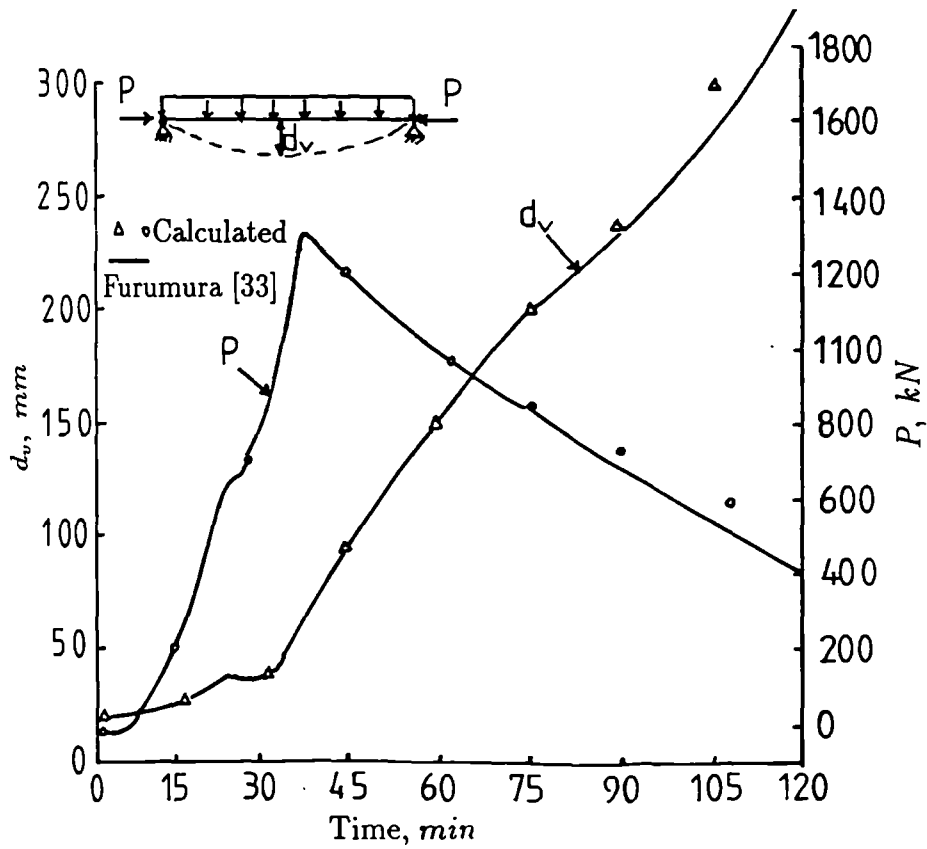


Fig. 5.12 - Comparison with Furumura [33] for hinge-ended beam.

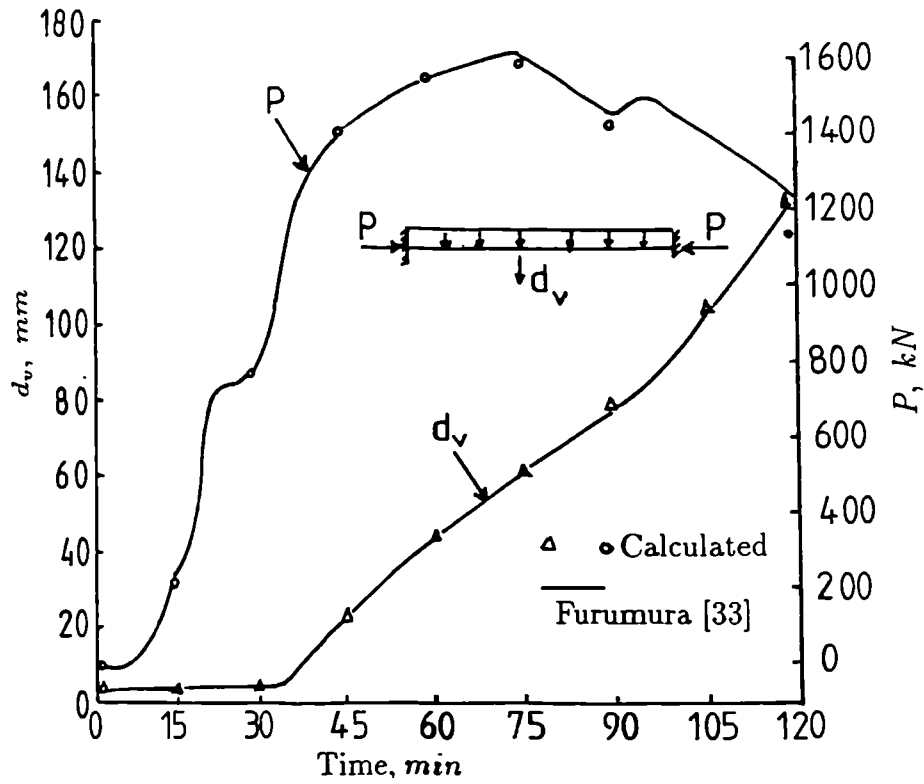


Fig. 5.13 - Comparison with Furumura [33] for fixed-ended beam.

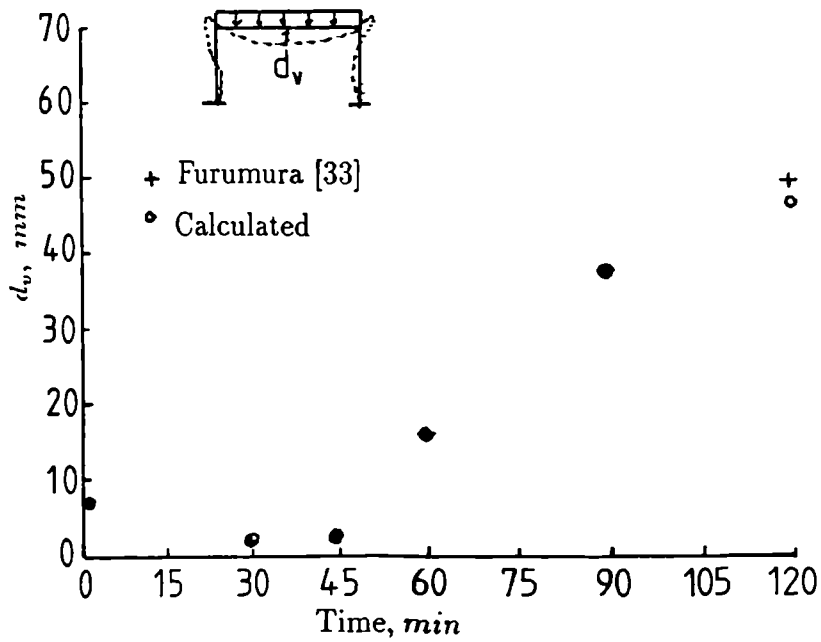


Fig. 5.14 - Comparison with Furumura [33] for frame results.



out at ambient temperature together with 15 column and 17 frame fire testing results. Four other calculations have been undertaken for comparison with analytical results.

The ambient temperature simulations have tested the basic ability of the program to deal with the load - deformation response of frames. It also investigated the effect of variation in input data on the response of frames. Different values of elastic modulus, yield stress and residual stress distribution were used in the analyses. In all cases, the numerical simulations correctly predicted the collapse load and deformational behaviour of the frame. The predicted results have also correctly followed the variation in input data.

Simulation of column tests have demonstrated the ability of the program to deal with a wide range of parameters at elevated temperatures. In these tests, temperature gradient both along and across the section were considered. The columns had a wide range of slenderness ratios and were subjected to an equally wide range of load ratios. The test specimens had pin ends but five columns were provided with a constant rotational restraint through cold beams at both ends of the column. This numerical simulation recognises any degree of restraint at the ends, and thus the reported values were assigned to the relevant degree of freedom. Initial out-of-straightness, residual stress and load eccentricities were also considered. In all cases, the analyses have resulted in very good agreement with the reported data.

Simulation of frame tests has similarly demonstrated the ability of the program to deal with a wide range of problem parameters. This was the only set of frame tests which has been located where sufficient input parameters for numerical simulation have been reported, and agreement between the predicted

and measured results was very good. The fact that tests *EGR5* and *EGR6* of table 5.3 have been carried out on the same frame and exhibited larger discrepancy than the numerical simulation shows that the program can reproduce test results with good accuracy if representative data is provided. The reported comparisons were the only test results provided by the authors.

Comparisons with the analytical results have tested the ability of the program to deal with the effect of axial forces due to thermal restraint and variation of these forces with the change of axial and flexural rigidities of the section. In all cases, the calculated results have correctly predicted the behaviour of the structures under fire conditions.

## 5.5 Conclusions

The above comparisons show that the approach described in Chapter 4 is an efficient numerical method for the analysis of structural elements under fire conditions. Prediction of failure temperature or collapse load and deformation history can be made with very good accuracy. Although the above tests were the only fire test results which have been located in which sufficient input parameters for numerical simulation have been reported, especially in the case of frame tests, the small discrepancy between the test results and predictions is due to the difficulty in reproducing exact representation and measurements taken during tests. These include material characteristics, temperature profiles both along and across each member, cross-section dimensions and geometry of the structure, end condition representations and initial imperfections. The effects of these parameters are studied in the next chapter.

# Chapter 6

## Behavioural Studies

In Chapter 4, a numerical approach for the analysis of the structural behaviour of steel frames at elevated temperatures based on a stiffness formulation was presented. The validity of this approach was then verified in Chapter 5 by comparing the results with the available data covering as wide a problem range as possible.

The aim of this chapter is to investigate the effects of some parameters which are known to affect the overall behaviour of fire exposed steel frames. First, elevated temperature buckling curves for uniformly heated steel columns are derived and compared to those of ECCS [29]. Then, the effects of these parameters are studied on a simple two-bar frame in which the complex interaction of an extensive frame is avoided. The effects of slenderness ratio, stress-strain representation and material models, various forms of protection, magnitude of residual strains and thermal gradient along and across the section are investigated. An approximate curve based on statistical analysis of the derived results is suggested as a simple means of predicting the critical temperature or collapse load of a uniformly heated steel frame. Further examples are presented which illustrate

the special form of moment redistribution that occurs at elevated temperatures for frames that contain partially heated elements.

## 6.1 Inelastic buckling of steel columns at elevated temperatures

Buckling of steel columns at elevated temperatures can occur in a variety of modes : local, interactive and overall. Which of these will govern a particular case depends on many factors such as the cross-sectional shape, slenderness ratio, magnitude and distribution of residual stresses, geometric imperfection, eccentricity of loading, end conditions and material properties.

The ECCS buckling curves at elevated temperatures [29] have been derived on the basis of the room temperature design curve but allowing for the influence of elevated temperatures on the yield stress (eq.3.6). The present work offers the opportunity to check these curves for pin-ended columns using the analysis described in Chapter 4. To this end, an IPE 80 section was analysed for a range of slenderness ratios  $L/r$  from 20 to 180. Since no perfectly straight member exists in practice, the analysis includes initial imperfection of a maximum of  $L/1000$  at mid-height. The initial deflected shape was assumed to be a half sine wave over the length of the member. residual strains, resulting from differential cooling during fabrication or manufacture, have been considered; their distribution over the cross section can be approximated by linear segments as shown by Fig.6.1 with a maximum magnitude of  $0.3\sigma_{y20}$ . No attempt has been made to redistribute these stresses in fire since no measurement of the reduction in their values has been reported. Heating is assumed to be uniform and the ECCS expressions for

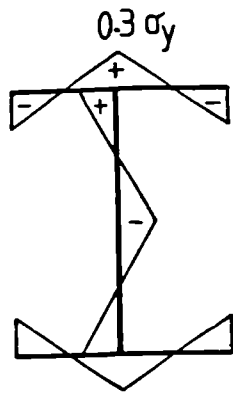


Fig. 6.1 - Residual stress distribution.

yield strength (eq.3.7) and modulus of elasticity (eq.3.3) were used along with an assumed elastic-perfectly plastic stress-strain relationship given by :

$$\sigma = E_{\theta} \{ \epsilon_{y,\theta} + \delta (\epsilon - \epsilon_{y,\theta}) \} \quad (6.1)$$

where :

$$\delta = \begin{cases} 1 & \sigma < \sigma_{y\theta} \\ 0 & \sigma \geq \sigma_{y\theta} \end{cases}$$

The ambient temperature yield strength and elastic modulus were assumed as  $400 \text{ N/mm}^2$  and  $210 \text{ kN/mm}^2$  respectively.

Fig.6.2 shows the relationship between failure stress  $\sigma_{cr}$  and slenderness ratio  $L/r$  with increasing temperature. The critical stress is nondimensionalised with respect to the ambient temperature yield stress  $\sigma_{y,20}$ . At ambient temperature, the familiar response of very stocky columns ( $L/r \leq 15$ ) being controlled by material yielding is clear while high slenderness columns ( $L/r \geq 70$ ) fail in an elastic overall buckling mode; the behaviour of intermediate slenderness columns is clearly influenced by both modes of failure. At  $200^{\circ}\text{C}$  and  $300^{\circ}\text{C}$  similar curves are obtained but at a reduced critical stress. This reduction in critical stresses becomes less with increasing slenderness up to  $L/r = 120$  after which it becomes negligible.

At higher temperatures, similar curves are obtained but at a much reduced critical stress due to further deterioration in material properties. The two distinctive influences of material yielding and elastic overall buckling are still shown by these curves for the stocky and high slenderness columns respectively, with the interaction between these two failure modes affecting a wider range of column slenderness ratios due to softening of the material. It is worth noting that the tendency of stocky columns to reach the effective squash load increases with

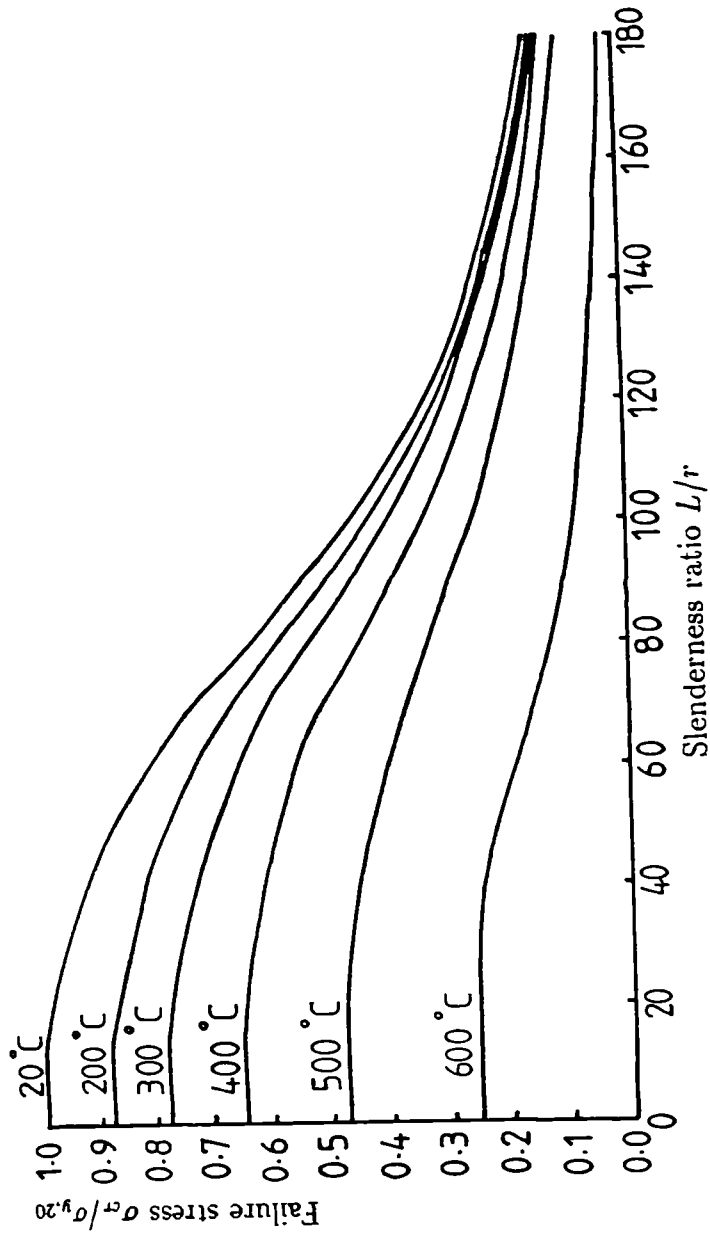


Fig. 6.2 - Variation of failure stress with column slenderness ratio at increasing temperature.

temperature. For example, the maximum slenderness to buckle at the effective squash load increases from 15 at room temperature to 40 at 600°C. This may be due to the use of an elastic-perfectly plastic stress-strain curve since the ratio  $\sigma_{y,\theta}/E_\theta$  increases with temperature. For further comparison, these curves are plotted against the ECCS curves in Fig.6.3.

The same information is plotted in Fig.6.4 as the nondimensionalised critical stress ( $\sigma_{cr}/\sigma_{y,20}$ ) against temperature. It is clear that, for very stocky columns ( $L/r \leq 15$ ), the critical stress decreases gradually and uniformly with increasing temperature in a similar fashion to the reduction in yield strength (curve (c), Fig.3.2). At increasing slenderness, critical stress continues to decrease with increasing temperature but at a much reduced rate due to the increasing influence of the modulus of elasticity. This influence is clear from the response of very slender columns ( $L/r = 180$ ) which show negligible loss in strength up to 400°C before a sudden drop in the curve similar to the reduction in the elastic modulus (curve(c), Fig.3.1) as temperature further increases.

It therefore seems reasonable to conclude that the behaviour of stocky columns is influenced by material yield strength while modulus of elasticity controls the response of slender columns at elevated temperatures. The behaviour of intermediate columns is influenced by both material strength and stiffness. It is important to note that eccentricity of loading affects these curves.

## 6.2 Frame response at elevated temperatures

An IPE 80 section frame is analysed over a range of frame slenderness ratios  $\bar{\lambda}$  from 0.27 to 0.89. The frame geometry is shown in Fig.6.5 while Table 6.1



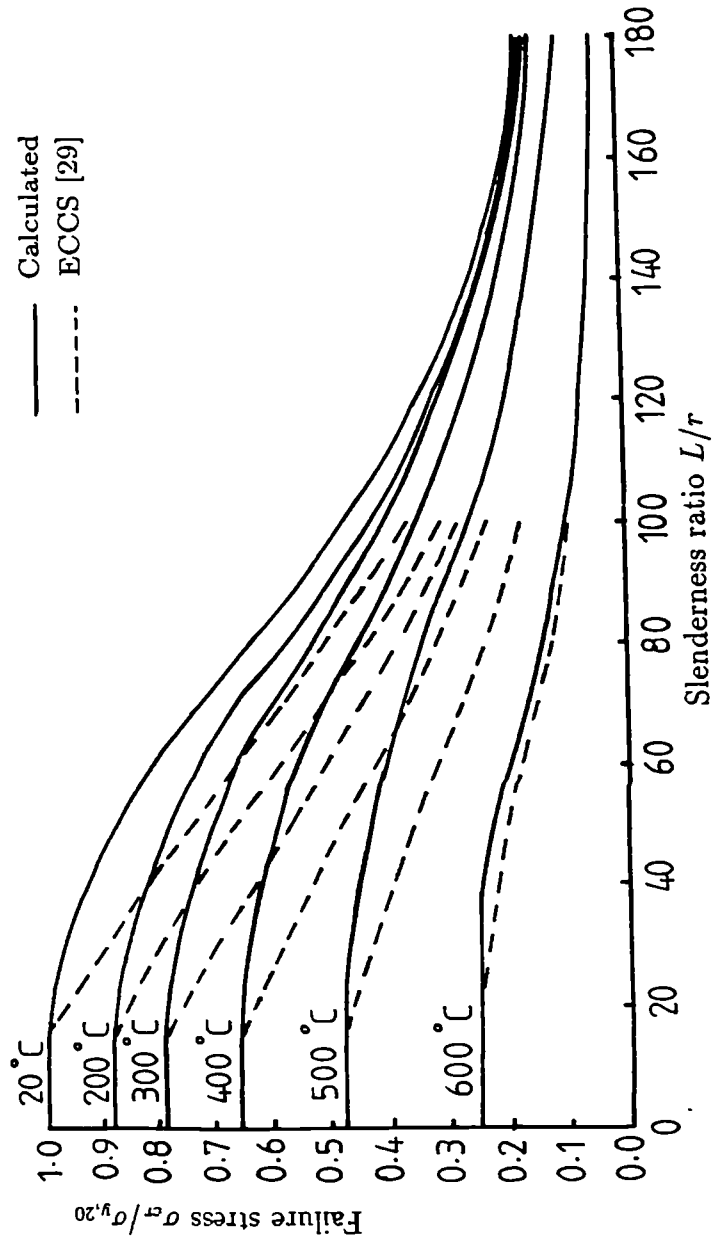


Fig. 6.3 - Comparison between calculated column buckling curves and ECCS [29] at increasing temperature.

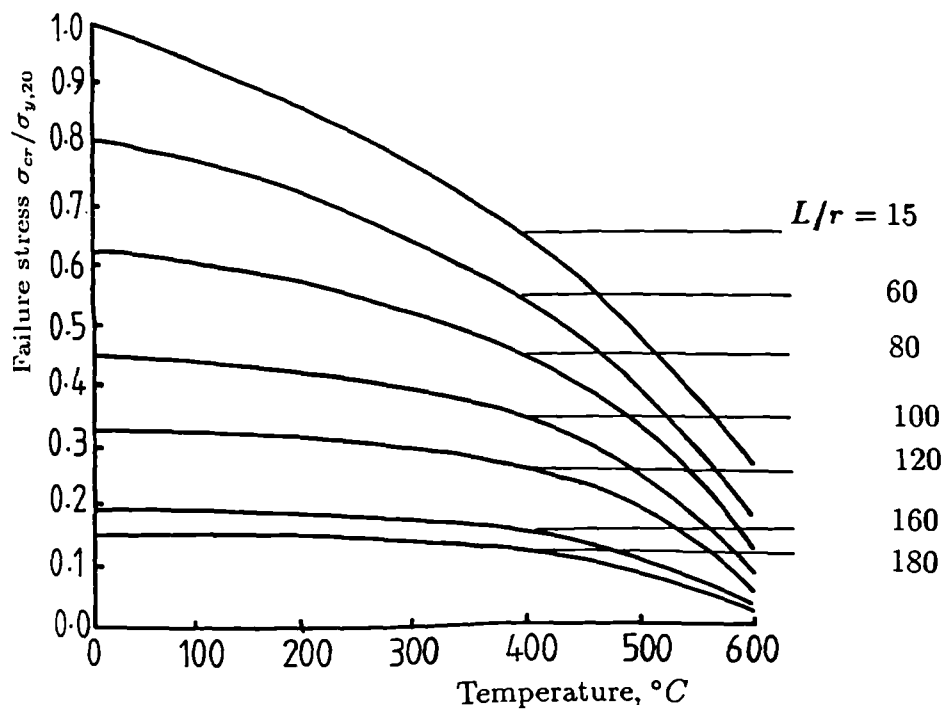


Fig. 6.4 - Variation of failure stress with temperature at increasing slenderness ratio.

summarises the input data for the calculation of  $\bar{\lambda}$  (eq.6.2). The ambient temperature yield strength and modulus of elasticity are assumed to be  $400 \text{ N/mm}^2$  and  $210 \text{ kN/mm}^2$  respectively. Uniform heating is assumed throughout this section unless otherwise stated.

### 6.2.1 Effect of slenderness ratio

The collapse of steel frames at ambient temperature usually occurs by a combination of instability and material yielding. Although these two modes of failure are distinct, a practical frame may fail in a combined mode, albeit in some cases with one mode of failure being predominant.

For the frame which fails purely by material yielding, its failure load depends only upon the material strength. By contrast, failure is elastic in nature for very slender frames and the critical load is therefore independent of the yield stress, being dependent upon the modulus of elasticity  $E$ , the moment of inertia  $I$ , the member lengths and the end conditions.

It is therefore essential to define a system slenderness ratio  $\bar{\lambda}$  upon which the inelastic behaviour of frames depends at ambient temperature. A representative expression for frame characteristics (geometry, material response, stability effects) can be defined in a system slenderness ratio as [77] :

$$\bar{\lambda} = \sqrt{\frac{F_u}{F_e}} \quad (6.2)$$

where  $F_u$  is the load bearing capacity of the frame using nonlinear inelastic analysis and  $F_e$  is the load bearing capacity of the frame using second order elastic analysis, both of which can be determined using the program. For a given load combination  $F$ ,  $F_u$  and  $F_e$  are multiples of  $F$ , and  $\bar{\lambda}$  can therefore be expressed

$l$ (mm)	$h$ (mm)	$F_e/F_u$	$\bar{\lambda} = \sqrt{\frac{F_u}{F_e}}$
1000	1000	13.5	0.27
1250	1500	11.5	0.3
1000	1500	9.0	0.33
1250	2500	3.5	0.54
1250	5000	1.25	0.89

Table 6.1 - Input data for calculation of  $\bar{\lambda}$ .

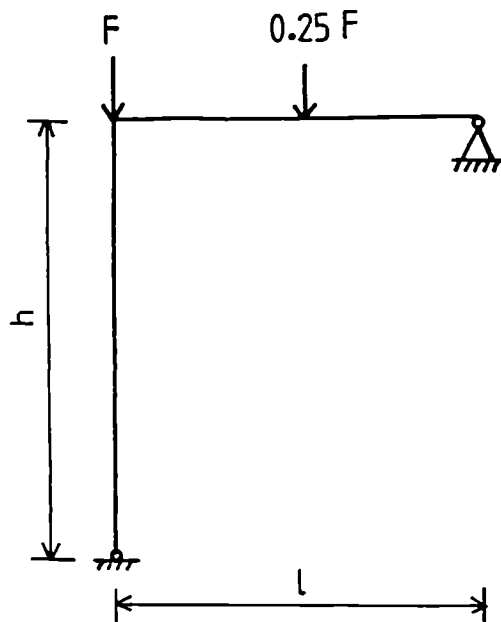


Fig. 6.5 - Frame geometry and loading for parametric studies.

in terms of the ultimate load factor  $\nu_u$  using nonlinear inelastic analysis and the elastic load factor  $\nu_e$  using second order elastic analysis as follows :

$$\bar{\lambda} = \sqrt{\frac{\nu_u}{\nu_e}} \quad (6.3)$$

Results of the analysis are shown in Fig.6.6 where relations between collapse load  $F_u$  and slenderness ratio  $\bar{\lambda}$  at increasing temperature are plotted. The collapse load is nondimensionalised with respect to room temperature collapse load  $F_{u,20}$ . It is shown that very low slenderness ratio frames ( $\bar{\lambda} = 0.27$ ) lose strength gradually up to  $400^\circ C$ ; beyond this temperature level, the decrease in frame strength becomes more rapid as the temperature further increases. This behaviour is very similar to that of the material yield strength (curve(a), Fig.3.2) which confirms that the collapse of very low slenderness frames is dominated by material yielding. For more slender frames ( $\bar{\lambda} \geq 0.5$ ), the loss of strength occurs at a more reduced rate between  $20^\circ C$  and  $250^\circ C$ . Loss of strength at a higher rate is exhibited by such frames as temperature further increases. For these frames, stability is more important and the pronounced influence of material stiffness is clear from the similarity between this curve and that of Fig.3.1 (curve(a)). For further comparison, the same information is plotted in Fig.6.7 as absolute collapse load - temperature relationships. This shows the diminishing effect of the slenderness ratio on the collapse load of frames.

The behaviour of intermediate slenderness frames ( $0.3 \leq \bar{\lambda} \leq 0.5$ ) is similar to that of low slenderness frames but at a reducing collapse load. These frames lose strength at a uniform rate with increasing temperatures and show no sudden drop. In this range of slenderness, collapse is dominated by interaction between instability and material yielding.

It therefore seems reasonable to conclude that frames lose strength at dif-

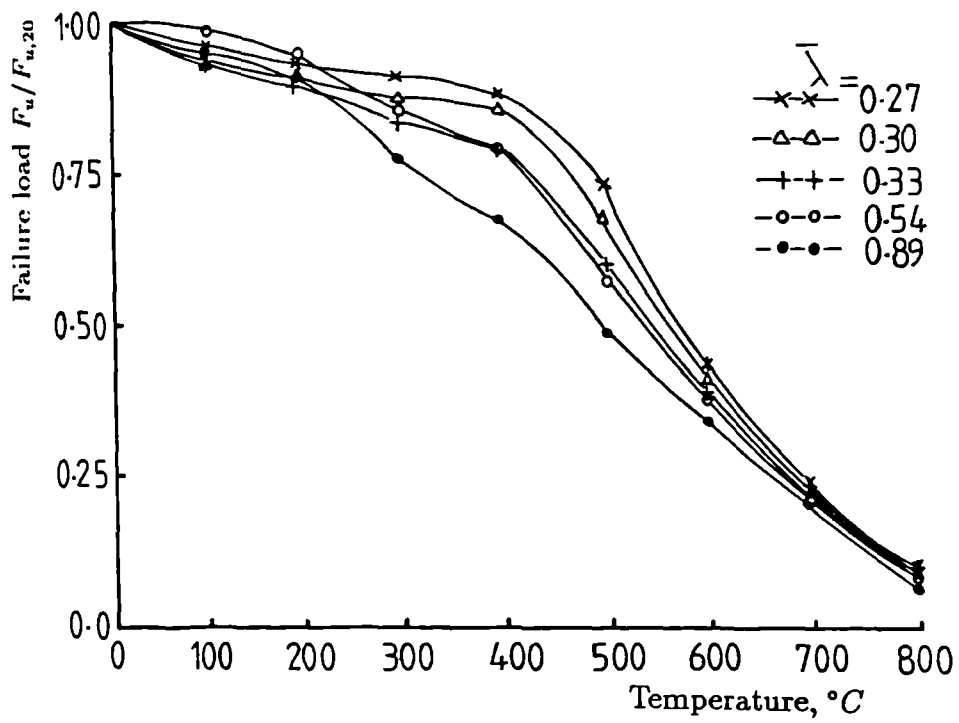


Fig. 6.6 - Variation of failure load with temperature at increasing slenderness using BS5950 expressions and continuous  $\sigma - \epsilon$ .

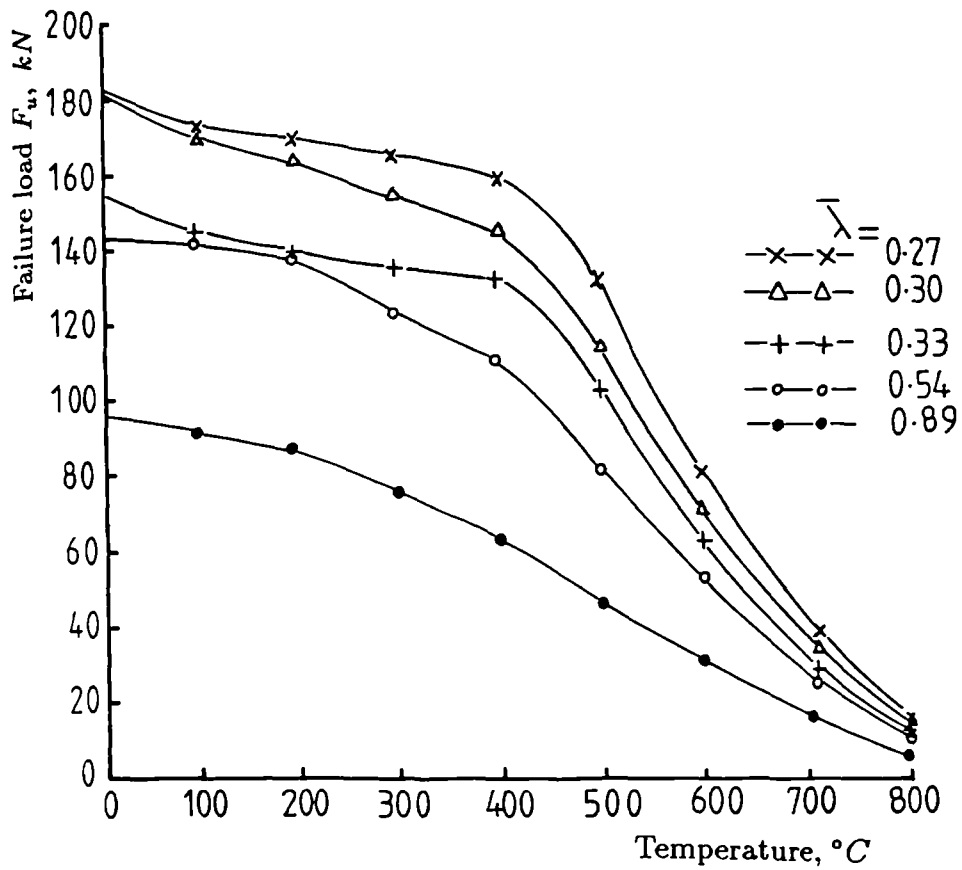


Fig. 6.7 - Variation of failure load with temperature at increasing slenderness.

ferent rates as temperature increases depending upon their failure modes at room temperature. The collapse of very low slenderness frames is influenced by material yielding while the elastic modulus variation controls the behaviour of high slenderness frames. The interaction between the yield strength and loss of stiffness is responsible for the behaviour of intermediate slenderness frames at elevated temperatures.

## 6.2.2 Effect of stress-strain relationships and material properties expressions

If material nonlinearity, which steel clearly exhibits at high temperatures, is to be taken into account, then a continuous form of the material constitutive relationship must be considered. However, a simplified form of the stress-strain relationship is frequently used owing to its simplicity. Such a form consists of two-straight-lines (eq.6.1) described only by the yield strength and the modulus of elasticity.

In this study, the effects of the form of stress-strain relationship on the behaviour of frames is investigated using the continuous (eq.3.11) and the bilinear (eq.6.1) expressions along with the ECCS (eqs.3.3 and 3.7) and CTICM (eqs.3.2 and 3.6) expressions relating the yield strength and the modulus of elasticity to their room temperature values and those derived on the basis of BS 5950 Pt.8. test data (eqs.3.4 and 3.8). The results are represented as failure load - temperature relationships at increasing slenderness. The failure load is nondimensionalised with respect to ambient temperature ultimate failure load  $F_{u,20}$ .

### 6.2.2.1 Comparison between bilinear and continuous stress-strain relationships using BS 5950 material models

Calculations of failure loads at increasing temperature using BS5950 Pt.8 data expressions and a continuous form of  $\sigma - \epsilon$  relationship were shown in Fig.6.6 and discussed in sec. 6.2.1. Results of a similar calculation but using an assumed bilinear representation for  $\sigma - \epsilon$  are presented in Fig. 6.8 for  $\bar{\lambda} = 0.27, 0.33, 0.89$ .

Again, the dominant effect of material yielding and elastic modulus on low ( $\bar{\lambda} = 0.27$ ) and high slenderness frames ( $\bar{\lambda} = 0.89$ ) respectively is clear. This influence is more pronounced when using a bilinear form of  $\sigma - \epsilon$  and the curves of low and high slenderness frames follow that of the yield strength and elastic modulus more closely. Moreover, the decrease in strength before  $250^{\circ}C$  and after  $550^{\circ}$  occurs at a more reduced rate for slender frames than for those of low to moderate slenderness, though the difference is small following those of yield strength and elastic modulus (Figs.3.2, 3.1 ) respectively. For example, at  $400^{\circ}C$  a slender frame ( $\bar{\lambda} = 0.89$ ) lost 15% of its room temperature strength while for the low slenderness frames ( $\bar{\lambda} = 0.27$ ) this loss was only 6%. Another important feature in the use of a bilinear relationship is that it leads to the behaviour of moderate slenderness ( $\bar{\lambda} = 0.33$ ) being similar to that of low slenderness ( $\bar{\lambda} = 0.27$ ), whereas a different behaviour is exhibited when a continuous form of this relationship was used.



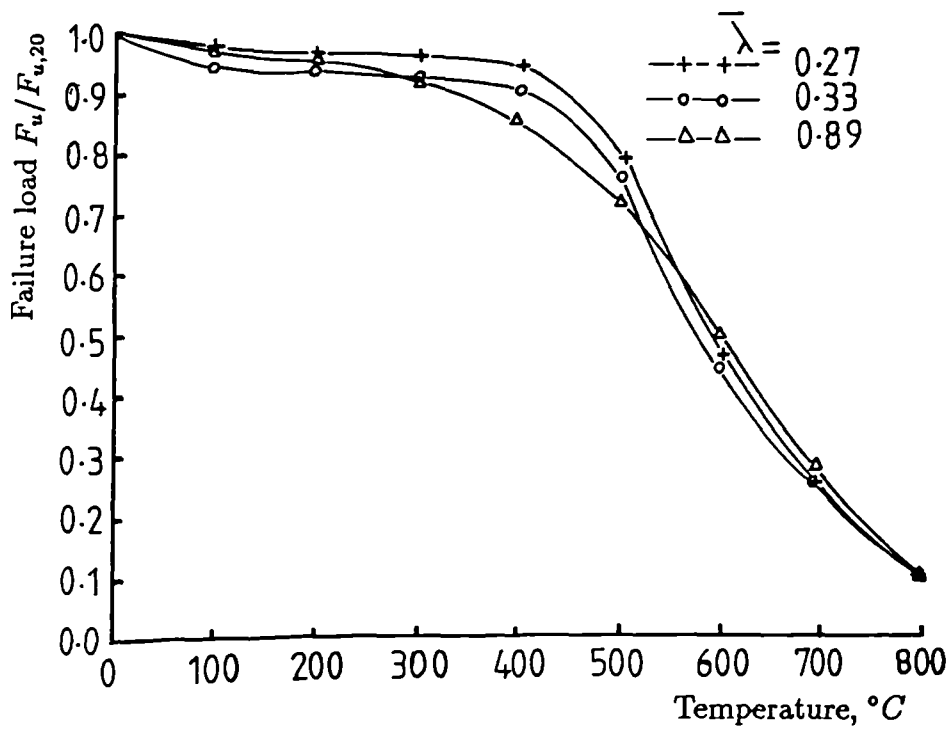


Fig. 6.8 - Variation of failure load with temperature at increasing slenderness using BS5950 expressions and bilinear  $\sigma - \epsilon$ .

### 6.2.2.2 Comparison between bilinear and continuous $\sigma - \epsilon$ relationships using CTICM material models

Similar calculations were carried out using the CTICM material expressions with continuous and bilinear  $\sigma - \epsilon$  representations. Results of the analysis are shown on Figs.6.9 and 6.10 respectively.

Once again, these curves demonstrate the dominant effects of material models used in the analysis on the strength-temperature response of steel frames. Following the variations of yield strength and modulus of elasticity with temperature (curves (b) in Figs.3.2 and 3.1 respectively), the curves shown in Figs.6.9 and 6.10 reflect the previously described effects of yield strength and elastic modulus on low and high slenderness frames respectively. Fig.6.10 also proves that the use of a bilinear stress-strain relationship has led to the behaviour of low to moderate slenderness frames being similar compared to the more distinctive curves ( $\bar{\lambda} = 0.27$  and  $0.33$ ) in Fig.6.9. For example at  $500^{\circ}\text{C}$  the difference between these two curves is negligible in Fig.6.10 whilst this difference amounts to approximately 10% in Fig.6.9.

### 6.2.2.3 Comparison between bilinear and continuous $\sigma - \epsilon$ relationships using ECCS material models

Results of similar calculations using ECCS material expressions with a continuous and an assumed bilinear form of  $\sigma - \epsilon$  relationship are presented in Fig. 6.11 and Fig.6.12. These results exhibit the same familiar response discussed earlier with the exception that both bilinear and continuous representations lead to the behaviour of low to moderate slenderness frames being similar when using ECCS

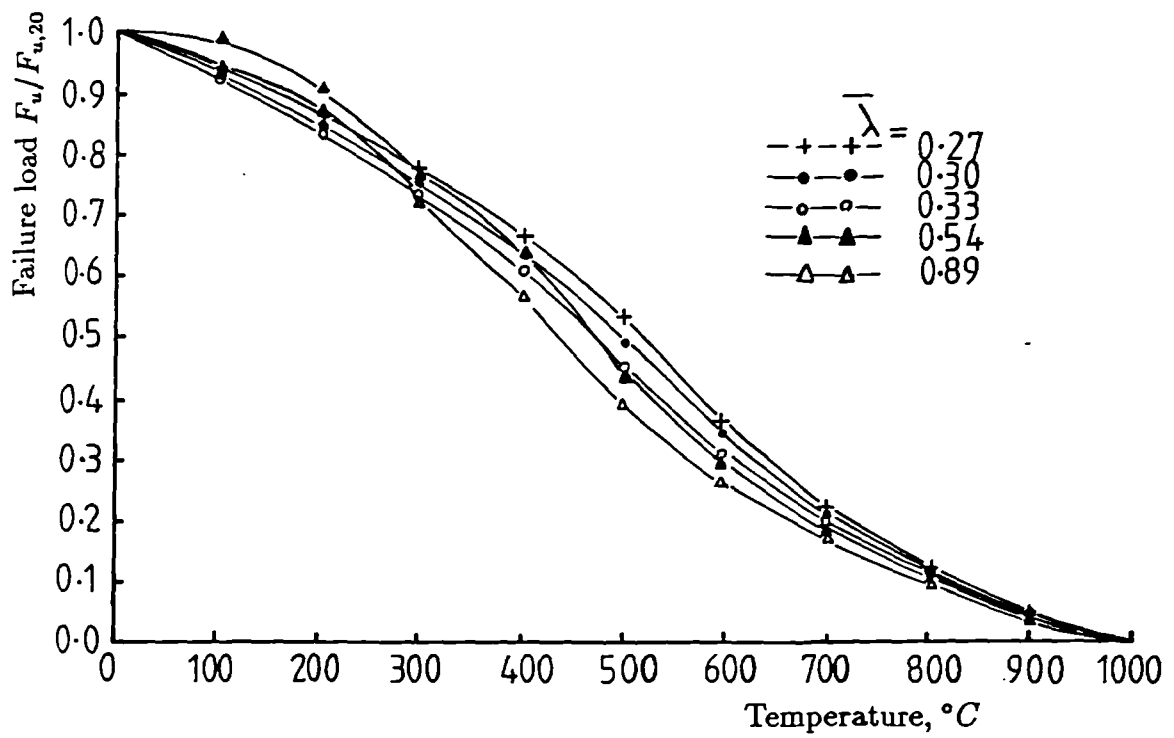


Fig. 6.9 - Variation of failure load with temperature at increasing slenderness using CTICM expressions and continuous  $\sigma - \epsilon$ .

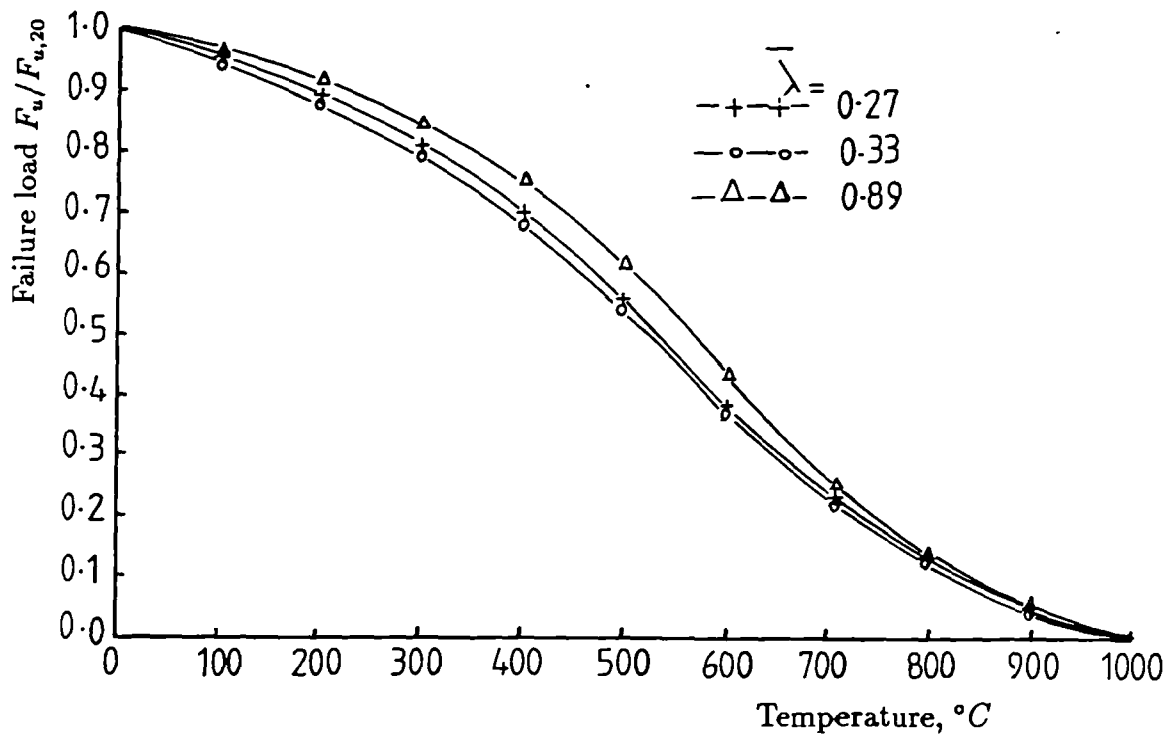


Fig. 6.10 - Variation of failure load with temperature at increasing slenderness using CTICM expressions and bilinear  $\sigma - \epsilon$ .

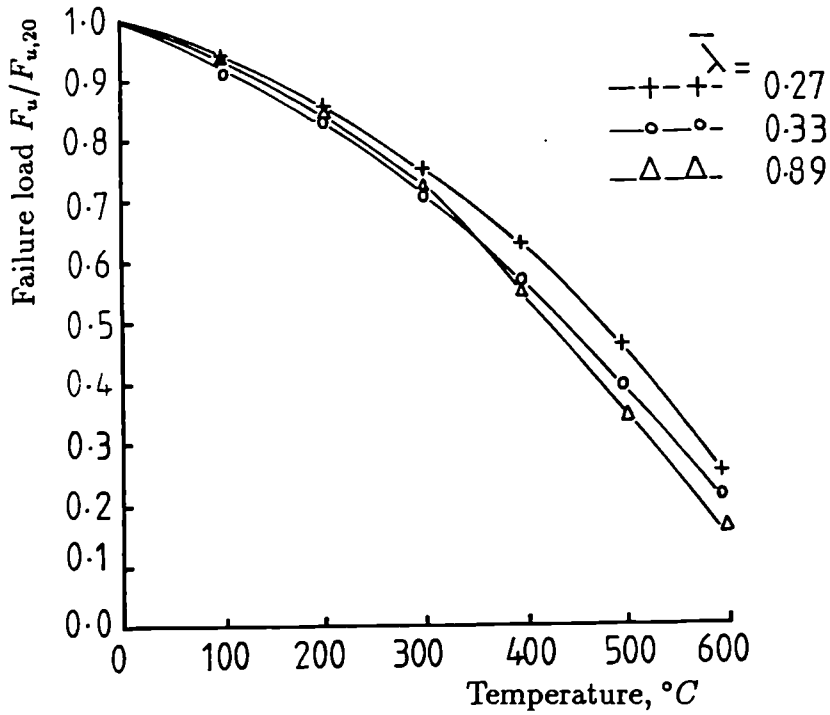


Fig. 6.11 - Variation of failure load with temperature at increasing slenderness using ECCS expressions and continuous  $\sigma - \epsilon$ .

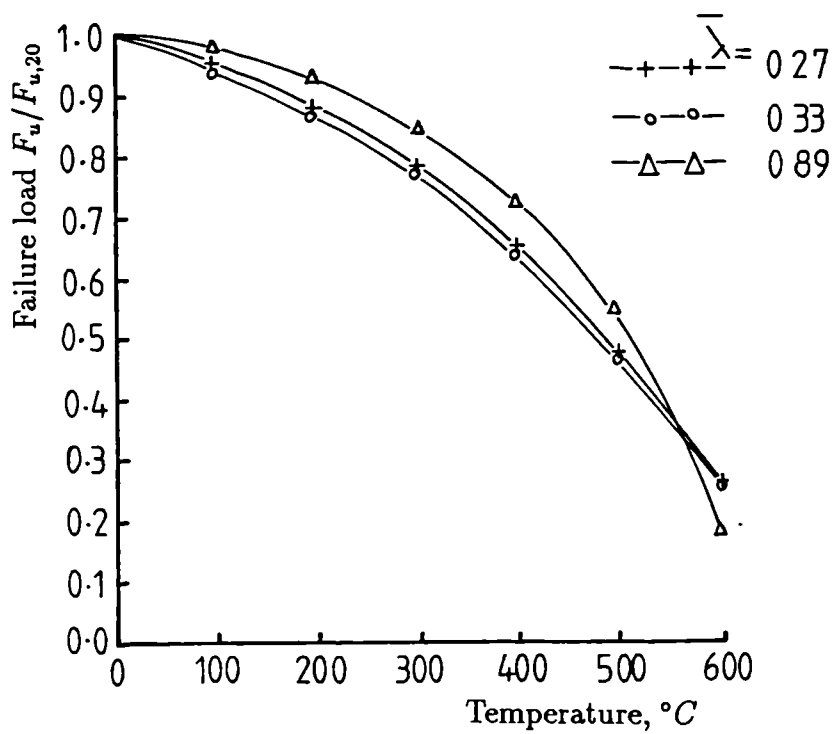


Fig. 6.12 - Variation of failure load with temperature at increasing slenderness using ECCS expressions and bilinear  $\sigma - \epsilon$ .

material expressions. In the next section, this behaviour will be compared with the previous responses using the three material models.

#### **6.2.2.4 Comparison between bilinear and continuous stress-strain representations using the three material models (BS 5950, CTICM, ECCS)**

For more comparison between results obtained using different material models, the same information presented in Figs.6.6 - 6.12 is plotted in Figs.6.13 - 6.16 for each frame representing the following slenderness :  $\bar{\lambda} = 0.27, 0.3, 0.54, 0.89$ .

It is clear that in all cases the use of an assumed bilinear stress-strain relationship results in a higher collapse load compared with the results based on a continuous material constitutive model. Moreover, the use of the three material models (BS 5950, CTICM, ECCS) has resulted in different collapse load levels with the BS 5950 results giving the highest load level. The use of the CTICM expressions has yielded higher collapse loads than those based on the ECCS expressions, although these results are closer to those of ECCS than BS 5950. The use of a continuous form of stress - strain relationship together with the BS5950 material data in Chapter 5 have resulted in closer simulation of the fire tests. This data has been recently derived using appropriate testing techniques and should therefore be adopted for numerical analysis.

### **6.2.3 Effects of various forms of protection**

The occurrence of partial heating is very common during building fires where only parts of the frame are heated while the rest of the structure is kept cold.

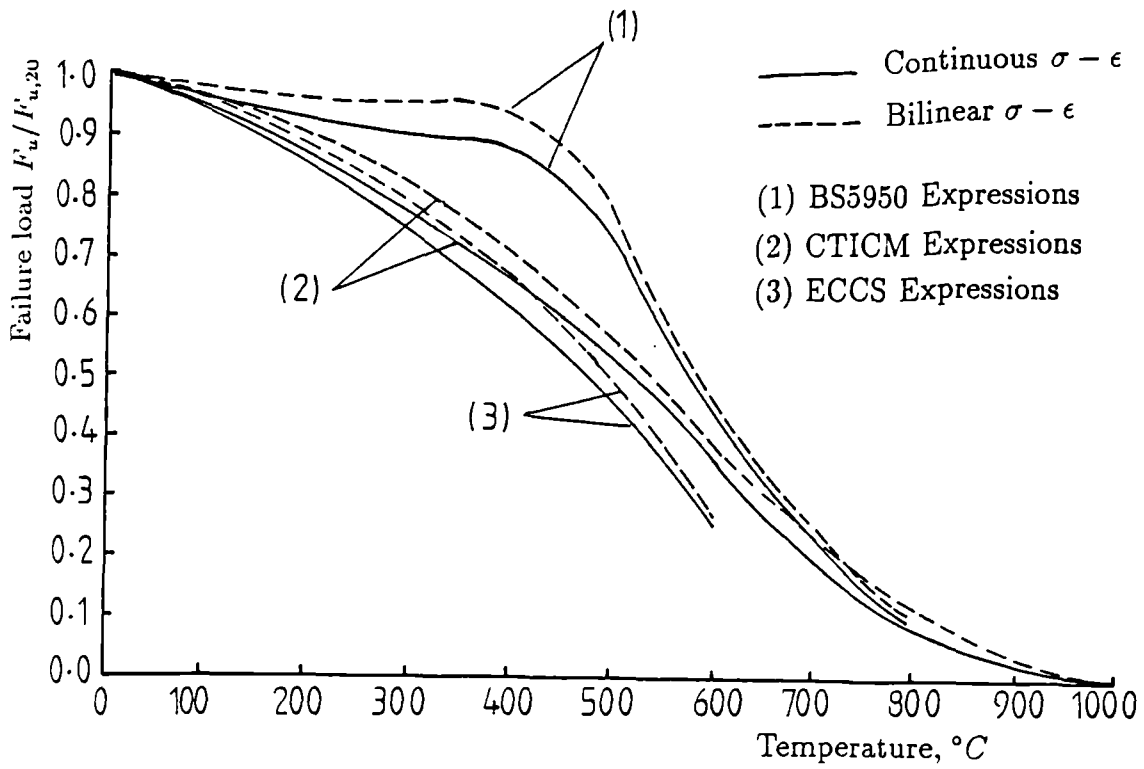


Fig. 6.13 - Comparison of frame response using different strength expressions ( $\bar{\lambda} = 0.27$ ).

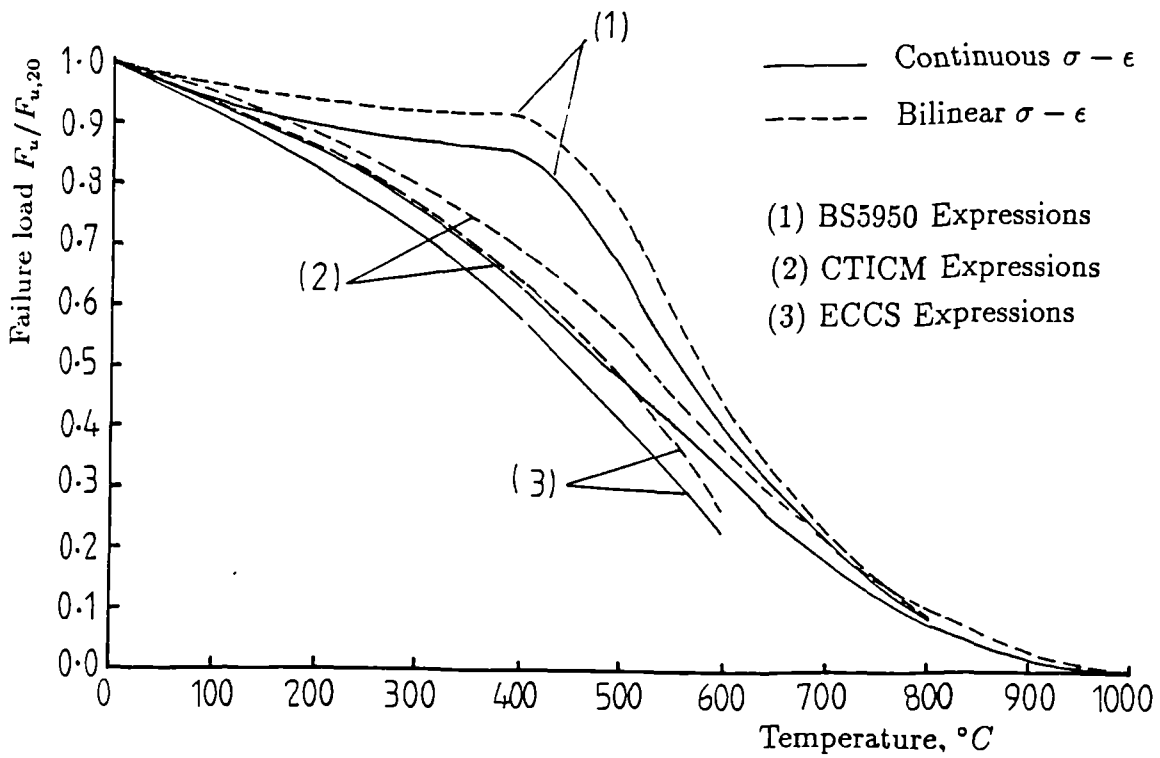


Fig. 6.14 - Comparison of frame response using different strength expressions ( $\bar{\lambda} = 0.30$ ).

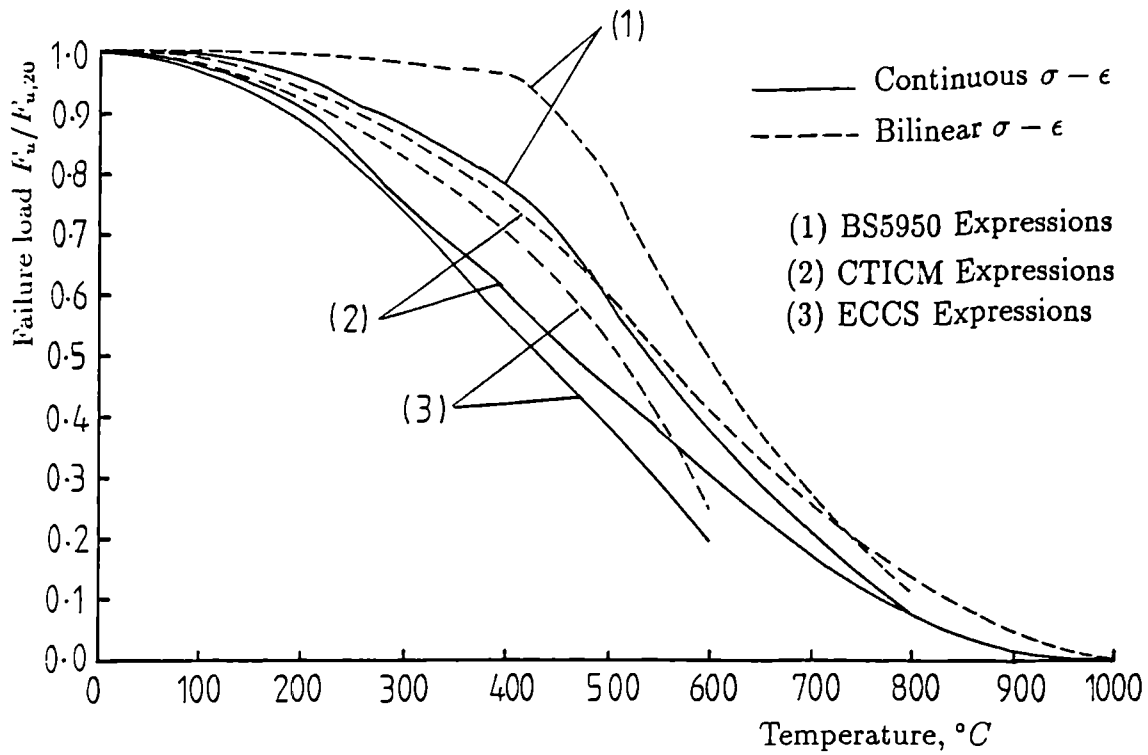


Fig. 6.15 - Comparison of frame response using different strength expressions ( $\bar{\lambda} = 0.54$ ).

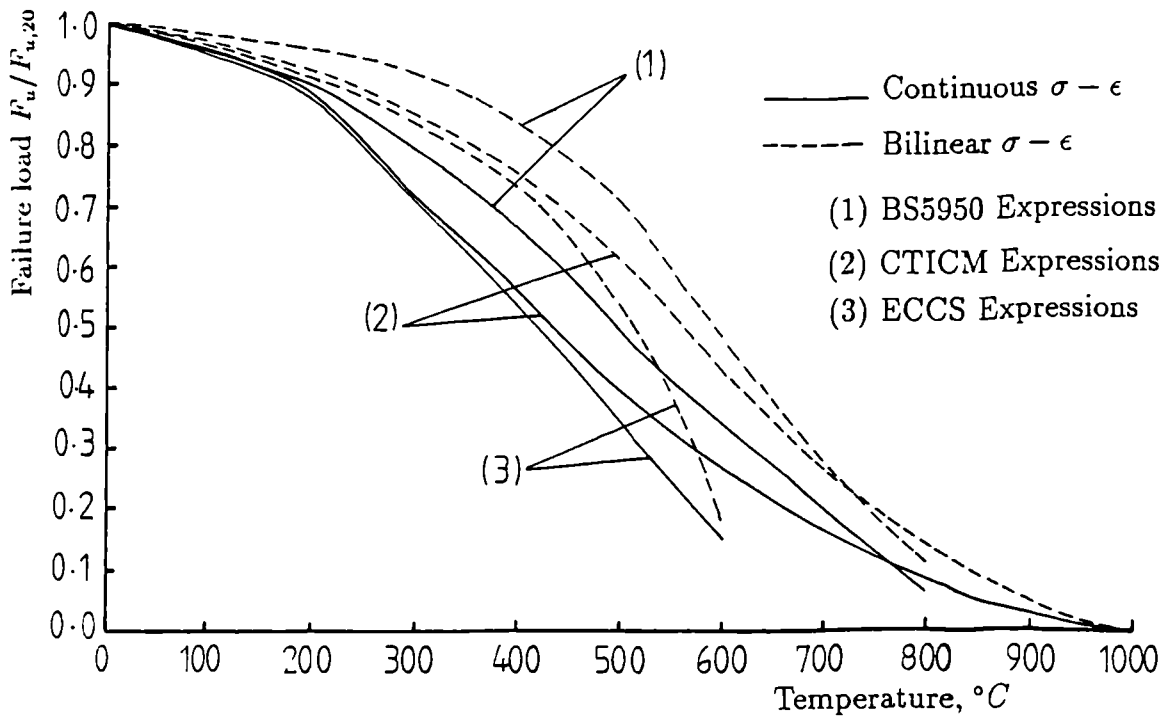


Fig. 6.16 - Comparison of frame response using different strength expressions ( $\bar{\lambda} = 0.89$ ).

This happens when members of the frame such as columns are totally embedded in the wall. This also occurs during a compartment fire when a locally intense heating moves throughout the compartment which leads to isolated members being subjected to a relatively very high temperature for a short time whilst other members are effectively cool. This variation in the temperature levels at various parts of a frame may be expected to affect the integrity of the structure depending upon the structural roles of these parts.

In order to study this effect, the two-bay frame of IPE 80 section shown in Fig.6.17 is analysed under various forms of insulation. The frame is comparatively slender having a value of  $\bar{\lambda} = 0.9$ . It is loaded with three column loads corresponding to 60% of the room temperature ultimate load capacity and a lateral load of 1.28% of the vertical load. The ambient temperature yield strength and modulus of elasticity were assumed as  $355 \text{ N/mm}^2$  and  $210 \text{ kN/mm}^2$  respectively. Calculations were made for five different insulation conditions as illustrated in Table 6.2. A uniform temperature distribution was assumed along and across the heated parts.

The results show that for uniform heating a critical temperature of  $425^\circ\text{C}$  was obtained. Protection of the beams only increased this to  $436^\circ\text{C}$ . Insulation of one beam and one column provided a 21% increase in critical temperature but protection of either all three columns or one complete ring frame increased the critical temperature to  $648^\circ\text{C}$  and  $634^\circ\text{C}$  respectively. The reason for the superior performance of the frames in which resistance to sway was preserved may be illustrated by a study of the deformed shapes of each of the five examples just prior to collapse, the mode of failure at room temperature already having been established as sway instability of the form shown in Fig.6.18a. For the uniformly heated frame (case 2), Fig.6.18b shows that failure occurs in a sway



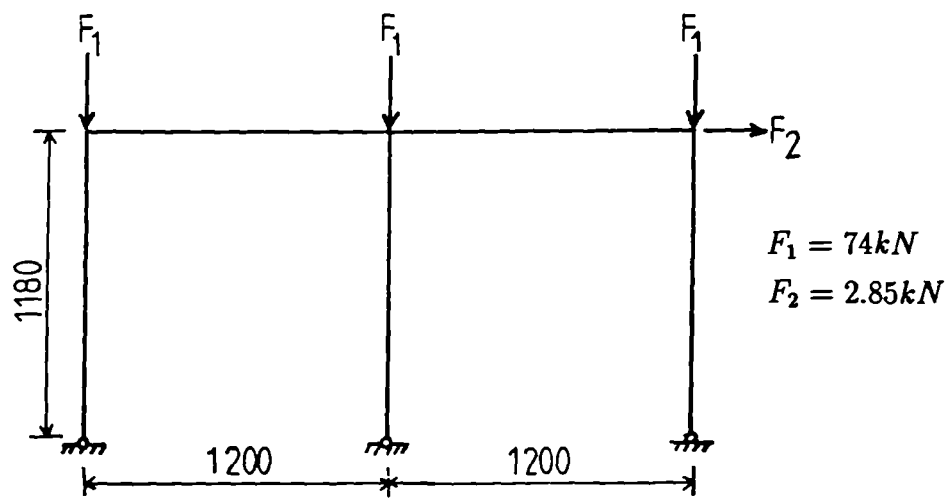
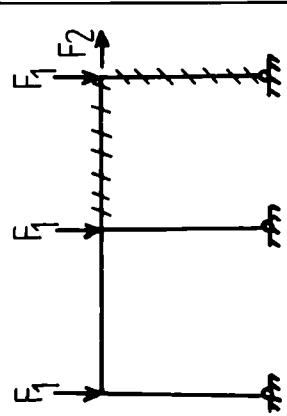
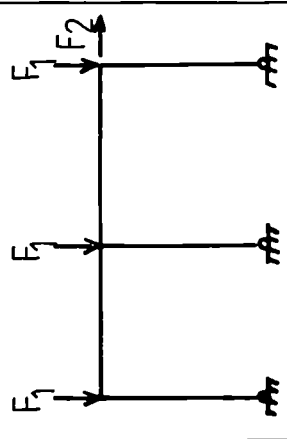
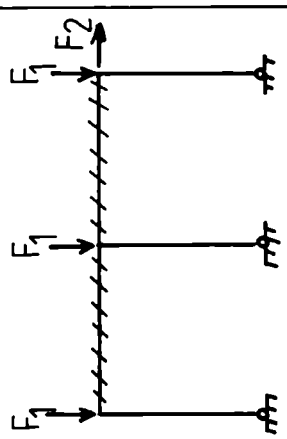
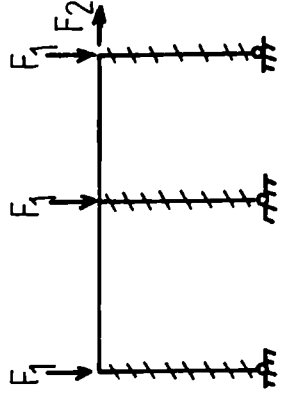
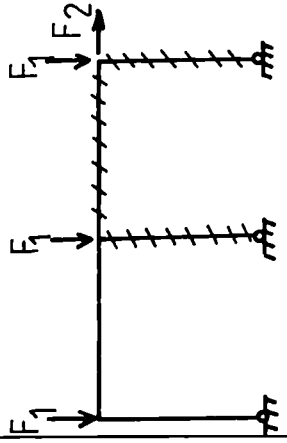


Fig. 6.17 - Frame geometry and loading.

Table 6.2 - Various forms of protection and corresponding critical temperatures.

Case 1	Case 2	Case 3	Case 4	Case 5
				
<p>Failure temperature</p> <p>528°C</p>	<p>425°C</p>	<p>436°C</p>	<p>648°C</p>	<p>634°C</p>

\*\*\*\*\* Cold element

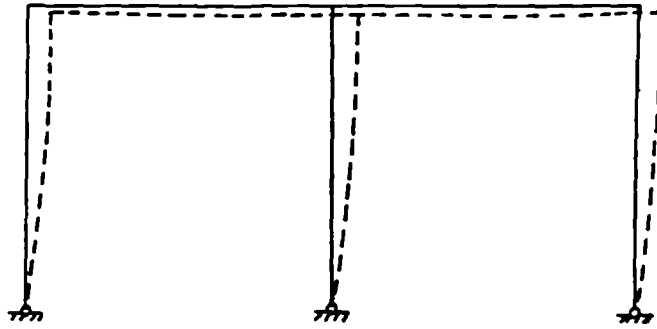


Fig. 6.18a - Ambient temperature failure mode.

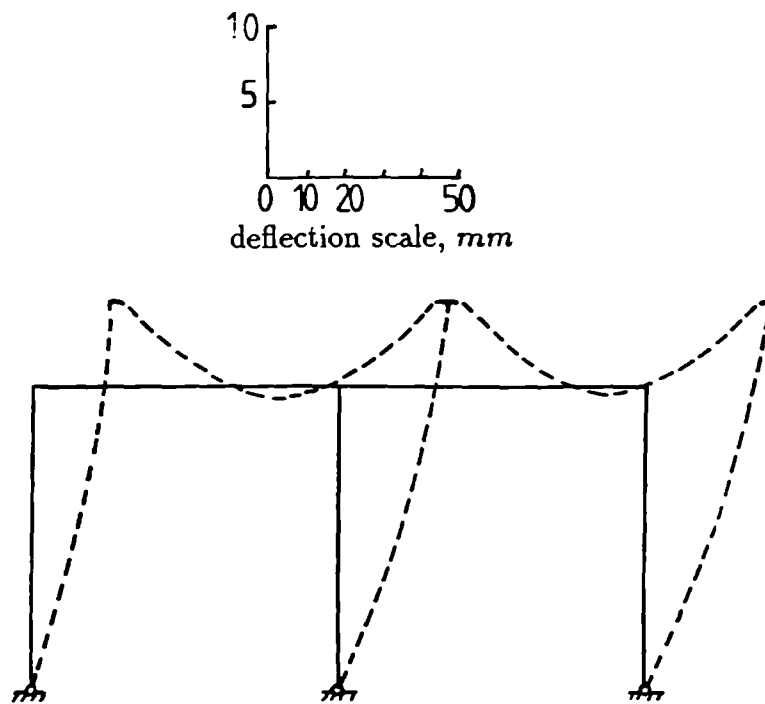


Fig. 6.18b - Failure mode of uniformly heated frame.

mode, which is an amplified version of the room temperature mode. Fig.6.19 shows that insulation of the type provided in case 3 does almost nothing to inhibit this type of deformation since those members whose stiffness is preserved (i.e the beams), do not really participate in resisting sway. On the other hand, preserving the stiffness in the columns limits sway of the frame, particularly when the structure is such that either all columns are protected (case 4) or the heated portion can 'lean' against a stiffer cold portion (case 5). These contrast with case 1 in which the insulated portion of the frame is much less able to act as sway bracing to the heated and thus less stiff part.

The temperature - sway deflection histories for the five cases given in Fig.6.20 proves that cases 4 and 5 are much more effective in limiting the development of a significant deformation until higher critical temperatures have developed.

#### **6.2.4 Effect of magnitude of residual strains**

Of all the imperfections that a steel section can have at ambient temperature, residual stresses are one of those generally regarded as among the most significant. These stresses, produced after the hot rolling process used in the manufacture of structural sections, or after welding and flame cutting of fabricated members, can cause their premature failure. Since subsequent cooling does not occur uniformly across the section, differential cooling results in a significant self-equilibrating pattern of stresses being retained in the member. Residual compression is developed in the parts of the cross section that cool first while residual tension is produced in the parts which cool later. The magnitude of these stresses depends on the relative sizes of the flange and the web, but in general the larger the cross-section

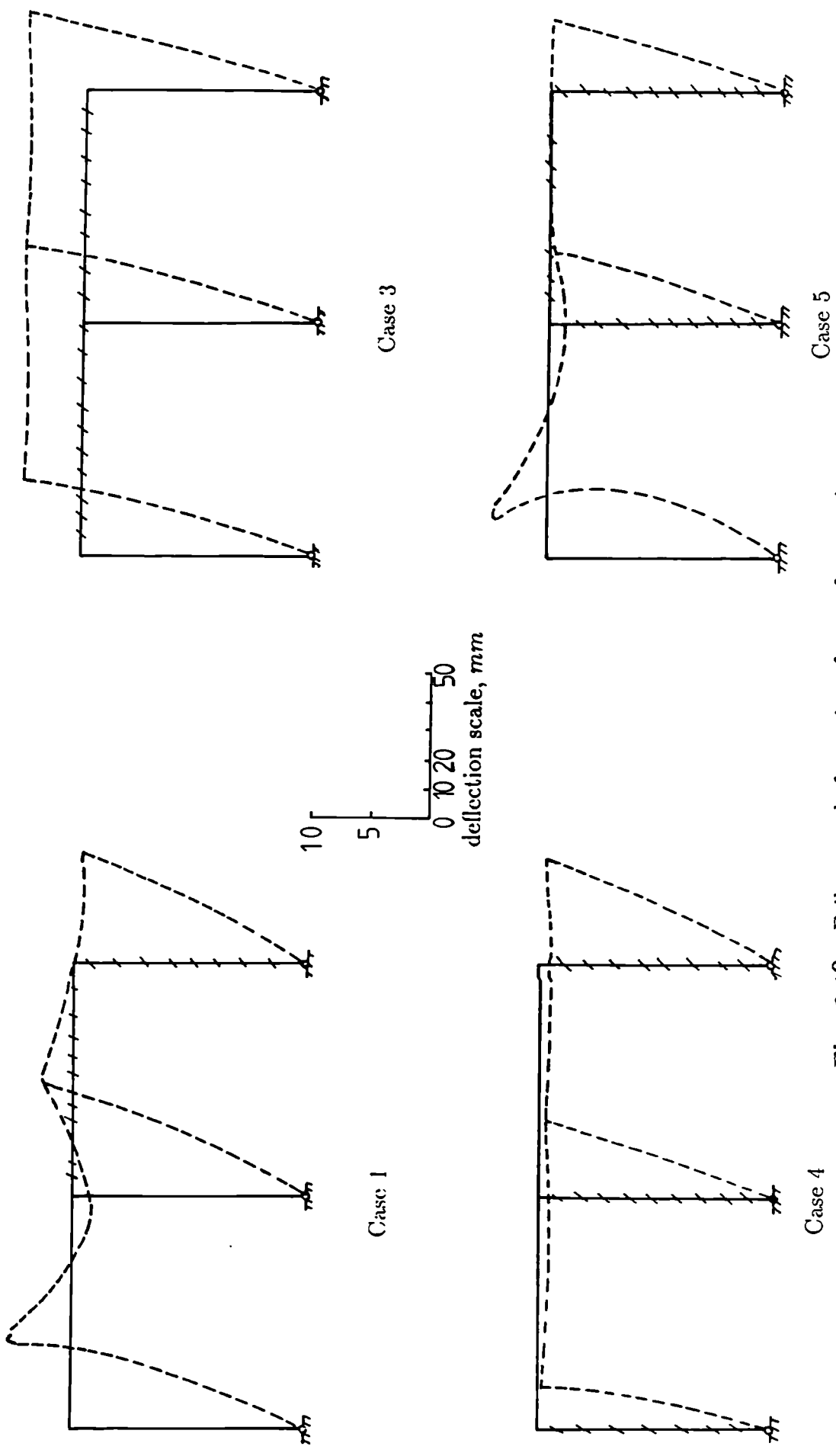


Fig. 6.19 - Failure mode for various forms of protection.

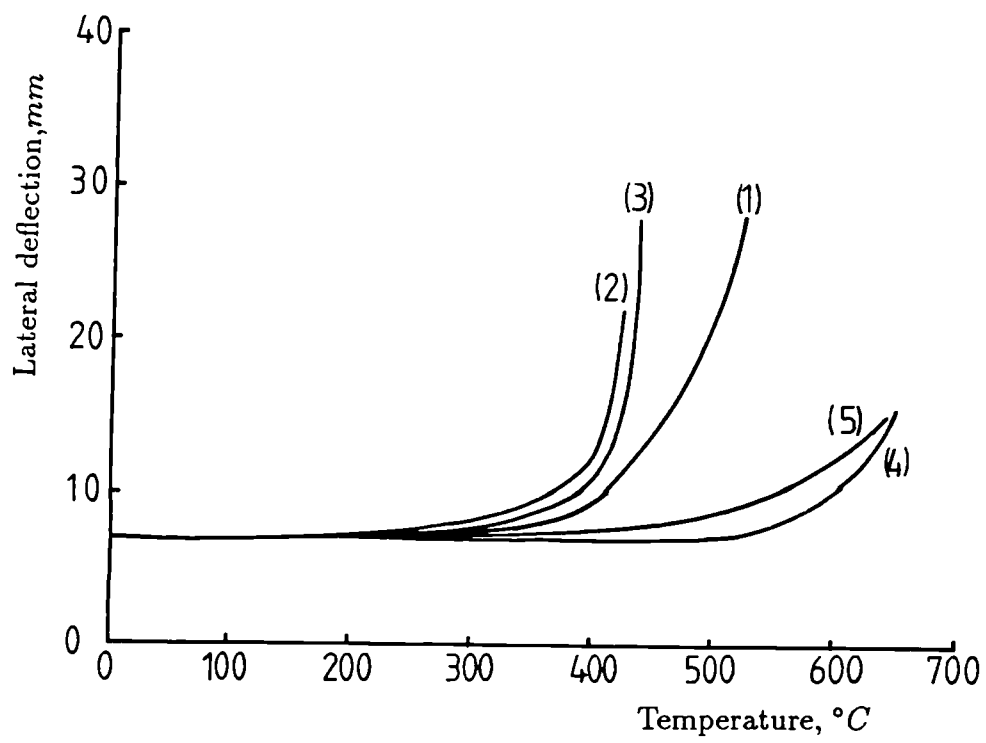


Fig. 6.20 - Temperature-sway deflection relationships for various forms of protection.

the bigger they become.

At elevated temperatures, residual stresses are known to undergo a decrease in magnitude and a redistribution over the cross section. No attempt has been made to measure these stresses at elevated temperatures and little has been reported on quantifying this effect. Aribert and Abdel-Aziz (1987) have, however, reported expressions relating the magnitude of these stresses to their ambient temperature values for nonuniformly heated cross sections. The values of the reported stresses are functions of the yield strength and they decrease with the reduction of the material strength at elevated temperatures.

In order to study the residual stress effect at increasing temperature, a residual stresses pattern was assumed as shown in Fig.6.1. Three frames of slenderness  $\bar{\lambda} = 0.27, 0.3, 0.89$  representing low, intermediate and high slenderness frames respectively were analysed under various levels of residual stress magnitude ( $0.1, 0.3, 0.5\sigma_{y,20}$ ). Results of the analysis have shown that these stresses have no effect on the low to moderate slenderness frames and that the high slenderness frame ( $\bar{\lambda} = 0.89$ ) shows only very little response to the level of residual stresses as indicated in Fig.6.21.

Similar calculations were carried out on the above frames but using the corresponding values of these stresses at elevated temperatures as calculated from Ref.[4]. As expected, since these stresses have negligible effect when their room temperature values are used, using temperature dependent values of residual stresses also reveals no effect.

To summarise, the residual stress distribution and magnitude has negligible effect on low to moderate slenderness frames at elevated temperatures beyond its ambient temperature effect. These stresses have shown no effect on very high

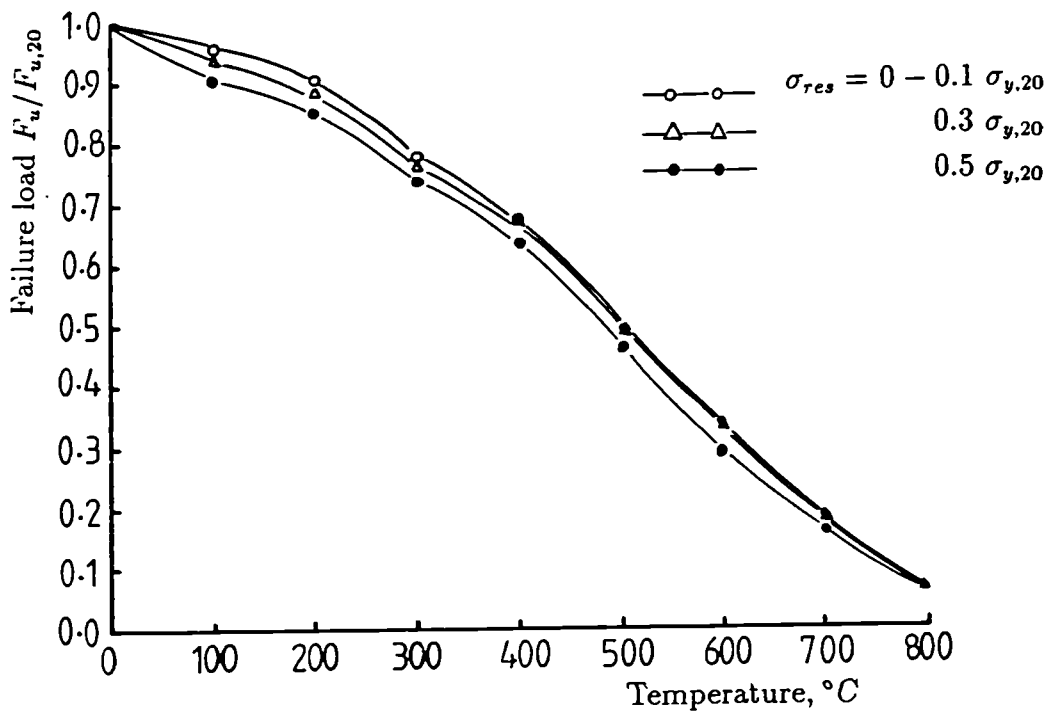


Fig. 6.21 - Variation of failure load with temperature at increasing residual stress level ( $\bar{\lambda} = 0.89$ ).



slenderness frames. No attempt is needed to measure these stresses at increasing temperatures since they have even less influence as temperature increases.

### **6.2.5 Effect of thermal gradient along and across the section**

Temperature distributions in structural steel elements are unlikely to be uniform during fire and may vary along and across each member. This may be due to the heating arrangements or to partial protection where the steel is in contact with another material. This thermal gradient can in general be of a beneficial effect as compared with the uniformly heated members since parts of the section preserve their strength and stiffness whilst remaining at low temperatures. However, an induced bowing towards the heat source is expected in these elements due to differential expansion between the hot and cold parts.

In order to study this effect, three frames representing various slenderness ratios ( $\bar{\lambda} = 0.27, 0.33, 0.89$ ) were analysed. Different temperature distribution patterns were assumed across and along the section.

#### **6.2.5.1 Effect of thermal gradient across the section**

Figs.6.22a-c show plots of collapse load nondimensionalised with respect to the uniformly heated collapse load for various temperature distribution patterns. The distribution was assumed to vary across the section with a constant gradient of  $300^{\circ}\text{C}$  between the hot and cold flanges.

It is clear from these figures that low to moderate slenderness frames

(Figs.6.22a and 6.22b) exhibit similar behaviour under thermal gradient. Differences in temperature distribution have negligible effect up to about  $500^{\circ}C$  compared with the uniformly heated section since material strength retains most of its room temperature value up to that temperature level. Bowing of the members, which can be approximately considered as constant throughout the heating history due to the constant thermal gradient, also appears to have a negligible effect, being at least compensated for by the shift of the effective neutral axis towards the cold part of the section. As temperatures increase further, a considerable increase in the load carrying capacity of the better protected structures is observed, especially between  $700 - 800^{\circ}C$ . No analysis was carried out beyond  $800^{\circ}C$  due to insufficient material data.

In contrast to the low to moderate slenderness frames, thermal gradient across the section has a diminishing effect on the very high slenderness frames ( $\bar{\lambda} = 0.89$ ) as shown in Fig.6.22c. This is due to the fact that bowing of the columns of these frames is much more serious, leading to an earlier collapse, even though parts of the protected frames do, of course, retain their better properties.

To summarise, thermal gradient across the section has in general a beneficial effect since parts of the section retain their room temperature strength. The potentially deleterious effect of bowing of the members due to this thermal gradient is negligible for low to moderate slenderness frames where it is compensated by the shift of the effective neutral axis towards the cold parts. However this bowing, which can be regarded as an enhancement of the initial out of straightness, has detrimental effects on very high slenderness frames where imperfections most affect the buckling behaviour.

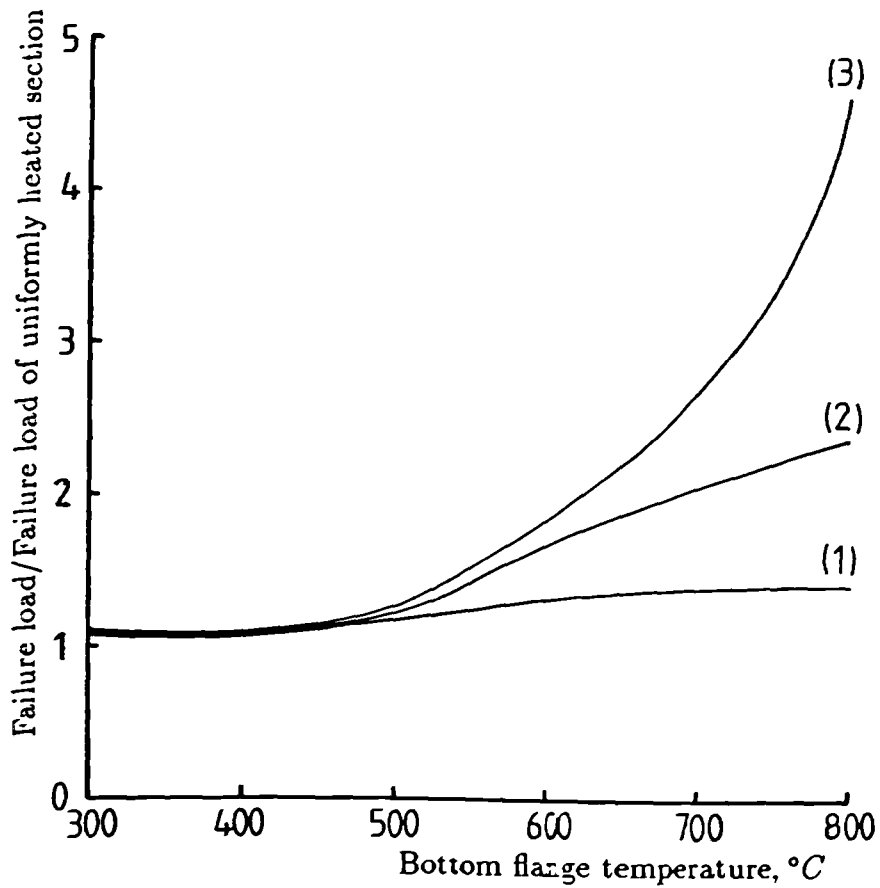
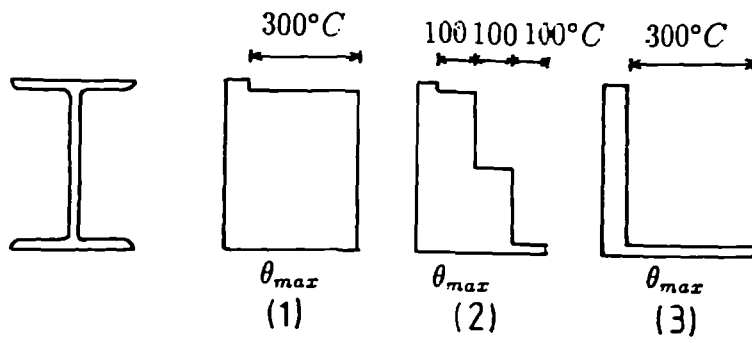


Fig. 6.22a - Variation of failure load/failure load of uniformly heated section with increasing temperature ( $\bar{\lambda} = 0.27$ ).

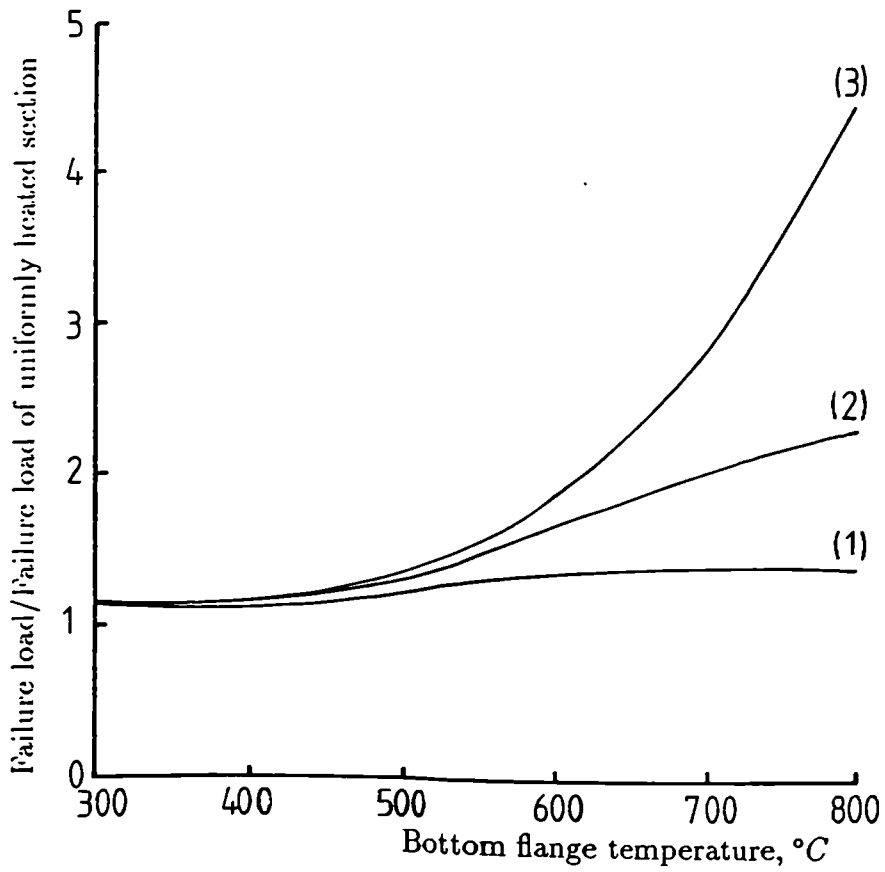


Fig. 6.22b - Variation of failure load/failure load of uniformly heated section with increasing temperature ( $\bar{\lambda} = 0.33$ ).

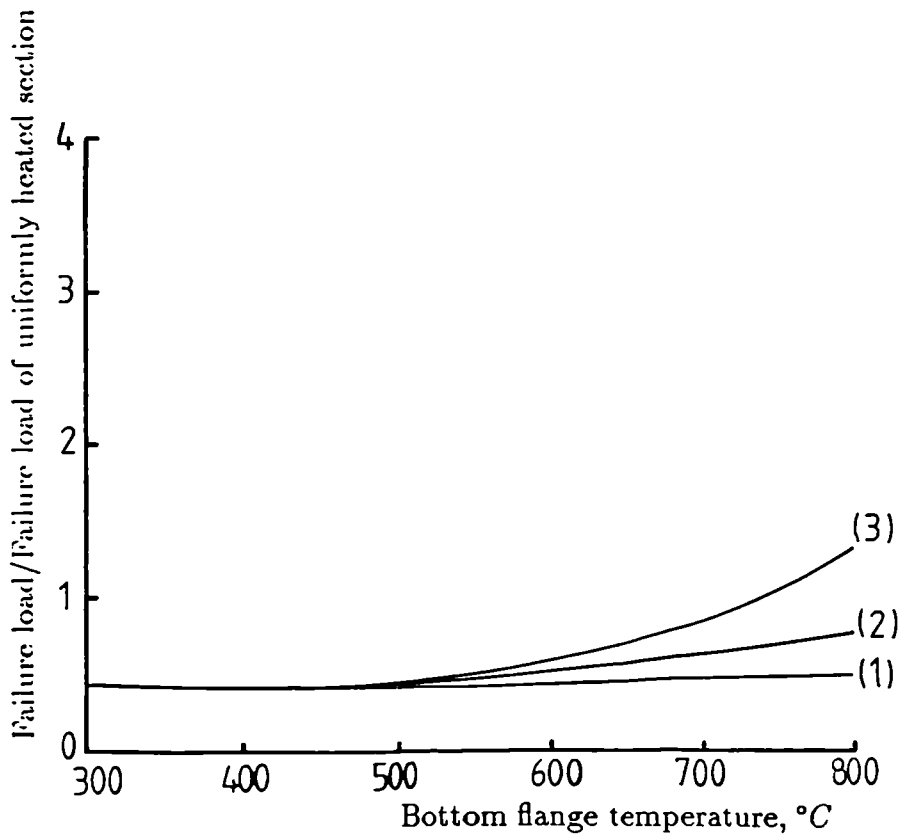


Fig. 6.22c - Variation of failure load/failure load of uniformly heated section with increasing temperature ( $\bar{\lambda} = 0.89$ ).

### 6.2.5.2 Effect of thermal gradient along the members

During fire tests, a uniform temperature distribution along the length of the structural members cannot normally be achieved. Depending on the heating characteristics of the furnace and the exposure procedure, the temperature may differ significantly along the length of the member, with the greater variation in the vicinity of its ends. A typical hot flange temperature distribution along a column length as measured in a furnace is shown in Fig.6.23 [92].

Witteveen and Twilt (1981/1982) found that for a realistic temperature distribution along the length of the column, the effect of nonuniform distribution is not very significant for all types of end conditions provided these columns are not heavily loaded and the slenderness is not very high.

In order to study this effect on steel frames, an assumed temperature distribution as shown in Fig.6.23 was considered. Results of the analysis for three frames representing various slenderness ratios ( $\bar{\lambda} = 0.27, 0.33, 0.89$ ) are shown in Fig.6.24. It can be seen that negligible variation from the wholly heated frames exist.

It therefore seems reasonable to assume that variations in temperature along the length of the members of the type shown in Fig.6.23 are unlikely to affect the structural response of either single members or frames. However, it is important to note that these variations will have considerable effect on the frame behaviour if connections change their degree of rotational restraints with temperature.

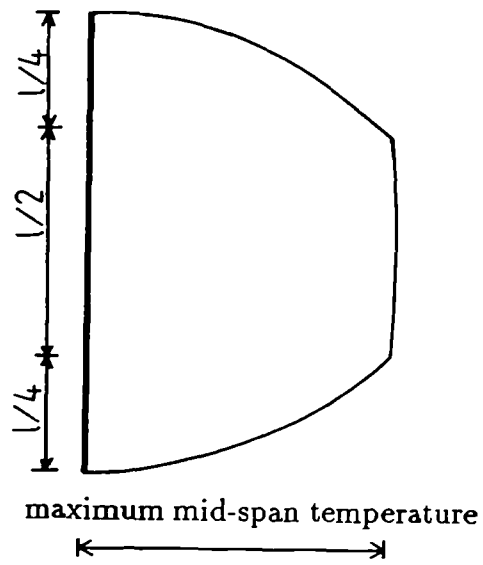


Fig. 6.23 - Typical temperature distribution along a column length [92].

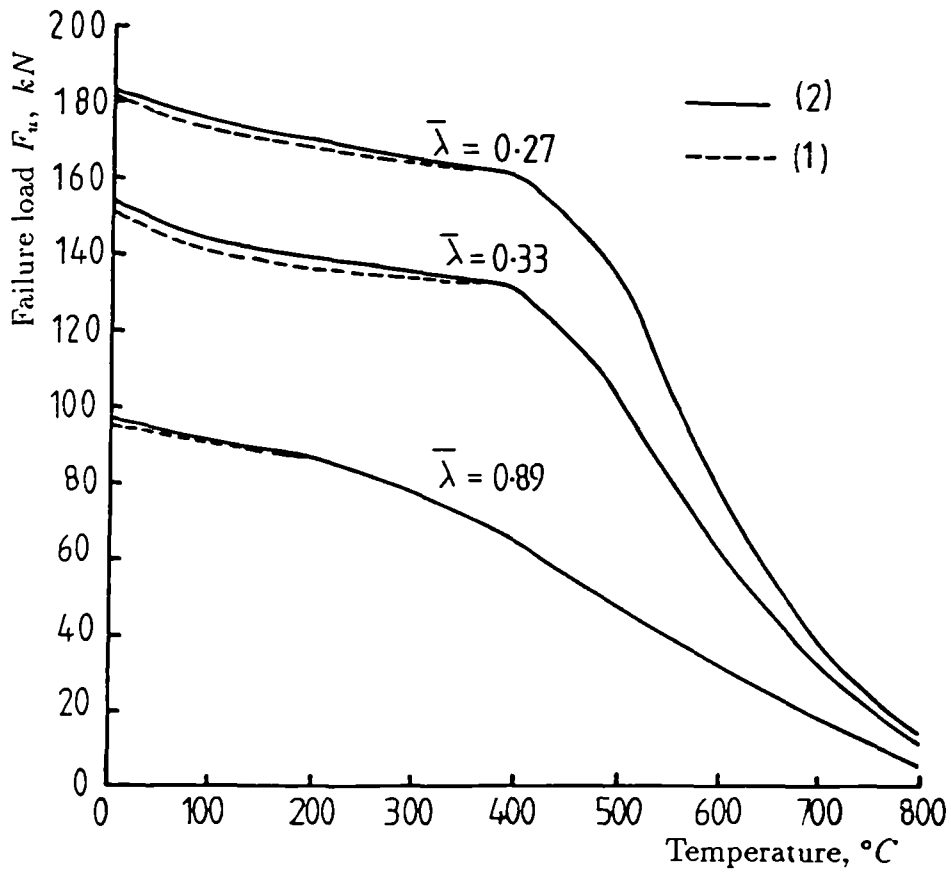
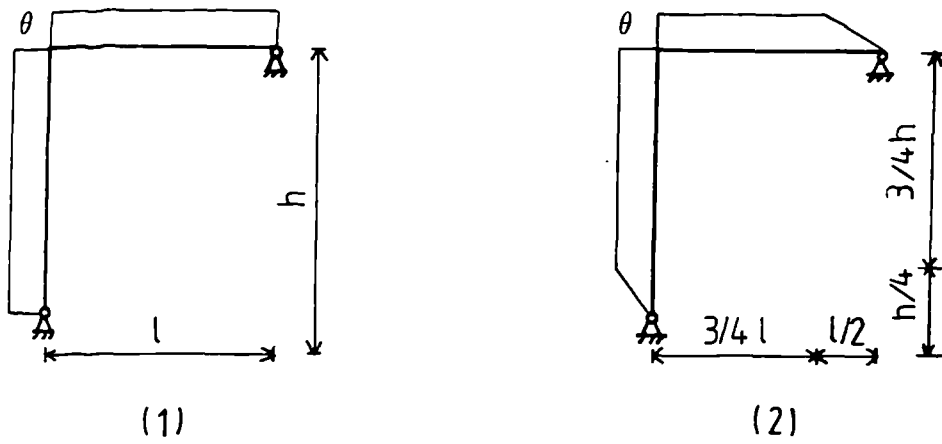


Fig. 6.24 - Variation of failure load with temperature using different longitudinal temperature distributions.

## 6.3 On the strength - temperature relationships of steel frames

Figs.6.6 to 6.16 have presented the strength -temperature relationships for uniformly heated non sway frames over a wide range of frame slenderness ratios using different stress - strain representations and using the most commonly used material characteristics. Although these curves differ somewhat from one another, it is clear that they all lie within a bandwidth with an upper bound representing frames having the highest slenderness ratio coupled with the least conservative elastic modulus assumption and a lower bound representing the stocky frames using the most conservative yield strength assumption. A single curve for all types of frames and load levels cannot therefore be achieved since the exact strength - temperature response depends on many factors such as slenderness ratio, end conditions, insulation arrangement and material properties. However, based on statistical analysis, an approximate curve can be postulated which can be used to predict the limiting temperatures of practical frames under uniform heating.

To this end, a sway frame is first analysed in order to generate more data on a wider basis for the statistical regression. The validity of the obtained curve is then checked against further cases representing different parameter variations.

### 6.3.1 The elevated temperature sway frame response

The sway frame of IPE 80 section shown in Fig.6.25a was analysed for various slenderness ratios under uniform temperature. The ambient temperature yield strength and modulus of elasticity were assumed as  $400 \text{ N/mm}^2$  and  $210 \text{ kN/mm}^2$



respectively. Results of the analysis of four frames representing various slenderness ratios ( $\bar{\lambda} = 0.32, 0.4, 0.48, 0.6$ ) are shown in Fig.6.25b. The collapse load is nondimensionalised with respect to the room temperature ultimate collapse load.

Fig.6.25b shows that these frames generally exhibited the familiar form of curves discussed in sections 6.3.1 and 6.3.2. However, for sway frames these curves are very similar for different slenderness ratios but at a gradually reduced collapse load due to the effect of sway.

Analysis was also carried out on the same frames at different percentages of the room temperature ultimate collapse load in order to find the corresponding critical temperatures under these loadings. This is to demonstrate the reciprocal strength - temperature relationship (i.e the critical temperature of a frame under sustained loading is approximately equivalent to the collapse load at that temperature level). Results of the analyses of the frames subjected to loads of between 20% and 80% of the corresponding room temperature ultimate collapse loads are shown in Fig.6.26a.

For comparison between Figs.6.26a and 6.25b, the same information contained in Fig.6.26a was then plotted in Fig.6.26b as nondimensionalised applied load against calculated critical temperatures. Comparison between Figs.6.25b and 6.26b reveals that the strength - temperature relationship is a reciprocal one. Thus, any subsequent relationship can therefore be used for the prediction of collapse load at a given temperature level and the critical temperature of a frame subjected to a given load level.

The above mentioned relationship can be illustrated with reference to Fig.6.27 in which path no.1 represents the analysis undertaken to predict the collapse load at given temperature level  $T$  while prediction of the critical temper-

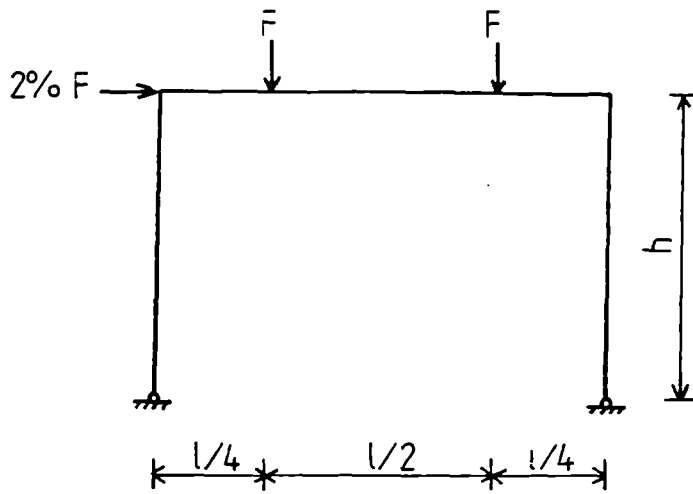


Fig. 6.25a - Frame geometry and loading.

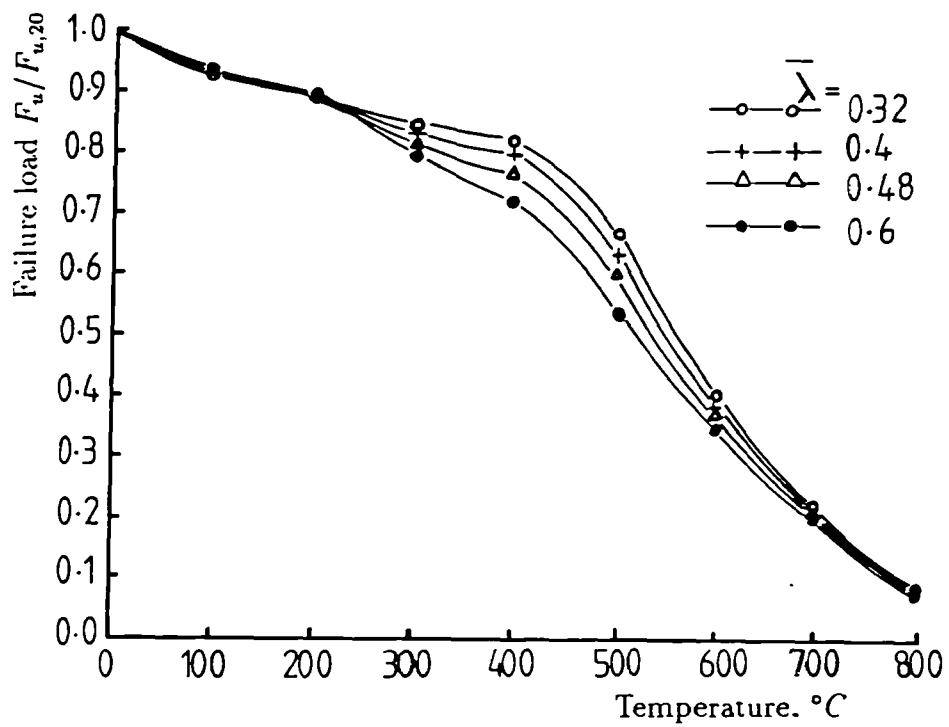
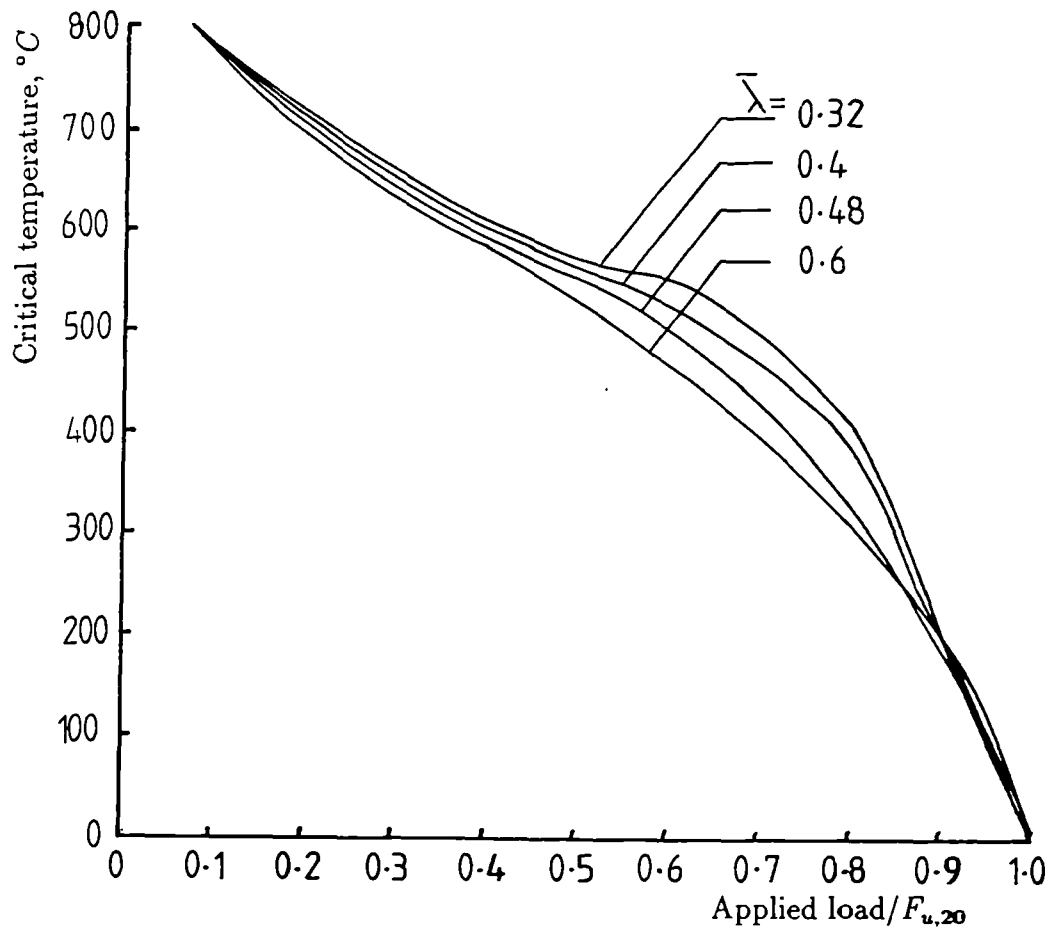
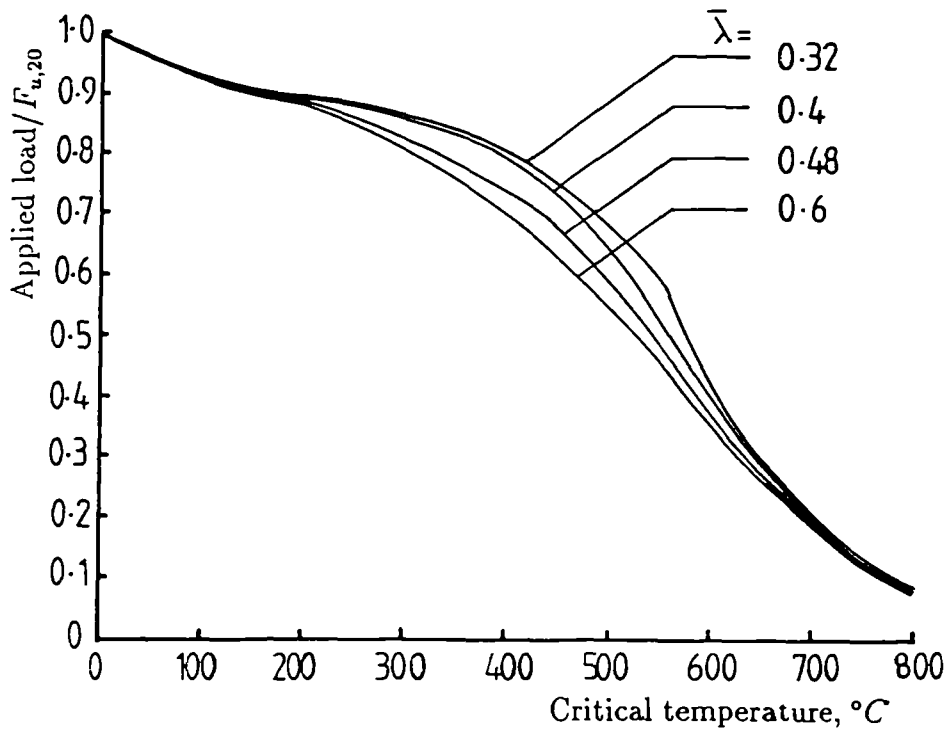


Fig. 6.25b - Variation of failure load with temperature at increasing slenderness for sway frame.



(a)



(b)

Fig. 6.26 - Applied load level Vs. critical temperature at increasing slenderness.

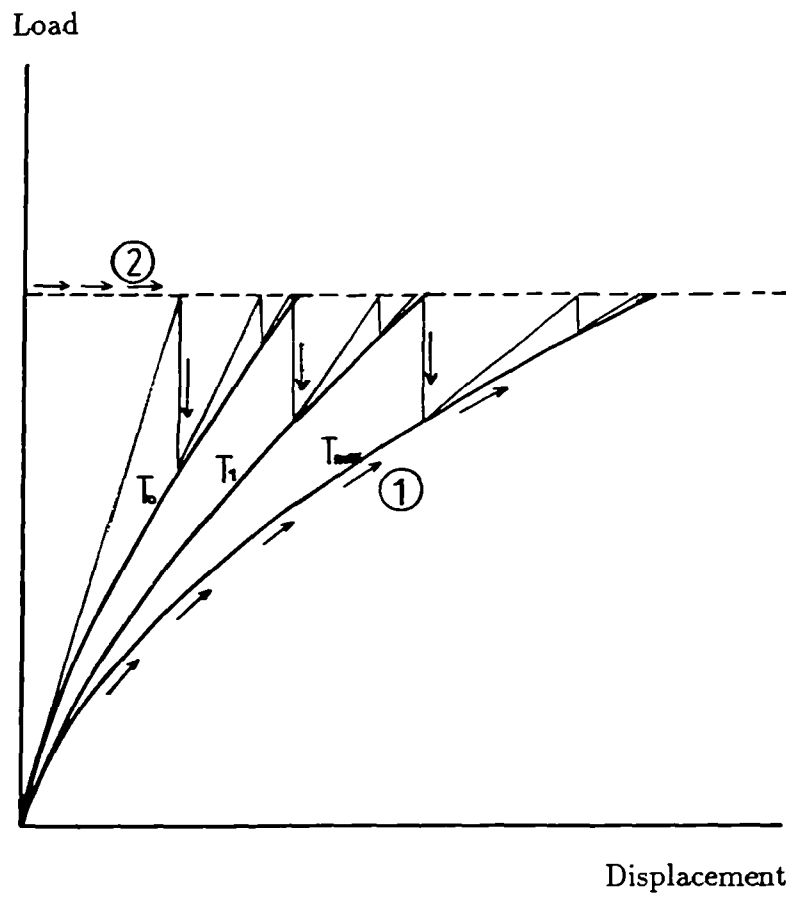


Fig. 6.27 - Schematic representation of method of analysis.

ature of a frame subjected to a certain load level  $P$  follows path no.2. It is clear from this figure that, both forms of analysis predict the deformational history and critical temperature or collapse load of a structure to be very similar.

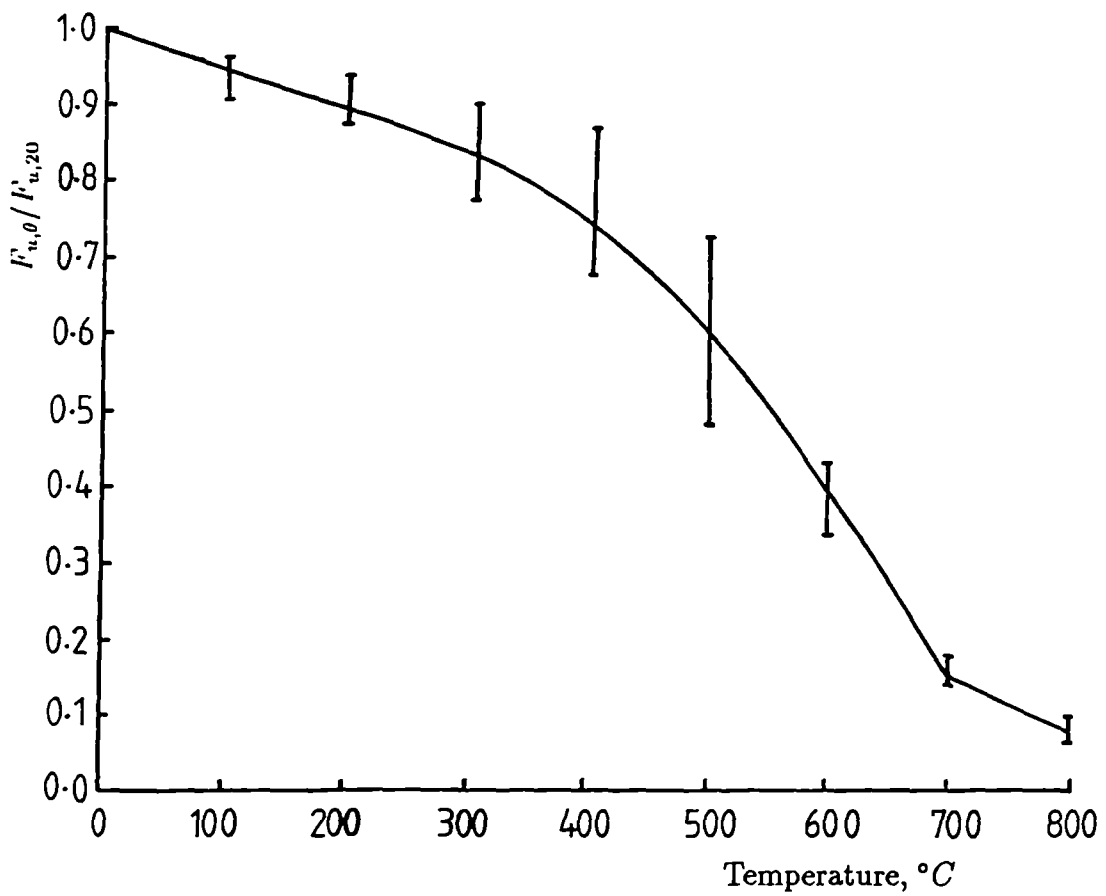
### **6.3.2 An approximate strength - temperature curve for uniformly heated steel frames**

Fig.6.28 shows the result of curve fitting the data obtained in the earlier analyses. Over 100 data points representing frames with a wide range of slenderness ratios, end conditions, material properties and loading level were used in order to derive a simple strength - temperature relationship. This curve comprises of two straight lines between  $20 - 300^{\circ}C$  and  $700 - 800^{\circ}C$  and a parabolic relationship in the temperature range  $300 - 700^{\circ}C$ . This curve can be of direct practical use as an approximate design estimation for the prediction of critical temperature and collapse load of frames subject to a given load and temperature level. Frames can also be designed to a specific load level if the structure is to achieve a given limiting temperature.

Checks will be made on this curve in the following section in order to further establish its validity.

### **6.3.3 Verification of the obtained curve**

To this end, the frame shown in Fig.6.29 of IPE 80 sections was analysed under different loading levels and temperatures. The predicted results are shown in Table 6.3. A three-storey non sway frame shown in Fig.6.30 was also analysed



$$\begin{aligned}
 20 < \theta \leq 300^\circ\text{C} \quad F_{u,\theta} / F_{u,20} &= 1 - 5.6742 \times 10^{-4}(\theta - 20) \\
 300 < \theta \leq 700^\circ\text{C} &= -2.8211 \times 10^{-6}\theta^2 \\
 &\quad + 1.096 \times 10^{-3}\theta + 0.766 \\
 700 < \theta \leq 800^\circ\text{C} &= 0.151 - 7.112 \times 10^{-4}(\theta - 700)
 \end{aligned}$$

Fig. 6.28 - Proposed strength-temperature curve for uniformly heated frames.

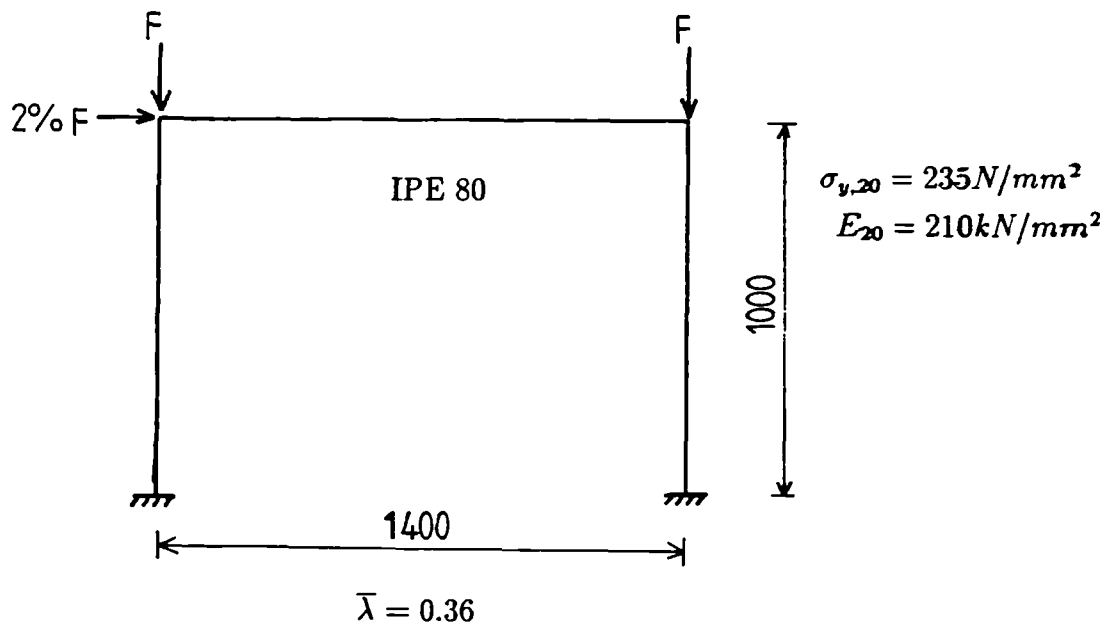


Fig. 6.29 - Frame geometry and loadings for curve verification.

	Input		Calculated	
	(°C)	$\frac{F_u}{F_{u,20}}$	$\frac{F_u}{F_{u,20}}$	(°C)
<i>Temperature level</i>	200		0.856	
	350		0.731	
	550		0.5	
<i>Load level</i>		0.7		402
		0.2		692

Table 6.3 - Input data and results for curve verification.

under the loading and temperature levels shown in Table 6.4. Fig.6.31 shows that the calculated results are in a very good agreement with the curve prediction.

Fig.6.31 also shows results of the analysis carried out on the frame shown in Fig.6.29 using yield strength characteristics of the fire resistant steel reported in section 3.3.2.5. The yield strength characteristics of this steel retain 2/3 of its room temperature value up to 600°C as can be seen from Fig.3.3. Whilst Fig.6.31 shows improvement in the frame performance when using this steel, the frame retains only half of its room temperature strength at 600°C. This is due to the fact that factors other than the steel properties influence the frame behaviour. Such factors include slenderness ratio and the load level.

## 6.4 Variation of internal moment with temperature

In the event of a fire in a multistorey steel frame building, it is possible that some members will develop certain temperature levels different from those of other members. This temperature variation occurs during a compartment fire or due to various protection patterns. Under these conditions, steel frames are likely to develop a pattern of internal moments at elevated temperatures which is different from the ambient temperature distribution. This is due to the fact that the inherent resistance of colder members can be utilised to support weak parts of the frame which are exposed to higher temperature levels, thus shifting the demand for resistance towards the sections whose ultimate capacity has not been exceeded. This enhances the fire endurance of the structure and consequently increases its limiting critical temperature.



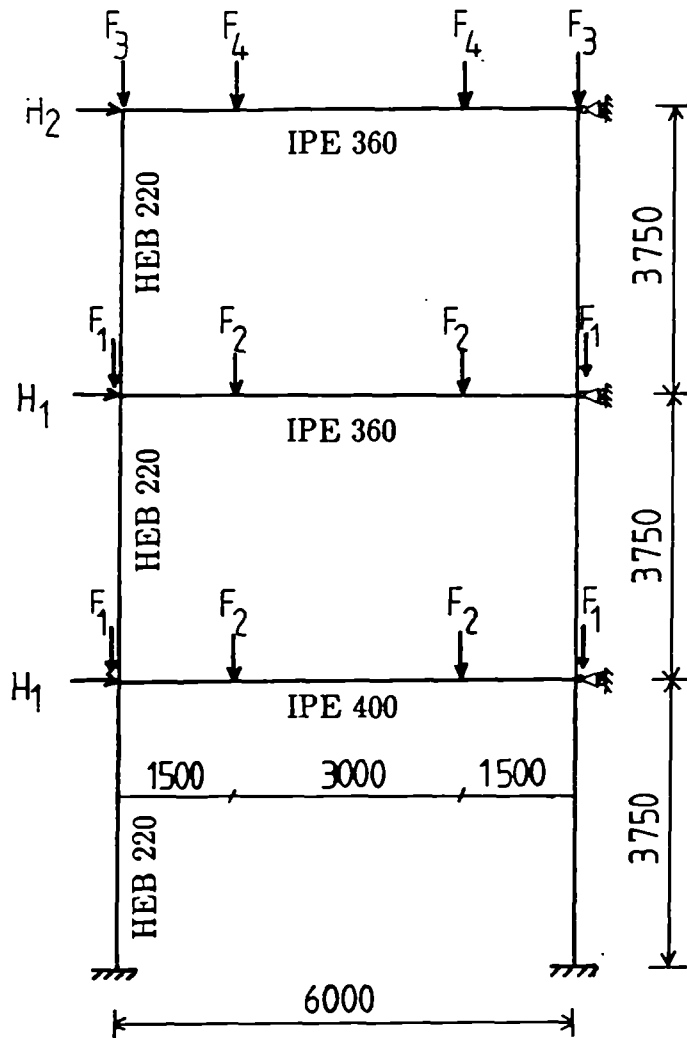


Fig. 6.30 - Frame geometry and loadings for curve verification.

	Input		Calculated	
	(°C)	$\frac{F_u}{F_{u,20}}$	$\frac{F_u}{F_{u,20}}$	(°C)
<i>Temperature level</i>	150		0.9606	
	250		0.9006	
	400		0.9	
	500		0.7806	
	600		0.4502	
<i>Load level</i>		0.35		662
		0.55		572

Table 6.4 - Input data and results for curve verification.

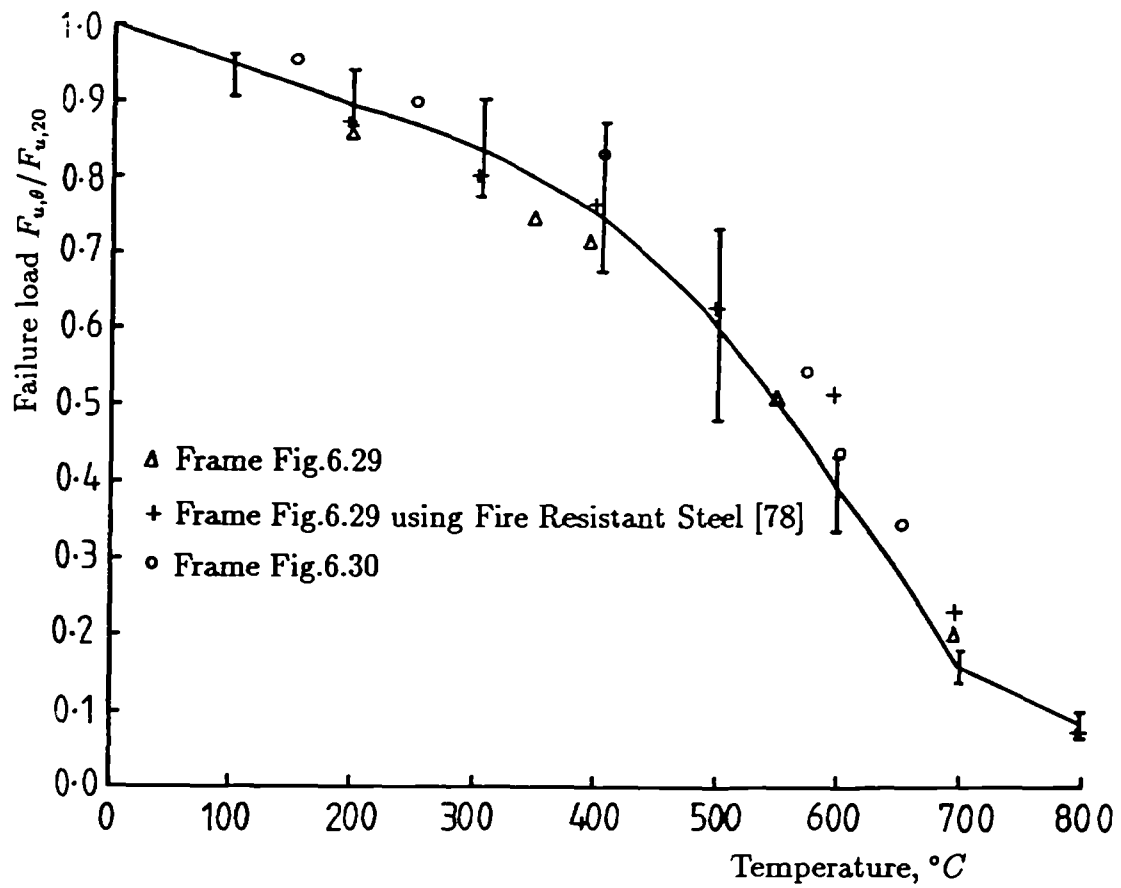


Fig. 6.31 - Verification of the proposed strength-temperature curve for uniformly heated frames.

To illustrate this phenomenon, the four frames shown in Figs.6.32a-d were studied under various heating patterns. Frames (a) and (b) were designed in order to obtain beam failure while frames (c) and (d) had high concentrated loads on their columns in order to produce column failure. In all cases, the load ratio was maintained at 60% of the ambient temperature ultimate load; the ambient temperature yield strength and modulus of elasticity were assumed as  $235 \text{ N/mm}^2$  and  $205 \text{ kN/mm}^2$  respectively. Imperfections were considered in the form of initial lack of straightness in the columns with a maximum of  $L/1000$  at mid-height and an assumed half sine wave distribution over the lengths of the members.

Consider now the example of the simple portal frame shown in Fig.6.32a with bracing members provided in order to prevent sway so that the change of internal moment of resistance can only be caused by temperature increase. Assume that both columns of the frame are uniformly heated while its beam is kept at room temperature. The reducing effect that the elevated temperature has on the moment of resistance of the heated columns is shown in Fig.6.33 in which the variation of the internal moment of resistance is plotted around the frame. The increase in the moment at mid-span of the beam with increasing temperatures is shown by Fig.6.34. It is shown that, as columns lose stiffness at increasing temperature, the contribution of the beam near its ends towards the load carrying capacity is also gradually decreasing as the beam mid-span moment tends to increase. Moreover, as temperature increases, a gradually reduced moment is resisted by ever less stiff columns, thus subjecting the mid-span of the beam to higher stresses up to the limit that can be resisted by the beam section. Furthermore, the inherent rotational restraint to the beam ends provided by the beam-to-column connection which is gradually decreasing under increasing temperature implies that the beam is gradually subjected to a higher load

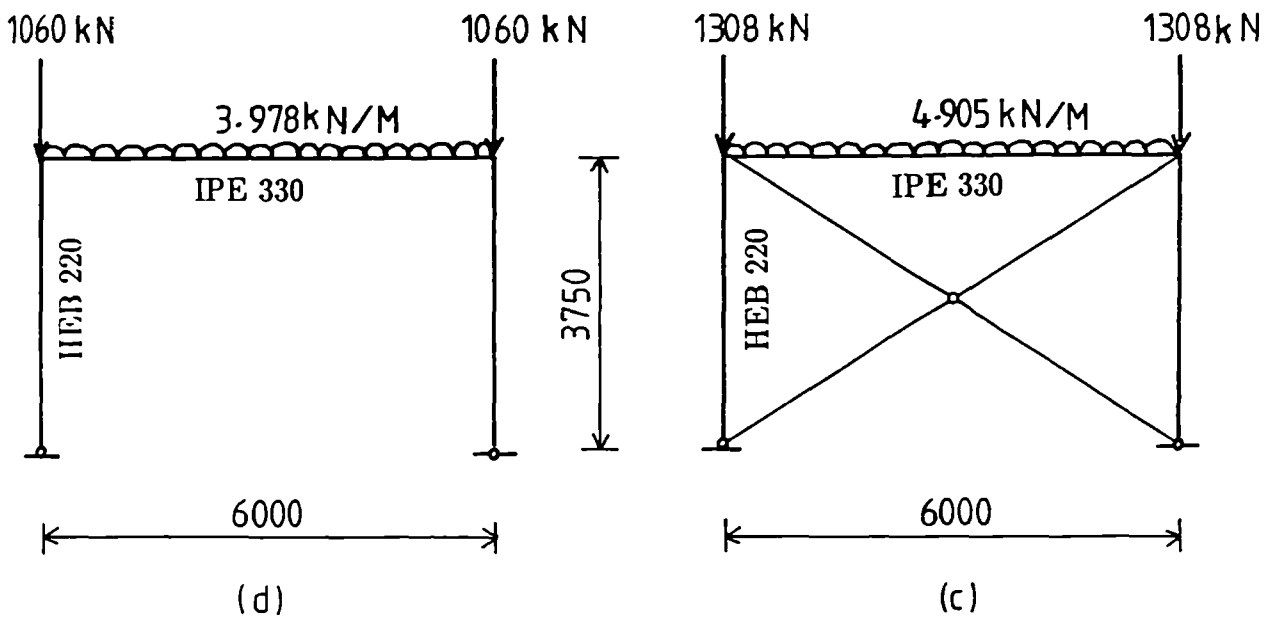
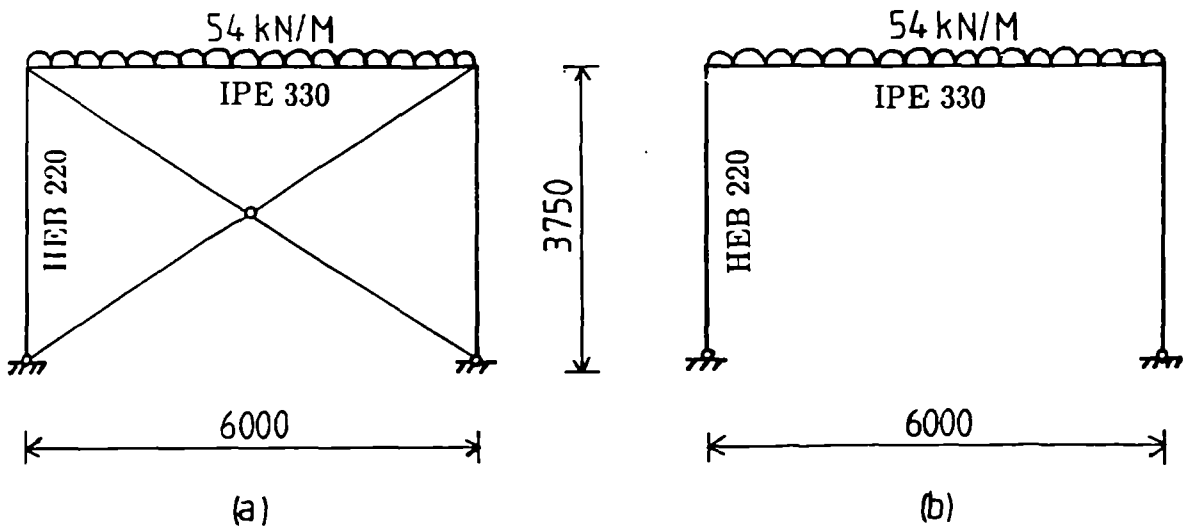


Fig. 6.32 - Frames geometry and loadings.

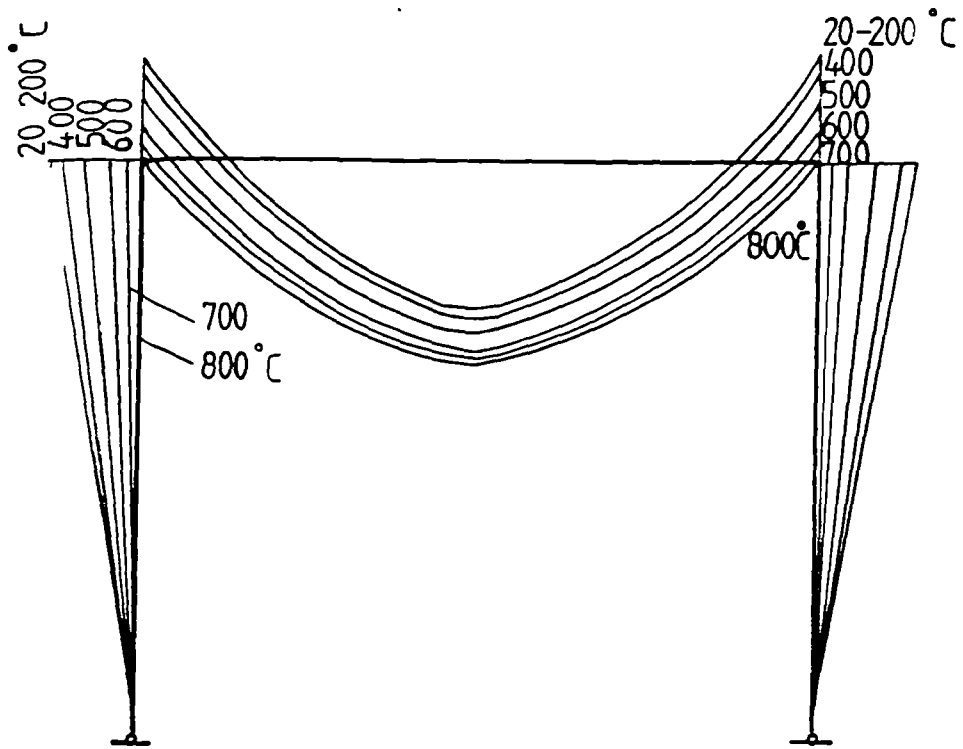


Fig. 6.33 - Variation of bending moment distribution with temperature.

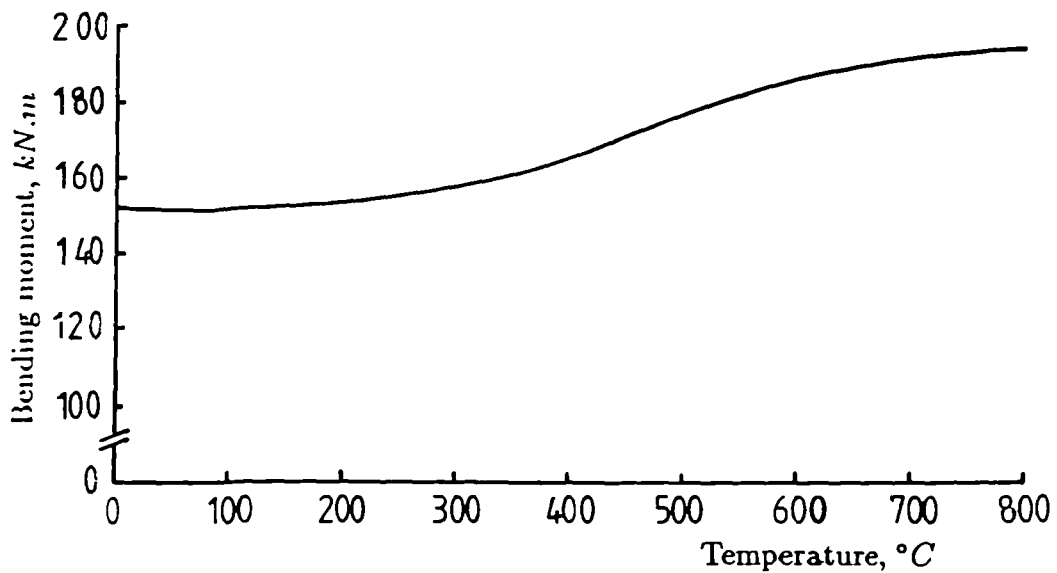


Fig. 6.34 - Variation of bending moment distribution with temperature at mid-span of the beam.

ratio due to the change in its effective end conditions. At  $800^{\circ}\text{C}$ , the beneficial contribution of beam-column interaction towards the beam's carrying capacity has become negligible, with the beam effectively having simple supports. It is therefore this beam with the relevant end conditions and load ratio that controls the collapse of the frame. For this frame, collapse occurs at a temperature level at which the load ratio of the beam, which now has only the degree of rotational stiffness at its ends corresponding to that temperature level, exceeds its ultimate load carrying capacity. This phenomenon should be reflected quantitatively in design requirements. A similar analysis was carried out on the sway frame shown in Fig.6.32b. The results show that the effects of this temperature scheme on unbraced frames are similar to those exhibited by the braced frames but at a reduced moment level and lower critical temperature due to the additional effects of sway. This is due to the influence of nonlinear effects on unbraced frames, which are enhanced by the decreasing stiffnesses of the heated columns.

Consider now the no-sway frame of Fig.6.32c which was designed to withstand high concentrated loads on the columns. Assume that only the columns are uniformly heated with the beam being kept at room temperature. Again, this frame exhibited similar response regarding loss of beam rotational end restraints due to the deterioration in column stiffnesses, though at a much reduced temperature level as shown in Fig.6.35. Because these columns are subjected to high concentrated load, collapse of the frame has occurred at  $555^{\circ}\text{C}$ . On the other hand, insulating the columns while the beam is subjected to increasing temperatures has led to the columns exhibiting a higher moment of resistance while the beam strength is gradually deteriorating. This is shown by Fig.6.36 in which the beam end restraints retain their ambient temperature values, thus providing quasi-fixed ends at high temperatures. This clearly affects the effective length factor of the column. At  $800^{\circ}\text{C}$  the moment at the beam ends has

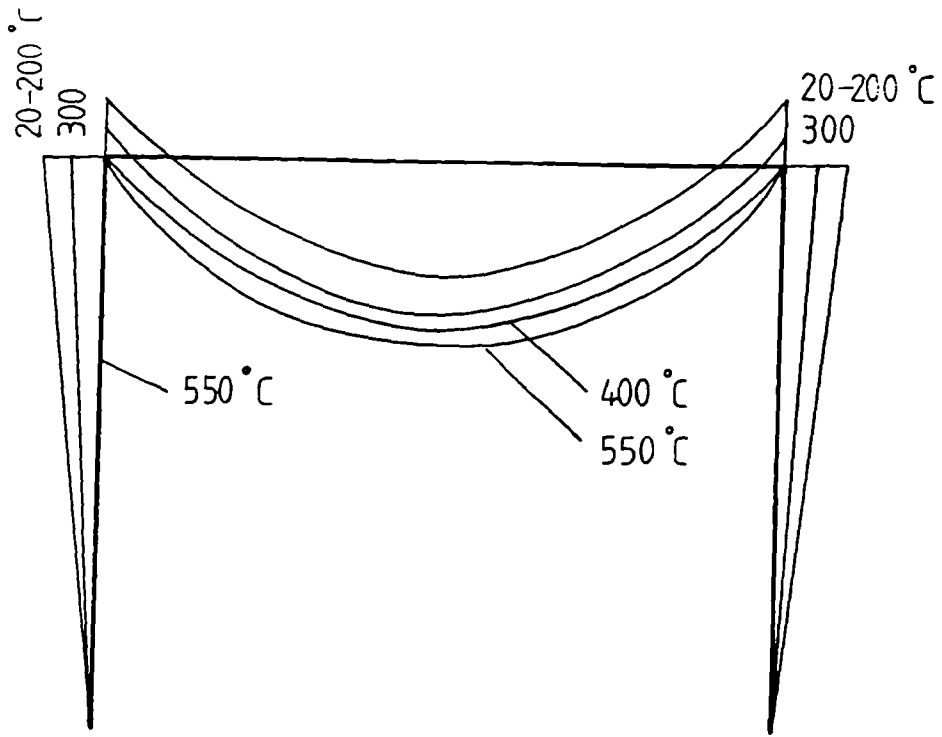


Fig. 6.35 - Variation of bending moment distribution with temperature.

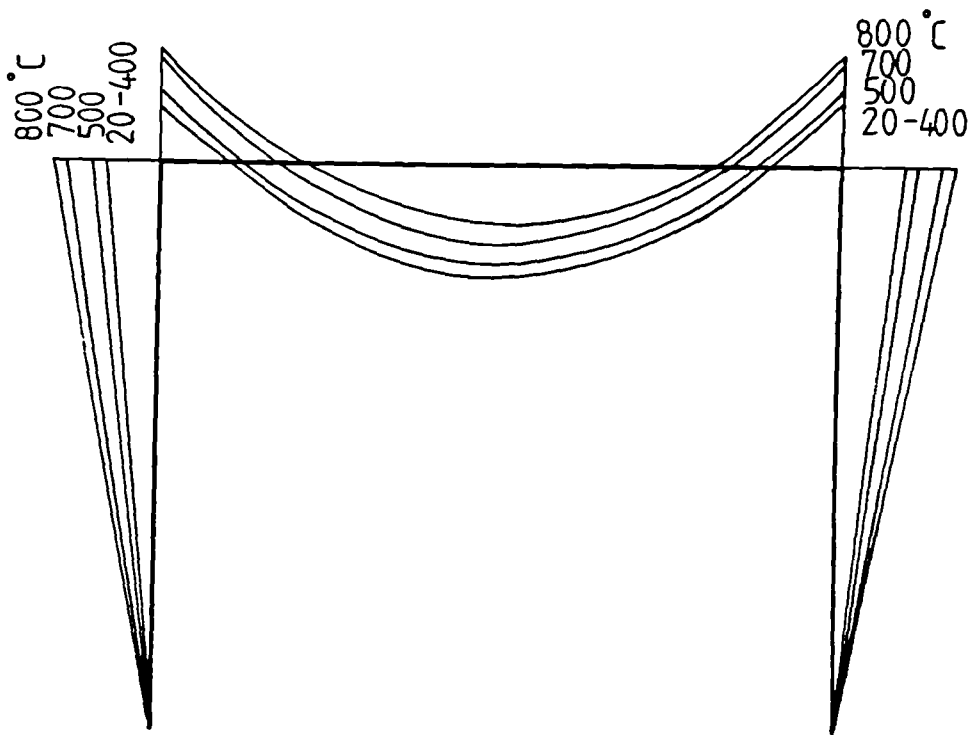


Fig. 6.36 - Variation of bending moment distribution with temperature.



approximately doubled its ambient temperature value, which in turn reduces the moment at mid-span to half its original value. Analysis has not been possible beyond  $800^{\circ}\text{C}$  due to lack of material data at these temperatures but the same tendency of the columns to resist higher moment is expected to continue at ever increasing temperatures, thus providing infinite end restraint stiffness. At this stage, collapse would be due to beam failure with infinitely stiff end restraints and an assumed very low load ratio. Only when the frame was totally and uniformly heated (Fig.6.37) was there a gradual loss of its member's stiffnesses and strengths which led to the collapse of the frame, controlled by deterioration of column bearing capacity, at  $525^{\circ}\text{C}$ . Similar analyses have been carried out on the unbraced frame of Fig.6.32d showed similar moment redistribution, but failure occurred at a much reduced temperature level. Although the braced and unbraced frames were subjected to the same load level, the reduction in critical temperature is due to the sensitivity of the unbraced frame to nonlinear effects. These effects become more detrimental to the behaviour of unbraced frames due to the decreasing stiffnesses of the heated columns, especially when these columns are subjected to high concentrated loads.

To summarise, the distribution of moment at elevated temperature in a partially heated frame is different from that at room temperature, being dependent upon the relative stiffnesses of different structural members under their corresponding temperature levels. The inherent beneficial effects of interaction between different elements is affected by the relative temperatures of these members; their response in a frame depends upon the heating pattern and load arrangement and therefore cannot be predicted simply from consideration of individual members. This is the case when beams, often designed with simple connections in practical frames, exhibit superior performance due to the relatively low temperature of the protected joints. This phenomenon should be considered when

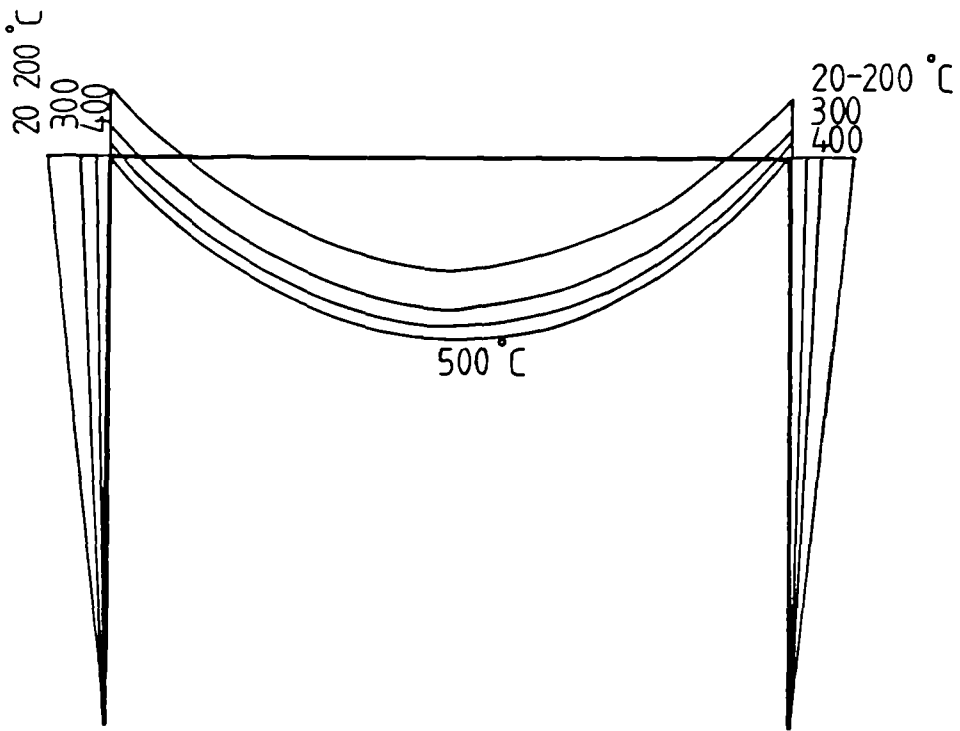


Fig. 6.37 - Variation of bending moment distribution with temperature.

analysing structural elements with the relevant end conditions at the corresponding temperature levels if individual element rather than interactive frame analysis is to be carried out. Any subsequent insulation arrangement can therefore ensure better fire endurance of the steel frame as a whole.

## 6.5 Concluding remarks

It is clear that many parameters affect the response of steel frames at elevated temperatures. Such parameters include : slenderness ratio, form of the stress-strain representation, partial protection, residual stresses and thermal gradient. Based on the studies reported in this chapter, the following conclusions may be drawn :

1. The familiar room temperature influence of yield strength and modulus of elasticity on frames is also apparent at elevated temperatures. The behaviour of low slenderness frames is largely controlled by the material yield strength while high slenderness frames are influenced principally by modulus of elasticity. The behaviour of intermediate slenderness frames is influenced by the interaction between material yielding and elastic overall buckling.
2. The markedly nonlinear response of steel at high temperatures is better represented by a continuous form of stress-strain-temperature relationship than by a bilinear form. The use of the bilinear form results in higher collapse loads and has led to the predicted behaviour of low to intermediate slenderness frames to be similar. A distinctive behaviour of any frame is exhibited when using the continuous representation.

3. Between the three material models used in the analysis, the ECCS expressions for yield strength and modulus of elasticity have resulted in the most conservative collapse loads while the prediction based on the BS5950 expressions results in the highest loads for all frames. Results of the analyses based on the CTICM expressions fall in between those two predictions.
4. The provision of a stiffer cold part of the frame as a result of partial protection of this part or of compartmentation improves its fire endurance considerably, especially if this part is such that it can support the rest of the structure.
5. It is noted that residual stress distribution and magnitude have negligible effects beyond those exhibited at ambient temperature on low to moderate slenderness frames. Their effects on very high slenderness frames are of no significance. It can be concluded that if the residual stress magnitude at room temperature does not have a significant influence then it will be even less important at elevated temperatures.
6. Generally thermal gradient across a section has a beneficial effect. Bowing of the members towards the heat source can be equated to an initial out-of-straightness which is partly compensated by the apparent eccentricity of loading caused by the shift of the effective neutral axis towards the colder parts. This bowing has shown negative effects on the very high slenderness frames where imperfections can most affect behaviour. The nonuniform longitudinal temperature distribution, especially in the vicinity of the ends, has negligible effect on frame behaviour provided that this longitudinal temperature distribution does not change the end stiffnesses.
7. The range of critical temperatures exhibited by different frames under various loading levels shows that uniformly heated frames with similar load

levels ( $F/F_{u,20}$ ) fail at approximately equal temperatures. The frame slenderness ratio ( $\bar{\lambda} = \sqrt{\frac{F_u}{F_c}}$ ) affects the predicted limiting temperatures especially for frames subject to moderate load levels. Critical temperature can therefore be determined as a function of frame slenderness ratio and load factor. These two parameters are ambient temperature design characteristics and can be determined using conventional methods.

8. Partial protection of a frame affects the interaction between its members, which alters their effective end restraint. This is the case when beams, often designed with simple connections in practical frames, exhibit superior performance in fire due to their relatively cold joints. The change in end restraint affects the load ratios and, in the case of columns, influences their effective lengths. The behaviour of various elements in a frame cannot be accurately predicted when these elements are individually analysed.

# Chapter 7

## Strength and Stability of Sway Frames in Fire

### 7.1 Introduction

In real building fires, temperature profiles will not be identical in all the structural members of a frame since these members cannot be expected to be exposed to the same heating conditions at any one time. The temperature distribution will therefore change according to the position of the member in the building relative to the fire source, and time. This often occurs during a compartment fire when locally intense heating affects members in and around the compartment, which leads to certain members being subjected to a relatively very high temperature for a relatively short time whilst other members are effectively quite cool. A similar situation occurs when fire takes place in one or two compartments at one time with the compartment floor acting as a heat sink and as a shield which keeps the rest of the structure relatively cool [34].

Such conditions are likely to have considerable effects on the strength and stability of sway frames. The behaviour of the heated members cannot be predicted if these members are individually considered; it is better to consider their interaction with the rest of the structure. This is because of the stabilising influence of the cooler parts of the structure located outside the fire compartment. A similar principle may be applied to the effects on the columns of the lateral restraint provided by the floor forming the roof of the fire compartment.

The heated members are expected to expand more than the adjacent cooler members, which will result in additional forces being induced in the structure due to partial restraint of thermal expansion and rotation. These forces can be neglected if the adjacent members can expand equally, or if the degree of rotational end restraint is relatively low. Furthermore, this degree of axial and rotational restraint becomes larger in a more extensive frame when a larger number of levels above and around the fire floor exist [9]. On the other hand, deterioration of axial and flexural rigidity of the heated members due to the reduction of their material strength and stiffness reduces these thermally induced forces as temperature increases. Moreover, the contribution of the heated members towards the overall resistance to the externally applied loading system reduces with increasing temperature, which leads to greater mobilisation of the inherent resistance of the cooler parts in order to preserve the integrity of the structure. Thus the distribution of the internal forces may differ from the ambient temperature distribution and cannot therefore be deduced from their ambient temperature values by an affine transformation.

The stabilising influence of the cooler parts of the structure is outlined in section 6.2.3. It has been shown that, depending upon the position of the cooler part in the frame, its fire endurance considerably improves especially if this part

can support the rest of the structure. For a column located outside the fire compartment, the degree of lateral support and rotational restraint provided by the floor forming the roof of the fire compartment decreases with increasing temperature. This significantly alters the effective length of the column and consequently its load capacity. The decrease in the column end restraint with increasing temperature will increase its effective length and reduce its load carrying capacity, although this column is not directly affected by the fire. It is not therefore accurate to assess the critical temperature and collapse load of individual elements using the effective length from the ambient temperature conditions.

This chapter aims to investigate the stabilising influence of the cool part of the frame and the effects of localised heating on the overall behaviour of sway frames. To this end two practical frames are considered in relation to local fires in which part of the frame is heated whilst the rest remains cool. The frames, with fixed and pinned column bases respectively, have similar geometry and member cross-sections, and are both subjected to 70% of their ambient temperature ultimate loads. In both cases the ambient temperature yield strength and modulus of elasticity were assumed to be  $235 \text{ N/mm}^2$  and  $205 \text{ kN/mm}^2$  respectively.

## 7.2 Behaviour of fixed base frames

The three-storey two-bay frame shown in Fig.7.1 was analysed under various schemes of heating. The frame is of intermediate slenderness, having a value of  $\bar{\lambda} = 0.38$ . The frame geometry and loading represent the lower part of a multi-storey steel frame. Calculations were made for six different heating conditions as illustrated in Table 7.1. A uniform temperature was assumed along and across the heated members of the frame while ambient temperature was assumed for the



Loads :  $F_1 = 292.275kN$      $F_2 = 974.25kN$   
 $F_3 = 147.30kN$      $H_1 = 10.44kN$

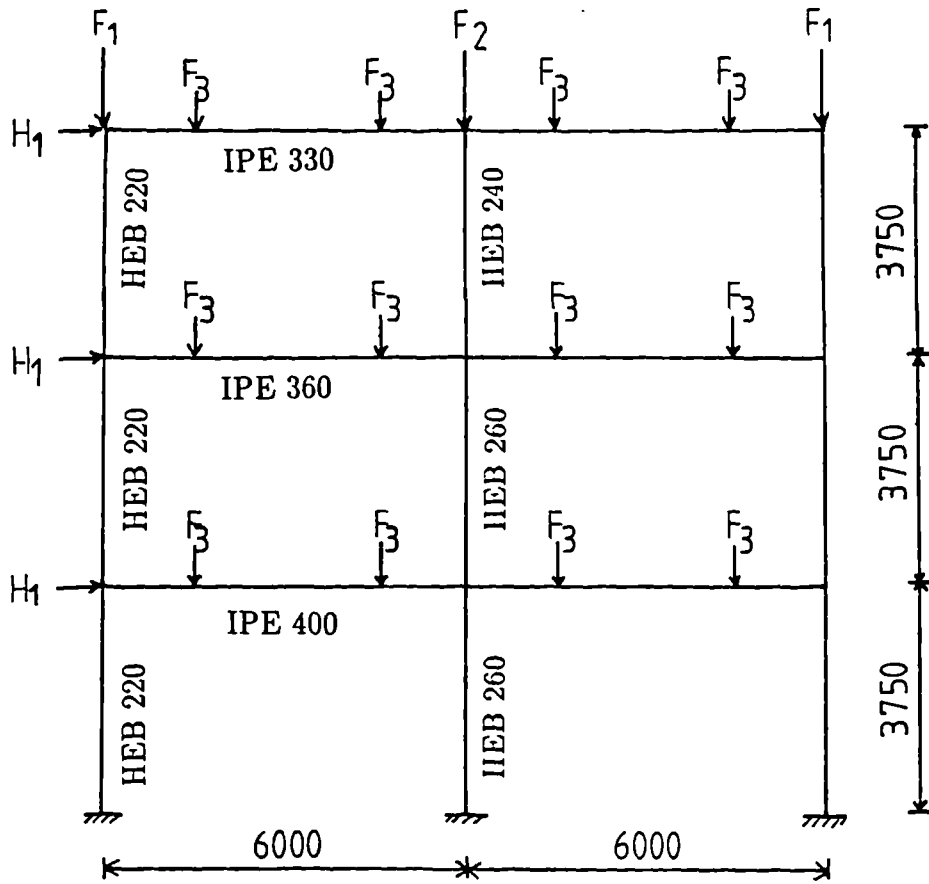
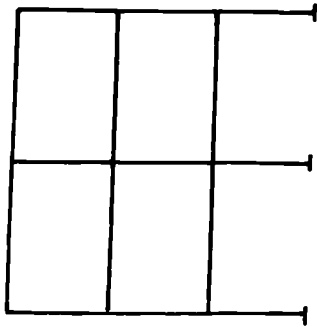
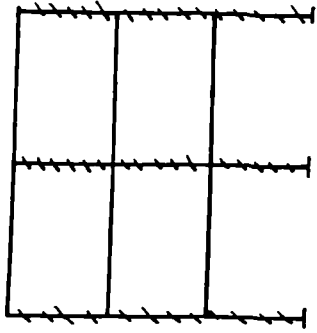


Fig. 7.1 - Frame geometry and loadings of fixed base frame.

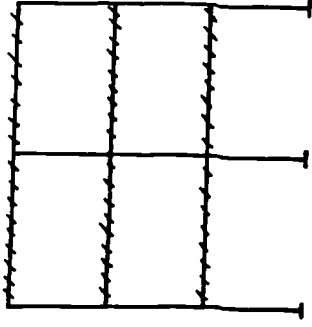


$F_1$   
 $\theta_{cr} = 441\text{ }^\circ\text{C}$

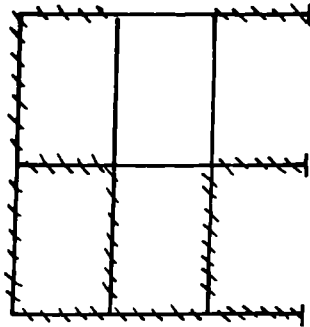


$F_2$   
 $\theta_{cr} = 552\text{ }^\circ\text{C}$

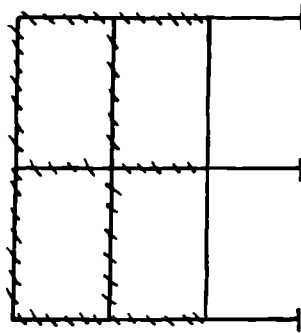
++++ Cold element



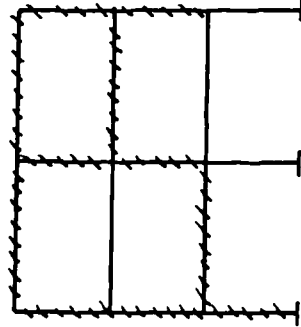
$F_3$   
 $\theta_{cr} = 455\text{ }^\circ\text{C}$



$F_4$   
 $\theta_{cr} = 552\text{ }^\circ\text{C}$



$F_5$   
 $\theta_{cr} = 453\text{ }^\circ\text{C}$



$F_6$   
 $\theta_{cr} = 551\text{ }^\circ\text{C}$

Table 7.1 - Various forms of heating conditions and corresponding critical temperatures.

rest of the structure.

Table 7.1 gives the predicted failure temperatures of the frame under the six different heating conditions. The results show that for total heating ( $F_1$ ), a critical temperature of  $441^\circ\text{C}$  was obtained. A considerable increase of 25% in this limiting temperature was provided by protecting all three columns in frame  $F_2$ . In this case, although the strength and stiffness of the columns themselves are preserved, the lateral support provided by the beams is reducing with increasing temperature due to the deterioration of the beam stiffness. Furthermore, the beneficial rotational restraint provided by the beams reduces with increasing temperature, which will change the effective length of each column. As temperature increases, the increase in the effective length of a column reduces its critical load leading to failure by instability. However, this lateral support provided by the heated beams does not vanish completely at high temperatures; a certain degree of rotational restraint will remain. If this column is assessed individually, then ambient temperature behaviour can be used provided that the effects of the temperature levels of the adjacent beams on its effective lengths are taken into account. On the other hand, the fact that insulating the beams only ( $F_3$ ) did very little to improve the critical temperature of the frame demonstrates that in this case the columns gradually lose strength and stiffness while the cold beams act as bracing against sway.

In Table 7.1, frame  $F_2$  demonstrates that the integrity of the structure can be preserved until a higher temperature is developed through the provision of a sway resisting assembly in the form of three stiff cold columns which, in the extreme case, can act as cantilevers. This phenomenon is also clear from frames  $F_4$ ,  $F_5$  and  $F_6$  in which fire is confined to one or two compartments only. It can be seen that under such heating conditions, the critical temperatures of

frames  $F_4$  and  $F_6$  have increased to  $552^\circ C$  and  $551^\circ C$  respectively whilst this temperature was only  $453^\circ C$  for the conditions shown in frame  $F_5$ . The relatively higher critical temperatures exhibited by frames  $F_4$  and  $F_6$  are due to the fact that the provision of a stiffer cool core has delayed the collapse of these frames whilst frame  $F_5$  represents a gradually deteriorating ground floor region with the upper floors acting as overload.

The effect of the various heating conditions on the lateral deflection of the frame is shown in Fig.7.2 in which the lateral deflection-temperature relationships are plotted. It is shown that these curves follow the ambient temperature deflection up to  $200^\circ C$ . Beyond this temperature level frames  $F_1$  and  $F_3$  start to exhibit larger deflection, reflecting the reduction in the value of the modulus of elasticity shown in Fig.3.1, though the sway exhibited by frame  $F_3$  occurs at a more gradual rate due to the bracing effect of its cool beams. A smaller increase in deflection is exhibited by frame  $F_5$  at temperatures below  $400^\circ C$  due to the small deterioration in the material strength of its ground floor below this temperature level. However, this frame exhibits a sudden increase in lateral deflection as temperature increases further. On the other hand, frames  $F_2$ ,  $F_4$  and  $F_6$  prove to be more effective in limiting sway until considerably higher temperatures are developed. This results from the provision of a stiff cooler core in the structure which is able to resist sway of the frame. In the case  $F_2$  the columns act as cantilevers against sway while a complete stiff assembly has delayed sway of frames  $F_4$  and  $F_6$ . More details of the deformed shapes are shown in Figs.7.3 to 7.6. Fig.7.3 presents the deformed shape of the frame at ambient temperature just prior to failure while Fig.7.4 shows that failure of the uniformly heated frame  $F_1$  occurred in a sway mode which is an amplified version of the room temperature mode. Comparison between the deformed shapes of frames  $F_2$  and  $F_4$  at  $550^\circ C$  shown in Figs.7.5 and 7.6 respectively reveals that frame  $F_4$  is more effective in

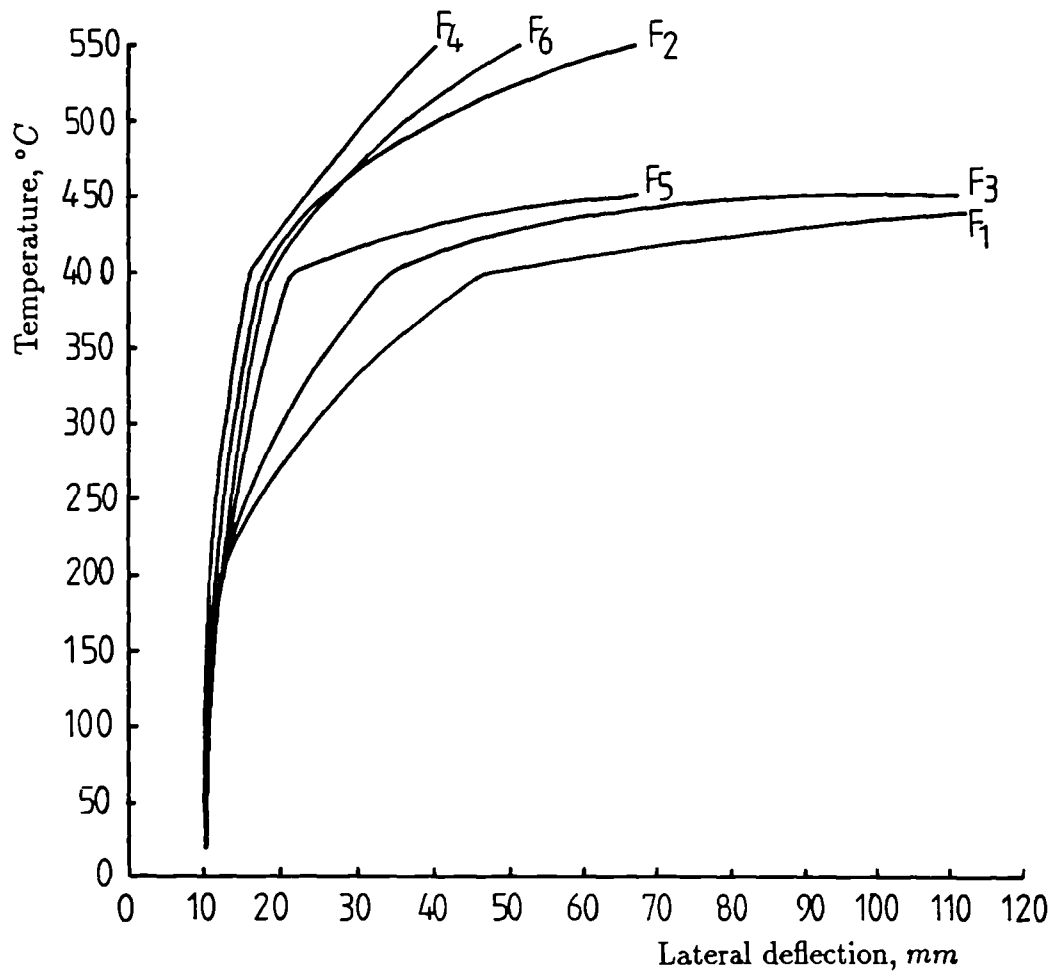


Fig. 7.2 - Lateral deflection-temperature relationships for heating conditions shown in Table 7.1.

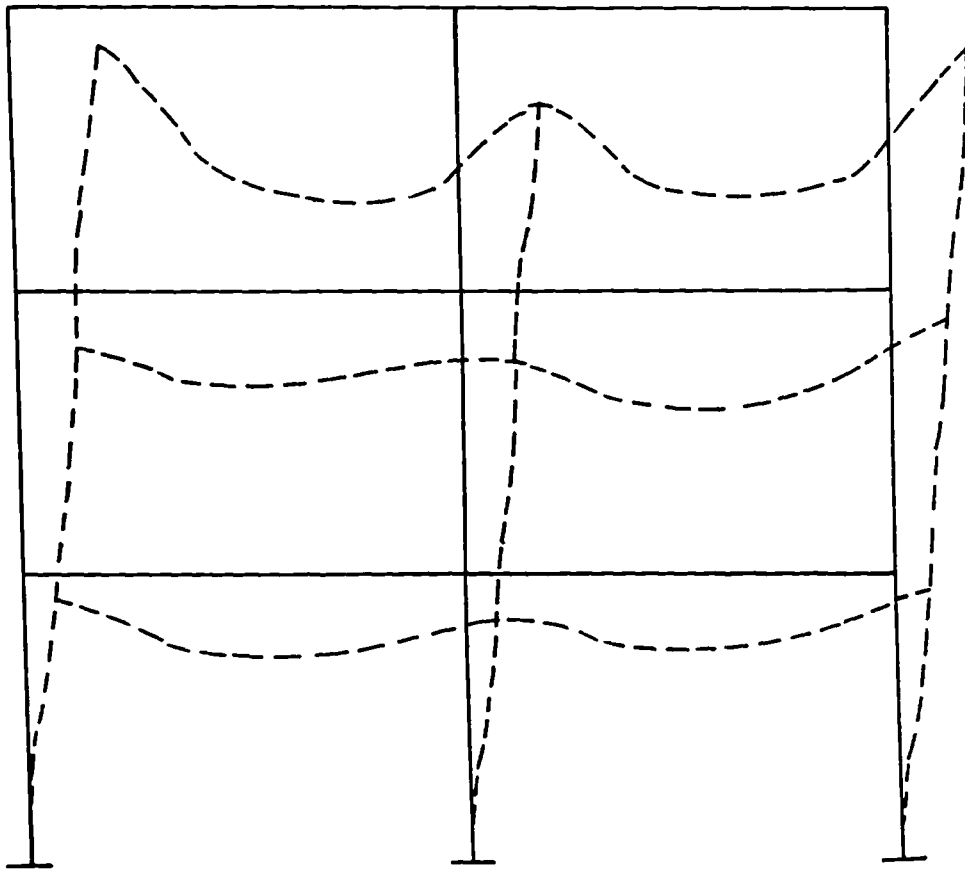
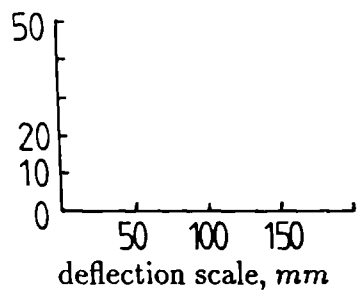


Fig. 7.3 - Ambient temperature failure mode.

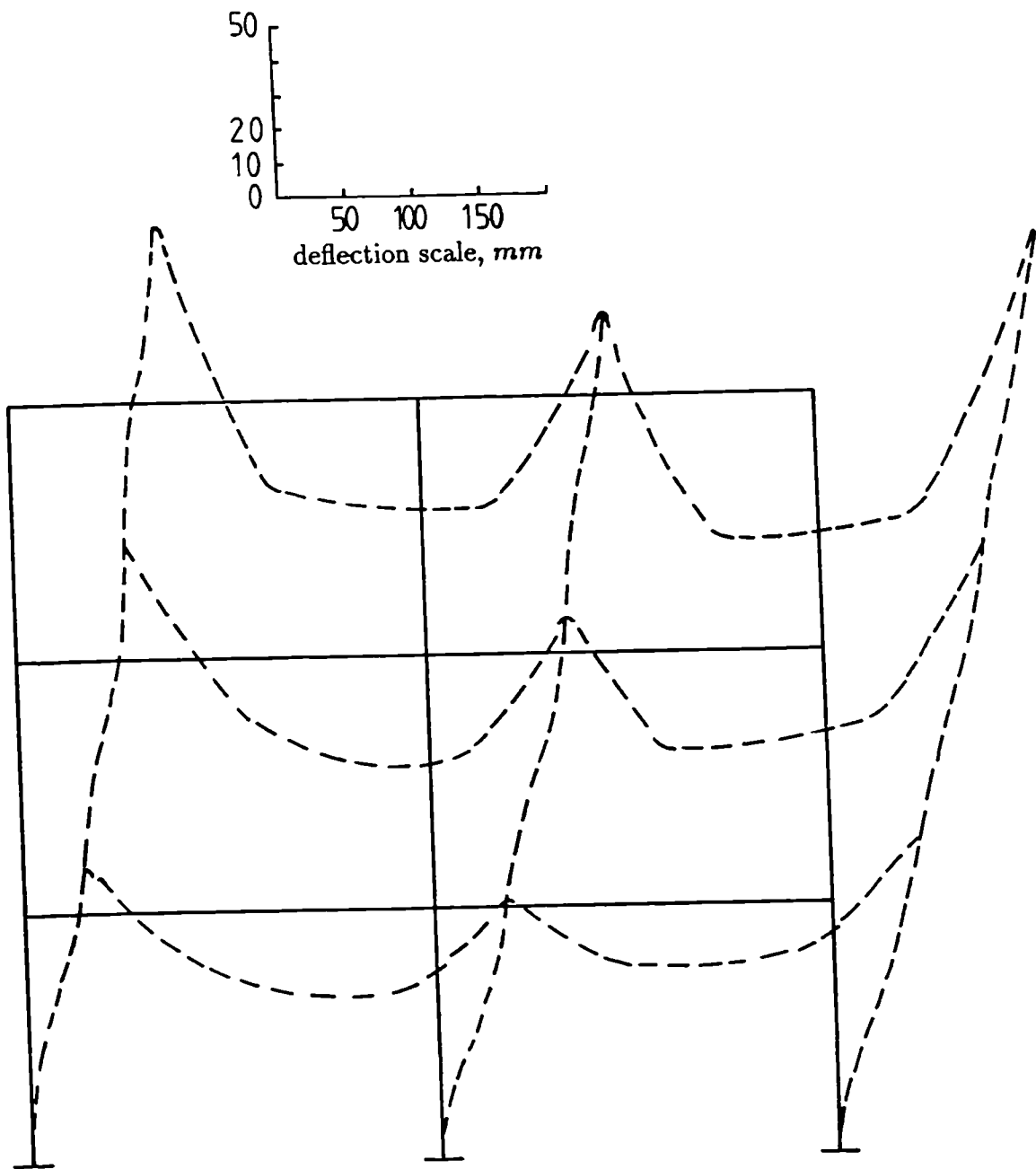


Fig. 7.4 - Deformed shape of uniformly heated frame ( $F_1$ ).

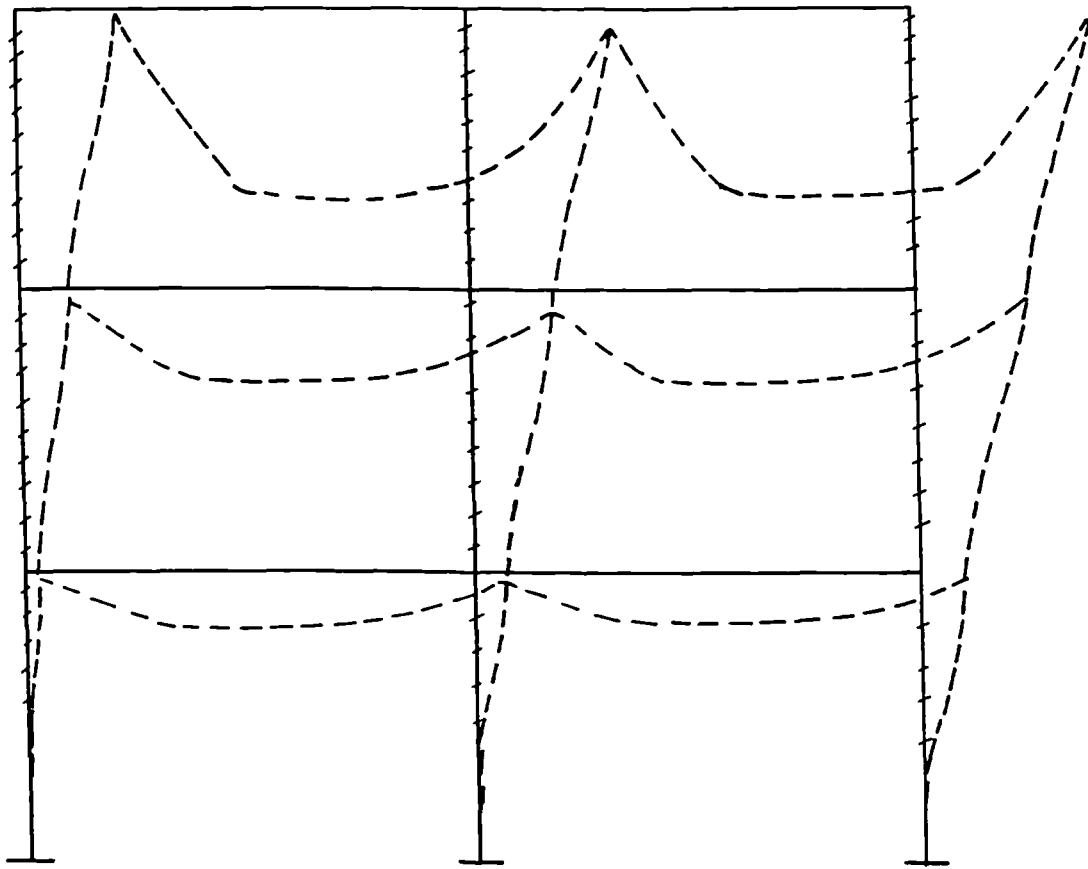
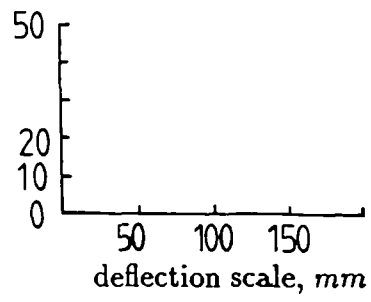


Fig. 7.5 - Deformed shape of frame ( $F_2$ ) at  $550^{\circ}C$ .



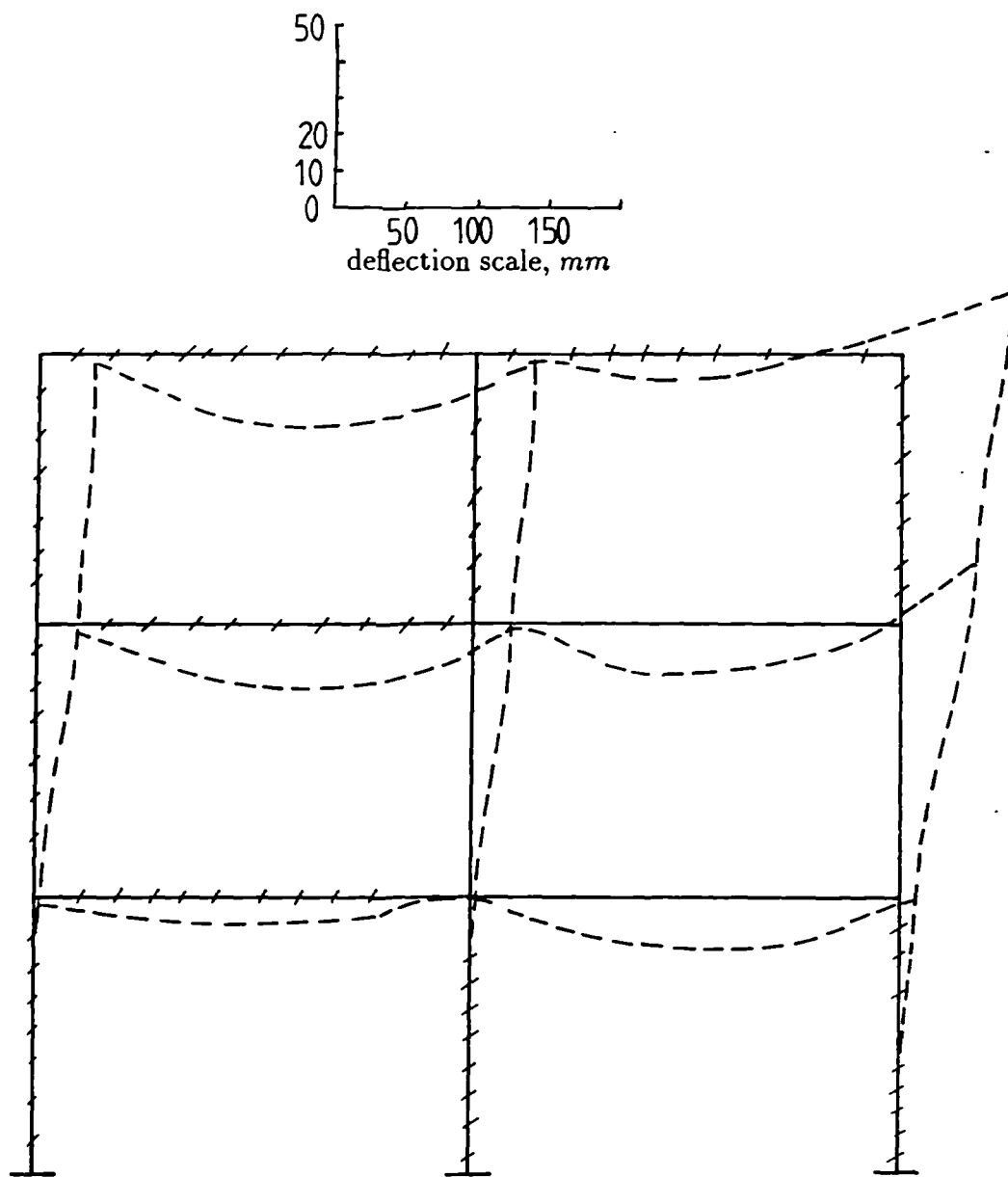


Fig. 7.6 - Deformed shape of frame ( $F_4$ ) at  $550^{\circ}C$ .

preventing sway.

The bending moment distribution at elevated temperatures depends upon the heating conditions, as can be seen from Figs.7.7 to 7.9 in which the internal moments for frames  $F_2$ ,  $F_4$  and  $F_6$  at  $550^\circ C$  are shown. The variation in the bending moment distribution results from the fact that additional forces are induced in the heated members by restraint of these members from expansion by their adjacent cooler members. These forces become larger in more extensive frames if a larger number of levels above and bays around the fire compartment exist. At the same time, these heated members are continuously losing their ambient temperature axial and flexural rigidity and strength as temperature increases, which transfers the resistance to the applied loading towards the cooler structural members of the frame. This is clear from Fig.7.8 in which the fire in compartment no.5 has induced additional moments in the left hand columns of compartments 1 and 2 compared with those when all columns are protected (Fig.7.7). This change is more pronounced in Fig.7.9 in which fire occurs in compartment no.6, due to the larger degree of restraint because of the larger number of levels which exist above the fire compartment.

### 7.3 Behaviour of pin ended frames

In order to develop more understanding of the effects of localised fire on frame behaviour, the frame shown in Fig.7.10 was analysed under various heating conditions as shown in table 7.2. The frame geometry was similar to the frame previously analysed except for the column bases which are assumed to be free to rotate, and the loading was proportionally reduced so as still to be 70% of the ambient temperature ultimate load capacity. With this loading arrangement and

0 100 200  $kN.m$

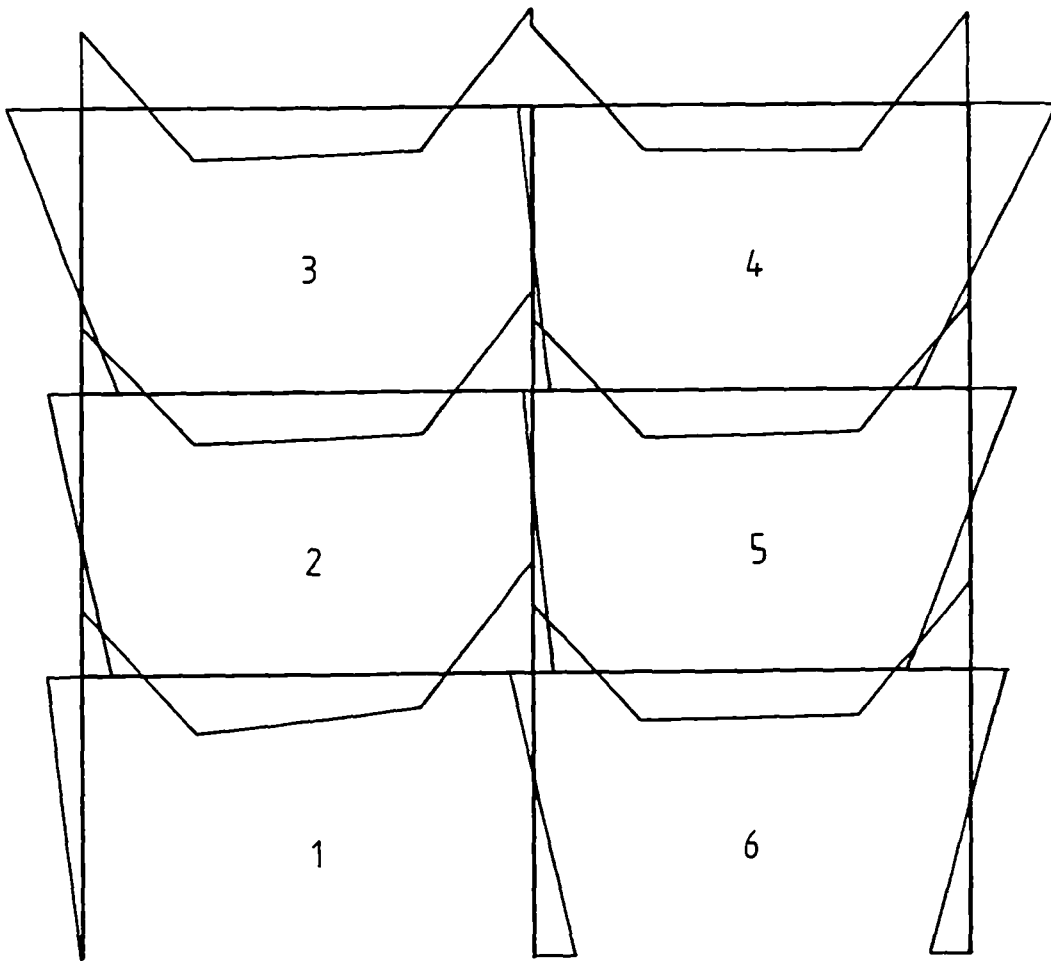


Fig. 7.7 - Bending moment distribution of frame ( $F_2$ ) at  $550^\circ C$ .

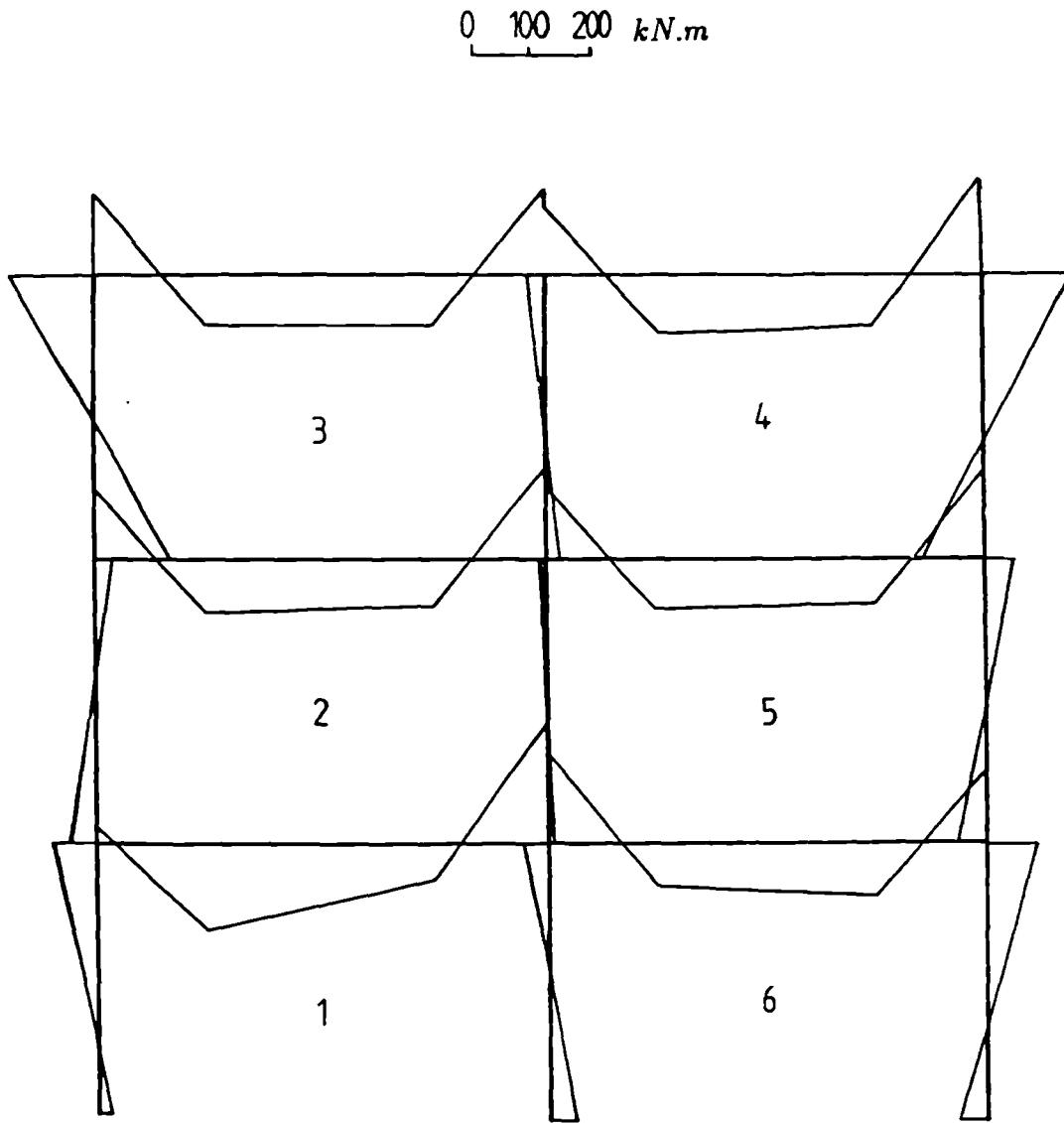


Fig. 7.8 - Bending moment distribution of frame ( $F_4$ ) at  $550^\circ\text{C}$ .

0 100 200 *kN.m*

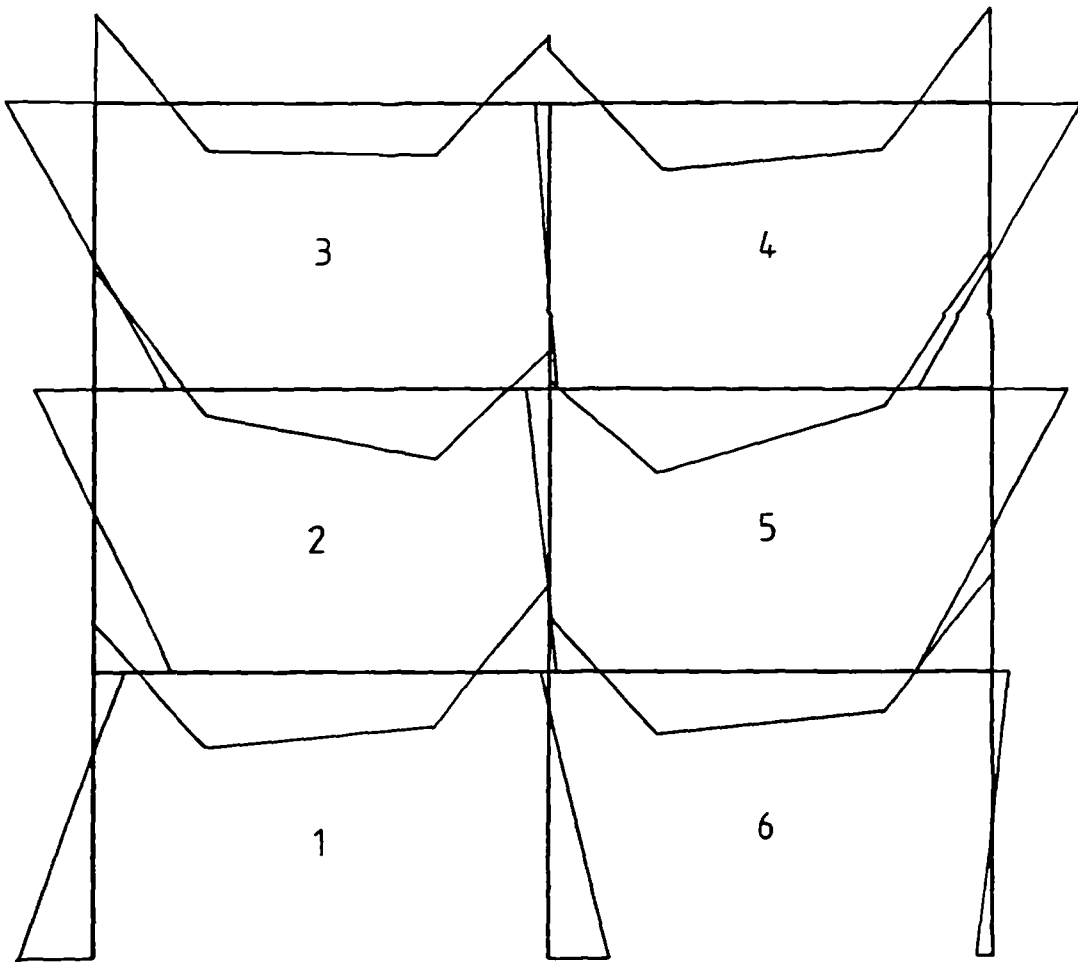


Fig. 7.9 - Bending moment distribution of frame ( $F_6$ ) at  $550^\circ\text{C}$ .

base conditions, the frame is more slender, having a slenderness ratio  $\bar{\lambda} = 0.6$ . Analyses were carried out for five different heating conditions as shown in Table 7.2.

Table 7.2 gives the critical temperatures for this frame under each of the heating schemes. This temperature was  $328^{\circ}\text{C}$  when the frame is fully and uniformly heated ( $P_1$ ) due to the high slenderness ratio which causes early collapse. Keeping the beams at ambient temperature ( $P_2$ ) has only a slight effect on the critical temperature since those members whose stiffnesses are preserved (i.e the beams), do not really participate in resisting sway. On the other hand, a significant increase of 66% in the critical temperature was exhibited by frame  $P_3$  in which the material properties of the columns are preserved. Protecting one column and three beams in case  $P_4$  resulted in a critical temperature of  $402^{\circ}\text{C}$ , whilst the highest critical temperature of  $582^{\circ}\text{C}$  was achieved in case  $P_5$  when a complete self-supporting part of the frame was protected. This confirms the effectiveness of providing a stiff self-supporting region of the frame in providing better fire endurance in general since the rest of the structure can be heated without causing early failure of the frame.

The effect of various heating conditions on the sway of the frame can be assessed from Fig.7.11 in which the lateral deflection-temperature relationships are shown. It can be seen that protecting all the beams in case  $P_2$  did not really limit the sway of the frame, nor did the protection offered in case  $P_4$  where the protected part of the structure simply followed the sway of the unprotected part. In case  $P_3$ , sway of the frame approximately retained its ambient temperature value up to  $400^{\circ}\text{C}$ . This sway increases more rapidly beyond this temperature level due to the loss of lateral support of the heated beams which, in this case, have an important role in acting as bracing elements. However, case  $P_5$  is most

Loads :  $F_1 = 227.97kN$      $F_2 = 759.915kN$   
 $F_3 = 114.89kN$      $H_1 = 8.143kN$

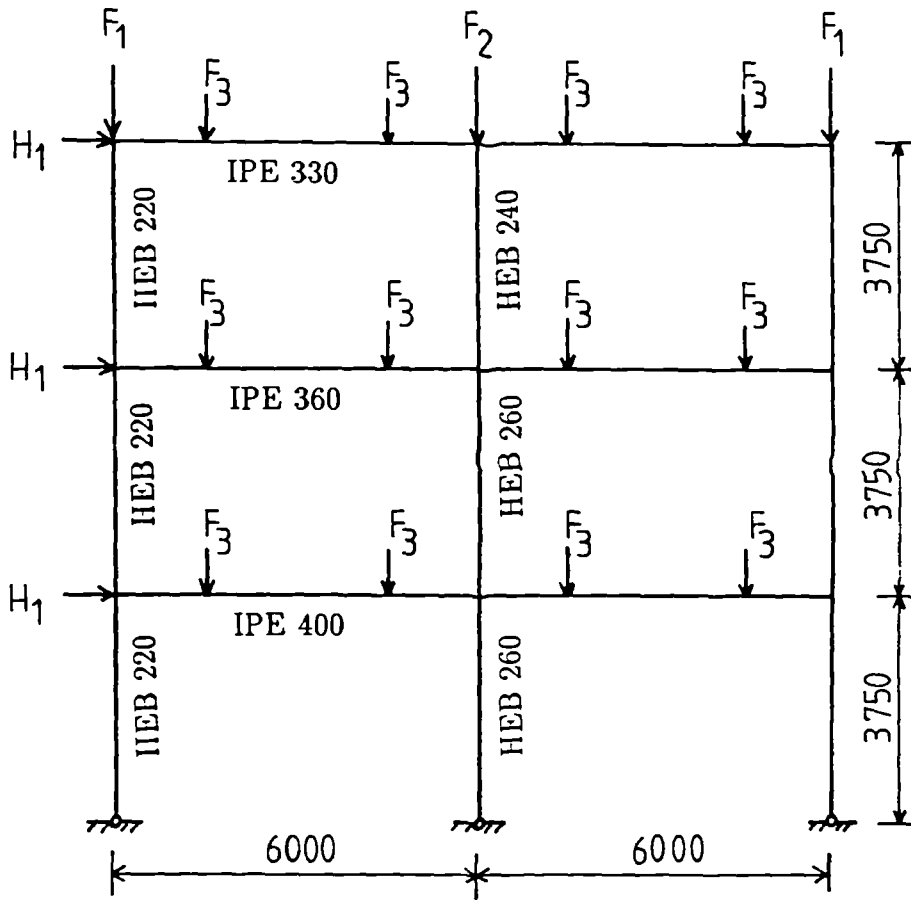
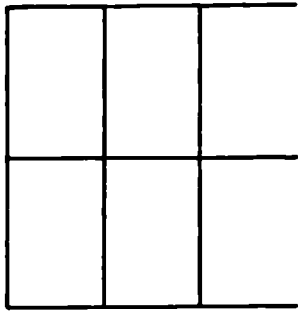
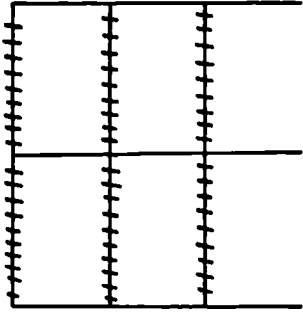


Fig. 7.10 - Frame geometry and loadings.

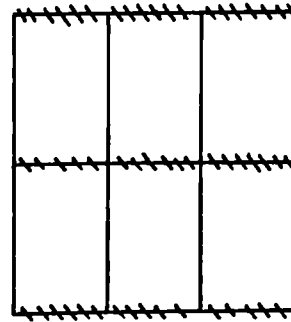
+++++ Cold element



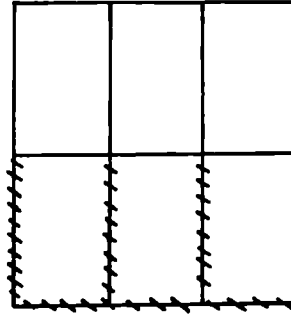
$P_1$   
 $\theta_{cr} = 328\text{ }^\circ\text{C}$



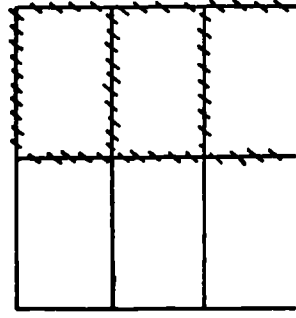
$P_2$   
 $\theta_{cr} = 352\text{ }^\circ\text{C}$



$P_3$   
 $\theta_{cr} = 566\text{ }^\circ\text{C}$



$P_4$   
 $\theta_{cr} = 402\text{ }^\circ\text{C}$



$P_5$   
 $\theta_{cr} = 582\text{ }^\circ\text{C}$

Table 7.2 - Various forms of heating conditions and corresponding critical temperatures.



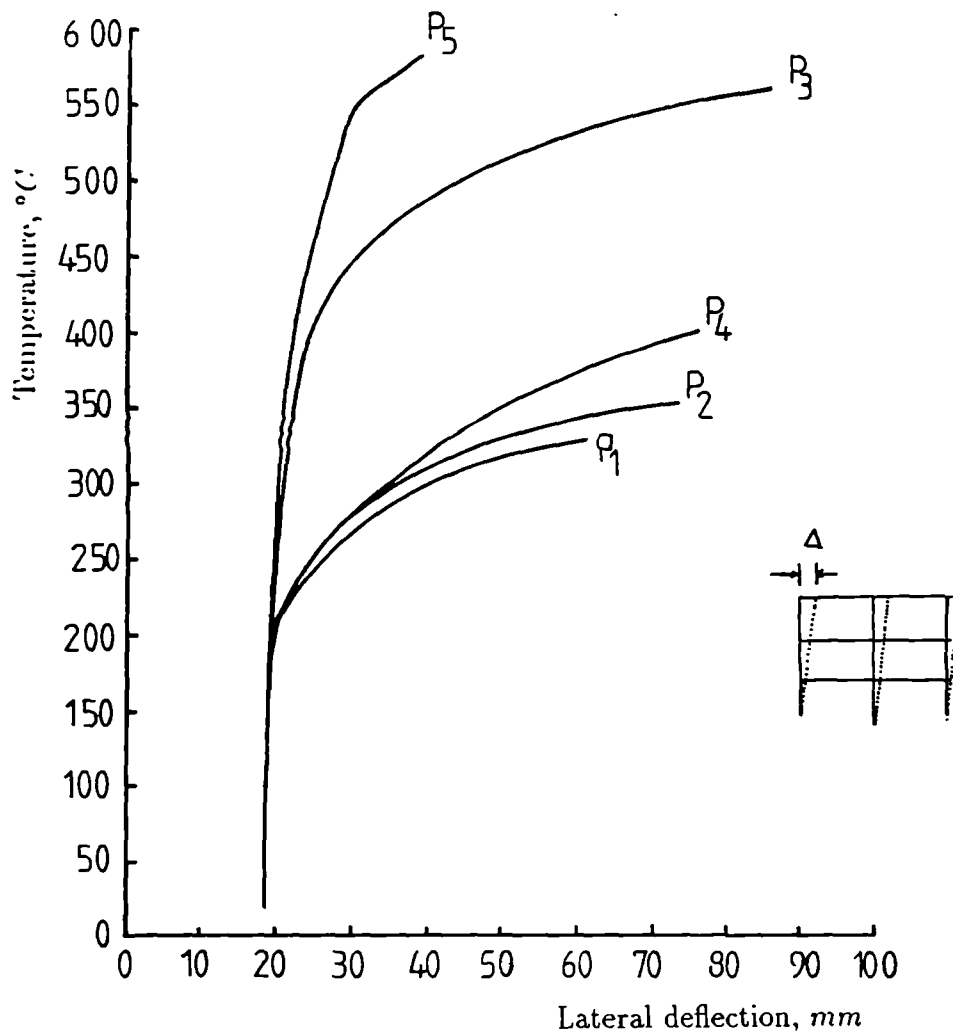


Fig. 7.11 - Lateral deflection-temperature relationships for the heating conditions shown in Table 7.2.

effective in preventing sway of this frame as shown by the appropriate curve in Fig.7.11. This can be explained by the fact that the heated part of the frame can 'lean' against a stiffer cold part which is self-supporting.

The mechanism of internal moment distribution under various heating conditions is similar to that discussed earlier as can be seen from Figs.7.12 to 7.15. Figs.7.12 and 7.13 show the distribution of the internal bending moment around frames  $P_4$  and  $P_5$  respectively at  $400^\circ C$ . Again, the familiar shift of the bending moment towards the cooler and thus stiffer part of the frame can be seen at the far left column of Fig.7.12. Moreover, Figs.7.14 and 7.15 show the distribution around frames  $P_3$  and  $P_5$  respectively at  $560^\circ C$  which, once again, confirms this phenomenon.

## 7.4 Concluding remarks

This chapter has outlined the effects of localised fire on the strength and stability of sway frames. Based on the above observations, the following conclusions may be drawn :

1. The stabilising influence of the cooler part of the structure located outside the fire compartments is apparent, especially if this part is self-supporting. This has shown to be effective in limiting sway of the frame and thus improving its fire endurance.
2. Deterioration of the stiffness of the beams forming the roof of a fire compartment has detrimental effects on columns located outside the fire compartment. The reduction in lateral support and rotational stiffness provided

by the heated beams increases the effective length of a column, thus reducing its critical load. Columns should therefore be assessed using the end conditions which are appropriate to the temperature levels of the adjacent members.

3. Additional forces are induced in the heated members due to the partial restraint to differential expansion between the heated and adjacent cooler members. At the same time, degradation of material strength and stiffness of the heated members reduces these forces. The contribution of the cooler part of the structure towards the load carrying capacity becomes larger. The distribution of the internal bending moment cannot therefore be deduced from that of the ambient temperature.

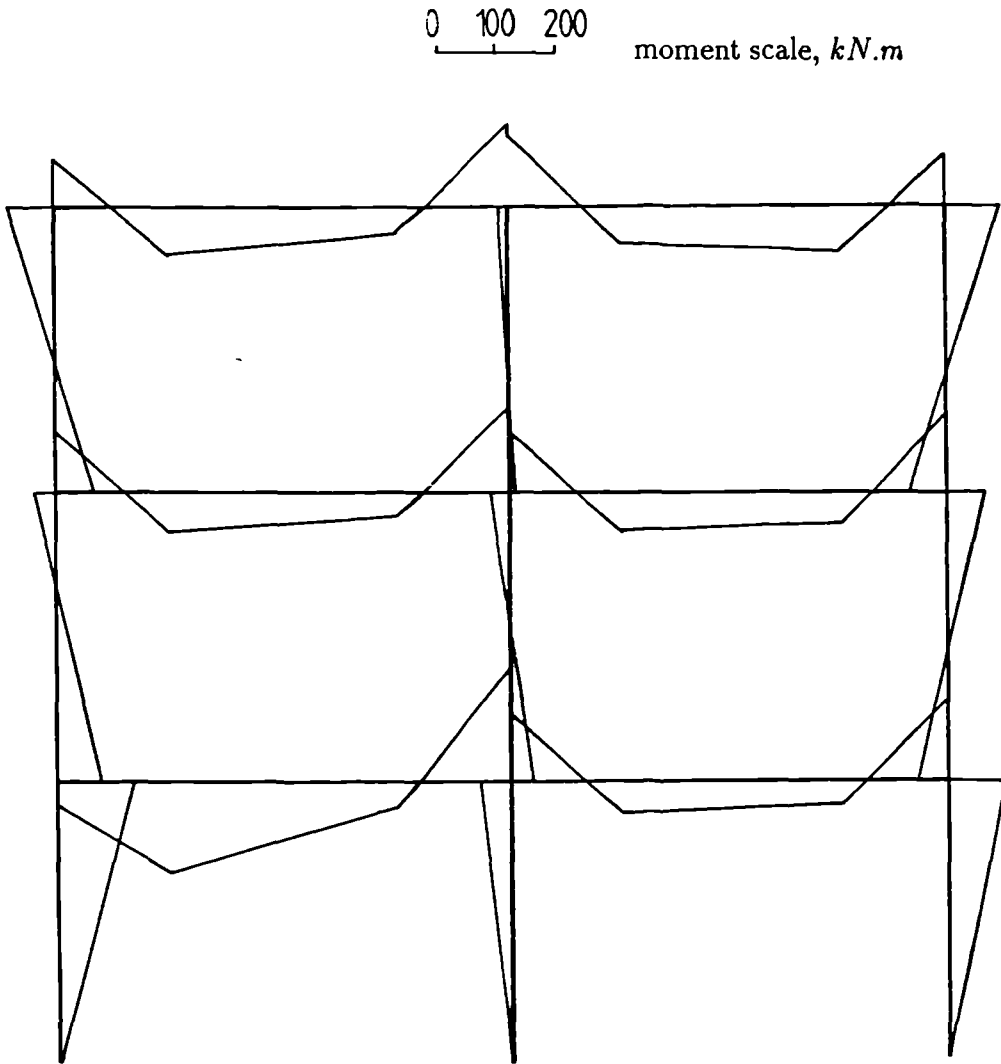


Fig. 7.12 - Bending moment distribution of frame ( $P_4$ ) at  $400^\circ C$ .

0 100 200 moment scale,  $kN.m$

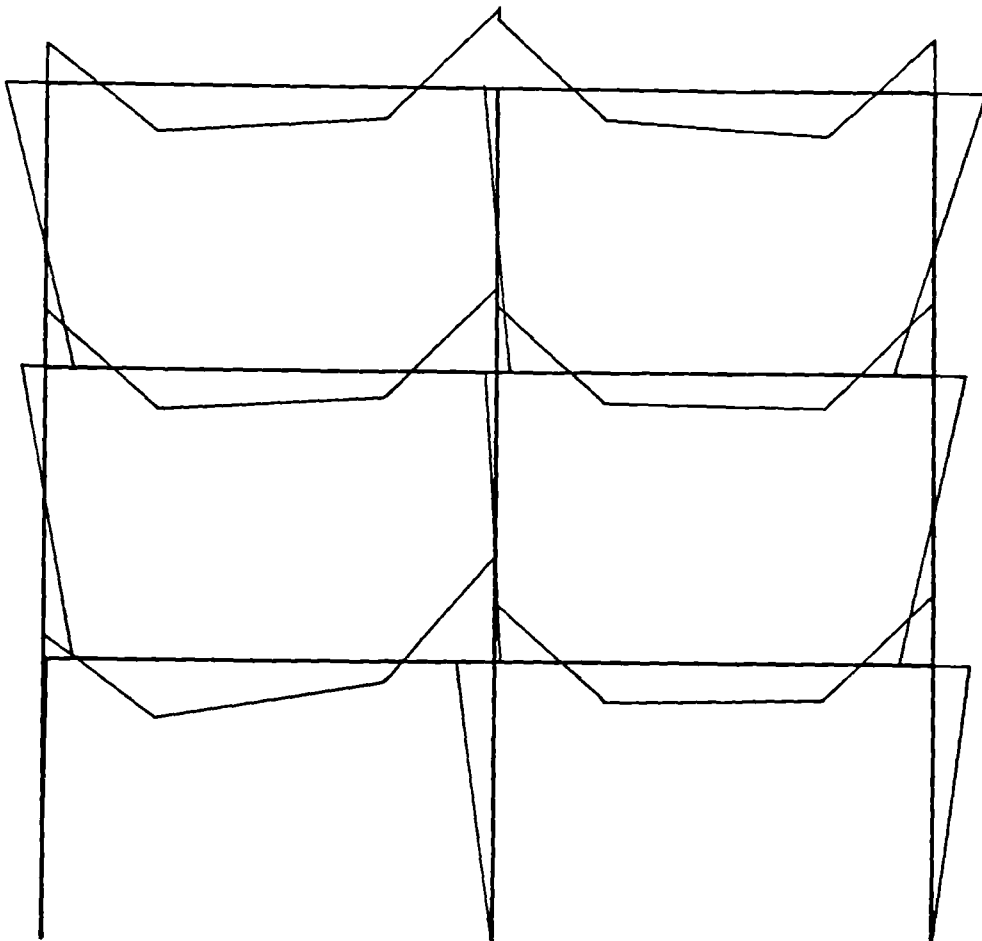
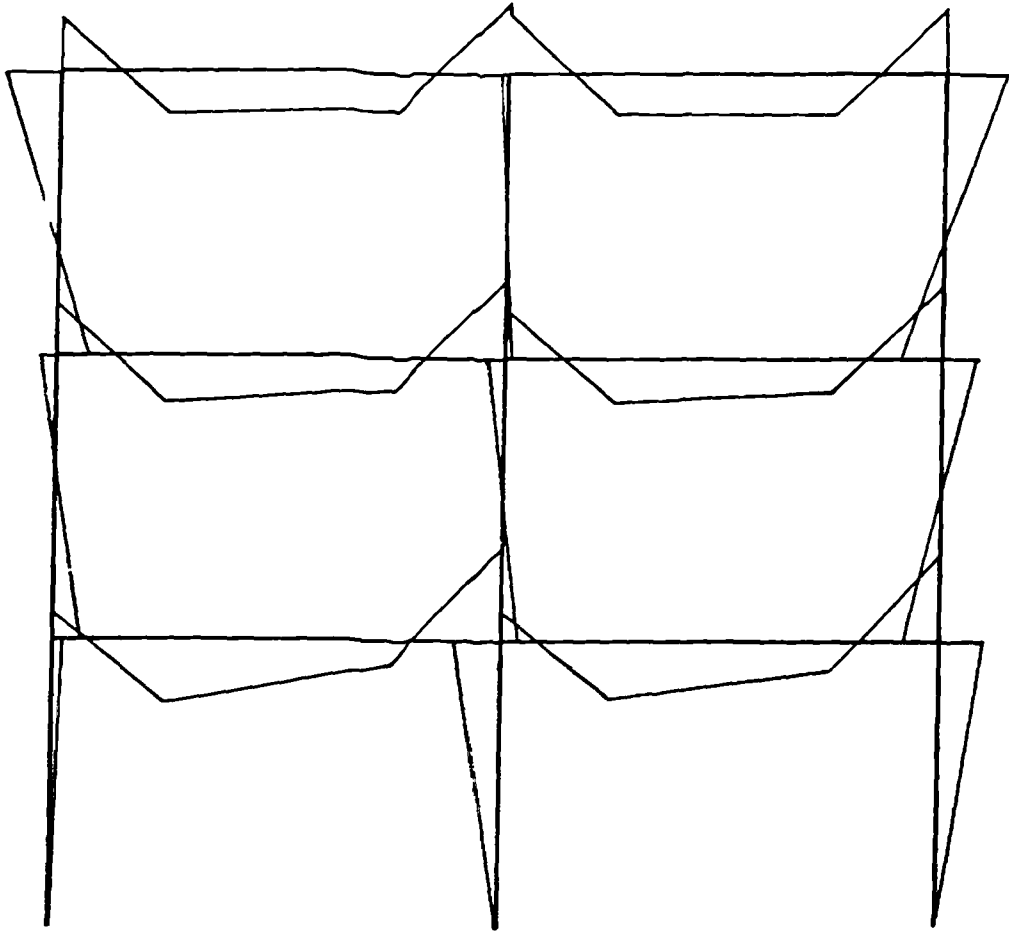


Fig. 7.13 - Bending moment distribution of frame ( $P_5$ ) at  $400^\circ C$ .

0 100 200 moment scale. *k.V.m*



**Fig. 7.14** - Bending moment distribution of frame ( $P_3$ ) at  $560^\circ C$ .

0 100 200 moment scale,  $kN.m$

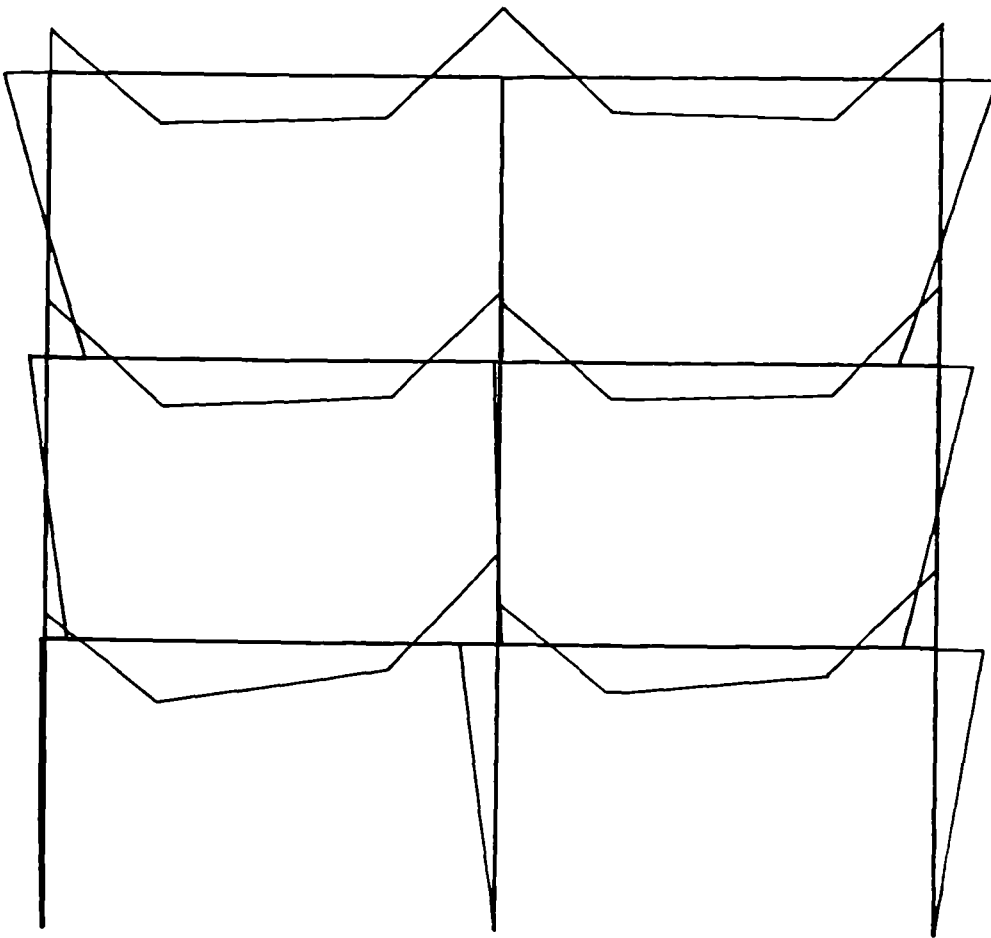


Fig. 7.15 - Bending moment distribution of frame ( $P_5$ ) at  $560^\circ C$ .

# Chapter 8

## Conclusions and Recommendations

The present work has been concerned with the development of a numerical approach and its subsequent use for behavioural studies on steel frames in fire conditions. The structural analysis is based on a tangent stiffness formulation using large deformation theory. A considerable amount of valuable data has been produced which provides the basis for a better understanding of the behaviour of steel frames in fire.

### 8.1 Scope of the work

A nonlinear finite element approach for the analysis of steel frames in fire has been presented. The analysis is based on a tangent stiffness formulation using large deformation theory. Structures subjected to increasing loads or temperatures are analysed using an incremental Newton-Raphson iterative procedure. The analysis



permits collapse load or critical temperature to be determined at a specified temperature or load level respectively, and provides a complete load-deformation and temperature-deformation history for two-dimensional multistorey steel frames.

The clearly nonlinear form of steel material properties at elevated temperatures has been represented as a set of continuous stress-strain relationships rather than in a bilinear form, although provision is made for any form of relationship to be included. Hence, a Ramberg-Osgood equation has been used to provide a set of nonlinear stress-strain-temperature relationships in which creep effects are implicitly included. The analysis includes the effect of geometric nonlinearity, temperature dependent nonlinear material behaviour and variation in temperature distribution both along and across the section. The effects of thermal strains, residual stresses and thermal bowing are also included and different values of the elastic stiffnesses of the support conditions can be considered. In the finite element formulation, a beam element with two nodes and three degrees of freedom at each node has been used. Gradual penetration of yielding through the cross-section is accounted for using the transformed area approach. The validity of this approach has been tested by comparing with experimental and analytical data covering as wide a range of problem parameters as possible. The comparisons show good agreement with this data.

The present method has been used to study a number of aspects of frame behaviour in fire. The influence of slenderness ratio, stress-strain representation and material models, various forms of protection, magnitude of residual stress and thermal gradient along and across the section of a frame have been investigated. An approximate curve based on statistical analysis of the derived results has been suggested as a simple means of predicting the critical temperature or collapse load of a uniformly heated steel frame. Results have also been presented that show

the effects of local fires and protection of only some parts of the steelwork which have revealed several interesting findings.

## 8.2 Concluding remarks

Behaviour of steel frames in fire has been investigated in Chapters 6 and 7. Results of the analyses have been discussed in detail and specific conclusions are provided at the ends of these chapters. However, based on the findings of the thesis as a whole, the following more general observations may be made.

The markedly nonlinear response of steel at high temperatures is better represented by a continuous form of stress-strain-temperature relationship than by an equivalent bilinear form. The use of such a bilinear form results in higher collapse loads with the three material models used in the analysis.

The familiar ambient temperature influence of yield strength and modulus of elasticity on frames is also apparent at elevated temperatures. The behaviour of low slenderness frames is largely controlled by the material yield strength while high slenderness frames are principally influenced by modulus of elasticity. The behaviour of intermediate slenderness frames is influenced by the interaction between material yielding and elastic overall buckling. On the other hand, between the three material models used in the analysis, the ECCS expressions for yield strength and modulus of elasticity have resulted in the most conservative collapse loads while the predictions based on the BS5950 expressions result in the highest collapse loads for all frames. Results of the analysis based on the CTICM expressions fall in between those two predictions. It is worth noting that analytical results based on the BS5950 expressions have shown the closest agreement with

fire test data.

The range of critical temperatures exhibited by different frames under various loading levels shows that uniformly heated frames with similar load levels fail at approximately equal temperatures. The frame slenderness ratio affects the predicted limiting temperatures especially for frames subject to moderate load levels. Critical temperatures of uniformly heated frames can therefore be determined as a function of frame slenderness ratio and load factor. These two parameters are ambient temperature design characteristics and can be determined using conventional methods.

As might be expected, residual stress distribution and magnitude have negligible effects at elevated temperatures beyond those exhibited at ambient temperature on low to moderate slenderness frames. Their effects on very high slenderness frames are of no significance. It can be concluded that if the residual stress magnitude at room temperature does not have significant influence then it will be even less important at elevated temperatures.

Variation of temperature across the section of a member generally has a beneficial effect since parts of the section retain their ambient temperature strength and stiffness. Bowing of the members towards the heat source can be regarded as an enhancement of the initial out-of-straightness and, is partly compensated by the apparent eccentricity of loading caused by the shift of the effective neutral axis towards the cooler parts of the section. It was shown that this thermal gradient has negative effects only on very high slenderness frames due to the thermal bowing since the equivalent imperfections have detrimental effects on the buckling behaviour of these frames. The nonuniform longitudinal temperature distribution, especially in the vicinity of the ends, has negligible effect

on the frame behaviour provided that this does not change the end connection stiffnesses.

The internal moment distribution at elevated temperatures in a partially heated frame is different from that at room temperature, being dependent upon the relative stiffnesses of different structural members at their corresponding temperature levels. The inherent beneficial effects of interaction between different elements is affected by the relative temperatures of these members; their response in a frame depends upon the heating pattern and load arrangement, and therefore cannot be predicted simply from the consideration of individual members. This is the case when beams, often designed with simple connections in practical frames, exhibit superior performance in fire due to the relatively low temperature of the protected joints. On the other hand, the stabilising influence of the cooler part of a frame as a result of partial protection of this part or of compartmentation is apparent. It has been demonstrated that partial protection can be effective in limiting sway of the frame and improving its fire endurance considerably, especially if this part is such that it can support the rest of the structure. A suitable partial protection scheme can therefore ensure better fire endurance of a frame as a whole.

For columns located outside a fire compartment, deterioration of the stiffness of the beam forming the roof of the fire compartment has detrimental effects on these columns. The reduction in lateral support and rotational stiffness provided by these heated beams increases the effective length of those columns, thus reducing their critical load. Columns should therefore be assessed in fire design using the end conditions which are appropriate to the temperature levels of the adjacent members. In partially heated frames, additional forces may be induced in the members due to the partial restraint from expansion as a result of differ-

ential expansion between the heated and adjacent cooler members. These forces become larger with greater numbers of levels above and bays around the fire compartment. At the same time, degradation of the axial and flexural rigidity of the heated section reduces these forces in the heated members. The contribution of the cooler part of the structure towards the load carrying capacity then becomes larger.

### 8.3 Recommendations for future work

The theory and analytical technique presented herein has been shown to be an efficient fire engineering approach to handle the structural analysis of steel frames in fire. It can nevertheless be extended to include further aspects of the problem.

Real connections in steel frames are neither fully rigid nor pinned. Modification to the existing program can be carried out to include the effect of semi-rigid connections by including experimental moment-rotation characteristics for different connections, with adequate provision for calculation of the joint stiffness matrix. A large amount of ambient temperature experimental moment-rotation characteristic data exists at Sheffield University, and this can be used as a basis for analysis using heated connections with minimum modification to the program.

Although the present theory considers only in-plane behaviour, out-of-plane collapse has been observed during fire tests. The present theory can be extended, with a substantial amount of work, to deal with three-dimensional analysis. In addition some other forms of construction, such as composite structures, can be studied with minimal modification to the program.

Temperature distribution is assumed in a stepped form over the cross-section, with four different temperature regions due to the large number of actual temperature patterns that may exist. Clearly any such distribution can be accommodated with very minimal modification.

Other aspects of the problem such as the cooling and extinguishing phase and reinstatement of damaged structures may also be studied.

Finally, only the structural response of frames under fire conditions can be predicted using this program. The heating schemes must be given in the input data, either in continuous form or as a set of data points. It would be more convenient if the program were extended to incorporate a thermal analysis of the structure.

Generally the present study provides a basis for further research into the behaviour of steel frames in fire. Attempts have been made to highlight the problem's features as widely as possible. An efficient analysis has been presented and a considerable amount of information has been produced. It is hoped that this information will form a valuable building-block in the growing body of understanding of the behaviour of steel frames in fire, which will eventually lead to a comprehensive philosophy for fire engineering design.

# References

- [1] Aasen, B.(1985),  
"An experimental Study on Steel Column Behaviour at Elevated Temperatures",  
Division of Steel Structures, The Norwegian Institute of Technology, University of Trondheim, Norway.
  
- [2] Anchor, R. D., Malhotra, H.L. and Purkiss, J.A. (ed.) (1986),  
Design of Structures Against Fire,  
Elsevier Applied Science Pub., London & NewYork.
  
- [3] Anderberg, Y.(1988),  
"Modelling Steel Behaviour",  
Fire Safety Journal, 13 ,P17-26.
  
- [4] Aribert, J.M. and Abdel Aziz, M.(1987),  
"Comportement a l'incendie de Poteaux Comprimés et Flechis en Presence de Gradients Quelconques de Temperature",  
Construction Metallique No.2.
  
- [5] Aribert, J.M. and Randriantsara, C.(1980),  
"Etude du Flambement a des Temperatures d'incendie.Action du Fluage",  
Construction Metallique No.4.

- [6] Aribert, J.M. and Randriantsara, C.(1983),  
 "Sur une modelisation du Flambement des Poteaux Metalliques dans des  
 Conditions d'incendie",  
 3<sup>rd</sup> Int. Col. on Stability of Metal Structures, Preliminary Report, CTICM,  
 Paris.
- [7] Arnold, P., Adams, P. and Lu, Le-Wu.(1968),  
 "Strength and Behaviour of an Inelastic Hybrid Frame",  
 ASCE Structural Division , V94,No.ST1,Jan.,P243-266.
- [8] Baba, S. and Nagura, H.(1985),  
 "Effect of Material Properties on the Deformation of Steel Frame in Fire",  
 JSCE Structural Eng./Earthquake Eng.,V2,No.1,P47-57,April.
- [9] Bennetts, I.D., Goh, C.C., O'Meagher, A.J. and Thomas, I.R.(1989),  
 "Restraint of Compression Members in Fire",  
 BHP Melb. Res. Labs. Rep. No. MRL/PS65/89/002, Sept.
- [10] Bennetts, I.D, Proe, D.J. and Thomas, I.R.(1985),  
 "Simulation of the Fire Testing of Structural Elements by Calculation.  
 Thermal Response",  
 Steel Construction, V19,No.3,Nov.
- [11] Bennetts, I.D., Proe, D.J. and Thomas, I.R.(1986),  
 "Simulation of the Fire Testing of Structural Elements by Calculation",  
 Steel construction, V19,No.3.
- [12] Bresler, B., Iding, R. and Nizamuddin, Z.(1977),  
 FIRES-T3, A Computer Program for the Fire Response of Structures -  
 Thermal,  
 Report No.UCB FRG 77-15, Univ. of California, Berkeley.



- [13] Bresler, B. and Iding, R.(1981),  
Effect of Fire Exposure on Steel Frame Buildings,  
Final Report, WJE No.78124, Sept.
- [14] Brockenbrough, R.L.(1970),  
"Theoretical Stresses and Strains From Heat curving",  
Journal of Structural Division , ASCE , No.ST7 ,V96 , July ,P1421-1444.
- [15] Brozzetti, J., Law,M. Pettersson, O. and Witteveen, J.(1983),  
Safety Concept and design for Fire Resistance of Steel Structures,  
IABSE Surveys S-22/83.
- [16] BS 5950 Pt.8(1990),  
Structural Use of Steelwork in Building : Code of Practice for Fire Resistant  
Design.
- [17] BSC Test No. RS/RSC<sup>10328</sup> /1 /87/B, Confidential Report.
- [18] Burgess, I.W., El-Rimawi, J.A. and Plank, R.J.(1988),  
"A Secant Stiffness Approach to the Fire Analysis of Steel Beams",  
J. Construc. Steel Research, 11, P105-120.
- [19] C.T.I.C.M.(1982),  
"Methode de Provision par le Calcule du Comportement au Feu des Struc-  
tures en Acier",  
Construction Metallique ,No.3, Sept.
- [20] Cheng, W.C.(1983),  
"Theory and Application on the Behaviour of Steel Structures at Elevated  
Temperatures",  
Computers and Structures, V16,No.1-4,P27-35.

- [21] Cheng, W.C. and Mark, C.K.(1975),  
"Computer Analysis of Steel Frame in Fire",  
J. of the Structural Division, ASCE, April.
- [22] Contro, R., Poggi, C. and Cazzani, A.(1987)  
"Numerical Analysis of Fire Effects on Beam Structures",  
Politecnico di Milano.
- [23] Cooke, G.M.E. and Latham, D.J.(1987),  
"The Inherent Fire Resistance of a Loaded Steel Framework",  
Steel Costruction Today, 1, P49-58.
- [24] Cooke, G.M.E.(1987),  
The Structural Response of Steel I-section Members Subjected to Elevated  
Temperature Gradients Across the Section,  
PhD Thesis, The City University, London, Sept.
- [25] Cooke, G.M.E.(1988),  
"An Introduction to the Mechanical Properties of Structural Steel at Ele-  
vated Temperatures",  
Fire Safety Journal , No.13 , P45-54.
- [26] Culver, C.G.(1972),  
"Steel Column Buckling under Thermal Gradients",  
J. of the Structural Division, Proc. ASCE, August,P1853-1865.
- [27] Culver, C.G., Aggarwal, V. and Ossenbruggen, P.(1973)  
"Buckling of Steel Columns at Elevated Temperatures",  
J. of the Structural Division, ASCE, April.

- [28] Dotreppe, J-C.(1986),  
"Structural Models for Fire Analysis",  
IABSE Proceedings P-101/86, August.
- [29] ECCS-T3 (1983),  
European Recommendations for the Fire Safety of Steel Structures,  
Elseviers Scientific Publishers Co.
- [30] Eggwertez, S.(1977),  
"Creep Buckling of a Steel Column in a Temperature-Time History Simu-  
lating a Fire",  
IABSE 10<sup>th</sup> Congress, Tokyo, Final Report, Zurich.
- [31] Fujimoto, M., Furumura, F. and Ave, T.(1982),  
"Creep Buckling of Steel Columns at High Temperatures",  
Report of the Research Lab. of Eng. Mat., Tokyo Inst. of Tech., No.7.
- [32] Fujimoto, M., Furumura, F., Ave, T., and Kin, W.J.(1983),  
"Further Studies of the Creep Buckling of Steel Columns at High Temper-  
atures",  
Rep. of the Res. Lab. of Eng. Mat., Tokyo Inst. of Tech., No.8.
- [33] Furumura, F. and Shinohara, V.(1978),  
"Inelastic Behaviour of Protected Steel Beams and Frames in Fire",  
Report of the Research Lab. of Eng. Mat., Tokyo Institute of Technology.
- [34] Goh, C.C., Bennetts, I.D., Foo, S.K. and Thomas, I.R.(1989),  
"Stability and Strength of Steel Columns in Fire",  
BHP Melb. Res. Labs. Rep. No. MPL/PS65/89/003, Oct.

- [35] Harmathy, T.Z.(1967),  
"A Comprehensive Creep Model",  
J. of Basic Eng., Trans. of the ASME, Semp.
- [36] Harmathy, T.Z. and Stanzak, W.W.(1972),  
"Behaviour of Steel Flexural Members in Fire",  
Applications of Solid Mechanics, Univ. of Waterloo, Study No.7, P291-310.
- [37] Hivid, N.J. and Olesen, F.B.(1980),  
" Fire Resistance of Bolted Steel Connections",  
Institute of Building Technology and Structural Eng., Danmark.
- [38] Hoffend, F. and Kordina, K.(1984),  
Versagenstemperaturen Crit T Von Brandbeanspruchten Stahlstutzen aus  
Walzprofilen,  
Stahlbau, 12.
- [39] Holmes, M., Anchor, R.D., Cooke, G.M.E. and Crook, R.N.(1982),  
"The Effect of Elevated Temperatures on the Strength Properties of Rein-  
forcing and Prestressing Steel",  
The Structural Engineer, V60B, No.1, March.
- [40] Horne, M.R.(1979),  
Plastic Theory of Structures,  
2<sup>nd</sup> Edition, Pergamon Press.
- [41] Horne, M.R. and Merchant, W.(1965),  
The Stability of Frames,  
Pergamon Press, Oxford.
- [42] ISO 834(1975),  
Fire Resistance Tests - Elements of Building Construction.

- [43] Jain, P.C. and Rao, M.N.G.(1983),  
"Analysis of Steel Frames Under Fire Environment",  
Int. J. for Num. Meth. in Eng., V19.
- [44] Janss, J. and Minne, R.(1981/1982),  
"Buckling of Steel Columns in Fire Conditions",  
Fire Safety Journal, No.4, P227-235.
- [45] Kerstma, J., Bijlaard, F.S.K. and Twilt, L.(1979),  
"Analyses of the Gap Between the TNO-IBBC Buckling Curves and the  
Results of Full-Scale Tests,  
Report No.BI-79-74, TNO, Delft.
- [46] Kirby, B.R.(1985),  
"Fire Resistance of Steel Structures",  
BSC, Jan.
- [47] Kirby, B.R.(1986),  
"Recent Developments and Applications in Structural Fire Engineering De-  
sign - A Review",  
Fire Safety Journal, No.11, P141-179.
- [48] Kirby, B.R. and Preston, R.R.(1988),  
"High Temperature Properties of Hot-Rolled Structural Steels for Use in  
Fire Engineering Design Studies",  
Fire Safety Journal, No.13
- [49] Kirby, P.A. and Nethercot, D.A.(1985),  
Design for Structural Stability,  
Collins Books, London.

- [50] Knublauch, E., Rudolphi, R. and Stanke, J.(1974),  
Theoretische Ermittlung der Feuerwiderstandsdauer von Stahlstützen und  
Vergleich mit Versuchen, Bestimmung der Kritischen Stahltemperatur,  
Stahlbau, 8.
- [51] Koike, S., Ooyanagi, N. and Nakamura, K.(1982),  
"Experimental Study on Thermal Stress within Structural Steelwork",  
Fire Science and Technology, V2, No.2, P137-150.
- [52] Kouhia, R., Paavola, J. and Tuomala, M.(1988),  
"Modelling the Fire Behaviour of Multistorey Buildings",  
13<sup>th</sup> IABSE Congress Report, Helsinki, June.
- [53] Kruppa, J.(1979),  
"Collapse Temperature of Steel Structures",  
J. of the Structural Division, ASCE, P1769-1788, Semp.
- [54] Kruppa, J.(1981/1982),  
"Some Results on the Behaviour of External Steel Columns",  
Fire Safety Journal, No.4, P247-257.
- [55] Lai, Y.F.W.(1988),  
Buckling Strength of Welded and Non-Welded Aluminium Members,  
PhD Thesis, Dept. of Civil and Struct. Eng., Sheffield Univ., Oct.
- [56] Law, M.(1983),  
"A Basis for the Design of Fire Protection of Building Structures",  
The Structural Engineer, V61A, No.1, Jan., P25-33.
- [57] Lawson, R.M.(1987),  
"Fire Engineering in the UK and Europe",  
Steel Construction Today, V1, No.5, Oct., P159-165.

- [58] Lie, T.T.(1972),  
Fire and Buildings,  
Applied Science Publishers Ltd., London.
- [59] Lie, T.T.(1978),  
"Fire Resistance of Structural Steel",  
Eng. Journal, AISC, 4 Quarter,P116-125.
- [60] Lie, T.T. and Stanzak, W.W.(1976),  
"Structural Steel and Fire - More Realistic Analysis",  
Eng. Journal, 2<sup>nd</sup> Quarter, P35-42.
- [61] Magnusson, S.E., Pettersson, O. and Thor, J.(1976),  
Fire Engineering Design of Steel Structures,  
Publication 50, SBI, Stockholm.
- [62] Malhotra, H.L.(1982),  
"Report on the Work of the Technical Committee 44-PHT, Properties of  
Materials at High Temperatures",  
Materials and Structures, V15, No.86, March - April, P161-170.
- [63] Ministry of Public Buildings and Works(1946),  
Post War Buildings Studies No.20, Fire Grading of Buildings, Part 1 :  
General Principles and Structural Precautions.
- [64] Muzeau, J.P. and Lemaire, M.(1980),  
"Modele Numerique du Comportement d'Ossatures en Acier sous Forte  
Elevation de Temperature",  
Construction Metallique, No.3.
- [65] Olawale, O.A. and Plank, R.J.(1988),  
"The Collapse Analysis of Steel Columns in Fire Using a Finite Strip

Method”,

Int. Journal for Num. Meth. in Eng., V26, P2755-2764.

- [66] Ooyanagi, N., Hirota, M. and Nakamura, K.(1983),  
”Experimental Study on Thermal Stress within Steel Frames”,  
Fire Science and Technology, V3, No.1, P45-55.
- [67] Ossenbruggen, P.J., Aggarwal, V. and Culver, C.G.(1973),  
”Steel Column Failure under Thermal Gradients”,  
J. of the Structural Division, ASCE, April, P727-739.
- [68] Petterson, O.(1988),  
”Practical Need of Scientific Material Models for Structural Fire Design -  
General Review”,  
Fire Safety Journal , No.13 , P1-8.
- [69] Petterson, O. and Witteveen, J.(1979/1980),  
”On the Fire Resistance of Structural Steel Elements Derived from Standard  
Fire Tests or by Calculation”,  
Fire Safety Journal, No.2,P73-87.
- [70] Proe, D.J., Thomas, I.R. and Bennetts, I.D.(1986a),  
”Simulation of the Fire Testing of Structural Elements by Calculation -  
Mechanical Response”,  
Steel Costruction, AISC, V19, No.4.
- [71] Proe, D.J., Bennetts, I.D. and Thomas, I.R.(1986b),  
”Simulation of the Fire Testing of Structural Elements by Calculation -  
Overall Behaviour”,  
Steel Construction, AISC, V19, No.4.



- [72] Peterson, A.(1984),  
"Finite Element Analysis of Structures at High Temperatures",  
Rep. TVSM-1001, Lund Inst. of Tech., Lund, Sweden.
- [73] Ramberg, W. and Osgood, W.(1943),  
"Description of Stress-Strain Curves by Three Parameters",  
NACA Technical Note No.902.
- [74] Robinson, J.T.(1989),  
"Fire Resistant Design of Steel Beams - Recent Developments in the UK",  
Pacific Structural Steel Conference, May, P532-543.
- [75] Rubert,A. and Schaumann P.(1985a),  
"Temperaturabhängige Werkstoffeigenschaften Von Baustahl bei Brandbeanspruchung",  
Stahlbau, V54, No.3.
- [76] Rubert, A. and Schaumann, P.(1985b),  
"Tragverhalten Stahlerner Rahmensysteme bei Brandbeanspruchung",  
Stahlbau, V54, No.9.
- [77] Rubert, A. and Schaumann, P.(1986),  
"Structural Steel and Plane Frame Assemblies under Fire Action",  
Fire Safety Journal, 10, P173-184.
- [78] S.A.I.S.C (1989),  
"Nippon Steel Develops a New Fire-Resistant Structural Steel",  
Steel Construction, V13, No.3, May, P27.
- [79] Saada, A.S.(1974),  
Elasticity Theory and Application,  
Pergamon Press Inc.

- [80] Schleich, J.B.(1988),  
"Fire Engineering Design of Steel Structures",  
Steel Construction Today, V2.
- [81] Schleich, J.B., Dotreppe, J.C. and Franssen, J.M.(1985),  
"Numerical Simulations of Fire Resistance Tests on Steel and Composite  
Structural Elements or Frames,  
Fire Safety Science - Proceeding of the 1<sup>st</sup> International Symposium, Oct.
- [82] Setti, P.(1983),  
"Buckling of Axially Loaded Steel Columns with Imperfections at Elevated  
Temperatures",  
Stability of Metal Structures, 3<sup>rd</sup> Int. Col., Preliminary Report, Paris, Nov.
- [83] Sharples, R.(1987),  
"The Strength of Partially Exposed Steel Columns in Fire",  
MPhil Dissertation, Dep. Civ. Str. Eng., Univ. of Sheffield,
- [84] Smith, C.I.(1986),  
"Structural Steel Fire Protection for Multistorey Buildings- Recent Devel-  
opments",  
Steel Construction, AISC, V20, No.2, August.
- [85] Thor, J., Pettersson, O. and Magnusson, S.E.(1978),  
"A Rational Approach to Fire Engineering Design of Steel Buildings",  
Steel Construction, AISC, V12, No.4, P2-7.
- [86] Twilt, T.(1988),  
"Strength and Deformation Properties of Steel at Elevated Temperatures :  
Some Practical Implications" ,  
Fire Safety Journal , No.13 , P9-15.

- [87] Uddin, T.A. and Culver, C.(1975),  
 "Effect of Elevated Temperature on Structural Members",  
 J. of the Structural Division, ASCE, P1531-1594, July, P1531-1549.
- [88] Vandamme, M. and Janss, J.(1981),  
 "Buckling of Axially Loaded Steel Columns in Fire Conditions",  
 IABSE Proc. P43/81, P81-95, August.
- [89] Wickstrom, U.(1979),  
 TASEF-2, A Computer Program for Temperature Analysis of Structures Exposed to Fire,  
 Report No.79-2, Dept. of Structural Mechanics, Lund Institute of Technology, Sweden.
- [90] Witteveen, J.(1985),  
 "Design Methods for Fire Exposed Steel Structures",  
 IABSE - ECCS Symposium, *Steel in Buildings*, Luxembourg.
- [91] Witteveen, J., and Twilt, L.(1972),  
 "Behaviour of Steel Columns under Fire Action",  
 Proc. Int. Col. on Column Strength, Paris
- [92] Witteveen, J. and Twilt, L.(1981/1982),  
 "A Critical View on the Results of Standard Fire Resistance Tests on Steel Columns",  
 Fire Safety Journal, No.4, P259-270.
- [93] Witteveen, J., Twilt, L. and Bijlaard, F.S.K.(1976),  
 "Theoretical and Experimental Analysis of Steel Structures at Elevated Temperatures",  
 IABSE 10<sup>th</sup> Congress, Tokyo, Final Report, Zurich.

- [94] Witteveen, J., Twilt, L. and Bijlaard, F.S.K.(1977),  
"The Stability of Braced and Unbraced Frames at Elevated Temperatures",  
Stability of Steel Structures, Liege, Preliminary Report.
- [95] El-Zanaty, M., Murray, D. and Bjorhovde, R.(1980),  
Inelastic Behaviour of Multistorey Steel Frames,  
Structural Engineering Report No.83, Dep. Civ. Eng., Univ. of Alberta,  
Canada.
- [96] Zienkiewicz, O.C.(1977),  
The Finite Element Method,  
3<sup>rd</sup> Edition, McGraw Hill, London.

# Appendix A

## Calculation of geometric deformation due to thermal gradient

### Assumptions

The following assumptions have been considered in order to calculate the geometric deformation due to thermal gradient across the section :

1. deformation shape is circular.
2. variation of temperature is linear across the section.
3. plane sections remain plane.
4. the coefficient of linear thermal expansion  $\alpha$  is constant with increasing temperature.

The member deformations are given by Fig.A.1 as :

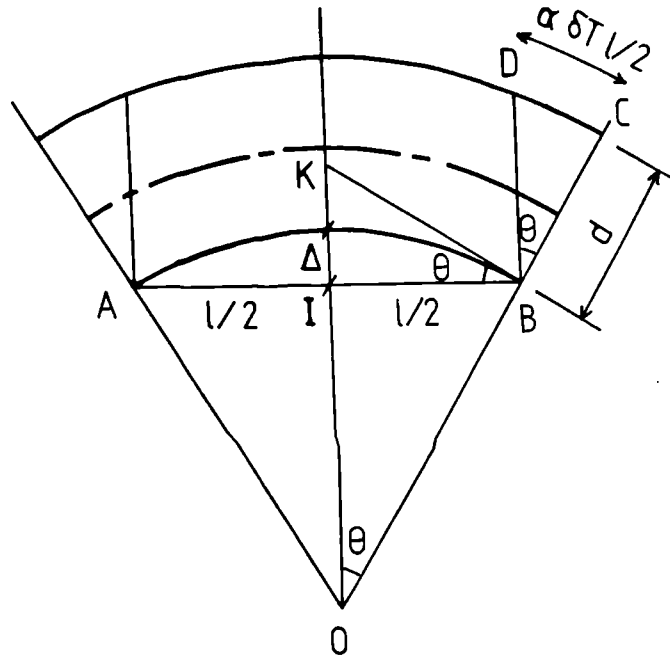
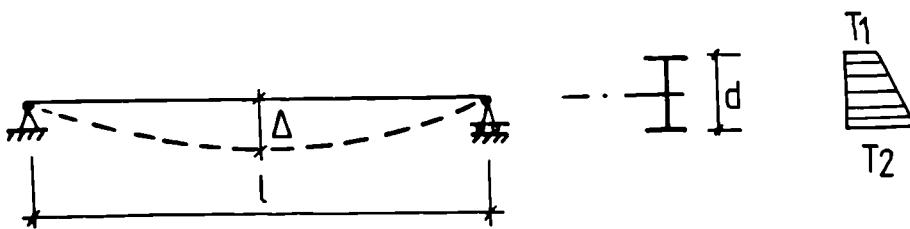


Fig. A.1 - Member deformations due to thermal bowing.

Pin ended members (Fig.A-2)



$$\theta = \alpha \delta T \frac{L}{2} \times \frac{1}{d} \tag{A.1}$$

from triangle *IKB* :

$$\theta = \frac{2\Delta}{L/2} = \frac{4\Delta}{L} \tag{A.2}$$

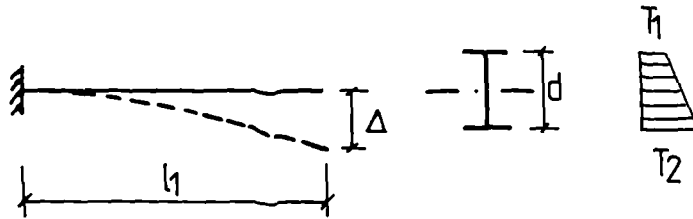
substituting eq.A.1 into eq.A.2 yields :

$$\alpha \frac{\delta T L}{2d} = \frac{4\Delta}{L} \quad (\text{A.3})$$

from which :

$$\Delta = \alpha \frac{\delta T L^2}{8d} \quad (\text{A.4})$$

Cantilever (Fig.A.3)



Rewriting eq.A.4 with  $L = 2L_1$  yields :

$$\Delta = \frac{\alpha \delta T}{8d} (2L_1)^2 = \frac{\alpha \delta T L_1^2}{2d} \quad (\text{A.5})$$

where :

$$\alpha = 1.4 \times 10^{-5} \text{ } / ^\circ\text{C},$$

$$\delta T = T_2 - T_1,$$

$d$  = section depth,

$L$  = member length.